CONF-980441--PROC.

DOE/EE-0188

Proceedings Geothermal Program Review XVI

A Strategic Plan for Geothermal Research

April 1-2, 1998

Berkeley, California

Sponsored by:

U.S. Department of Energy
Assistant Secretary for Energy Efficiency and Renewable Energy
Office of Geothermal Technologies

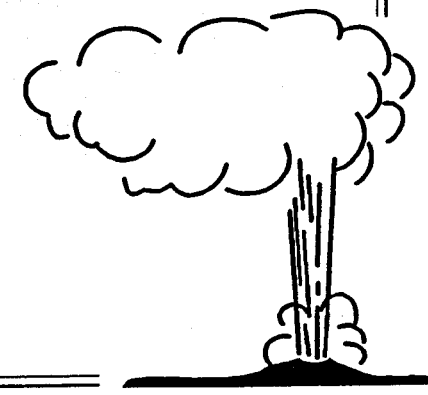

DISCLAIMER

DISCLAIMER

DISCLAIMER

Portions of this document may be illegible in electronic image products. Images are produced from the best available original document.

TABLE OF CONTENTS

RESERVOIR TECHNOLOGY (continued)

ENERGY CONVERSION TECHNOLOGY

DRILLING TECHNOLOGY

DIRECT USE AND GEOTHERMAL HEAT PUMP TECHNOLOGY

WORKSHOP

APPENDIX A:

APPENDIX B:

Preface

The U.S. Department of Energy's Office of Geothermal Technologies conducted its annual Program Review XVI in Berkeley on April 1-2, 1998. The geothermal community came together for an in-depth review of the federally-sponsored geothermal research and development program. This year's theme focussed on "A Strategic Plan for Geothermal Research."

This annual conference is designed to promote technology transfer by bringing together DOE-sponsored researchers; utility representatives; geothermal developers; equipment and service suppliers; representatives from local, state, and federal agencies; and others with an interest in geothermal energy.

Program Review XVI consisted of seven sessions chaired by DOE, industry, and contractor representatives. Introductory and overview remarks were presented during each session followed by detailed reports on specific DOE-funded research projects. The progress of R&D projects over the past year and plans for future activities were discussed. The government-industry partnership continues to strengthen -- its success, achievements over the past twenty years, and its future direction were highlighted throughout the conference. DOE's strategic plan for geothermal research was also presented at a panel discussion.

The comments received from the conference evaluation forms are published in this year's proceedings. I thank all of you who took time to give us your thoughts and suggestions. Your comments will help make next year's program review even better. I want to express my thanks to all who participated and contributed to this year's successful Geothermal Program Review.

Allan J. Jelacic, Director
Office of Geothermal Technologies
Energy Efficiency and Renewable Energy

Session 1:

Overview

Securing Our Investment

The CEC's Michal Moore Describes Programs to Preserve and Promote Renewables as California's Electric Industry Restructures

***Note*: The following article has been reprinted from the April/May 1998 issue of the GRC Bulletin. It was edited from a Keynote Presentation delivered by Commissioner Michal Moore, California Energy Commission (CEC), at the 16th U.S. Department of Energy Geothermal Program Review on April 1, 1998, in Berkeley, CA.**

The world for regulators at the California Energy Commission (CEC) changed dramatically on March 31, with the opening of the state's new, competitive retail market for electricity. With my colleagues at the CEC, we are working hard to reinvent ourselves, to understand the new market for electricity in the not too distant future, and how to keep up with the issues that this new market will generate.

Part of our mission as public servants is to make sure that the geothermal industry's journey into a competitive future is easier and more productive, while giving back more to the public with the least amount of regulation possible. As we reinvent the regulatory framework for electricity markets, we hope you will see positive results during the four-year transition period to full electric competition, with less regulatory burdens and greater productive output as your bottom lines increase.

The CEC was created in 1975, with five commissioners responsible for programs involving energy efficiency standards, conservation, and to a limited extent, resource planning. With retail electric competition, the agency's entire regulatory role has changed as we help usher in California's new, competitive market for electric power.

We still perform energy efficiency research and broader-scale research, development and demonstration (RD&D) projects, and now preside over a large fund of money meant to help California's renewable energy industries meet the challenge of the new electric market. In addition, we oversee the siting of new power plants. An impressive—and relatively sudden—number of proposed power plants are now before us for consideration. It is all gas-fired, but we believe that new renewable energy facility applications will come our way in the future.

In September 1996, Gov. Pete Wilson signed Assembly Bill (AB) 1890. California's electric utility restructuring law is driving the evolution of the electricity market, and influencing the structure and mission of regulatory bodies like the CEC. Development and passage of AB 1890 came about for some pretty logical reasons. First, with Federal Energy Regulatory Commission (FERC) Order 888 in the spring of 1996, restrictions on fair and open access to the electric transmission system were lifted, creating a need to develop a viable retail electricity market. Second, California has relatively high rates for electricity, which sparked efforts by business and industry in the state to seek relief through the legislative process. Third, the state's investor-owned utilities were saddled with assets and contracts for alternative power that rendered those companies less competitive.

AB 1890 turned the regulatory world on its top. The CEC has a responsibility to promote the public interest by helping electricity generators successfully meet market challenges during the state's four-

year transition to competition. We're working to implement AB 1890's renewable energy provisions and to distribute transition funding provided by the law as equitably as possible.

Several programs imposed on investor-owned utilities over the years by a regulatory compact to promote renewable energy represent stranded benefits which otherwise might have been lost if not for AB 1890. The law has moved some of those programs out of the regulatory arena, including low-income assistance and energy efficiency programs. As we make mid-course corrections to our application of the law, the CEC's Renewable Energy and Public Interest Energy Research (PIER) programs are off to a successful start in ensuring that California's investment in the public and environmental benefits of renewable energy will not be lost.

Geothermal is California's largest developed renewable power resource, and is a baseload electricity provider. A competitive retail electric market challenges all facets of the geothermal industry, especially new resource development sites and financing. But we believe opportunities exist that will transform geothermal into an even more significant and successful player in future electricity markets and CEC programs. Geothermal and the other renewable power industries provided the basis for public understanding of the intangible benefits they offer to the environment and society. Hopefully, when we start to peg the value of these benefits, public preference for energy alternatives like geothermal will rise.

AB 1890 provides $540 million to the CEC's Renewable Energy Program to help California develop a self-sustaining, consumer-driven market for renewables, and help renewable energy suppliers become cost effective and successfully market their products. Our goal is to encourage development of new, market-based facilities; and maintain California's portfolio of renewable electric generation options. As head of the Renewable Energy Program, my objective is a zero balance at the end of our four-year transition period to full market competition. Hopefully with our help, survivors of the transition will be healthy, competitive, and confident in the future.

Of the $540 million provided for renewables by AB 1890, $243 million (45% of the total) is allocated to assist existing resources, with $135 million for biomass and solar, $72.2 million for wind, and $37.8 million for a variety of technologies that include geothermal. This funding was allocated in tiers during a contentious set of hearings, with the highest tier viewed as the least competitive today. As a compliment to your industry, geothermal was deemed the healthiest, most competitive and least in need of public assistance. If electricity prices fall significantly in the future, however, our guidelines include a price cap vs. market price formula that provides an opportunity for geothermal to find necessary funding.

The Renewable Energy Program also provides $54 million (10% of the total) for emerging technologies. It's uncertain whether this account will apply to geothermal, but we have $162 million (30% of the total) for new technologies that does. Finally, we have $81 million for customer assistance (15% of the total). We believe that a fair amount of these dollars will come back to geothermal in the form of customer preference, where ratepayers will receive credits toward their electricity bills if they designate a green power producers.

Fixed price, qualifying facility (QF) contracts for renewable energy are creating some problems for our programs. That's because a lot of the renewable energy we would like to make available for

customer choice is tied up in those contracts. It's uncertain what the future of QF contracts will be, but they shouldn't continue in their present form. The renewables industry ought to become more competitive; the declining commitments in our renewables assistance program reflect that policy.

Our renewables programs are designed to be transitional, with the assumption that they will die after four years. That's important, because the environmental community has asked if the legislature will support reinvigoration of the renewables program at the end of the transition period (March 2002). I have no knowledge of any such legislation that is planned, and none of the CEC's transitional programs are designed to stretch beyond that date.

The CEC also administers the PIER Program, which promotes energy research not adequately addressed by competitive markets or regulated entities. Utility spending in support of public interest RD&D declined 60 percent from 1991 to 1995. The steepest declines were in environmental protection, development of advanced generation technologies, and improvements in system reliability. In the corporate world, work toward providing collective goods is suffering at the hands of the bottom line. Government is no different as we emulate private industry.

With the PIER Program we're reversing that trend by focusing on areas that need public support. Our objectives include development of a robust portfolio of public interest RD&D projects covering short-, mid-, and long-term objectives. We're also firming up the connection between research and the intangible benefits of renewable energy. The PIER Program, which traditionally would have looked only at hardware, has this broader perspective and will support projects that may not have been traditionally funded.

The PIER Program provides $62.5 million annually for RD&D projects that include geothermal technologies. Our 1997/98 budget includes $25.8 million for partial-year funding. In February, the first partial solicitation went out, and to my knowledge, it was very successful. It offered about $15 million for public interest RD&D projects including renewable generation, environmentally preferred advanced generation, and environmental research. A second quarter general solicitation has been released for end-use energy efficiency and strategic energy research, and we intend to follow that with a small grants solicitation.

During its approximately 17-year history, the CEC's grant and loan program has awarded funds to over 150 geothermal projects spanning the length of the state, that produce about 141 billion Btus of geothermal energy annually. That's not trivial, but we are also aware of the limitations that can come with geothermal energy development, such as depleted steamfields. That is why the CEC is committed to supporting the Santa Rosa Wastewater Project to The Geysers, a plan that can achieve the long-terms goals of helping a municipality dispose of its wastewater in an environmentally safe manner while helping preserve the stability of an important geothermal reservoir to the state.

The CEC will hold additional workshops this summer to solicit ideas on how to revise the PIER Program for subsequent years, and we hope the geothermal industry will participate. You should, because the needs of the geothermal community have changed since the program was first initiated, and the program is generally under-subscribed by geothermal projects. We can turn that around with enough pressure from the industry.

We need your help in defining and developing an effective, long-term program that helps us wisely use restructuring transition funds provided by AB 1890. The geothermal and other renewables industries have to read our turgid and lengthy documents, beat on our door, and tell us what you like and what you don't like about CEC programs. You've got to participate in the process. But don't complain if you don't have an alternative. Only with a product can we make progress.

The world is changing at a rapidly escalating rate. With that in mind, there are a number of areas where the CEC and the geothermal industry can work together. First, we can restructure the financing and attractiveness of the geothermal industry, as the state proves your importance though policies and funding. Second, we can capitalize on geothermal's position as a baseload electricity provider, expand the base you already have, and encourage new exploration and construction. Third, we encourage geothermal energy providers to participate as a vital and strong contributor in the CEC's RD&D program

We also want to create a renewables knowledge base to educate the public and decision makers. We can create all the hardware and establish all of the economic statistics and trends we want, but if we can't translate them convincingly to those who must make local or regional land-use decisions, we have failed in our mission of protecting your investments and the environment. Distribution of geothermal knowledge—and our ability to translate that knowledge to top decision makers—is paramount.

Finally, I hope the geothermal industry will work to better educate both state and local governments about the interconnectivity of geothermal energy development and land-use planning. How tough will it be in the future to build new geothermal facilities and transmission lines if you don't stake out that territory today? Together, we must work with local governments to ensure that developed geothermal fields continue producing electricity, and that new geothermal resources can be developed to meet future needs.

I applaud the geothermal industry's contributions to the energy supply and the natural environment of California. The challenges we face today are real. I urge you to leverage your comparative advantage to become stronger in the new market for electricity. Our work isn't over, and I trust that you will work with the CEC to create an even brighter and more successful future.

Michal C. Moore was appointed to the California Energy Commission by Gov. Pete Wilson in October 1995. By law, four of the CEC's five commissioners must be professionals in engineering or physical science, environmental protection, economics, and law. Moore fills the economist position. He serves as Presiding Member of the AB 1890 Renewables Implementation Committee, the Ad Hoc Committee on Information and the 1998 Electricity Report Committee. He serves as associate member of the 1996 Energy Plan Committee, the Efficiency Standards Committee and the Fuels Report & Planning Committee. Prior to accepting his current position with the CEC, Moore was a consulting economist. He has served on the State Board of Landscape Architects, was chief economist for Landmark Land Co., and deputy director for local government at the Governor's Office of Planning & Research. He was elected supervisor of Monterey County from 1976 to 1985, and has served on the Seismic Safety Commission. Moore earned a B.S. in geology and natural resources from Humboldt State University, a master's in land economics from the Ecology Institute at the University of California Davis. He is a candidate for a Ph.D. in land economics at Cambridge University, England.

The Biggest Bang for the Buck

R&D Focus on Reduced Drilling Costs, Improved Drilling Success and Injection Will Ensure the Future of Geothermal Development

***Note*: The following article has been reprinted from the April/May 1998 issue of the GRC Bulletin. It was edited from an Industry Keynote Presentation by Randolph L. Howard,Group Vice President, International Operations/Geothermal, Unocal Corp. (Brea, CA), at the 16th U.S. Department of Energy Geothermal Program Review on April 1, 1998, in Berkeley, CA.**

The U.S. Department of Energy (DOE) is a partner with industry in developing geothermal resources. The bottom line is that finding and developing economic geothermal energy reserves is not an easy task. Taking on that task depends on results-oriented research and development (R&D) projects that will help the geothermal industry move forward.

Installed geothermal generation capacity worldwide is almost 8,000 megawatts (MW), and promises to increase by as much as tenfold. Reservoir capacity around the world is not the issue. We have plenty of resources identified. The real issues are more fundamental.

Basically, the geothermal industry seeks development projects in regions where we have an adequate market, we have customers, we have a marketplace that can sustain new electric generation development, we have appropriate government laws and regulations, and where we can competitively accomplish our goals to develop sustainable energy resources at a profit.

DOE's annual geothermal R&D budget was $150 million several years ago, but today it is only $30 million. It's time for some tough decisions. We must prioritize areas of research and select projects that can generate new ideas to lower our cost of development. That's the reality today. Clearly, our focus must be directed toward spending that $30 million and additional R&D grants from other sources like the California Energy Commission (CEC) on geothermal projects that yield the most cost reduction in the shortest possible time.

We cannot afford to dilute our limited funding by working on "interesting" technologies. Geothermal development is on the brink of moving forward, but if we can't cut costs and become more competitive, it won't happen. All research projects should be reviewed and ranked on the basis of benefit vs. cost. It's a matter of first things first, and getting the biggest bang for the buck.

Let me suggest areas where this goal might be accomplished. **The most impact from geothermal R&D can be gained by reducing drilling costs, increasing drilling success by better targeting fractures, and learning how to benefit from injection.**

One of the biggest development costs for geothermal projects is drilling. Unocal invited DOE scientists from Sandia National Laboratories to visit our rigs, discuss real-life problems and brainstorm solutions with Unocal engineers. This effort was very successful in helping us to drill

smarter, and we believe there is more that the geothermal industry can do with DOE to improve drilling success and achieve lower costs.

Learning how to develop geothermal resources with half as many wells would have a tremendous impact on our cost structure. One of the best ways to lower drilling costs is to better target fractures. In Unocal's research partnership with DOE, continuous cores from three of the largest geothermal reservoirs are providing a tremendous opportunity to better understand fractures and stimulation deep underground. We're also excited about DOE research programs to improve fracture mapping.

Geothermal operations rely on two different subsurface systems—production and injection. Managing injection systems affects not only the life of geothermal resources, but their productivity. Though we are learning a lot from the Lake County Geysers Pipeline & Injection Project in Northern California, there is still much we don't know about injection. To help ensure a positive impact on steam capacity, we must continue to develop technologies that increase our understanding of how injected fluids move within a steam reservoir.

Forward-looking technological developments like hot dry rock are too far from being commercial to justify investment in demonstration projects. DOE should focus first on making conventional geothermal development more cost effective. Systems technologies we need today for developing high-enthalpy geothermal resources are precursors of technologies that will be needed for successful hot dry rock ventures in the future.

Drilling research focused on cost reduction will benefit future hot dry rock projects, as will sophisticated fracture mapping techniques and new high-temperature logging tools. Further development of mechanical and chemical stimulation technologies are also necessary to create sustained, fractured reservoirs. In addition, hot dry rock projects will need tracers and tracer modeling software to determine flow path and heat transfer characteristics of fractured reservoirs.

DOE should focus on these technologies to ensure the viability of the geothermal industry today, while securing a future for hot dry rock projects. I'm not saying that hot dry rock should not be pursued as a future energy source, or that projects aimed at that end shouldn't be identified and put on the map. But let's work on the most important things first.

We have only limited dollars to spend on R&D efforts. After the cost of drilling is refined, fracture mapping is improved, and high-temperature tools, tracers and reservoir stimulation technologies are developed and tested, hot dry rock may become a viable energy resource.

Geothermal energy is the most economical of all renewables. With geothermal development, we don't have to pray for wind, rain or sunshine. And with the highest electric generation capacity factors compared to other forms of renewable energy, geothermal is closest to meeting competition from fossil fuels.

Our biggest competitor right now—especially overseas—is coal. Unocal and other geothermal development companies have worked hard to reduce costs so we can better compete with fossil fuels, but it's a moving target. Our fossil-fuel competitors keep lowering their costs, and we need to do the

same. We believe that helping geothermal development meet that competition should be a high priority by DOE.

Some say that geothermal is a proven technology, that it needs no further R&D. I would argue that geothermal has a proven return on the research dollar, and further investment—with a focus on development costs—will increase that return. Research to date has helped geothermal become viable and reliable. Now we must work on lowering our costs, so geothermal development can grow in the future.

An exciting opportunity right now is the geothermal industry's wastewater pipeline to The Geysers in Northern California. The Lake County project is up and running, and ongoing studies will determine injection flow and how The Geysers reservoir responds to it. When it becomes a reality, a proposed pipeline from Santa Rosa will continue to test our ingenuity with even higher injection flows into The Geysers that will help guarantee the reservoir's productive life well into the future.

The geothermal industry's partnership with government is a true commercial venture. It's important to remember that the federal government and California both benefit directly from geothermal production. Over $200 million in tax and royalty revenues have flowed into the federal, state and local coffers from geothermal projects. In addition, there are the external values of geothermal energy to society, including clean air, fuel diversity, small environmental footprints, and incremental development costs. We must develop techniques to better quantify and publicize these external benefits.

The CEC recently signed a memorandum of understanding with DOE on R&D cooperation. Working with the industry, these agencies can now focus their efforts toward making geothermal R&D more cost effective and results oriented with programs and projects that will promote near-term industry growth and lead the way to future technologies.

DOE efforts to facilitate international geothermal market development with government-to-government collaboration is appreciated, so long as those programs do not interfere with private business. Continued, open communication between the geothermal industry and DOE is an essential ingredient in that relationship. The Geothermal Energy Association is a critical focal point of our communication with DOE, and I am pleased with their efforts.

Another area of concern for the geothermal industry is more subtle—the U.S. role in geothermal science. We are the international leader in this area, and we must cultivate and preserve our position. DOE should assist us in our efforts to attract young scientists to geothermal research. As key research people retire or move on to other endeavors, I urge DOE to take the same approach that the industry has taken in succession planning. We need initiatives to attract new blood into geothermal technology development, so we can maintain our technical leadership for the long-term.

In summary, the focus of geothermal R&D should be on projects that provide the most effective cost-reduction potential. We also believe that cooperative projects with DOE's national labs are important. And industry/government workshops are helpful in improving our focus on combined efforts, providing technology transfer from successful R&D projects, and ensuring that DOE and the CEC better understand the needs of the geothermal industry.

Borrowing from recent testimony in the U.S. House of Representatives by DOE Assistant Secretary for Energy Efficiency & Renewable Energy Dan Reicher, "We need to extend the life of our reserves, reduce our foreign oil dependence, minimize health risks of greenhouse gases, make our industries more competitive. These are the cheapest and least intrusive investments we can make." Geothermal R&D offers the greatest payoff for these objectives, and this is no time to abandon our technological leadership in the worldwide geothermal community.

Randolph L. Howard joined Unocal in 1973 after graduating with a B.S. in Chemical Engineering from the University of California (Berkeley). Prior to his current position of Group Vice President, International Operations/Geothermal, he held positions with Unocal as Vice President-Refining; Vice President-Supply, Transportation & Planning; General Manager-Los Angeles Refinery; General Manager of Product Supply & Refinery Sales; and Manager of Strategic Planning, Refining & Marketing Division. In addition, Howard has performed a variety of engineering, operations and planning assignments at Unocal's San Francisco, Los Angeles and Chicago Refineries.

Where Do We Go From Here?

ORMAT's Dan Schochet Urges Stakeholders in the Geothermal Industry to Develop a Near-Term Tactical Plan for U.S. Development

***Note*: The following article has been reprinted from the April/May 1998 issue of the GRC Bulletin. It was edited from an Industry Keynote Presentation delivered by ORMAT International, Inc. Vice President Daniel N. Schochet at the 16th U.S. Department of Energy Geothermal Program Review on April 1, 1998, in Berkeley, CA.**

Any definition of the U.S. geothermal industry includes all of us—developers, operators, suppliers, consultants, the U. S. Department of Energy (DOE), the California Energy Commission (CEC), the national labs, our associations and academia. It's quite a large group, and it represents a huge pool of geothermal technology that's been developed over the years.

With worldwide geothermal development slowing down, the survival of our industry is at stake. The world is changing, and unless we change with it, I'm afraid that we might go the way of the buggy whip and the typewriter industry. DOE has a long-term strategic plan, but what are our short-term issues?

We need a tactical plan. Stakeholders in the geothermal industry need to focus on such a plan, and we must coordinate our efforts. Most importantly, we must recognize that industry competitors are not our adversaries. The beast we have to control is market forces.

What should be our vision? There's no question that the industry needs new projects to survive. And our survival must be pegged to the U.S. geothermal market. The U.S. market must be revived. Ours is the marketplace with no political or currency risks, with credit-worthy power purchasers, with a stable economy and predictable growth. The United States is the easiest place in the world to build power plants, and the easiest place to operate them. Considering the problems facing geothermal developers in other regions of the world, there is no doubt about these facts.

In the past, risks that inhibited investment in U.S. geothermal project development were exploration and drilling, but now it is market forces. Competition from natural gas-fired power plants has hurt us, and utility industry deregulation has changed the outlook for power marketing.

The U.S. geothermal market has been flat since the early 1990s. There are no new long-term power purchase agreements, no new projects, and very little new exploration. More problematic, there is almost no recognition of geothermal benefits among U.S. regulators, legislators and consumers. Our industry is shrinking. There are fewer geothermal developers and suppliers. Many of our old friends in consulting and services are no longer with the industry, and the U.S. membership of the Geothermal Resources Council is on the decline.

Regrettably, we also have an unwarranted negative image. In many cases, when we speak of geothermal, we are told that we are expensive or experimental, that projects are not sustainable, that

geothermal development poses environmental problems. We've also been hurt by "greener grass" opportunities. Over the past few years, as our domestic market waned, our industry—including my company—understandably looked at overseas projects and other technologies. Now, in order to survive, we must again turn our eyes to reviving the U.S. geothermal market.

What must we do? The geothermal industry needs more exploration and identification of new resources that can be developed, and we must lower development costs if we are to provide competitively priced electrical power. We need to improve exploration techniques. We must improve geological understanding, mapping and assessment as we decrease well-drilling costs and improve well-siting technology. And we need to again implement cost sharing with DOE and the CEC for new resource exploration.

New power sales arrangements must be developed as we seek innovative project financing alternatives. What will these tools look like in the future? The industry's future is market-based power, with electrical power portfolio requirements that should and will include geothermal as reliable baseload power. Because we will be selling power at market-based prices, financable projects must be redefined. The geothermal industry will to have to provide bankable reports on market growth for renewable power as a basis for project financing, as opposed to the previous standard power sales arrangements that will no longer be available in a competitive marketplace.

One of the goals of DOE's strategic plan is removing market inequities. This must be done by recognizing that geothermal power is not based on combustion. It is sustainable and renewable, with a baseload capacity factor of 95 percent or greater. Geothermal resources supply many times the kilowatt-hours of energy supplied by all other renewables in the United States. And geothermal power developers can build plants with near-zero emissions of greenhouse gases.

The geothermal industry needs recognition and evaluation of geothermal benefits as we focus on projects that are reliable and sustainable. We absolutely need federal support for the external, or intangible, benefits of geothermal power. They must be quantified in value. I believe that tax credits are the logical way to go. These would not be subsidies, but recognition by government that the external benefits of geothermal energy represent avoided costs of societal damages. Determining the value of geothermal development should be a high priority, as well as passing on to the public the costs for those benefits. There is no reason why the avoidance of societal damages offered by geothermal power should not have the same credit value ascribed to wind and solar power, which is 1.5-cents per kilowatt-hour (kWh).

In summary, geothermal power market stakeholders must develop new methods to abate development and credit risks. Though the industry has the risks of above-ground, power plant development largely under control, minimization of exploration and drilling risks will require DOE and CEC assistance.

The geothermal industry also needs innovative financing. All project financing in the past has been based on long-term, front-loaded power purchase agreements, but those arrangements are "Gone With The Wind." Geothermal power purchases now and in the future will be dictated by the market. Our price need not be totally competitive with natural gas-fired power, but it should and can be the most competitive within the renewables market.

Developers must prove the long-term viability of geothermal operations. They must erase the image that geothermal projects are not sustainable. In fact they are sustainable, and there has not been a single case of a geothermal power plant closure due to a lack of geothermal fuel.

Cost-effective geothermal power should be based on the cost of generation minus an externality tax credit. Again, geothermal power need not be the lowest cost alternative—we don't have to beat the cost of natural gas-fired electricity. But we can be the lowest cost renewable power alternative. The industry should target a power generation cost in the five-cent per kWh range. With a credit of 1.5 cents, we can market power for about 3.5 cents per kWh. This would put geothermal in a competitive position with natural gas as well.

To meet the future, the geothermal industry needs a coordinated and aggressive outreach program. Too often, when government agencies and other organizations summarize the benefits of renewable power, geothermal is left out of the discussion, even though the sum of wind, solar and biomass is less than the total output of geothermal developments around the country.

Stakeholders must target increasing geothermal's share of renewable energy portfolios. We need to identify new geothermal resources. We should identify an additional 2,500 megawatts of geothermal power that can be developed over the next five years, to effectively double the amount of electrical power we have on-line in the United States today. We need to improve and lower the cost of geothermal drilling and exploration methods. We need to establish power market parameters that are bankable, and we must work to develop new financing models.

The geothermal industry should create a committee with representation by all stakeholders to develop the issues I've outlined into a tactical plan that can be implemented with available human and financial resources as early as the 1998 GRC Annual Meeting in September. Our target should be 500 MW of new geothermal power in the pipeline for development by 2001-2002 . This would be the beginning of a U.S. geothermal market revival, which, when coupled with DOE's strategic plan, would ensure a healthy and viable industry well into the future.

Daniel N. Schochet joined ORMAT International, Inc. as an overseas consultant in 1975, and served as marketing director from 1979 through 1984, with responsibility for international marketing and sales. Since then, he has been involved in power project and business development. He serves on the Geothermal Resources Council Board of Directors, and has advised the U.S. Department of Energy Office of Geothermal Technologies on its strategic plan for research and development. Prior to joining ORMAT, Schochet held a number of technical and management positions in the fields of power systems, aerospace, biomedical, aircraft and pipeline engineering. He earned a bachelors degree in electrical engineering from Cooper Union School of Engineering, and a masters degree in electrical engineering from Columbia University.

Planning: Creating the Path to Success

Allan Jelacic, Director
Office of Geothermal Technologies
U.S. Department of Energy

Presentation notes included in Appendix A

Concurrent Session 2:

Exploration Technology

The Promise of Electrical Geophysics in Developing Geothermal Resources

Alan C. Tripp, University of Utah

SUMMARY

The rising tide of computational resources has lifted electrical geophysics to a level in which truly three-dimensional conductivity images can be produced. The challenge for the next decade is to learn how to use electrical data cooperatively with other data types to increase resolution and decrease ambiguity. This paper illustrates some concepts useful in cooperative interpretation using two examples. In the first, adaptive focussing is used to increase the resolution of inductive logging. In the second, an invariaint physical property is detemined for an SP survey over a forced convection geothermal system.

INTRODUCTION

For more than one hundred years, geoscientists have recognized that electrical conductivity is a fundamental physical property of geological materials - a physical property whose variations can be related to variations in the geological materials. Such dependency has been used with spectacular success, in many cases, to advance economic and speculative investigations. the very success of electrical methods, combined with increasingly stringent needs to discover and manage a broad range of earth resources, has motivated startling advances in electrical probing over the past decade. It is the author's thesis that the stage is now prepared for a paradigm shift in research - a shift which will consolidate the advances of the past decade in an information theoretic context - leading to interpretational possibilities startlingly unlike any realized to date.

The past decade might be characterized as one in which the increasing power and availability of computer facilities has made computational electromagnetics a mature science. By this I mean that the canons of the field are being quickly established and revolutionary themes are increasingly unlikely. Brilliant analysis in pursuit of a particular result is increasingly yielding to massive computation using generally applicable schemes.

What are the milestones of this evolution? In the decade, three-dimensional modeling has moved from an esoteric art - practiced by computing the response of simplistic electrical conductivity models in a cut-and-try random search for a model which would match some particular data set, to automated inversion of data sets to conductivity models with tens or hundreds of thousands of model variables. And all graphically presented in living color! Much of this evolution was funded by the DOE - the history of the funding and the progress facilitated thereby would make interesting reading!

So with the ability to invert EM data to thousands - soon to be millions - of parameters, have we arrived in the promised land where research can stop and we can begin to invert the world ? No - the null-space stands in the way of such a situation. Actually one might imagine two "null -spaces" for the EM interpretation problem. First there is the space of conductivity features which have no expression in a particular EM data set; there is also the "null-space" of earth features which have negligible conductivity expression.

Thus any "EM image", no matter how colorful and attractive it may be, is deceptive if the viewer embraces it without a critical appreciation of its limitations. Nor does EM face this inditement alone - human science is by its nature inexact and ANY method, used by itself, will only give half-truths. The key to improvement, of course, is to characterize the relevant null-spaces carefully and then to use the information which is available **cooperatively** with other data sets to resolve the problem at hand. This effort constitutes the challenge for future applications of electrical geophysics in developing geothermal resources.

Much could be written characterizing this program - and indeed its true character will evolve. However, a short description of two projects currently being pursued at the University of Utah might serve to illuminate some of the features which I believe will characterize work in reservoir directed EM research in the next decade.

The first example, which involves developing triaxial induction measurements in anisotropic materials, illustrates how conductivity estimation can be improved by shaping source fields from a knowledge of the borehole environment. The second example involves determining flow invariants determined from surface SP data.

TRIAXIAL MEASUREMENTS AND ADAPTIVE FOCUSSING

Long-offset borehole, cross-borehole, and surface-to-borehole EM induction probing have been suggested as means of delineating and monitoring geothermal reservoirs. Certainly many of the physical processes encountered in a geothermal reservoir have an electrical expression. One major problem encountering EM probing in such an environment is that the environment can be very heterogeneous, which can manifest itself in macroscopic anisotropy. Now traditional EM data collection and interpretation has assumed model isotropy - for the very good reason that interpreting data over an isotropic earth was challenging enough given the technology in place. However, given the recent advances in interpretation theory, it is now possible to conduct feasiblity studies examining the effects which anisotropic materials might have on conventional measurements and to design new modalities to adequately resolve anisotropic structures.

The approach which we will discuss here involves optimization of borehole triaxial magnetic dipoles. In this approach, the strengths and/or phases of the sources are all linked in such a way as to optimize perturbations about an a-priori model. The waveforms of the sources may also be optimized. More background for the theory and practise of this approach is found in a series of papers by Cherkaeva and Tripp (1996a,b; 1997; 1998) .

Consider the electrical structure of a geothermal reseervoir. Broad isotropic zones of alteration are adjacent to very narrow features such as fractures. Contrasts between resistivities of adjacent zones can be extreme. Moreover, many of the features of interest to the reservoir engineer, such as fracture zones, can be electrically subtle and are certainly not macroscopically isotropic. From the point of view of borehole methods, the problem is exacerbated if boreholes are deviated.

For the present discussion, let's concentrate on a particularly simple case of electrical anisotropy.

Consider a borehole penetrating a series of beds, consisting of alternating fractured zones and competent zones. Then the fracture zones and competent zones will have different resistivities, but if the the sequence is viewed macroscopically, then the bed sequence will be anisotropic. The resistivities of the sequcnce transverse and perpendicular to the sequence are described by the equations

$$\rho_T = H_{\mu 1}\,\rho_{\mu 1} + H_{\mu 2}\,\rho_{\mu 2} \qquad (1)$$

and

$$\rho_L = [\, H_{\mu 1}/\rho_{\mu 1} + H_{\mu 2}/\rho_{\mu 2}\,]^{-1}, \qquad (2)$$

where ρ_T is the transverse or vertical resistivity and ρ_L is the longitudinal or horizontal resistivity. The terms vertical and horizontal in this context assume a vertical borehole and horizontally layered strata. $H_{\mu 1}$ and $H_{\mu 2}$ are the volume fractions of the materials $\mu 1$ and $\mu 2$, such that $H_{\mu 1} + H_{\mu 2} = 1$, while $\rho_{\mu 1}$ and $\rho_{\mu 2}$ are the intrinsic resistivities of the component materials.

Symmetry suggests that when source dipoles are aligned along the borehole, the received magnetic field contains no information concerning the vertical conductivity, assuming that the borehole is perpendicular to the bedding planes. Examination of the analytic expressions or the operant equations for the numerical modeling algorithms shows that a source perpendicular to bedding does indeed decouple from the conductivity perpendicular to bedding. An estimate of the additional information added by multi-source measurements can be accomplished by a sensitivity analysis, such as that offered by Kriegshäuser and Tripp (1997). Such an analysis could be based on analytic expressions or on numerically computed expressions.

There is a limited literature concerning the possibilities of triaxial induction logging in resolving anisotropic conductivities. These works include Moran and Gianzero (1979), Howard (1981), Nekut (1994), and deCarvalho and Verma (1994). All of these works conclude that resolution of an anisotropy tensor using triaxial measurements is possible, but would be difficult in practise due to borehole effects. Subtracting a borehole response calculated numerically might be a possibility, but a better option seems to be to tailor the source waveforms to minimize the borehole effects.

Let $H_\gamma(f)$ be the measured log response for a source distribution f and a background earth conductivity distribution γ over the domain Ω. Suppose that we wish to resolve a perturbation σ on the background conductivity distribution. Then the goal of source optimization is to find the $f \in L_2(\partial\Omega)$, $\| f \| = 1$, which maximizes the functional $\| H_{\gamma+\sigma}(f) - H_\gamma(f) \|$.

Now the optimization can be with respect to the waveform of a particular source - as in the case of Kriegshauser and Tripp (1997) and Cherkaeva and Tripp (1997), or with respect to the relative amplitude weighting of an array of sources, as in the case of Cherkaeva and Tripp (1996a,b; 1998). In any case, knowledge of the borehole can be used to focus current in the perturbation σ.

At present, the theory has been developed only for an isotropic earth and a uniaxial measurement, but generalizing the technique to a triaxial measurement should be immediate. The array weights are also developed supposing that all transmitters of the array are in-phase, but phased array weights would be better in maximizing resolution of the conductivity of the formation.

In the DC case, adaptive focussing provides the basis of an effective inversion technique. A similar technique should be possible for EM fields.

In conclusion, adaptive focussing techniques can be a means of minimizing the effects of structures, such as boreholes, which are known at the time of the survey. This is of particular note in high resolution triaxial logging. They are also useful for cooperative data interpretation with other logs.

SP SOURCE CHARACTERIZATION

The spontaneous potential (SP) method measures the electrical manifestation of other primary flows, such as heat flow or fluid flow. As such, it has been often used successfully as a method of detecting geothermal systems (Zohdy et al., 1973; Corwin and Hoover, 1979; Ross et al., 1990). However, since the SP method is sensitive to so many different phenomena modeling the data with a determinate physical model can be daunting.

Difficulties can occur in several forms. There can be uncertainties in the values of the cross-coupling coefficients linking the primary flows and the subsequent electric manifestation. A critical compilation of published coefficients is under preparation (Tripp and Ross, 1998). Interpretational uncertainty can also arise from the difficulty of rigourously calculating electrical potentials arising from multi-dimensional flows. Under DOE sponsorship, Sill (1983) developed a technique for numerically modeling SP and demonstrated it for a two dimensional earth. This method has recently been extended to three-dimensions (Tripp et al., 1998).

Thus at present, there are effective means of calculating the multidimensional electrical response of primary flows in a model of given physical properties. A more difficult problem, which is directly involved in the use of SP for monitoring and delineating geothermal resources, is to deduce physical properties from the measured electrical field. This is the inverse problem.

In forward modeling, we use primary flow patterns and cross-coupling coefficients to calculate equivalent sources, which can then be used to calculate electric potentials at any point in the model earth. This process is well-posed in that any flow and cross-coupling model has a unique electrical response. It is well-conditioned in that a small amount of noise in the flow and cross-coupling parameters is not amplified in the electrical response.

In the inverse problem, this sequence of steps is reversed. First, measured electric potentials are used to determine equivalent electric sources. These sources are then used to determine the flow parameters.

The first stage of this process is equivalent to solving the integral equation (Hohmann, 1987),

$$\Phi(\mathbf{r}) = \int S(\mathbf{r}') G_0(\mathbf{r}, \mathbf{r}')\, dv', \qquad (3)$$

for the electric source distribution $S(\mathbf{r}')$. In this equation, $\Phi(\mathbf{r})$ is the distribution of measured electric potentials at the observation sites $\mathbf{r}$, $G_0(\mathbf{r}, \mathbf{r}')$ is the Green's function for the background earth, and the integration is over the support for the source distribution. The source distribution $S(\mathbf{r}')$ also has the representation $S(\mathbf{r}') = \nabla'\sigma(\mathbf{r}') \cdot \nabla' \Phi(\mathbf{r}') / \sigma(\mathbf{r}')$ where $\sigma(\mathbf{r}')$ is the conductivity distribution.

The second step of the process is to use the distribution $S(\mathbf{r}')$ in the equation

$$\nabla.(L_{e,h}\,\nabla\zeta_{Heat} + L_{e,m}\,\nabla\zeta_{Mass}) = \nabla'\sigma(r').\ \nabla'\Phi(r')/\sigma(r'), \quad (4)$$

in the case of a flow arising from a gradient or the equation

$$\nabla.(L_{e,m}\,V/k) = \nabla'\sigma(r').\ \nabla'\Phi(r')/\sigma(r'), \quad (5)$$

for a non-conservative flow (Sill,1982,1983).

Following this solution stream in the case of real field data is a non-trivial task. The source identification problem is equivalent to solving a Fredholm Integral Equation of the First Kind, and as such is an archetypal ill-posed and ill-conditioned problem (Tripp et al., 1998). This type of problem has been encountered in many fields, including cardiology, antenna analysis and design, and signal processing. The classic "fix" for the ill-posedness and ill-conditioning is to impose some a-priori information in the form of a "regularization condition". In our application, the a-priori information must be geological.

One fairly simple geological assumption would be that the source of the anomaly possesses a particular geometry. For example, suppose that an anomaly occurs from forced convection up an intersection of two faults, as is the case at Newcastle (Ross et al., 1990; Tripp et al., 1998). Then in this case the electrical response is uni-axial and the source is the flow along the intersection. This model can be represented as

$$\phi(r) = -\int (\rho(z)\,\mu(z)C_o(z)Q(z))/2\pi k(z)\,\|(r,z)\|_2\,dz, \quad (6)$$

which is the response of a line source of varying physical properties. In this equation, $\rho(z)$ is the resistivity profile, $\mu(z)$ is the viscosity, $C_o(z)$ is the cross-coupling coefficient, $Q(z)$ is the flow, and $k(z)$ is the permeability. Thus, a radially symmetric SP response can support only a line source interpretation, and the data only gives an estimate of the line integral of the source term $S(z) = (\rho(z)\,\mu(z)C_o(z)Q(z))/2\pi k(z)$. Estimation of the source term is an ill - posed and ill-conditioned problem and requires additional geological information for its complete solution. Even given an estimate of S(z), deconvolution of the source into physical parameters requires a great deal of a-priori information to begin. An elaborate flow parameter interpretation of this SP data set, by itself, clearly would be mis-leading.

Although these conclusions might be viewed as disparaging the use of SP, they actually support its use by defining its role. Some salient points are:

1) Evaluating an integral is not a bad application. It is, after all, an invariant which is proportional to flow magnitude and as such might be viewed as an ideal surface indicator of a flow source.

2) Subsequent flow inverse modeling might well use the SP defined invariant as a constraint on the interpretation.

3) The ill-posed and ill-conditioned nature of the SP inverse problem is a consequence of the fact that there are many different source mechanisms for SP and hence many different applications. However, an application must be carefully defined and constrained so that the exact nature of the information to be derived from the SP is understood.

CONCLUSIONS

It is now possible to compute three-dimensional models which "fit" electrical data. The edifying task for the next decade is to more fully assess the information content of such "images" and to find effective means of cooperatively gathering and interpreting complementary data sets.

ACKNOWLEDGEMENTS

This work was supported by the DOE under grant DE-FG03-93ER14313 and under contract no. DE-AC07-95ID13274. Such support does not constitute an endorsement by the Department of Energy of the views expressed in this publication. The contributions of E. Cherkaeva, H.P Ross, and P.M. Wright to this work are gratefully acknowledged.

REFERENCES

Cherkaeva, E. and Tripp, A. C., 1996a, Optimal survey design using focused resistivity arrays: IEEE Trans. on Geoscience and Remote Sensing, 34, no. 2, 358 - 366.

Cherkaeva, E. and Tripp, A. C., 1996b, Inverse conductivity problem for inaccurate measurements: Inverse Problems, 12, 869 - 883.

Cherkaeva, E. and Tripp, A. C., 1997, On optimal design of transient electromagnetic waveforms: presented at the 67th SEG Annual Meeting.

Cherkaeva, E. and Tripp, A.C., 1998, Optimal focussing in inductive logging: Submitted for presentation at the 68th SEG Annual Meeting.

Corwin, R.F. and Hoover, D.B., 1979, The self-potential method in geothermal exploration: Geophysics, v. 44, p. 226-245.

deCarvalho,P.R. and Verma, O.P., 1994, Coplanar coil system in electromagnetic induction well-logging tool: SPWLA 35th Annual Logging Symposium.

Hohmann, G.W., 1987, Numerical modeling for electromagnetic methods in geophysics: *in* Electromagnetic Methods in Applied Geophysics, ed. M.N. Nabighian.

Howard, A.Q., Jr., 1981, Induction logging for vertical structures in the presence of a borehole fluid: Geophysics, v. 46, 68-75.

Kriegshauser, B. and Tripp, A.C., 1997 , Probing strata of anisotropic complex conductivity using surface-to-borehole methods, 1997, accepted for presentation at the 67th Annual SEG Meeting.

Moran, J.H. and Gianzero, S., 1979, Effects of formation anisotropy on resistivity logging measurements: Geophysics, v. 44, 1266-1286.

Nekut, A.G., 1994, Anisotropy induction logging: Geophysics, v. 59, 345-350.

Ross, H.P., Blackett, R.E., Shubat, M.A., and Mackelprang, C.E., 1990, Delineation of fluid upflow and outflow plume with electrical resistivity and self-potential data, Newcastle geothermal area, Utah: Geothermal Resources Council Transactions, v. 14, part II, p. 1531-1536.

Sill, W.R., 1982, Self-potential effects due to hydrothermal convection-velocity cross-coupling: DOE/DGE Report, Contract DE-AC07-80ID12079, Department of Geology and Geophysics, University of Utah.

Sill, W.R., 1983, Self - potential modeling from primary flows: Geophysics, v. 48, p. 76 - 86.

Tripp, A.C., Ross, H.P., and Cherkaeva, E., 1998, Three-Dimensional Modeling of SP Data: Proceedings of the Twenty-Third Workshop on Geothermal Reservoir Engineering, Stanford University, Stanford, California, January 26-28, 1998.

Tripp, A.C. and Ross, H.P., 1998, SP heat and fluid flow cross -coupling coefficients - A compilation: In preparation.

Zohdy, A.A.R., Anderson, L.A., and Muffler, L.J.P, 1973, Resistivity, self - potential, and induced polarization surveys of a vapor - dominated geothermal system: Geophysics, v. 38, p. 1130 - 1144.

GEOTHERMAL CHEMISTRY/EXPLORATION INVESTIGATIONS AT DIXIE VALLEY, NEVADA

Fraser Goff
Los Alamos National Laboratory
505-667-8060

Cathy J. Janik
U.S. Geological Survey
650-329-5213

Deborah Bergfeld and Dale Counce
Los Alamos National Laboratory
505-667-1812

Carol J. Bruton and Gregory Nimz
Lawrence Livermore National Laboratory
510-423-1936

ABSTRACT

Dixie Valley geothermal field has continuously produced electric power since 1988. At the request of Oxbow Geothermal Corp. and the U.S. Department of Energy, we have organized an inter-agency team of investigators to examine several topics of concern regarding management and behavior of the resource. These topics include scaling of the injection system, recharge of the reservoir, geochemical monitoring of the reservoir, and development of increased fumarolic activity north of the power plant.

INTRODUCTION

The Dixie Valley geothermal system is located in west-central Nevada between the Stillwater and Clan Alpine ranges (Fig. 1) and produces electricity from a 62 MWe double-flash power plant that began operations in 1988. Fluids are produced from depths of 2450 to 3050 m at an average temperature of about 250°C. The plant and geothermal wells are owned and operated by Oxbow Geothermal Corp. The geologic setting of the field was most recently described by Lutz et al. (1997).

During FY97 we began an inter-agency collaboration to investigate scaling in injection pipelines and wells. In FY98 we expanded this collaboration to evaluate recharge sources and ages of the geothermal system, to monitor geochemical changes in production fluids, and to investigate time-series changes in CO_2 flux and temperature distribution on the recently discovered "dead zone." The object of this contribution is to summarize the status of these tasks.

SCALE FORMATION

Carbonate scaling in Dixie Valley production wells was described by Benoit (1987). Silica scaling in pipelines and

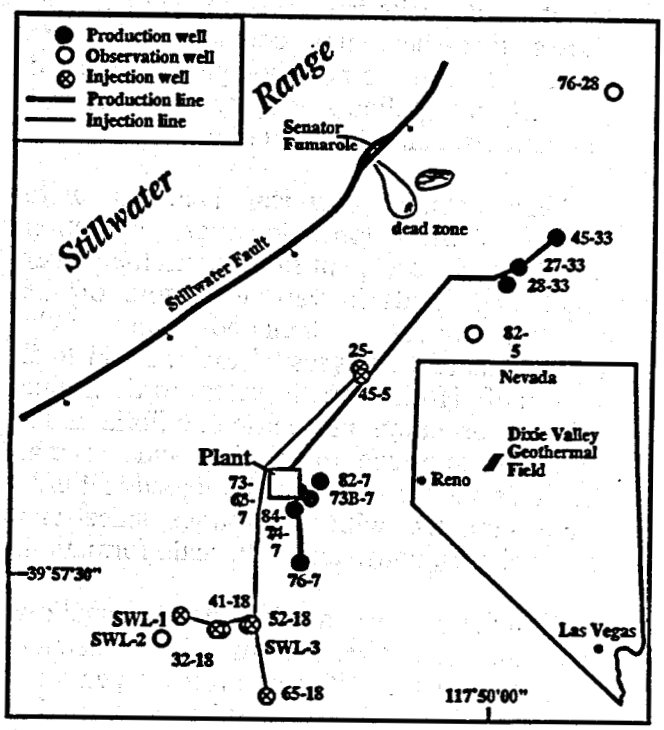

Figure 1. Map showing location of Dixie Valley geothermal system, Nevada.

injector wells downstream of the power plant has been a problem for a number of years. Some initial investigations were previously carried out by Oxbow to determine the nature of the scale. A team from Lawrence Livermore National Laboratory, Los Alamos National Laboratory, and Energy & Geoscience Institute was created at the request of Oxbow to address the scaling issue.

A report on the initial results of this effort was presented in early FY98 (Bruton et al., 1997). Several questions were considered:

* What is the source and composition of the scale that forms and how can it be controlled?

* Will scale form if reinjection is supplemented with local groundwater to maintain reservoir pressure?

* Will reinjection damage the reservoir over time?

Chemical and XRD analyses of scales from the Oxbow test bed revealed that they were composed primarily of amorphous silica with minor to trace amounts of quartz, calcite, magnetite, goethite, and clays. A variety of deposits from pipelines in the field shows that they may contain pebble-size clasts of reservoir lithologies cemented primarily by opaline silica, minor calcite and rare greenish, clay-like material.

Very detailed chemical analyses were made of shallow domestic water, production brines and gases, spent fluids from the power plant, and fluids in various sectors of the injection lines. Included were field extractions and analyses of ionized and total Al and of pH/Eh from all waters to determine mineral speciation and phase equilibria under various conditions of heating and mixing. Calculations showed that the injection fluids were saturated with amorphous silica and other phases, consistent with scale formation.

Simulation of the heating of shallow domestic groundwater from 34°C (collection temperature) to 250°C (reservoir temperature) indicated that carbonates, sulfates, and Mg-silicates will precipitate if this fluid is used for re-injection but that the potential for silica precipitation will decrease. Mixing of power plant injectate with reservoir waters is a more complicated issue (Fig. 2). Bruton et al. (1997) simplified the simulations into near and far wellbore cases. Near the wellbore, temperatures and salinities decrease as cool injection water dilutes the reservoir fluid. Silica saturation decreases but carbonate saturation increases as the injection fluid is progressively diluted. Away from the wellbore, temperatures and salinities rise as injection water mixes with reservoir fluids. Silica saturation decreases as the proportion

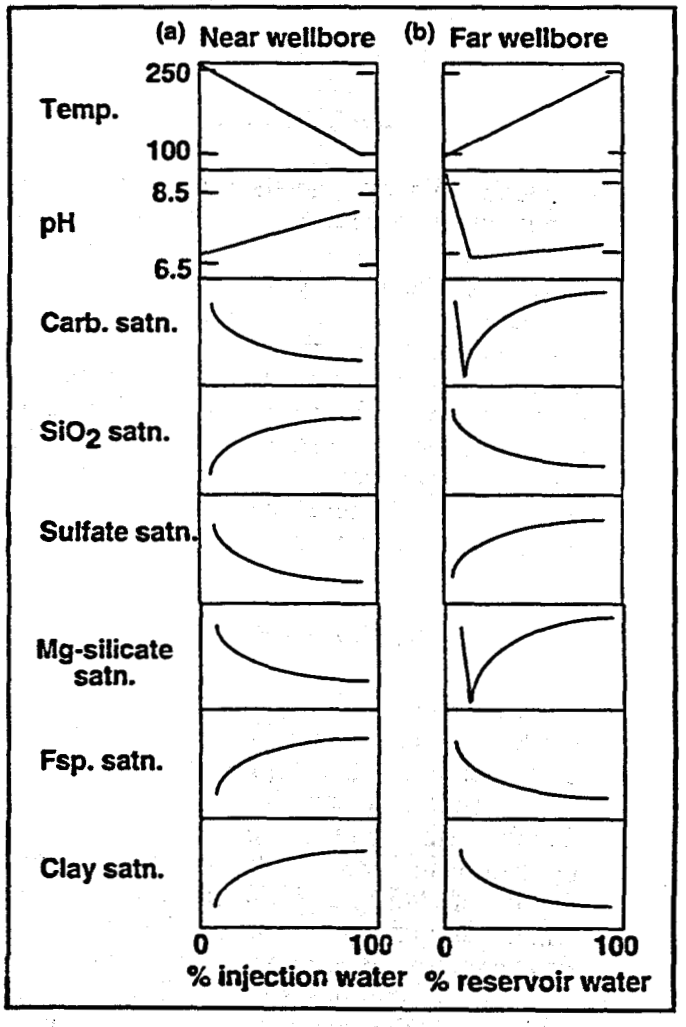

Figure 2. Summary of chemical-mineral trends during gradual mixing of (a) injectate into reservoir fluid and (b) reservoir fluid into injectate. Abbreviations: Carb. = carbonates, satn. = saturation, SiO_2 = silica polymorphs, Mg-silicate = Mg-bearing silicates, Fsp = feldspar (from Bruton et al., 1997).

of reservoir fluid increases. The far wellbore scenario is more sensitive to pH variations caused by more complicated precipitation responses from carbonates and Mg-silicates.

SYSTEM RECHARGE

Since exploitation began in 1988, the Dixie Valley geothermal reservoir has experienced a systematic decline of water levels and pressures in production wells. This has created a need to more thoroughly evaluate such processes as recharge to the geothermal system. We are presently collaborating on a combined chemical and isotopic study of regional springs and aquifers to help understand where recharge fluids primarily come from and to constrain how fast recharge occurs. The isotope studies will include analyses of deuterium/oxygen-18, tritium, carbon-13, carbon-14, chlorine-36, and strontium 87/86 in regional waters and production fluids. Sampling for this task began in November 1997 so a complete data set has not yet been obtained.

Figure 3 is a plot of deuterium vs. oxygen-18 for over 50 fluid samples collected in 1997. The gray cloud shows the range of 24 regional meteoric waters from Dixie Valley, the Stillwater Range, and the Clan Alpine Range that do not show any isotopic modifications due to evaporation or rock- water exchange. These waters form a trend that we refer to as the Dixie Valley meteoric water line (DMWL) and this trend is shifted by about +1 ‰ in oxygen-18 relative to the world meteoric water line (WMWL, Craig, 1961). The equation for the DMWL is $\delta D = 7.42\ \delta^{18}O - 8.91$ (n = 24, r = 0.91). A similar shift was found by Goff et al. (1994) for background waters in the Railroad Valley and Pine Valley regions, Nevada (SE and E of Dixie Valley). A slope of 7.55 was determined for cold springs throughout the Great Basin by Flynn and Buchanan (1993).

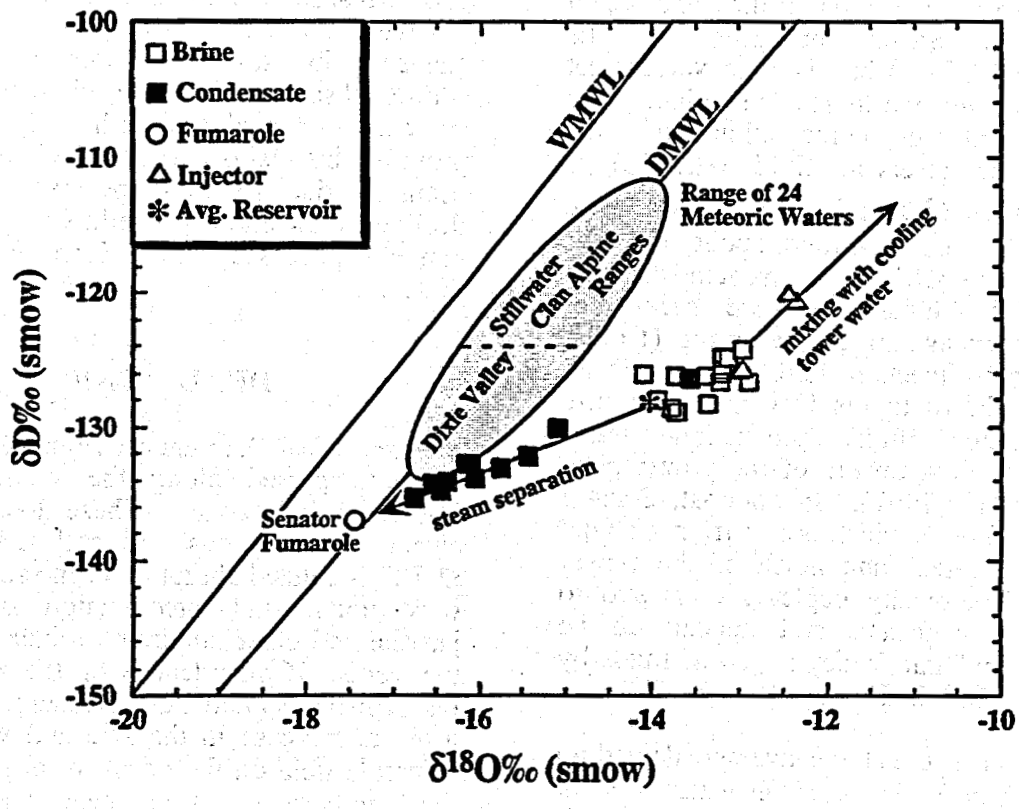

Figure 3. Plot of δD vs. $\delta^{18}O$ for various production fluids and regional waters in the Dixie Valley geothermal system and adjacent ranges.

Of the 24 meteoric waters represented by the gray cloud, 10 issue from the floor of Dixie Valley and their isotope compositions fall within the most depleted sector of the cloud (Fig. 1). Fourteen of the remaining 24 waters issue in the Stillwater and Clan Alpine ranges and 13 of these have isotope values that are enriched compared to those in Dixie Valley. Normally, the reverse relation would be expected because waters precipitated at higher elevation (such as in a mountain environment) would have isotope values that are more depleted than those in adjacent basins (Hoefs, 1973; Vuataz and Goff, 1986). The implication is that waters in Dixie Valley were either recharged at elevations higher than those we collected in the ranges or originated from an earlier time when precipitation was isotopically different. Flynn and Buchanan (1993) noted similar isotope relations between thermal and nonthermal waters and stated that most geothermal fluids in the Great Basin were recharged in the Pleistocene, 10 to 30 ka.

Dixie Valley production fluids form two major clusters of residual brines and steam condensates. Steam produced in the separators (~165°C) has isotope values that are depleted relative to residual brine. The average isotopic composition of the reconstructed reservoir fluid (~250°C) is about -130 ‰ (δD) and -14 ‰ ($\delta^{18}O$). The oxygen-18 value is shifted about +2.3 ‰ relative to the DMWL, a characteristic best explained by high-temperature rock-water isotopic exchange in the reservoir (Hoefs, 1973). Some injection fluids are isotopically enriched relative to residual brines because they are mixed with highly evaporated water from the cooling towers of the power plant (Bruton et al., 1997). In contrast, Senator Fumarole (97°C), which issues from a strand of the Stillwater Fault north of the power plant, is isotopically depleted compared to separator condensates and appears to be derived from Dixie Valley reservoir fluids by boiling at ~180°C (Henley et al., 1987).

If we accept that the average deuterium value of Dixie Valley reservoir water is about -130 ‰, it would appear that the reservoir does not contain fluids resembling those presently precipitated in the ranges. Tritium in reservoir fluids that were analyzed in 1996 contain ≤0.12 T.U. Using a well-mixed reservoir model (Shevenell and Goff, 1995), the maximum mean residence times of these fluids would be ≥10 ka. Additional tritium and future carbon-14 analyses should provide a much better handle on the age and recharge of Dixie Valley geothermal fluids.

MONITORING

Tracer tests conducted since 1989 have shown that there is some breakthrough of injection fluids into production wells of the geothermal reservoir (Adams et al., 1993). In addition, analysis of noncondensible gases have shown systematic decreases in CO_2 and H_2S during the first six years of power plant operation (Benoit and Hirtz, 1994).

Geochemical data obtained by our group in November 1997 was limited to just two production separators whereas data obtained in November 1998 included the entire geothermal field. At this time we can't make reliable statements regarding temporal changes in reservoir composition. As additional sample suites are collected, we will compare our analyses with early analyses provided by Oxbow to see if changes have occurred due to fluid removal, pressure decline, reinjection procedures, and other reservoir processes (i.e., Mariner and Janik, 1995).

DEAD ZONE

Areas of weak to intense fumarolic activity are interspersed along the NNE-trending Stillwater fault zone. These locations are characterized by gas and soil temperatures ≤97°C, localized alteration of the surrounding rock units, and precipitation of sulfur, jarosite and other sublimate minerals around the vents. Coincident with the decline in reservoir levels and fluid pressures has been a recent increase in the size and vigor of a fumarole field on the northwestern border of the geothermal system near the Senator Fumarole (Fig. 1). In 1997 dramatic changes occurred around the alluvial fan that extends

east from the fumaroles. These changes include partial to total die off of woody shrubs and formation of an area of steaming ground fractures at the base of the fan. This general area is now referred to as the "dead zone." Another group of dry fractures occurs in the basin northeast of the dead zone.

The two sets of ground fractures are noticeably different in character. Dead zone fractures (steaming ground) are associated with high temperatures, dead vegetation, moist soil, and formation of a soil crust. Basin soil fractures (dry cracks) have no thermal signature but are more laterally extensive and deeper than surface fractures in the dead zone. These fractures were first noticed in 1996 and visual observations suggest that they are growing with time.

Measurements of diffuse soil CO_2 flux are being used in volcanic and geothermal environments to provide information on transient processes (Farrar et al., 1995). We measured soil CO_2 flux along regularly spaced traverses within, across, and bordering the dead zone. Additional traverses were located around the area of dry cracks. CO_2 concentrations were obtained using a LI-COR brand infrared CO_2 gas analyzer in a closed loop with an accumulation chamber. This system delivers a well-mixed gas sample from the chamber to the analyzer and back at the rate of one sample per second. This instrument can measure very low CO_2 concentrations (signal noise is below 0.2 ppm) with an accuracy of ±2 ppm at high CO_2 concentrations (1000 ppm). For the purposes of this study flux is reported as grams of CO_2 per m^2 per day. Data is contoured using a software package that applies kriging statistics to determine a minimum error-variance estimate of the flux for unsampled locations. The contouring eliminates extremely high flux values from the resulting map (Fig. 4).

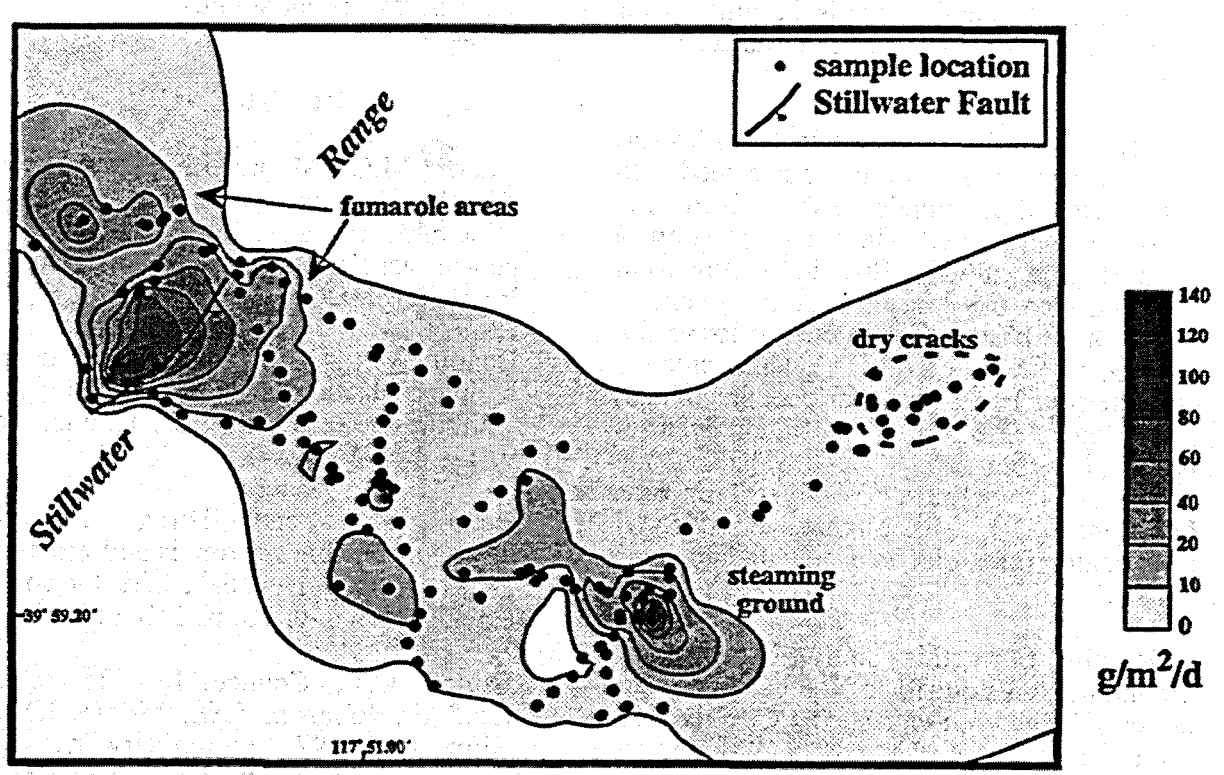

Figure 4. Map of contoured CO_2 flux over the dead zone and adjacent areas, Dixie Valley, Nevada. A contour map of soil temperature has a similar appearance. White regions lack sufficient data to be contoured.

The dry cracks area shows no CO_2 anomaly associated with ground fractures. Ambient CO_2 concentration at the soil surface is approximately 370 ppm and CO_2 flux across this area averages 1.8 $g/m^2/d$. CO_2 flux across the dry cracks area is comparable with other basin measurements located far away from steaming ground and essentially defines the local background flux.

It was not possible to obtain flux measurements directly over fumaroles because high CO_2 concentrations quickly exceeded the measurement capabilities of the analyzer. Maximum flux measurements of around 200 $g/m^2/d$ were obtained near fumaroles located along the Stillwater fault zone (Fig. 4). CO_2 flux rapidly decreases away from the fumaroles but all sample locations along a range front traverse yield a flux well above the local ambient value. Sample locations within the steaming ground area display elevated CO_2 concentrations and have flux magnitudes similar to those measured near fumaroles. Average flux for sample localities in this area is 52 $g/m^2/d$ with a maximum of 170 $g/m^2/d$ adjacent to fractures.

Four down-fan traverses in NW-SE and N-S orientations were performed to investigate flux trends away from the Stillwater fault zone. The traverses show a steep decline in CO_2 flux in a down-fan direction with the exception of the steaming cracks in the basin and a middle to lower fan region of elevated flux. This area is characterized by diffuse surface precipitates and moderate to high soil temperatures ranging between 24° to 59°C. The mid fan region helps to define a NW-SE striking zone of enhanced CO_2 emission that is bounded by the Senator fumarole field and the steaming cracks.

Results from this study indicate that ground fractures outside of the dead zone are not correlative with enhanced CO_2 flux. As such we feel that the dry cracks are not related to expansion of the fumarole field and are more likely related to another process, possibly subsidence within the basin.

In contrast, the steaming cracks at the base of the dead zone show soil temperatures and CO_2 flux similar to areas around the fumaroles. Although the causes of cracking are not understood, the steam must come from boiling of underlying geothermal reservoir fluids or from vaporization of shallow meteoric water that overlies the geothermal reservoir. Chemical and isotopic analyses of the steam suggest that it originates by the latter process. Another set of flux measurements will be obtained later this year to assess the rate of growth of the dead zone, if possible.

ACKNOWLEDGMENTS

This work is funded by the Geothermal Division, U.S. Department of Energy (Marshall Reed). We thank Joe Moore (Energy & Geoscience Institute) for getting us involved with the Dixie Valley effort in FY96. S. Johnson and W. Benoit (Oxbow Geothermal Corp.) have been instrumental in the progress of our studies.

REFERENCES

Adams, M.C., Moore, J.N., Benoit, W.R., Doughty, C., and Bodvarsson, G.S., 1993, "Chemical tracer test at the Dixie Valley geothermal field, Nevada", Univ. Utah Res. Instit., Rept. DOE/EE/12929-H1, 36 p.

Benoit, W.R., 1987, "Early stage carbonate scaling characteristics in Dixie Valley wellbores", Geotherm. Res. Counc. Trans., v. 11, p. 495-502.

Benoit, D., and Hirtz, P., 1994, "Noncondensible gas trends and emissions at Dixie Valley, Nevada", Geotherm. Res. Counc. Trans., v. 18, p. 113-119.

Bruton, C.J., Counce, D., Bergfeld, D., Goff, F., Johnson, S.D., Moore, J.N., and Nimz, G., 1997, "Preliminary investigation of scale formation and fluid chemistry at the Dixie Valley geothermal field, Nevada", Geotherm. Res. Counc. Trans., v. 21, p. 157-164.

Craig, H., 1963, "Isotopic variations in meteoric waters", Science, v. 133, p. 1702-1703.

Farrar, C.D., Sorey, M.L., Evans, W.C., Howle, J.F., Kerr, B.D., Kennedy, B.M., King, C.-Y., and Southon, J.R., 1995, "Forest-killing diffuse CO_2 emission at Mammoth Mountain as a sign of magmatic unrest", Nature, v. 376, p. 675-678.

Flynn, T., and Buchanan, P.K., 1993, "Pleistocene origin of geothermal fluids in the Great Basin, western United States", Resource Geol. Spec. Issue, No. 16, p. 60-68.

Goff, F., Hulen, J.B., Adams, A., Trujillo, Counce, D., and Evans, W.C., 1994, "Geothermal characteristics of some oil field waters in the Great Basin, Nevada", in (Schalla, R.A., and Johnson, E.H., eds.) Oil Fields of the Great Basin, Nevada Petrol. Soc., Reno, Nevada, pp. 93-106.

Henley, R.W., Truesdell, A.H., Barton, P.B., and Whitney, J.A., 1984, "Fluid-mineral equilibria in hydrothermal systems", Reviews in Economic Geology, Vol. 1, Soc. Economic Geologists, 267 p.

Hoefs, J., 1973, Stable Isotope Geochemistry, Springer-Verlag, N.Y., 140 p.

Lutz, S.J., Moore, J.N., and Benoit, D., 1997, "Geologic framework of Jurassic reservoir rocks in the Dixie Valley geothermal field, Nevada: Implications from hydrothermal alteration and stratigraphy", Proceed. 22nd Wksp. on Geotherm. Reservoir Engineering, Stanford Univ., 8 p.

Mariner, R.H., and Janik, C.J., 1995, "Geochemical data and a conceptual model for the Steamboat Hills geothermal system, Washoe County, Nevada", Geotherm. Res. Counc. Trans., v. 19, p. 191-200.

Shevenell, L., and Goff, F., 1995, "The use of tritium in groundwater to determine fluid mean residence times of Valles caldera hydrothermal fluids, New Mexico, USA", Jour. Volcanol. Geotherm. Res., v. 67, p. 187-205.

Vuataz, F.-D., and Goff, F., 1986, "Isotope geochemistry of thermal and nonthermal waters in the Valles caldera, Jemez Mountains, northern New Mexico", Jour. Geophys. Res., v. 91, p. 1835-1853.

A TECTONIC MODEL FOR THE COSO GEOTHERMAL AREA

J. Douglas Walker and Richard S. Whitmarsh
Department of Geology, University of Kansas

ABSTRACT

New geologic mapping in the Coso Range, eastern California, has resulted in a revised model for the geologic and tectonic development of the area. This model reassesses the relative roles of strike-slip and normal faults in the range. Two aspects of this work and model have bearing on the geothermal resource in the area. First, most of the resource appears to be localized within a pre-middle Pleistocene graben. Second, the eastern extension of the resource may be limited or offset by a newly recognized fault zone.

INTRODUCTION

The Coso Range and associated geothermal resource (Figure 1) have been the subject of geologic investigation for some time (e.g., Duffield and Bacon, 1981; Duffield et al., 1980; Roquemore, 1980; Stinson, 1977a, 1977b). These previous studies mostly have emphasized mapping of Tertiary volcanic and sedimentary rocks in the range. Although the Miocene to Recent igneous activity clearly is the main source of heat for the KGRA, the main reservoir is hosted in the Mesozoic basement rocks in the range. These Mesozoic rock have been the subject of some previous studies, but none of those studies were range-wide in scope or had significant geochronologic or structural aims. For this reason, the authors, in conjunction with the Geothermal Program Office, Naval Air Warfare Center, China Lake, CalEnergy Company, and the Department of Energy, have undertaken a systematic study of the basement rocks in the Coso Range.

Results for basement lithologies and ages (summarized in Figure 1) have been presented elsewhere (Whitmarsh, 1998; Walker and Whitmarsh, 1995, 1996) and maps are available via the Internet (http://geomaps.geo.ukans.edu). This report covers new tectonic and structural interpretation for the Coso Range based on mapping of the Mesozoic basement rocks and reexamination of the Miocene to Recent cover sequence.

GEOTHERMAL AREA

New geologic mapping and refinement of work by Duffield and Bacon (1981) reveals two dominant fault sets in the area of the Coso KGRA in the Coso Range. These are WNW- and NNE-trending structures (Figure 2). In general, WNW-trending faults appear to be dominantly strike-slip in nature and the NNE faults are mostly normal slip. In addition, the WNW faults appear to offset and segment the NNE-trending ones. We use basement rock characteristics, fault characteristics, and the Tertiary section to reconstruct the area for these fault sets. Features used in the reconstruction are discussed briefly below.

Important NNE structures consist of the Joshua Ridge fault and a sequence of west-facing normal faults (Figure 2). The Joshua Ridge fault is marked by cataclasis and brecciation. Slip on this fault is interpreted to be about 1 km based on the offset of distinct sill in the hanging wall and footwall (Black Spot pluton, Figure 2). Slip on the west-facing faults is uncertain, but is probably dip-slip and of normal sense (although displacement is inferred only on the basis of topography).

Other important features in the area includes breccia zones along the Airport Lake faults zone and along the Hot Springs fault zone near the Coso Hot Springs. Timing of development of these breccias, however, is uncertain. Breccia in the southeast part of the area is overlain by basalt dated at 3.6 Ma (Figure 2; Whitmarsh, 1998). Another important structural marker is the Rosevel shear zone - a Mesozoic-age ductile shear zone - in the northwest part of the area.

The features discussed above can be used to reconstruct deformation in the area. Figure 3 highlights the features used in the reconstruction. Because the WNW-trending faults appear to offset the NNE-trending ones, the Rosevel shear zone, and the breccia zones, we interpret these faults to be the younger feature. Restoring strike-slip motion on the WNW faults to line up the NNE-trending features yields about 5.5 km of cumulative slip across the area. Motion along the WNW-

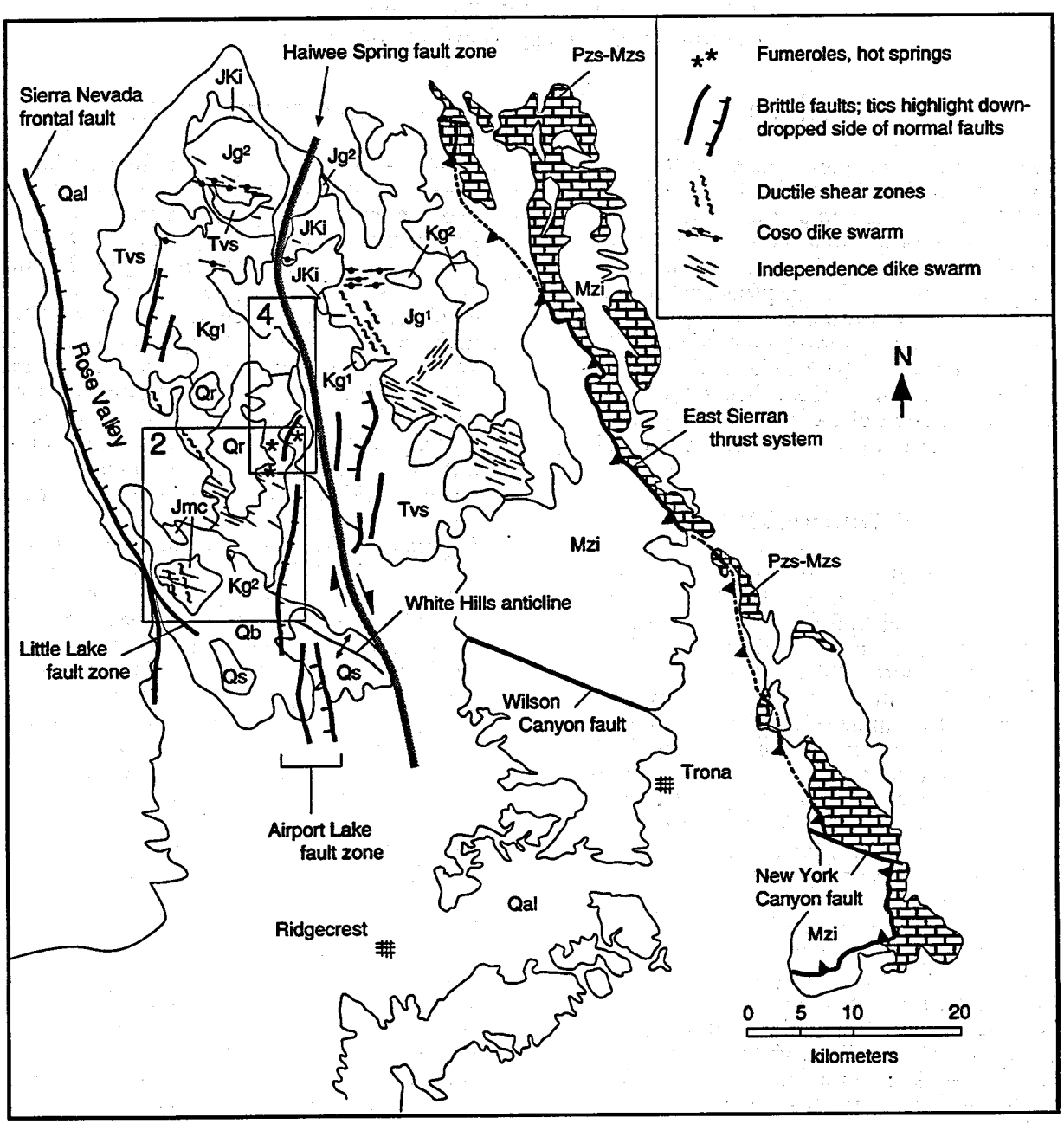

Figure 1. Generalized geologic map of the Coso, Argus, and Slate ranges with major tectonic features highlighted. Jg1, older Jurassic granitoid; Jg2, younger Jurassic granitoid; Jmc, Jurassic mixed complex; JKi, Jurassic-Cretaceous intrusive complex; Kg1, older Cretaceous leucogranite; Kg2, younger Cretaceous leucogranite; Mzi, Mesozoic intrusive rocks; Pzs-Mzs, Paleozoic-Mesozoic strata; Tvs, Tertiary volcanics and sediments; Qal, Quaternary alluvium; Qb, Quaternary basalt; Qr, Quaternary rhyolite; Qs, Quaternary sediments. Note boxes that delineate the areas of Figures 2 and 4 as noted in upper-left corner of each.

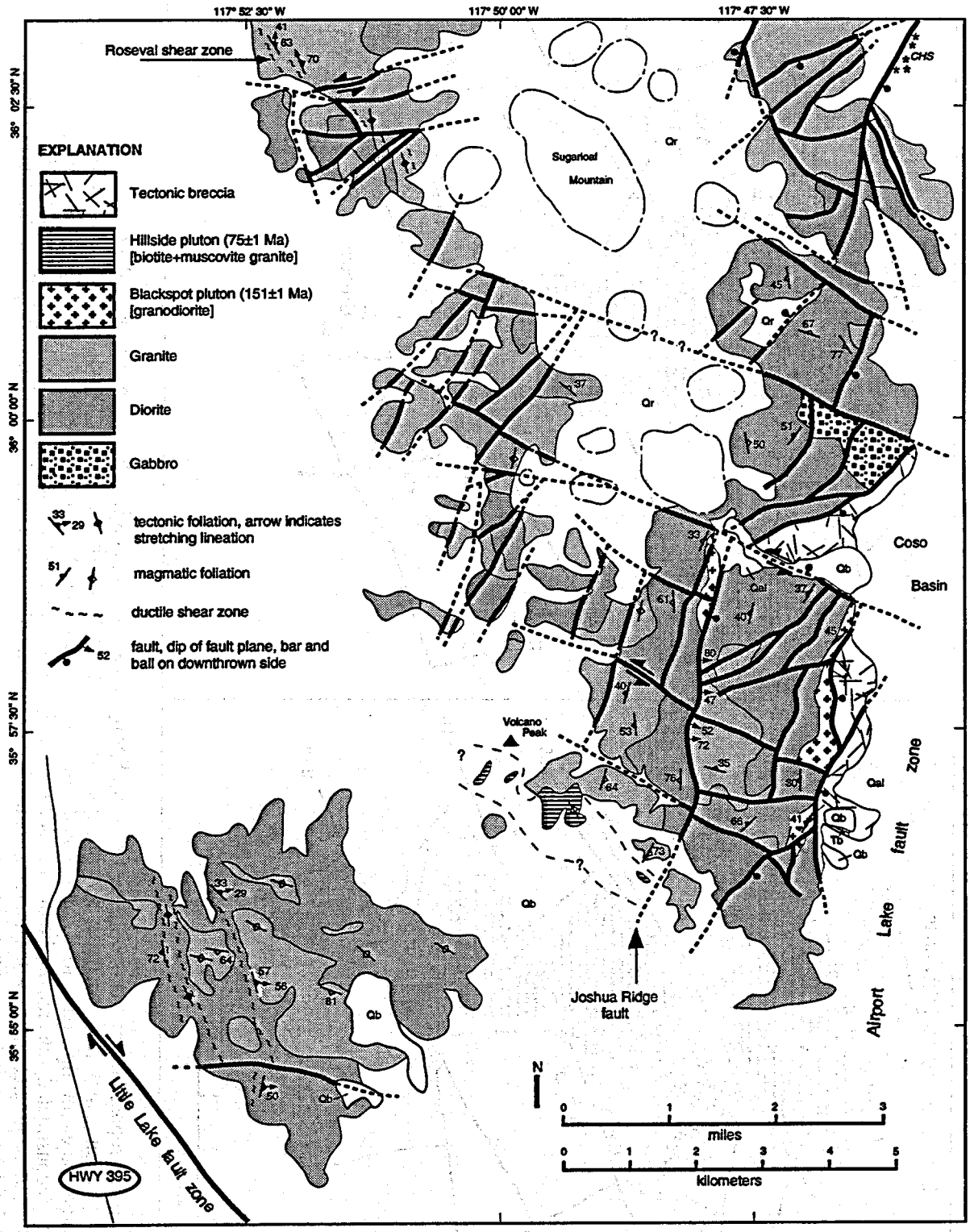

Figure 2. Generalized geologic map of the southwestern Coso Range. CHS, Coso Hot Springs; Qal, Quaternary alluvium; Qb, Quaternary basalt; Tb, Tertiary basalt. Dash-dot contacts outline rhyolite domes within the pyroclastic cover.

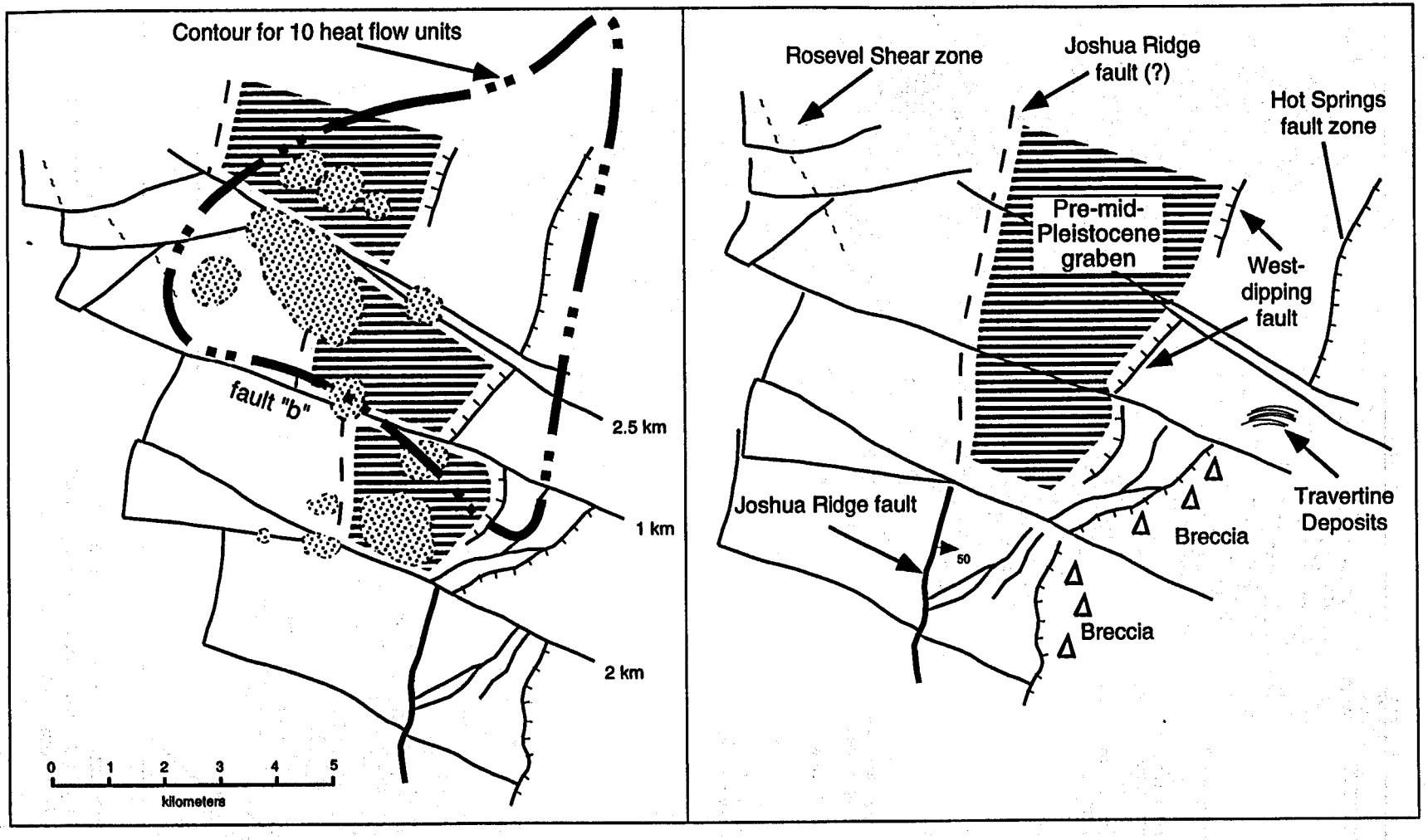

Figure 3. Proposed reconstruction for the Coso Hot Springs area. Diagram on left shows the current geologic configuration (simplified from that shown in Figure 2). Area of high heat flow is shown, as well as the position of the rhyolite domes (in stiple pattern). Diagram on the right shows the area restored for inferred motion on strike-slip faults. When reconstructed, the area of the rhyolite domes and high heat flow lies between the zone of west-dipping normal faults and the projection of the Joshua Ridge fault. For this reason, the domes are interpreted to mostly lie within a pre-middle Pleistocene graben (horizontal rule).

trending faults probably occurred prior to 1.07 Ma, because a basalt flow of this age overlies one of the faults.

Most of the KGRA (with its associated rhyolite domes) lies between the restored positions of the west-facing normal faults and the northward projection of the Joshua Ridge fault. (It is likely that the Joshua Ridge fault continues to the north, because when last observed it has 1 km of down-to-the-east slip along it.) This indicates that the domes and KGRA appear to be located in a pre-1.07 Ma graben in the west-central part of the Coso Range. This suggests that Basin and Range structures may have in part influenced the location of the resource.

The area of highest heat flow for the Coso KGRA is bound to the south by fault "b". It may have more slip on it than 1 km (as inferred by the model above), with most of the slip predating the graben. This interpretation fits well with regional considerations discussed below.

HAIWEE SPRING FAULT ZONE

A somewhat different structural configuration is observed in areas farther to the north. From the Coso Hot Springs northward through Haiwee Spring, the dominant fault trend is roughly north-south (Figures 1 and 4). In this region, the most conspicuous faults are NE- to NW-trending normal faults and N- to NW-trending strike-slip faults. These are clearly young faults in that they disrupt the Pliocene cover sequence in the area.

Also present in this area are several E-W-trending contractional faults. Slip on these structures is small to large, but slip is consistently south-directed (Figure 4). The largest structure offsets a gabbro body by 1 km. The age of these structures is somewhat uncertain because they mostly only cut Mesozoic rocks. One small fault in the northern part of the area, however, clearly cuts the Cenozoic cover sequence. This fault is cut by both normal and strike-slip faults in the area. We interpret these faults to be late Tertiary in age.

The pattern of faulting in this area can be interpreted to represent a strike-slip fault zone with associated normal faults and thrust faults. Because of the complex structural relations, the slip on the zone is probably significant. Overall slip can be interpreted by examining relations to the north of the Haiwee Spring area. If the Haiwee Spring fault zone is projected to the north, it crosses the Coso dike swarm (an roughly E-W-trending swarm of 88 Ma granitic dikes mapped in the area; Whitmarsh, 1998). The main locus of the Coso dike swarm appears to be offset 5 to 6 km across the projection of this fault (Figure 1). Therefore, we interpret there to be significant right-lateral slip, 5 to 6 km, on the Haiwee Spring fault zone.

TECTONIC MODEL FOR THE COSO RANGE

The interpretation of the Haiwee Spring fault zone as a major structure in the Coso Range, along with mapping an identification of area of normal faulting and strike-slip faulting, form the basis of a new model for the tectonic development of the Coso Range. This model is consistent with the area experiencing right-oblique extension (a previously accepted overall strain interpretation for the area). This is accommodated by both normal and strike-slip faults within the Coso Range (Figure 5). Areas of extension include the graben discussed above, as well are the Airport Lake/Coso Basin system and an area of faulted basalt flows to the east of Coso Basin. It is also clear that the right oblique extension is expressed as a combination of strike-slip and normal faults within much of the range (e.g., Figures 2 and 3 and discussion above).

Interpretation of the Haiwee Spring fault zone as a major strike-slip fault with 5 km or more of right-lateral slip also has implications for the regional geologic picture. One fault zone of major regional importance is the Wilson Canyon fault (Figures 1 and 5). Restoration of 5 km of slip on the Haiwee Spring fault zone lines the Wilson Canyon fault with fault "b" in the Coso Range. Fault "b", therefore, is interpreted as a major structural zone. Given that movement along the Wilson Canyon fault was mostly pre-middle Pliocene (Whitmarsh, 1998), significant motion on fault "b" may have occurred. (We interpret fault "b" to have only about 1 km of slip since formation of the graben in the KGRA vicinity.) This is consistent with the observation that fault "b" forms the southern boundary to the KGRA.

IMPLICATION FOR GEOTHERMAL EXPLORATION

We interpret the Coso KGRA to be mostly located in a pre-middle Pleistocene graben located north of the extension of the Wilson Canyon fault. This latter fault, therefore,

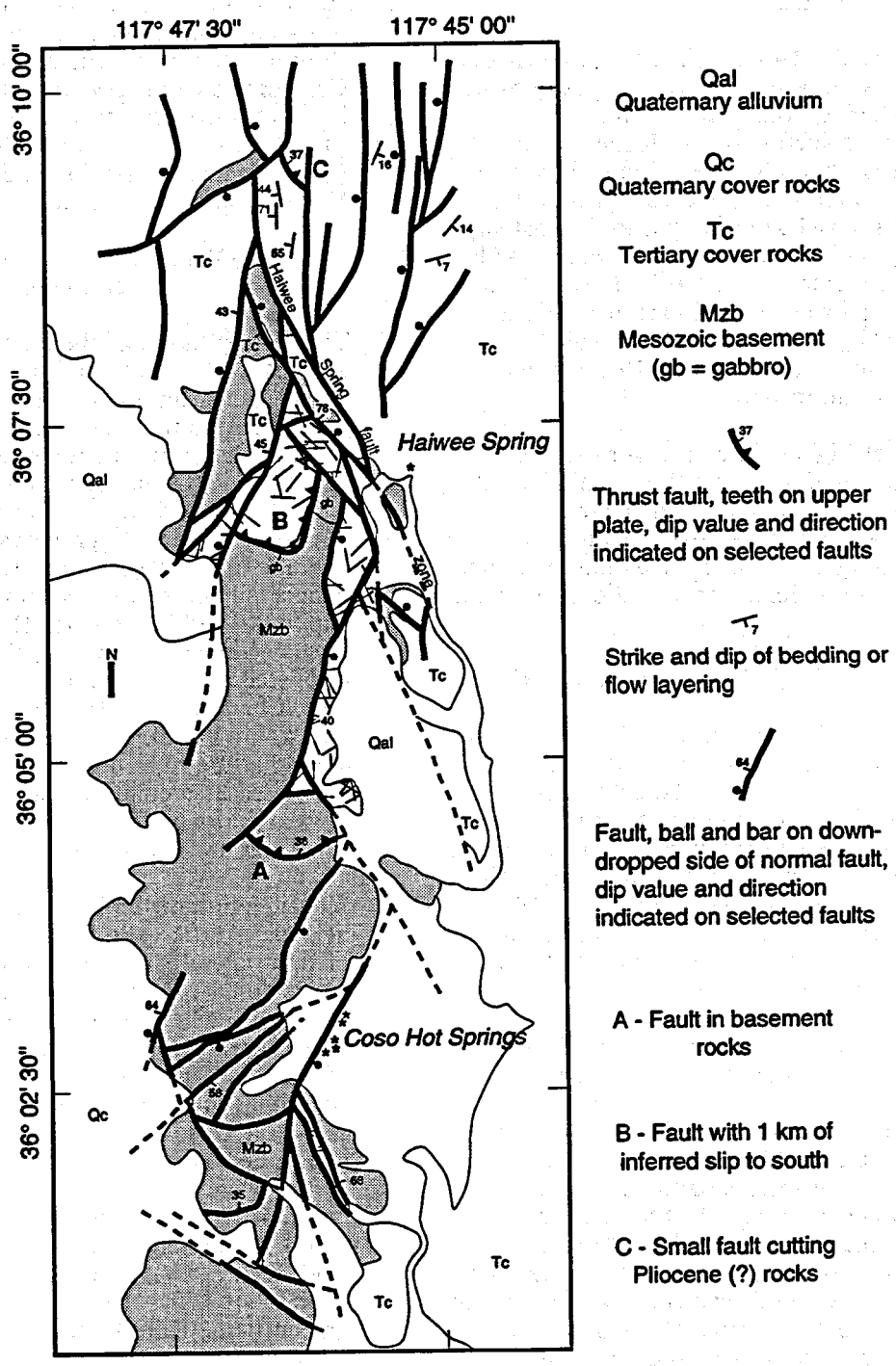

Figure 4. Generalized geologic map of the Haiwee Spring fault zone. Map shows many strike-slip faults, south-directed reverse faults, and normal faults.

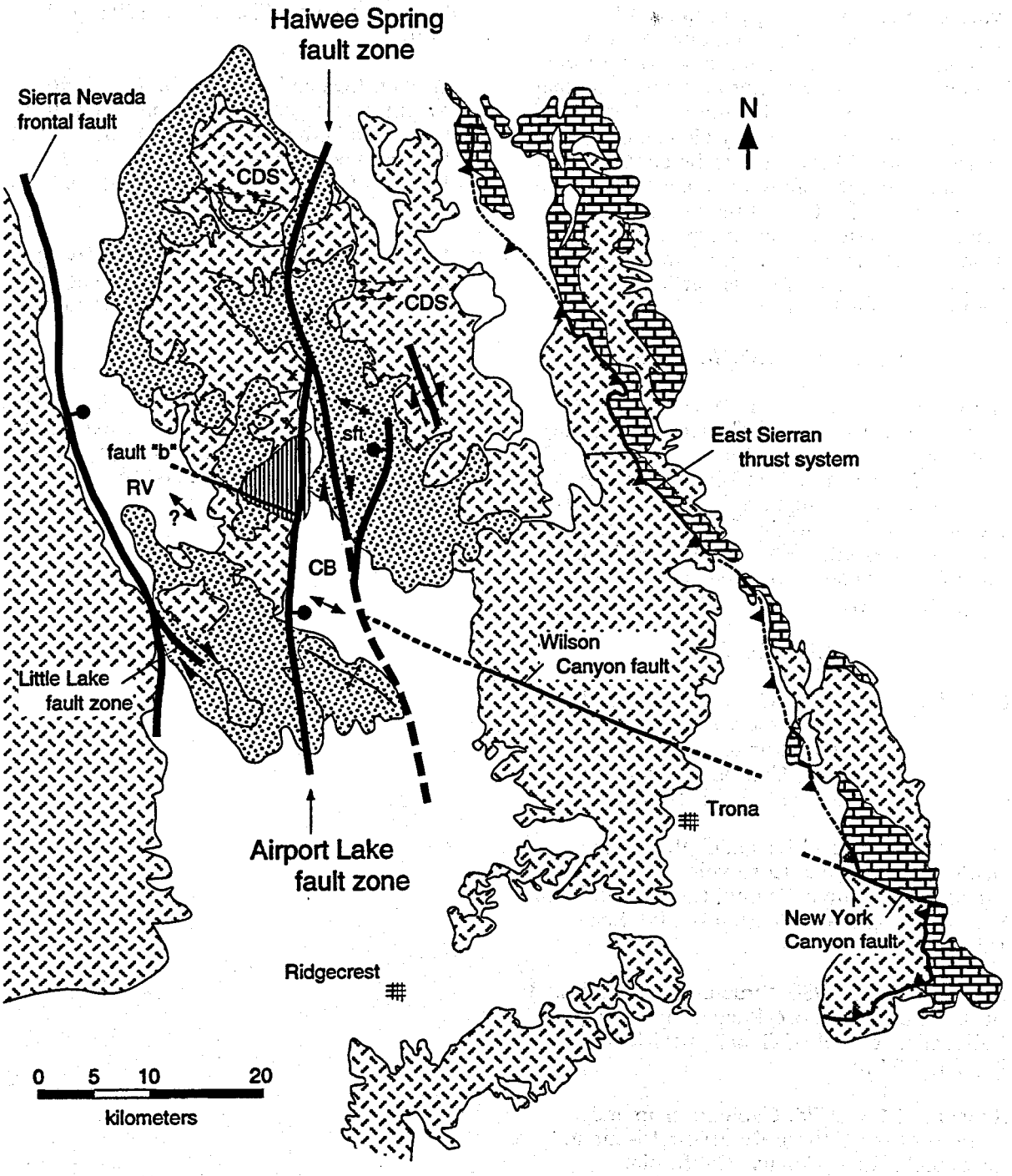

Figure 5. Tectonic model for the Coso Range and adjacent areas. The model interprets the area to be undergoing right-oblique extension. Major strike-slip fauts consist of the Haiwee Spring and Little Lake fault zones. Normal faults are somewhat more widely distributed. CB, Coso Basin; CDS, Coso dike swarm; RV, Rose Valley; sft, step faulted basalt flow terrane.

appears to be a deeply penetrating feature that bounds the KGRA. It appears to form a major hydrologic and/or enthalpy barrier. We therefore suggest that exploration in areas to the south of fault "b" should have low priority. In addition, the Haiwee Spring faults zone may form a similar barrier, therefore exploration to the east of this structure may also be of lower priority. Most likely areas to be connected hydrologically, therefore, are areas to the west of the current KGRA and the northern Coso Basin area. Based on the interpretations present here, these are the areas that may be most favorably explored for further geothermal development.

ACKNOWLEDGMENTS

The Geothermal Program office of the US Navy (Naval Air Warfare Center, China Lake), CalEnergy Company, and the Department of Energy Geothermal Technology Organization provided financial support for this work. The authors would like to thank Frank Monastero, David Meade, Allen Katzenstein, and John Copp for stimulating discussion of Coso Range Geology.

REFERENCES

Duffield, W.A, Bacon, C.R., and Dalrymple, G.B, 1980, Late Cenozoic volcanism, geochronology, and structure of the Coso Range, Inyo County, California: Journal of Geophysical Research, 85, 2381-2404.

Duffield, W. A., and Bacon, C. R., 1981, Geologic map of the Coso volcanic field and adjacent areas, Inyo County, California: United States Geologic Survey Map I-1200, Scale 1:50,000.

Roquemore, G., 1980, Structure, tectonics, and stress field of the Coso Range, Inyo County, California: Journal of Geophysical Research, 85, 2434-2440.

Stinson, M.C. 1977a. Geologic map and sections of the Haiwee Reservoir 15-minute quadrangle, Inyo County, California. California Division of Mines and Geology, Map Sheet 37.

Stinson, M.C. 1977b. Geologic map and sections of the Keeler 15-minute quadrangle, Inyo County, California. California Division of Mines and Geology, Map Sheet 38.

Walker, J.D., and Whitmarsh, R.S., 1995, Mapping and geologic interpretation in the Coso Geothermal area: U.S. Department of Energy, Federal Geothermal Research Program Update, Fiscal Year 1994, p. 2-21 to 2-26.

Walker, J.D., and Whitmarsh, R.S., 1996, Mapping and geologic interpretation in the Coso Geothermal area: U.S. Department of Energy, Federal Geothermal Research Program Update, Fiscal Year 1995, p. 2-71 to 2-78.

Whitmarsh, R.S., 1998, Structural development of the Coso Range and adjacent areas of east-central California: Doctoral Dissertation, University of Kansas, Lawrence.

Whitmarsh, R.S., Walker, J.D., Monastero, F.C., 1996, Structural domains within the Coso Range: A case for right-oblique extension: Geological Society of America Abstracts with Programs, v. 28, no. 7, p. A-116.

THE AWIBENGKOK, INDONESIA, GEOTHERMAL RESEARCH PROJECT

Jeffrey B. Hulen
Energy & Geoscience Institute (EGI), University of Utah
Salt Lake City, Utah

Introduction

The Awibengkok geothermal field, in West Java, Indonesia (Fig. 1) is the biggest by far in the entire Indonesian archipelago. Operated by Unocal Geothermal of Indonesia (UGI), the field has an installed electrical generating capacity of 330 MW (Glen Melosh, UGI, pers. comm., 1998). It is an excellent proxy for neutral-chloride, composite-volcanic ("andesitic")-hosted Cenozoic geothermal systems along the entire island arc and, indeed, anywhere in the world. We are therefore fortunate to have obtained, for focused geothermal research, a 1.1-km long continuous core from the heart of the Awibengkok system.

The core, from well Awibengkok ("Awi") 1-2, was retrieved by UGI late in 1995, with the understanding that it could become this important research tool. In mid-1997, the U.S. Department of Energy's (DOE) Office of Geothermal Technology (OGT), working through EGI, finalized negotiations with UGI to obtain a one-half, longitudinal split of the core. With selected corresponding logs, analyses, measurements, and imagery provided by UGI, the core will underpin a 2-3 yr research effort designed to improve significantly our understanding of reservoir controls in andesitic systems in all similar settings worldwide.

The Awibengkok field was discovered in 1983 by UGI working as contractor to PERTAMINA, the Indonesian National Oil Company. The core from Awi 1-2 is one of only two such cores from andesitic systems which is not only of such great length and completeness, but is available for non-proprietary research for the benefit of the entire geothermal community (the other core is from the Tiwi system, Philippines).

Geologic and Geothermal Setting

The Awibengkok geothermal field is situated in the Salak contract area of West Java, encompassing much of the Quaternary-age Salak-Kiaraberes-Gagak-Perbakti (SKGP) volcanic complex (Effendi, 1974; Ganefianto and Shemeta, 1996). These overlapping composite volcanoes are typical of the Javanese sector of the Sunda-Banda volcanic arc (Fig. 1), which marks the juncture between the northward subducting Indo-Australian tectonic plate and the overriding Eurasian Plate. The volcanoes of this portion of the arc, as throughout the archipelago, are associated with numerous active geothermal systems, including the productive Awibengkok, Kamojang, and Darajat fields and numerous promising prospects (Fig. 1).

Within the SKGP complex, the Awibengkok field and the Ratu geothermal area to the west (Fig. 2) occur mainly in complexly interstratified, intermediate- to felsic-composition flow and dome rocks, lahar breccias and tuffs. These rocks are intruded locally by hypabyssal and subvolcanic plutons – likely dikes and sills – of similar composition. Of the four major volcanic centers of the SKGP, only Salak has erupted juvenile magmatic material in recorded history

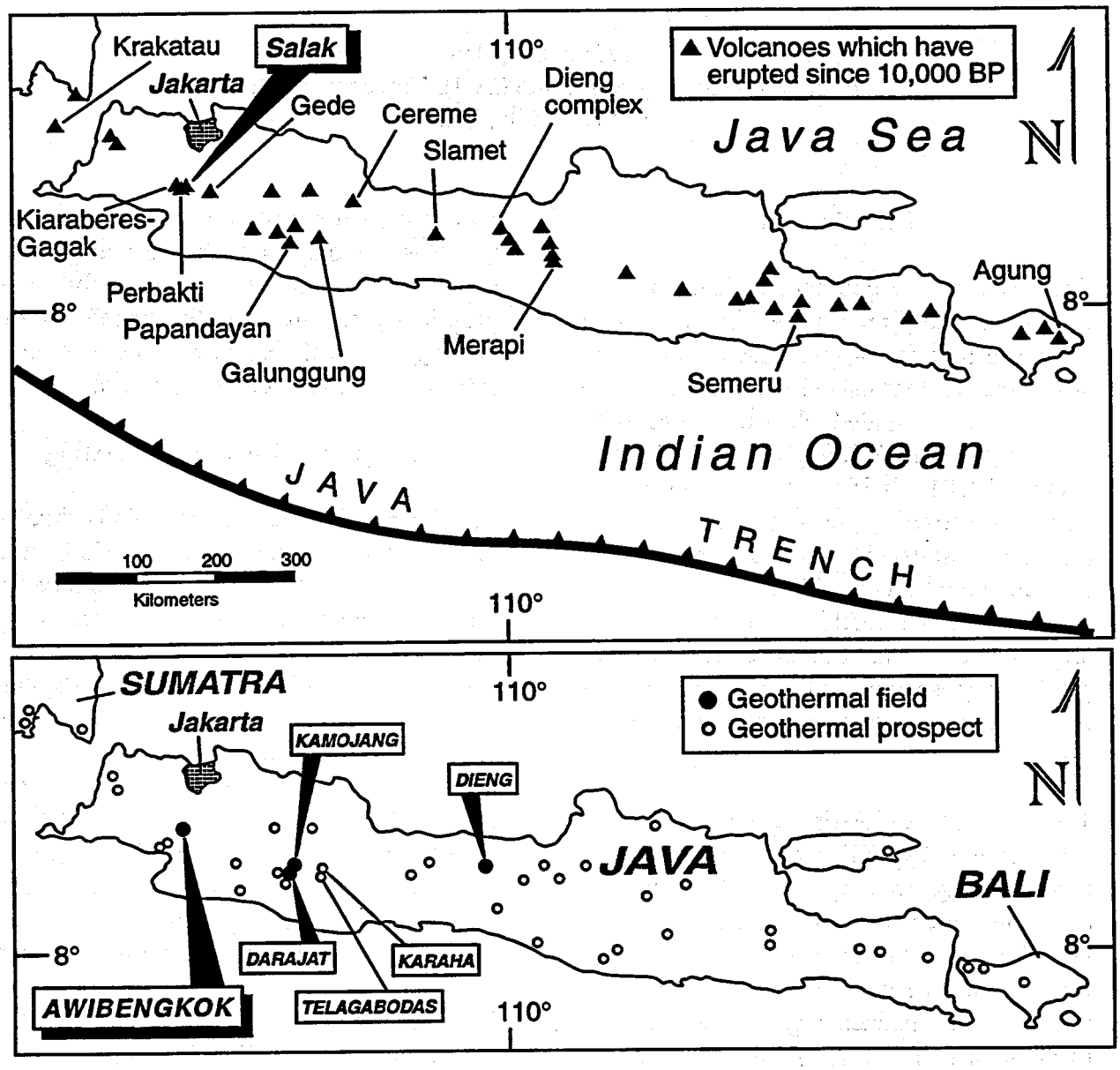

Figure 1. Maps of Java, Bali, and southernmost Sumatra, Indonesia, showing (top) volcanoes with documented Holocene eruptions (including hydrothermal eruptions) and (bottom) geothermal fields and prospects. Volcanoes from Simkin and Siebert, 1994. Geothermal sites synthesized from Radja, 1990; Effendi, 1991; Ganda et al., 1992; and Rachman et al., 1995 (site numbers and locations differ slightly among these sources).

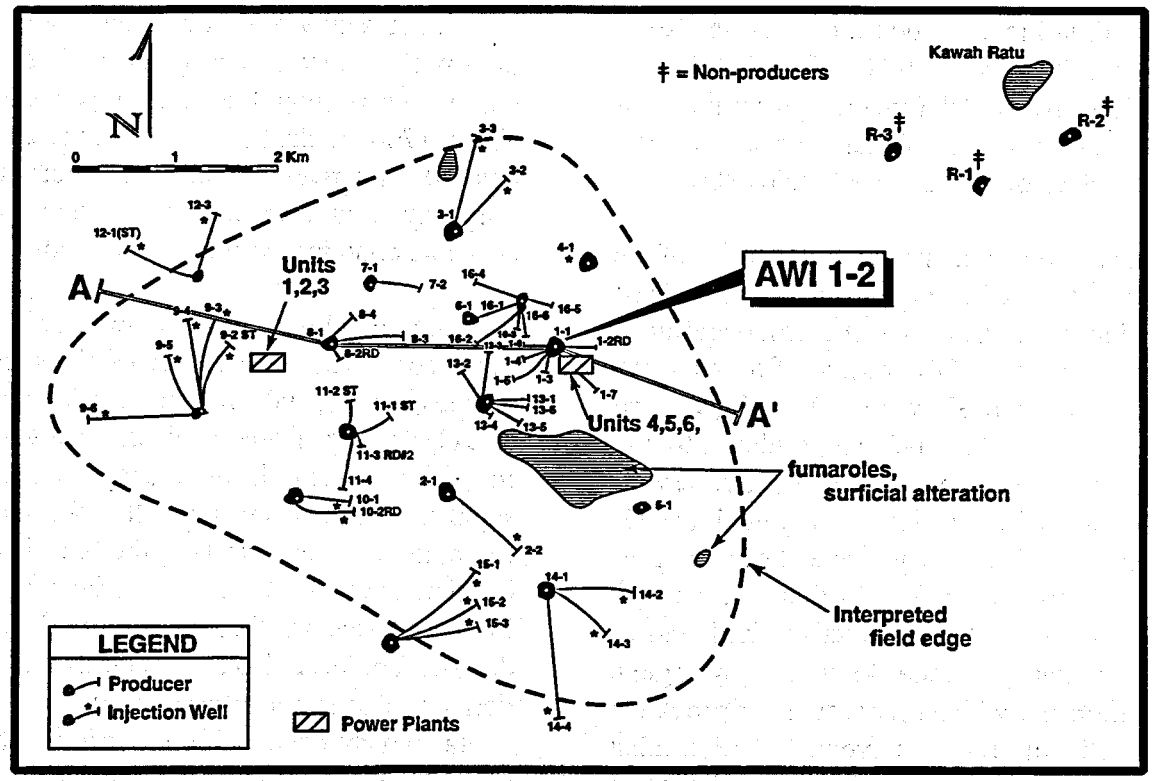

Figure 2. Well map of the Awibengkok geothermal field and Ratu geothermal area, showing location of corehole Awi 1-2. Modified slightly from Unocal et al., 1997.

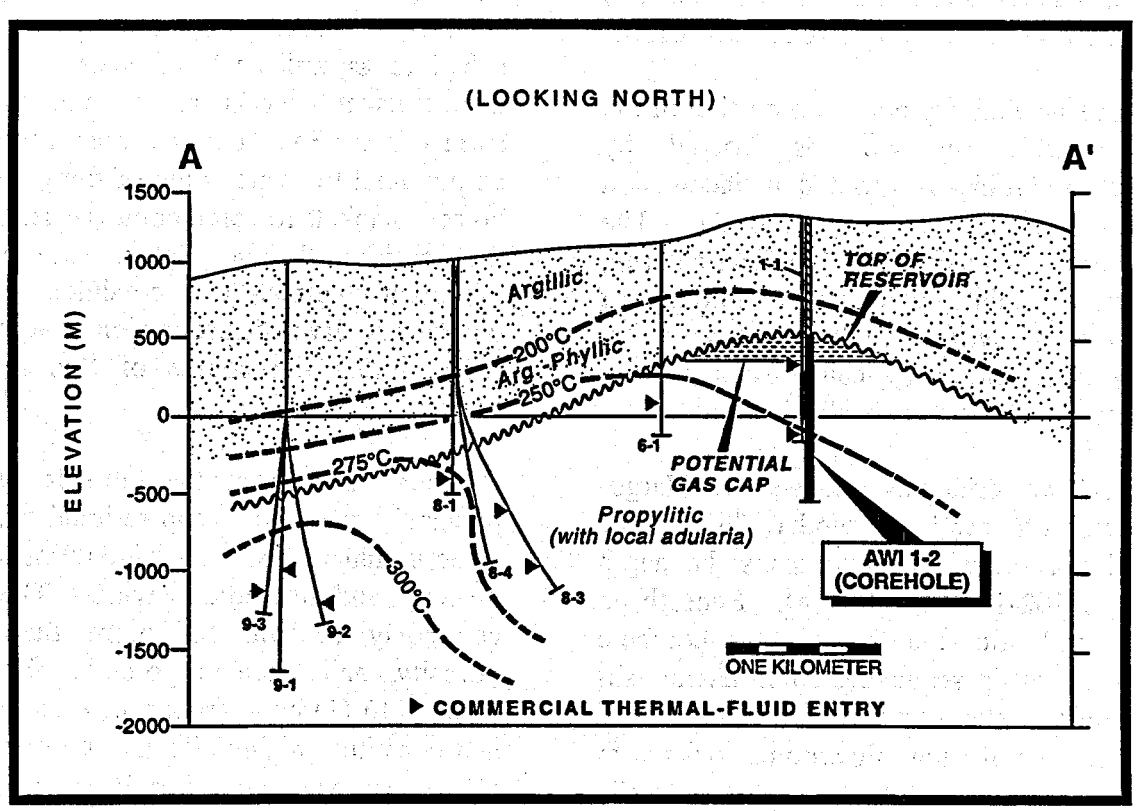

Figure 3. Highly generalized west-to-east cross section through the Awibengkok geothermal field. Modified from Murray et al., 1995; and Unocal et al., 1997.

(a small-volume pyroclastic flow in 1699; Simkin and Siebert, 1994). Other Holocene eruptions from Salak (including from the Ratu vent area) have been phreatic events, yielding localized aprons of unsorted lithic debris.

Temperatures in the productive portion of the Awibengkok field range from 220 to at least 300 degrees Celsius, and the produced fluids typically have a TDS content of about 1.3% (Ganefianto and Shemeta, 1996; **Figs. 2** and **3**). Corehole Awi 1-2 was drilled into the shallowest portion of the geothermal reservoir, a "cupola" within which Murray et al. (1995) postulated there may have been a pre-exploitation gas cap. Within the cupola, uncharacteristically, productive fluid entries occur within the zone dominated by argillic alteration and which serves as the caprock for the bulk of the reservoir. The argillic alteration is dominantly smectite at shallower levels, mixed-layer illite/smectite at greater depth, and in some cases entire lithologic units have been >90% converted to layer silicates.

The overwhelmingly dominant portion of the Awibengkok reservoir is hosted by propylitized rocks overprinted by silicification and adularization (**Figs. 2** and **3**). The propylitic phases consist of epidote, chlorite, calcite, and albite, with varying amounts of hematite and pyrite, anhydrite, and wairakite. The adularization is typically associated with increased sulfidation and silicification.

Awi 1-2 was drilled as a conventional large-diameter rotary well to a depth of 762 m. The cored portion of the hole spans the depth interval 762-1830 m (**Fig. 4**). Beneath an upper andesitic lahar breccia, the corehole encountered, in sequence: a thin dacite ash-flow tuff; another thin andesitic lahar breccia; a thick zone of dacite flow/dome rocks with prominent quartz phenocrysts; a totally argillic-phyllic-altered pyroclastic horizon; and a thick but relatively thin-bedded sequence of flow rocks, lahar breccias, and tuffs to total depth. Disrupting this deeper sequence at about 1700 m depth is a distinctive, dark-colored, relatively unaltered microdiorite porphyry which unlike other units in the corehole contains fresh mafic minerals.

Hydrothermal breccias are a common feature of the core. They include pebble dikes, jigsaw puzzle breccias, and adjacent "crackle zones". The clasts range from locally derived varieties to those which have clearly undergone significant vertical transport. It is possible, for example, that some clasts in the breccias may be microcrystalline limestone derived from the Miocene "basement" complex more than a km deeper. There are also tabular clasts which are derived from hydrothermal quartz veins containing abundant sulfide (pyrite withtraces of chalcopyrite, galena, and sphalerite). The matrices of these breccias are invariably altered and cemented by such phases as quartz, adularia, wairakite, epidote, pyrite, and anhydrite as well as layer silicates. Since hydrothermal breccias are so common at the surface in the Salak contract area, there may be potential to relate some of these surficial breccia blankets to cored counterparts. Also, the breccias by their very nature are potentially important thermal-fluid conduits, and in our view deserve a disproportionate amount of study during the course of this research project.

Obvious porosity in the core is of four principal types – vugs and residual cracks in veins; unmineralized cracks; interclast voids in breccias; and dissolution cavities. The latter commonly account for more than 10% porosity, and there is potential for these features to (1) be interconnected extensively and constitute highly effective porosity; and (2) to serve as storage sites for thermal fluids which will ultimately supply larger productive

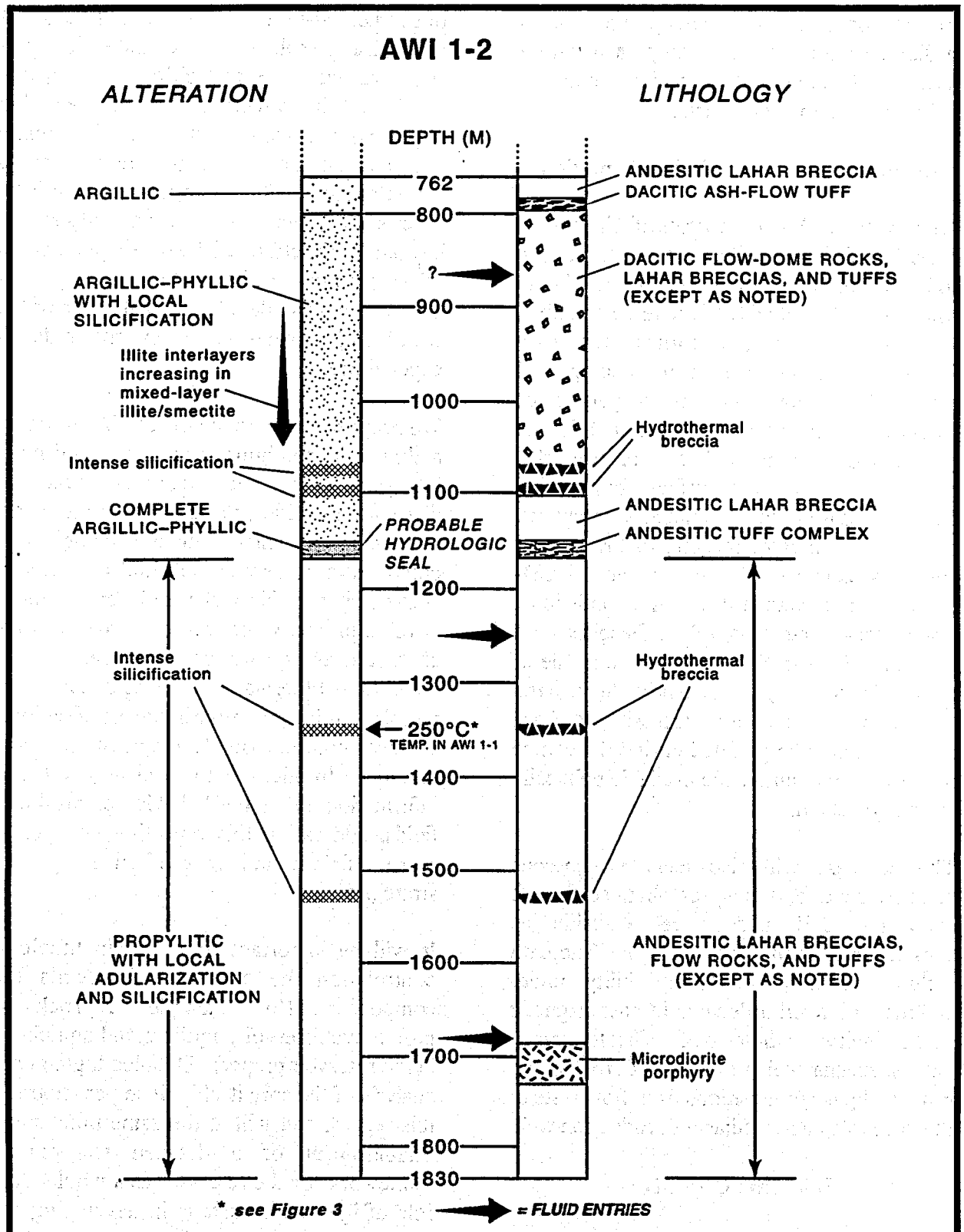

Figure 4. Highly generalized lithologic and alteration columns for corehole Awi 1-2. Simplified and modified from field geologic log prepared in late 1995 by J. Hulen and D. Nielson. Fluid entries inferred from prominent local excursions on UGI injection-temperature-gradient log.

fracture zones. The voids are up to several cm in diameter, and are commonly lined with a variety of euhedral secondary minerals including adularia and quartz.

Accompanying Technical Information

Along with the Awi 1-2 core itself, Unocal has provided a highly detailed and comprehensive collection of wireline logs and analytical data which will be invaluable to the research effort. The logs, in digital format for easy distribution, include total-count and spectral gamma; injection temperature; caliper; vector magnetic intensity; dual-induction; SP; and full-waveform sonic. The core was also analyzed at the well site (surface) for porosity, density, and total-count gamma. Continuous, high-resolution color imagery of the slabbed core was also obtained. This imagery, on CD-ROM format, was distributed to individual researchers at the inaugural Awibengkok core workshop held in Salt Lake City on June 2, 1998. The imagery will also provide the basis for a comprehensive, easily accessible database to be continually upgraded during the course of the research, and made available publically at its conclusion.

The database will also include numerous measurements and analyses obtained for the core by UGI and made available as background for this investigation. The data include porosity and permeability under ambient and overburden conditions; magnetic susceptibility; whole-rock silicate-oxygen values; mechanical properties of rocks; and brine and gas compositions from flow tests of the corehole and an adjacent production well.

Scientific Objectives

Through detailed study of the Awi 1-2 core and accompanying data set, described above, we plan to significantly improve understanding of geothermal-reservoir controls in a large but otherwise typical, island-arc, andesitic, high-temperature, neutral-chloride, liquid-dominated hydrothermal system (see also Hulen and Anderson, 1998). We will compare and contrast the new information obtained from this study with corresponding data from other such systems, both local and global. A key part of the effort will be timely publication of the research results, so that these systems can be found and developed in all parts of the world with greater efficiency and reduced expenditure.

We propose to determine the origins, measure and map the configurations, and establish the interrelationships of fractures, breccias, dissolution cavities, vesicles, interclast vugs, and other voids which singly or in combination could serve as geothermal-fluid conduits or storage sites. This will ideally enable us to develop predictive concepts for the location, character, and quality of permeable zones in andesitic geothermal systems as a class. We will also study the relative influence of regional vs local controls on development of these features. In addition to furnishing valuable information about the behavior of produced fluids, addressing this objective will permit more efficient and cost-effective injection strategies.

It will be important to ascertain lithologic controls on the geothermal system's key components (for example, caprock vs productive reservoir; aquifers and aquicludes in the reservoir proper). Detailed logging and analysis of the core itself will be paramount in this regard, and will at the same time enable establishment of a detailed stratigraphic framework for the reservoir as a whole. The role of igneous intrusions in developing and sustaining the geothermal system will become much clearer as a result of this module of the investigation.

Hydrothermal alteration mineralogy and zoning can often be directly related to the effective "plumbing system" of an active geothermal system. We will map this alteration at the scale of the core, and if permissible will relate this to the configuration of alteration zones throughout the reservoir. Particular alteration assemblages and textures will be compared with active thermal fluid conduits to develop more effective predictive tools for the location of these features.

Reconstruction of the hydrothermal history of the Awibengkok system will be much more readily achieved through this research project, and with continuous core, than with the use of small-diameter drill cuttings alone. The resulting information will allow more confident prediction of future changes in reservoir characteristics with time and progressive fluid depletion.

Measurement of multiple physical and mineralogic properties of the rocks penetrated by the corehole, particularly under simulated reservoir pressures and temperature, will permit more informed and realistic reservoir models, and allow more refined forecasts of future reservoir behavior.

Approach

A detailed summary of the methods and procedures by which we hope to reach the goals outlined above is presented in Hulen and Anderson (1998), and will not be fully reproduced here; the interested reader is referred to that paper for elaboration.

An inaugural workshop on the Awibengkok Geothermal Research Project was held in Salt Lake City, Utah, on June 2, 1998. At this meeting, interested researchers debated the preliminary site-specific Science Plan presented in Hulen and Anderson (1998), refined the plan, and developed guidelines for the most effective sampling of the retrieved core, now at the EGI Geothermal Sample Library. The collective expertise of the assembled researchers more than adequately addressed the multiple scientific objectives envisioned for the project. Of particular importance for this effort will be a highly coordinated sampling effort, so that to the full extent possible, the individual researchers' results can be compared, contrasted, and correlated with those of others. This approach will also minimize the extent of destructive sample analysis, thereby preserving this valuable core for future research efforts. A final Science Plan for the Awibengkok project will be available to the entire geothermal research and development community by the end of Fiscal Year 1998. It should be stressed that other scientists with independent funding are more than welcome to participate in this project if their interests and approaches technically enhance it, and they do not substantially duplicate efforts already in progress.

Significance of Expected Results

The new information obtained from this investigation will: (1) improve the odds of finding similar andesitic systems anywhere on Earth; (2) help reduce costs in exploiting those systems already secured, including Awibengkok itself; and (3) help enable reservoir engineers to prolong the systems' productive lives through more informed long-term development strategies. The work will also inevitably yield a detailed picture of the Awibengkok system's evolution since inception, especially; (A) the nature and timing of events specifically linked to the creation or modification of porosity and permeability; (B) fluid sources, volumes, pathways, chemical transformations, and thermal histories. This knowledge will be valuable not only in

geothermal exploration, development, and research, but also in the search for and mining of analogous, low-sulfidation, volcanic-hosted epithermal mineral deposits.

Acknowledgements

DOE support for the Awibengkok project's Chief Scientist, the author of this summary, is being provided by OGT under Contract No. DE-AC07-95ID13274. Much of this summary is abstracted from Hulen and Anderson (1998), and for that effort the writer is indebted to Tim Anderson, Research Coordinator for Unocal Geothermal. Other Unocal scientists who are providing valuable advice and insight include Glen Melosh, Tom Powell, Brian Koenig, Jim Stimac, Iwan Prihaswan, and Birean Sagala.

Illustrations by Ron Wilson and Doug Jensen

References

Effendi, A.C., 1974, Geologic map of the Bogor quadrangle, Java (Indonesia): Geological Survey of Indonesia, Ministry of Mines, Scale 1:100,000.

Effendi, A.C., 1991, Peta sebaran lokasi lapangan panasbumi di Indonesia (Map of localities of geothermal fields in Indonesia): Volcanological Survey of Indonesia, Directorate General of Geology and Mineral Resources, Department of Mines and Energy, Scale 1: 6,000,000.

Ganda, S., Sunaryo, D., Hantono, D., and Tampubulon, T., 1992, Exploration progress of high-enthalpy geothermal prospect(s) in Indonesia: Geothermal Resources Council, Transactions, v. 16, p. 83-88.

Ganefianto, N., and Shemeta, J., 1996, Development strategy for the Awibengkok geothermal field, West Java, Indonesia: Indonesian Petroleum Association, 25th Anniversary Convention, Proceedings, 11 p.

Hulen, J.B., and Anderson, T.A., 1998, The Awibengkok, Indonesia, geothermal research project: Stanford University, 23rd Workshop on Geothermal Reservoir Engineering, Proceedings (in press), 8 p.

Murray, L.E.,., Rohrs, D.T., and Rossknicht, T.G., 1995, Resource evaluation and development strategy, Awibengkok field: Florence, Italy, World Geothermal Congress, Proceedings, p. 1415-1420.

Rachman, A., Lubis, L.K., Boedihardi, M., Suroto, and Mulyono, A., 1995, Geothermal prospects in Indonesia – Prospect status and development opportunity: Florence, Italy, World Geothermal Congress, Proceedings, p. 531-535.

Radja, V.T., 1990, Review of the status of geothermal development and operation in Indonesia, 1985-1990: Geothermal Resources Council, Transactions, v. 14, p. 127-145.

Simkin, T., and Siebert, L., 1994, Volcanoes of the world (2nd edition): Tucson, Arizona, Geoscience Press, in association with the Smithsonian Institution, 349 p.

Unocal Geothermal Indonesia, PERTAMINA, PLN, and Nusamba Geothermal, 1997, Gunung Salak geothermal project guidebook, 21 p.

Concurrent Session 3:

Reservoir Technology

MULTIPHASE INVERSE MODELING: AN OVERVIEW

Stefan Finsterle
Lawrence Berkeley National Laboratory
Earth Sciences Division, Mail Stop 90-1116
Berkeley, CA 94720
(510) 486-5205
SAFinsterle@lbl.gov

ABSTRACT

Inverse modeling is a technique to derive model-related parameters from a variety of observations made on hydrogeologic systems, from small-scale laboratory experiments to field tests to long-term geothermal reservoir responses. If properly chosen, these observations contain information about the system behavior that is relevant to the performance of a geothermal field. Estimating model-related parameters and reducing their uncertainty is an important step in model development, because errors in the parameters constitute a major source of prediction errors. This paper contains an overview of inverse modeling applications using the ITOUGH2 code, demonstrating the possibilities and limitations of a formalized approach to the parameter estimation problem.

INTRODUCTION

Numerical modeling of nonisothermal multiphase flow in fractured-porous media has reached a level of sophistication that allows one to accurately simulate coupled flow, transport, and heat exchange processes in a geothermal reservoir under a variety of natural and production-induced conditions (Pruess et al., 1997). However, uncertainties in the parameters describing the hydrogeologic properties of the geothermal reservoir often obliterate the theoretically high precision of numerical simulations. An even greater impact on the predicted system behavior is generated by errors in the conceptual model, making the identification of the relevant features and parameters the most important step in model development.

Data describing the geothermal reservoir characteristics are usually obtained using a variety of methods, each of which producing information pertinent to a specific scale and a particular process. In previous publications (Finsterle and Pruess, 1995; Finsterle et al., 1997) we have argued that hydrogeologic parameters should be determined based on production data (flow rates, enthalpies, and temperatures) and using a model with a structure similar to that employed for the subsequent predictions. Automatic history matching of relevant test and production data assures that *model-related* parameters are estimated, thus increasing the reliability of the predictions.

The project described in this paper aims at enhancing automatic history matching and optimization techniques for analyzing problems in geothermal reservoir engineering. Developing inverse modeling capabilities for a nonisothermal multiphase reservoir simulator provides the means to reduce errors and uncertainties in the input parameters. The fact that parameter uncertainties constitute a major source of prediction uncertainty emphasizes the importance of the parameter estimation process in general, and the assessment of parameter sensitivities and estimation errors in particular.

We have developed inverse modeling capabilities for the TOUGH2 simulator (Pruess, 1991) for applications in nuclear waste isolation, environmental sciences, and geothermal engineering. The ITOUGH2 code ("Inverse TOUGH2") permits the estimation of TOUGH2 input parameters based on any type of observation for which a corresponding TOUGH2 output can be calculated (Finsterle, 1997a). Furthermore, a detailed residual and error analysis can be performed, and the uncertainty of model predictions can be evaluated using either a linear analysis or Monte Carlo simulations.

The purpose of this paper is to provide an overview of ITOUGH2 applications to a variety of multiphase flow problems on a wide range of scales and involving different processes. The ability of inverse modeling to extract information from measured data will be demonstrated, along with its limitations, which are usually a consequence of systematic errors in either the model or the data.

ELEMENTS OF INVERSE MODELING

In this section, we briefly summarize the various steps involved in the iterative procedure of automatic model calibration. A detailed discussion of inverse modeling theory can be found elsewhere (e.g., Carrera and Neuman, 1986).

The flow chart shown in Figure 1 illustrates the process and main elements of inverse modeling.

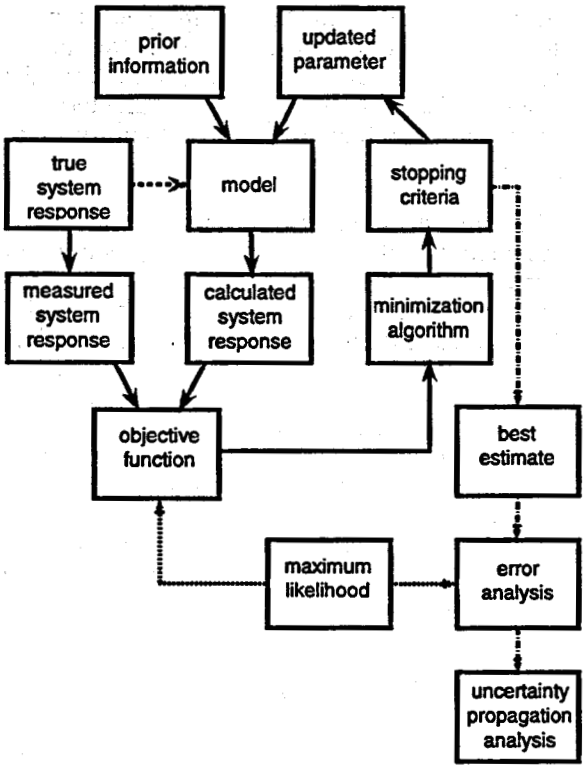

Figure 1. Inverse modeling flow chart showing main elements of automatic model calibration procedure.

The core of an inverse modeling code is an accurate, efficient, and robust simulation program that solves the so-called forward problem. It must be capable of simulating the flow and transport processes that govern the observed system response. As mentioned above, we use TOUGH2 (Pruess, 1991) to model multiphase fluid and heat flow in fractured-porous media. In addition to selecting the simulator, a problem- and site-specific conceptual model has to be developed. Note that any error in the conceptual model leads to a bias in the parameter estimates, which is usually much larger than the uncertainty introduced by random measurement errors.

Next, an objective function has to be selected to obtain an aggregate measure of deviation between the observed and calculated system response. The choice of the objective function can be based on maximum likelihood considerations, which for normally distributed measurement errors leads to the standard weighted least squares criterion (Carrera and Neuman, 1986):

$$S = \mathbf{r}^T \mathbf{C}_{zz}^{-1} \mathbf{r} \qquad (1)$$

Here, $\mathbf{r}$ is the residual vector with elements $r_i = z_i^* - z_i(\mathbf{p})$, where z_i^* is an observation (e.g., pressure, temperature, flow rate, etc.) at a given point in space and time, and z_i is the corresponding simulator prediction, which depends on the vector $\mathbf{p}$ of the unknown parameters to be estimated. The i-th diagonal element of the covariance matrix $\mathbf{C}_{zz}$ is the variance representing the measurement error of observation z_i^*. Note that alternative objective functions are available, which may have significant advantages over the traditional least-squares formulation (Finsterle and Najita, 1997).

The objective function S has to be minimized in order to maximize the probability of reproducing the observed system state. Due to strong nonlinearities in the functions $z_i(\mathbf{p})$, an iterative procedure is required to minimize the objective function S. A number of minimization algorithms are available in ITOUGH2. They reduce the objective function by iteratively updating the parameter vector $\mathbf{p}$ based on the sensitivity of z_i with respect to p_j. Details about the minimization algorithms implemented in ITOUGH2 can be found in Finsterle (1997a).

Finally, under the assumption of normality and linearity, a detailed error analysis of the final residuals and the estimated parameters is conducted. As demonstrated in Finsterle and Pruess (1995a,b), these analyses provide valuable information about the estimation uncertainty, the adequacy of the model structure, the quality of the data, and the relative importance of individual data points and parameters. In addition to its efficiency, it is mainly the formalized sensitivity, residual, and error analyses that make inverse modeling preferable over the conventional trial-and-error model calibration.

APPLICATIONS

ITOUGH2 has been applied to a number of synthetic and actual multiphase inverse problems on different scales and with different objectives. Applications to geothermal engineering problems have been described in Finsterle and Pruess (1995b), White (1995), Finsterle and Pruess (1997), Finsterle et al. (1997), and Guerrero et al. (1998). An additional set of sample problems with a detailed description of the ITOUGH2 program options can be found in Finsterle (1997b). Table 1 shows the four selected applications of increasing scale that will be discussed in the remainder of this paper.

Table 1. Summary Description of Selected ITOUGH2 Applications

#	Application	Parameters	Observations
1	Gas-pressure-pulse-decay experiment	Permeability Porosity Klinkenberg factor	Pressure in upstream and downstream gas reservoir
2	Ventilation experiment	Permeability van Genuchten parameters	Water potentials Pressures Evaporation rate
3	Atmospheric pressure fluctuation	Gas diffusivity	Pneumatic pressure
4	Calibration of geothermal reservoir model	Permeability Porosity Steam saturation van Genuchten parameters	Pressure Enthalpy

In Application 1, permeability and porosity of a very tight fine-grained graywacke core plug from the Geysers Coring Project are determined using the gas-pressure-pulse-decay (GPPD) method, in which a reservoir attached to the dry sample is rapidly pressurized using nitrogen gas (see Figure 2). Gas starts flowing through the sample, and the pressure change over time is observed in both the upstream and downstream reservoirs. Using nitrogen gas as opposed to water has the advantage of shorter test duration due to the increased mobility of the fluid. Furthermore, the high compressibility allows the determination of a relatively independent porosity estimate from the steady-state pressure data. Knudsen diffusion effects, however, lead to increased gas fluxes and thus require estimating a third parameter, the Klinkenberg gas slip factor b, along with absolute permeability and porosity. Details can be found in Finsterle and Persoff (1997).

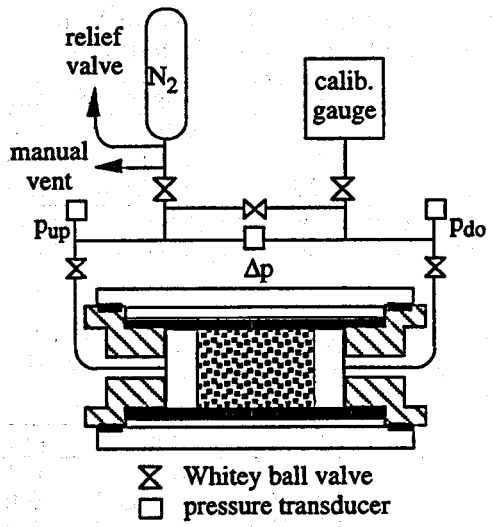

Figure 2. Gas-pressure-pulse-decay apparatus.

Figure 3 shows the data (symbols), the simulated pressures with an initial set of parameters (dash-dotted lines), and the match obtained after 5 ITOUGH2 iterations (solid lines).

The almost perfect match shown in Figure 3 may lead to the conclusion that the parameters were estimated with a high degree of precision. However, the covariance matrix of the estimated parameters (Table 2) reveals that the very strong negative correlation between the permeability k and the Klinkenberg factor b yields an estimation uncertainty of more than an order of magnitude.

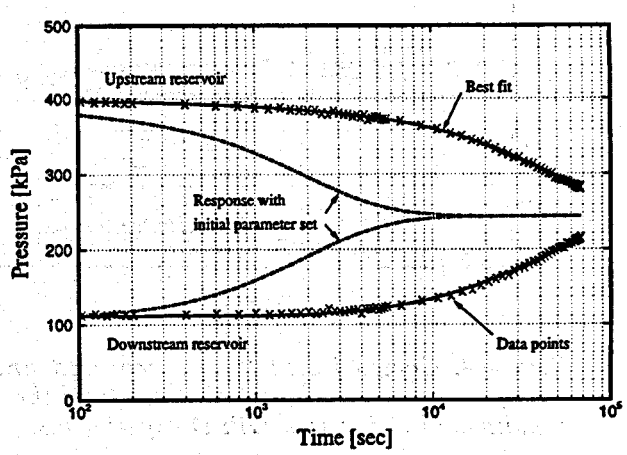

Figure 3. Inversion of data from a GPPD experiment. Comparison between measured and calculated pressure transient curves in the upstream and downstream gas reservoirs.

Table 2. Estimation Covariance Matrix, Inversion of One GPPD Experiment

	log(k)	log(b)	porosity
log(k)	1.67	-0.99	-0.87
log(b)	-1.90	2.16	0.87
porosity	-5.79E-4	6.59E-4	2.64E-7

Diagonal contains variances, lower triangle is covariance matrix, upper triangle is correlation matrix.

Table 3. Estimation Covariance Matrix, Simultaneous Inversion of Three GPPD Experiments.

	log(k)	log(b)	porosity
log(k)	1.05E-4	-0.52	-0.12
log(b)	-1.07E-4	4.10E-4	-0.02
porosity	-1.30E-6	-3.62E-7	1.06E-6

Diagonal contains variances, lower triangle is covariance matrix, upper triangle is correlation matrix.

The two highly correlated parameters can be effectively decoupled by simultaneously inverting data from three experiments performed at three different pressure levels. Weakening the correlation coefficient from -0.99 to -0.52 allows for a more independent determination of all parameters, thus significantly reducing the estimation uncertainty as shown in Table 3. The match to all three GPPD experiments is shown in Figure 4.

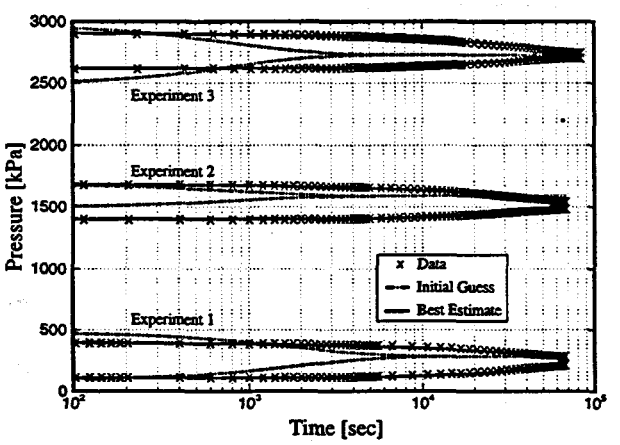

Figure 4. Comparison between measured and calculated pressure transient curves from three simultaneously inverted GPPD experiments.

This example shows the importance of a formalized error analysis for a comprehensive interpretation of inverse modeling results. More details about correlations, the impact of systematic errors and their removal by parameterization, and the use of robust estimators can be found in Finsterle and Persoff (1997) and Finsterle and Najita (1997).

Application 2 demonstrates the flexibility of inverse modeling. A variety of different data from an unconventional experiment are used for the determination of two-phase hydraulic properties.

Figure 5 shows a schematic of a ventilation experiment performed at the Grimsel Rock Laboratory, Switzerland. In order to determine the macropermeability of crystalline rocks, the total inflow of moisture into an isolated, ventilated drift section is measured in a cooling trap. Due to ventilation, the initially saturated granodiorite formation starts to dry out radially from the drift despite a strong water pressure gradient. By measuring the water potential using thermocouple psychrometers (TP), the gas pressure in two boreholes (see Figure 6), and the average evaporation rate, it was possible to determine the absolute permeability as well as the two-phase flow parameters of the van Genuchten model (Luckner et al., 1989). The example demonstrates that virtually any type of sensitive data can be used in a joint inversion to estimate parameters that affect the observed system behavior. This flexibility of inverse modeling can be exploited to conceive new experimental designs and to analyze a larger variety of observations obtained under natural and testing conditions. The ventilation experiment, the problem of nonuniqueness, and a nonlinear error analysis are discussed in detail in Finsterle and Pruess (1995).

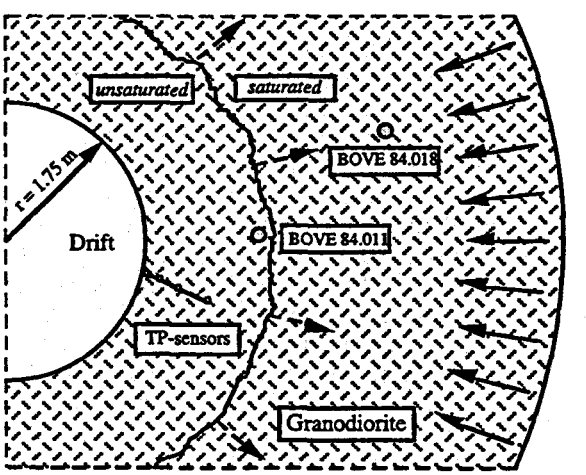

Figure 5. Schematic of ventilation experiment, showing thermocouple psychrometer (TP) and borehole locations.

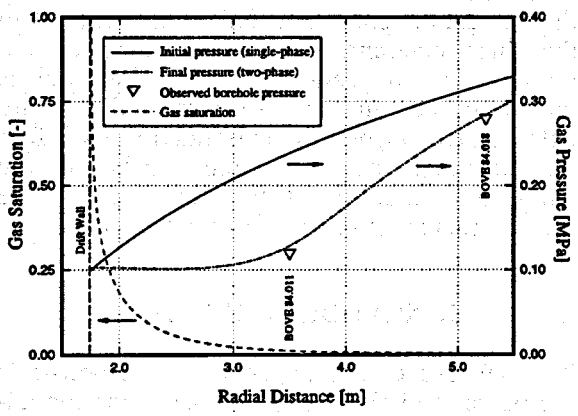

Figure 6. Calculated gas saturation and pressure profiles after 80 days of ventilation. The measured borehole pressures are shown as triangles.

Application No. 3 uses transient gas pressure data on a regional scale to estimate gas diffusivity of a thick, heterogeneous, unsaturated zone. Atmospheric pressure variations at the land surface are damped as they propagate through the formation. The pneumatic pressure signals observed at several levels in a deep borehole exhibit a specific time lag and reduction in amplitude depending upon gas diffusivity. Figure 7 shows the pressure fluctuations at the land surface, and the comparison between the measured and calculated pneumatic signals. Analyzing pneumatic pressures by inverse modeling provides a means to determine effective fracture network properties in the unsaturated zone on a large scale. More details can be found in Finsterle (1997b).

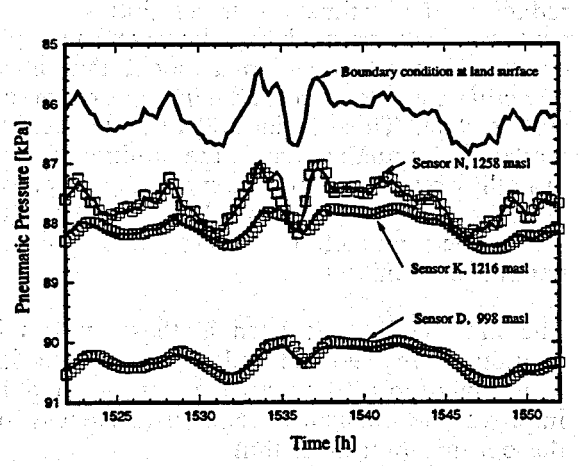

Figure 7. Match of pneumatic pressures at three elevations in a deep borehole. The applied boundary pressure fluctuations at the land surface (1371 masl) are also shown.

The final application presents preliminary results of an inversion of pressure and enthalpy data from a geothermal well, using a simple, one-dimensional, radial model with homogeneous rock properties. The thickness of the reservoir is assumed to be 200 m; the feed zone is at a depth of about 1600 m. Initial reservoir temperature was measured to be 336 °C.

Note that the pressure and enthalpy data were obtained at the wellhead, whereas the simulation results refer to downhole conditions. While heat loss and enthalpy changes along the wellbore are not expected to be large, the pressure drop, a function of flow rates and phase composition, is significant. Here, we assume that the pressure drop is independent of flow rate; it will be treated as an unknown parameter to be estimated simultaneously with the reservoir properties.

The parameters to be estimated are selected based on a sensitivity analysis. Only the most sensitive parameters of relative low overall correlation are subjected to the estimation process. They include the logarithm of the absolute permeability, porosity, initial vapor saturation, residual liquid saturation, the van Genuchten parameter n in the relative permeability function (Luckner et al., 1989), and a constant c_{well} representing the pressure drop along the wellbore.

Data from 85 days of production were used to calibrate the model. The production rate during this period varied around 4 kg/s. Data are again available after t=106 days, when production rate was increased to about 10 kg/s. This latter period was not used for calibration but for testing the model predictions. Figure 8 shows the prescribed production rate, the observed and calculated enthalpies and pressures for the initial parameter set as well as the best estimate, along with the 95% error band. The corresponding parameter sets are given in Table 4.

Comparison of the responses obtained with the initial and final parameter set demonstrates the sensitivity of the modeling results with respect to the relatively minor updates needed to improve the match. More important, it reveals the difficulties of the current model to simulate the relatively strong pressure drop between t=55 and t=70 days, without resulting in excessively low pressures once the production rate is increased. Recall that wellbore effects are not modeled. While the enthalpies are matched reasonably well (except at early times,

when fracture flow may be dominant), the model fails to predict the enthalpy during the last period of high production, when most of the produced fluid in the model consists of vapor.

Table 4. Initial Guess, Best Estimate, and Estimation Uncertainty

Parameter	Initial Guess	Best Estimate	Standard Deviation
log (perm. [m^2])	-14.50	-14.48	0.01
porosity [-]	0.02	0.05	0.01
initial vapor sat. [-]	0.02	0.01	0.01
res. liq. sat. [-]	0.20	0.18	0.04
vG parameter *n* [-]	3.00	2.45	0.08
c_{well} [bar]	40.00	45.40	1.14

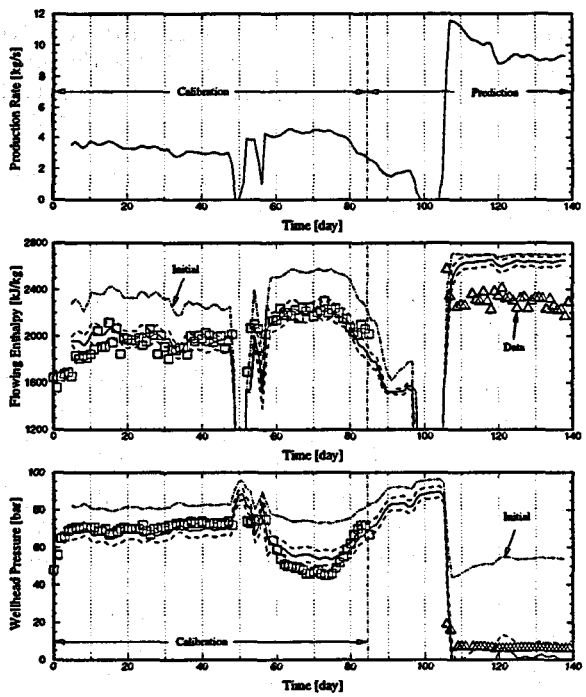

Figure 8. Calibration and prediction of flowing enthalpy and wellhead pressure. The top panel shows the prescribed production rate. Squares are measured data used for calibration. Triangles are measured data used for validation. The dash-dotted lines are the model results with the initial parameter set (see Table 4). Simulation results based on the estimated parameter set are shown as solid lines. Error bands (dashed lines) are calculated using linear uncertainty propagation analysis.

It should be realized that the conditions during the validation phase are quite different from the ones encountered while calibrating the model. Vapor saturation near the well is increased, i.e., the relative permeabilities are extrapolated beyond the calibrated range. It is obvious that the systematic errors in the simplified model must be eliminated before the parameter set can be further assessed.

CONCLUDING REMARKS

The purpose of this paper was to demonstrate the power and flexibility of an inverse modeling approach for automatic history matching. Four selected ITOUGH2 applications on different scales have been discussed. It was shown that model-related parameters can be estimated by performing a joint inversion of a variety of data collected under testing conditions or during production. The advantages of inverse modeling procedures are that they overcome the time and labor-intensive tedium of trial-and-error model calibration. More importantly, the formalized approach allows one to obtain objective measures of estimation uncertainty, parameter correlation, and overall goodness-of-fit.

Forward and inverse modeling improve our understanding of the basic multiphase flow processes and allow us to study the impact of parameters on model predictions. The reliability of model predictions in complicated nonisothermal multiphase flow systems strongly depends on the accuracy with which the input parameters can be determined. Inverse modeling aims at assessing and reducing the estimation uncertainties. The success of inverse modeling, however, depends on our ability to develop a model that is *in principle* capable of reproducing the observed system state. This crucial and difficult step of model conceptualization is the limiting factor in both forward and inverse modeling, because any error in the conceptual model leads to systematic prediction errors and biased parameter estimates.

The ITOUGH2 code used in these studies is continually revised and updated to account for newly incorporated physical processes, and to improve the robustness and effectiveness of the optimization algorithm.

ITOUGH2 is planned to be released through DOE's Energy Science and Technology Software Center in the summer of 1998. More

information can be obtained at the following web site:
http://www-esd.lbl.gov/ITOUGH2

ACKNOWLEDGMENT

This work was supported, in part, by the Assistant Secretary for Energy Efficiency and Renewable Energy, Office of Geothermal Technologies, of the U.S. Department of Energy under Contract No. DE-AC03-76SF00098. We would like to thank K. Pruess and G. Moridis for thoughtful reviews.

REFERENCES

Carrera, J. and S. P. Neuman, "Estimation of Aquifer Parameters Under Transient and Steady-State Conditions, 1, Maximum Likelihood Method Incorporating Prior Information," *Water Resour. Res. 22*(2), 199-210, 1986.

Guerrero, M. T., C. Satik, S. Finsterle, and R. Horne, "Inferring Relative Permeability From Dynamic Boiling Experiments," *Proceedings*, 23rd Workshop on Geothermal Reservoir Engineering, Stanford University, Stanford, Calif., January 26-28, 1998.

Finsterle, S., "ITOUGH2 Command Reference, Version 3.1," Report LBNL-40041, Lawrence Berkeley National Laboratory, Berkeley, Calif., 1997a.

Finsterle, S., "ITOUGH2 Sample Problems," Report LBNL-40042, Lawrence Berkeley National Laboratory, Berkeley, Calif., 1997b.

Finsterle, S. and J. Najita, "Robust Estimation of Hydrogeologic Model Parameters," Report LBNL-40684, Lawrence Berkeley National Laboratory, Berkeley, Calif., (submitted to *Water Resour. Res.*), 1997.

Finsterle, S. and P. Persoff, "Determining Permeability of Tight Rock Samples Using Inverse Modeling," *Water Resour. Res., 33*(8), 1803-1811, 1997.

Finsterle, S. and K. Pruess, "Solving the Estimation-Identification Problem in Two-Phase Flow Modeling," *Water Resour. Res., 31*(4), 913-924, 1995a.

Finsterle, S. and K. Pruess, "Automatic History Matching of Geothermal Field Performance," *Proceedings*, 17th New Zealand Geothermal Workshop, p. 193-198, Auckland, New Zealand, November 8-10, 1995b.

Finsterle, S. and K. Pruess, "Development of Inverse Modeling Techniques for Geothermal Applications," *Proceedings*, DOE Geothermal Program Review XV, p. 2-47 - 2-54, San Francisco, Calif., March 24-26, 1997.

Finsterle, S., K. Pruess, D. P. Bullivant and M. J. O'Sullivan, "Application of Inverse Modeling to Geothermal Reservoir Simulation," *Proceedings*, 22nd Workshop on Geothermal Reservoir Engineering, Stanford University, Stanford, Calif., p. 309-316 January 27-29, 1997.

Luckner, L., M. T. van Genuchten, and D. Nielsen, "A Consistent Set of Parametric Models for the Two-Phase Flow of Immiscible Fluids in the Subsurface," *Water Resour. Res., 25*(10), 2187-2193, 1989.

Pruess, K., "TOUGH2-A General-Purpose Numerical Simulator for Multiphase Fluid and Heat Flow," Report LBL-29400, Lawrence Berkeley National Laboratory, Berkeley, Calif, 1991.

Pruess, K., C. Oldenburg, G. Moridis and S. Finsterle, "Water Injection into Vapor- and Liquid-Dominated Reservoirs: Modeling of Heat Transfer and Mass Transport," *Proceedings*, DOE Geothermal Program Review XV, p. 2-55 - 2-62, San Francisco, Calif., March 24-26, 1997.

White, S. P., "Inverse Modelling of the Kawerau Geothermal Reservoir, NZ," *Proceedings*, 17th New Zealand Geothermal Workshop, p. 211-216, Auckland, New Zealand, November 8-10, 1995.

WATER ADSORPTION AT HIGH TEMPERATURE ON CORE SAMPLES FROM THE GEYSERS GEOTHERMAL FIELD

Miroslaw S. Gruszkiewicz
Juske Horita
John M. Simonson
Robert E. Mesmer
Oak Ridge National Laboratory
(423) 574-4965

ABSTRACT

The quantity of water retained by rock samples taken from three wells located in The Geysers geothermal field, California, was measured at 150, 200, and 250 °C as a function of steam pressure in the range $0.00 \leq p/p_0 \leq 0.98$, where p_0 is the saturated water vapor pressure. Both adsorption and desorption runs were made in order to investigate the extent of the hysteresis. Additionally, low temperature gas adsorption analyses were made on the same rock samples. Mercury intrusion porosimetry was also used to obtain similar information extending to very large pores (macropores). A qualitative correlation was found between the surface properties obtained from nitrogen adsorption and the mineralogical and petrological characteristics of the solids. However, there was no direct correlation between BET specific surface areas and the capacity of the rocks for water adsorption at high temperatures. The hysteresis decreased significantly at 250 °C. The results indicate that multilayer adsorption, rather than capillary condensation, is the dominant water storage mechanism at high temperatures.

INTRODUCTION

The decline in reservoir pressures observed at The Geysers after a period of rapid development (Barker, 1992) prompted an increase in the research of the mechanisms of water storage. There is no doubt that at various locations in the reservoir and at various stages in production history, water can be present as bulk liquid, steam, capillary condensate and surface adsorbate. For the purposes of performance modeling and forecasting it is important to know the proportions between these storage mechanisms, since the expected reservoir responses to the production of geothermal steam would be different. It is expected that adsorption can control the response of the reservoir to both production of steam and injection of water in the wells where the pressure falls significantly below its original level in the undisturbed reservoir.

The goal of this study was to expand our understanding of the adsorption/desorption processes occurring in geothermal reservoir rocks. The desired outcome is an improvement of the efficiency of the recovery of geothermal energy through more accurate inputs to both simple empirical reservoir performance forecasting schemes and comprehensive reservoir models, so that the life of the reservoir can be sustained for the most economical exploitation of the resource.

The reservoir pressure affects directly the economics of geothermal energy production. The rates of both pressure and flow rate decline during production are used as an indicator of the size of the resource and the expected life and performance of the reservoir (Sanyal *et al.*, 1992; Enedy, 1992). It was determined that the initial pressure at sea level in the central part of The Geysers reservoir was 35.4 bars (Lippmann *et al.*, 1978), which corresponds to a boiling temperature of 243.3 °C. Since this temperature is close to the measured well temperatures, the reservoir must contain some amount of free water present in wide pores and fractures (Pruess and O'Sullivan, 1992). The steam produced by a vapor-dominated reservoir initially comes from the evaporation of the excess liquid water. After the reserves of this bulk liquid are, at least locally, exhausted, the water retained in smaller pores and adsorbed on the surfaces starts to evaporate, and the pressure starts to decline. The process of depletion of a steam-dominated reservoir, assuming thermodynamic equilibrium over all the volume of a closed system (i.e. slow production rate), is shown schematically in Figure 1.

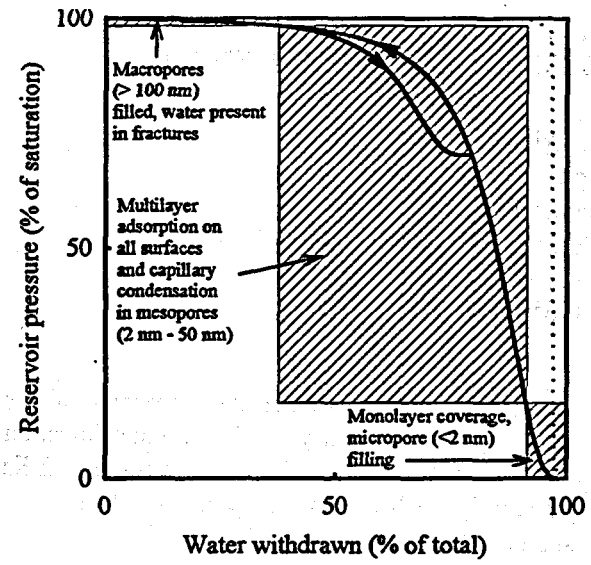

Figure 1. Equilibrium pressure decline during depletion of a vapor-dominated geothermal reservoir.

The actual, dynamic response of the reservoir may not follow closely the adsorption isotherm if the production rate is high compared to the relaxation rate of the reservoir, or if the reservoir is being recharged. The flat (nearly horizontal) part of the solid curve in Figure 1 indicates that it would be rather difficult to accurately estimate the amount of water present initially in the reservoir by measuring the reservoir equilibrium pressure decline. At this stage, the withdrawal of even large amounts of water is associated with an immeasurably small (long-term) pressure drop. In the later stages of reservoir depletion, the amount of water left in the reservoir can be determined in principle from reservoir pressure data, if the water retention capacity as a function of pressure (i.e. an adsorption isotherm) and the reservoir size are known.

The shapes of the pressure decline curves can be significantly different from that shown in Figure 1, in particular in their high-pressure portions, where a hysteresis loop usually occurs. The particular shape depends on the properties of the reservoir rocks, such as mineral compositions, porosities, pore size distributions, and the predominant pore shapes. It can also depend on the way the pores are filled or emptied and on the temperature. Generally, adsorption, or any other mechanism of water pressure lowering, makes the pressure decline more gradual. Since steam pressure is the driving force for further depletion, pressure lowering acts as a mechanism delaying a complete dry-out. Adsorption properties of geothermal reservoir rocks have the greatest impact on the behavior of vapor-dominated geothermal reservoirs, with the steam pressure substantially lower than the saturation pressure, but which still contain a considerable amount of water held by the solid-liquid interactions. The knowledge of adsorption characteristics can also help in better understanding of the reservoir's response to water injection. The time needed for the injected water to reach the production wells may be longer with adsorption since the injected water will at first readsorb on the surface of fractured rocks. The amount of water needed during injection may be different from the amount of water previously withdrawn, due to hysteresis, and to different conditions at the injection well.

Possible mechanisms of water storage based on solid-fluid interactions include micropore filling, cooperative adsorption (involving interactions between adsorbate molecules), monolayer and multilayer adsorption, capillary condensation, and interactions similar in varying degrees to chemical bonding. Since physical models developed to describe these phenomena are different, it would be desirable to determine the prevailing water storage mechanism at the actual reservoir temperature, so that an adequate model can be developed.

One of the reasons for measuring adsorption isotherms over a range of temperatures is to be able to distinguish between capillary condensation and multilayer adsorption. This distinction is possible because multilayer adsorption isotherms as a function of the relative pressure p/p_0 are expected to change only very little with temperature, while capillary condensation is temperature dependent. According to the established simplified model of multilayer physical adsorption, represented most often by the BET equation (Brunauer *et al.*, 1938), a single layer of adsorbed molecules is sufficient to screen the subsequent layers from interactions with the solid surface. The creation of an adsorption layer and condensation into bulk liquid are then thermodynamically similar processes. Since the associated enthalpy changes and volumetric properties are nearly the same, p/p_0 at a particular extent of adsorption is expected to remain constant with temperature.

In contrast to multilayer adsorption, the saturated vapor pressure over capillary condensate should be strongly affected by temperature as predicted by the Kelvin equation (Defay *et al.*, 1966). In fact, the surface tension of any fluid decreases to zero as the temperature approaches the liquid-vapor critical point. However, at a given temperature, the experimental relationship between relative pressure and the amount of water retained can be described equally well either in terms of the Kelvin equation or an adsorption equation like the BET adsorption isotherm. Hsieh and Ramey (1978) noted that experimental data are sometimes described in the literature in terms of capillary condensation, using the Kelvin equation, at conditions where the capillary condensation model is no longer valid. They suggested that the multilayer adsorption model (and the BET equation) would provide a more appropriate description. Even at conditions where capillary condensation certainly occurs, a substantial part of the condensed phase may be more properly described in terms of the multilayer adsorption concept.

Studies of high temperature water adsorption in porous materials in general and rocks in particular have been rather scarce (Shang *et al.*, 1995). The temperatures did not exceed 150 °C, with most of the reported measurements done at 120 °C and below. Recently, Bertani *et al.* (1996) reported adsorption (but not desorption) isotherms on several geothermal reservoir rocks at temperatures between 170 °C and 200 °C. They found no temperature dependence of the amount of water adsorbed in this temperature range. Shang *et al.* (1995) found an increase in the amount of water adsorbed as the temperature increased from 80 °C 130 °C. This increase was more pronounced at high relative pressures.

EXPERIMENTAL

The measurements were performed on core samples of rocks taken from the productive steam reservoir at The Geysers. Well numbers and approximate depths were as follows:

- MLM-3, 4336 - 4336.3 ft (1322 m)
- Prati-State 12, 6261.7 - 6261.8 ft (1909 m)
- NEGU-17, 8530 - 8530.5 ft (2600 m).

The rocks were fine to medium grained graywacke, which had been intensely hydrothermally altered during the time the reservoir was liquid-dominated, and the calcite, originally present in veins, was largely replaced by calc-silicates (Hulen *et al.*, 1991, 1992). Hydrothermal mineralization, alteration, mineral dissolution, and fracturing are the causes for the significant porosity and permeability of the reservoir rocks in comparison with the caprock (Gunderson, 1992).

The mineral compositions of the metagraywacke samples taken from the three wells were more diverse than expected. The percentages of the component minerals are given in Table 1.

Table 1. Mineral percentages of the metagraywacke samples (Hulen, 1997).

	MLM-3	NEGU-17	PS-12
quartz	38	19	45
albite	30	16	21
chlorite	14	31	13
illite	11	14	4
epidote	1	2	11
adularia	traces	8	3
sphene + anatase	2	2	2
calcite	2	-	traces
ferroaxinite	-	2	-
organic	2	6	1

All three core samples contained traces of actinolite, apatite, and zircon, and traces of rutile were found in the MLM-3 and NEGU-17 cores. Additionally, prehnite was found in the MLM-3 sample, and pyrite, garnet, and clinopyroxene were found in the Prati-State sample. The compositions shown in Table 1 indicate that the fine grained NEGU-17 metagraywacke differs significantly from the other two more coarse grained samples in the relative amounts of quartz, albite, and chlorite. NEGU-17 also contains much more organic matter. The core from the Prati-State 12 well contains more quartz and epidote but less illite than either NEGU-17 or MLM-3.

The rocks were crushed and screened into three fractions with the following grain sizes: 2.00 - 4.25 mm ('coarse'), 0.355 - 2.00 mm ('medium'), and 0 - 0.355 mm ('fine'). Two aliquots of each of the medium fractions were loaded in the autoclave in order to evaluate possible random differences due to the heterogeneity of the samples.

The ORNL high-temperature isopiestic apparatus has been described previously. (Holmes *et al.*, 1978; Gruszkiewicz *et al.*, 1996). Briefly, the samples were placed inside a high-pressure, high-temperature autoclave in titanium pans fitting in holes in a disk which was rotated by the operator. The pans were positioned in turn on the torsion-suspension electromagnetic balance and weighed *in situ* by adjusting the electric current through the balance coil. Since the weighings were made by comparison with a set of standard weights placed inside the pressure vessel together with the samples, the method's susceptibility to significant systematic errors was greatly reduced.

In addition to the high temperature water adsorption experiments, nitrogen adsorption and desorption measurements were made across the whole pressure range for selected samples. Multipoint BET specific surface area analyses and pore size distributions were obtained from these data. Adsorption results were supplemented with mercury intrusion tests. Mercury pressure scans extended from 1.59 psia (0.110 bar) to 60000 psia (4.14 kbar), providing a nominal pore diameter range from 114 μm to 3 nm.

RESULTS

Since the properties of the rocks vary significantly with depth, it is difficult to compare directly the results obtained on different samples, even if they come from the same well. In this work, the samples are named by the well numbers, even though they do not represent the entire respective well cores. There was very good agreement between the present results and those obtained by Satik and Horne (1995) where a direct comparison could be made for an adsorption isotherm (Gruszkiewicz *et al.* 1996). However, the agreement of the desorption isotherms was not satisfactory, as the hysteresis loops obtained in this work were closed or nearly closed, while extensive low pressure hysteresis and irreversible water retention were observed by Satik and Horne (1995) and Shang *et al.* (1995) on all their samples.

Figure 2 shows the experimental results for water sorption on the medium fractions of MLM-3, NEGU-17 and Prati-State 12 cores, respectively, at 150, 200 and 250 °C.

In all the figures open symbols represent experimental results on the adsorption branches,

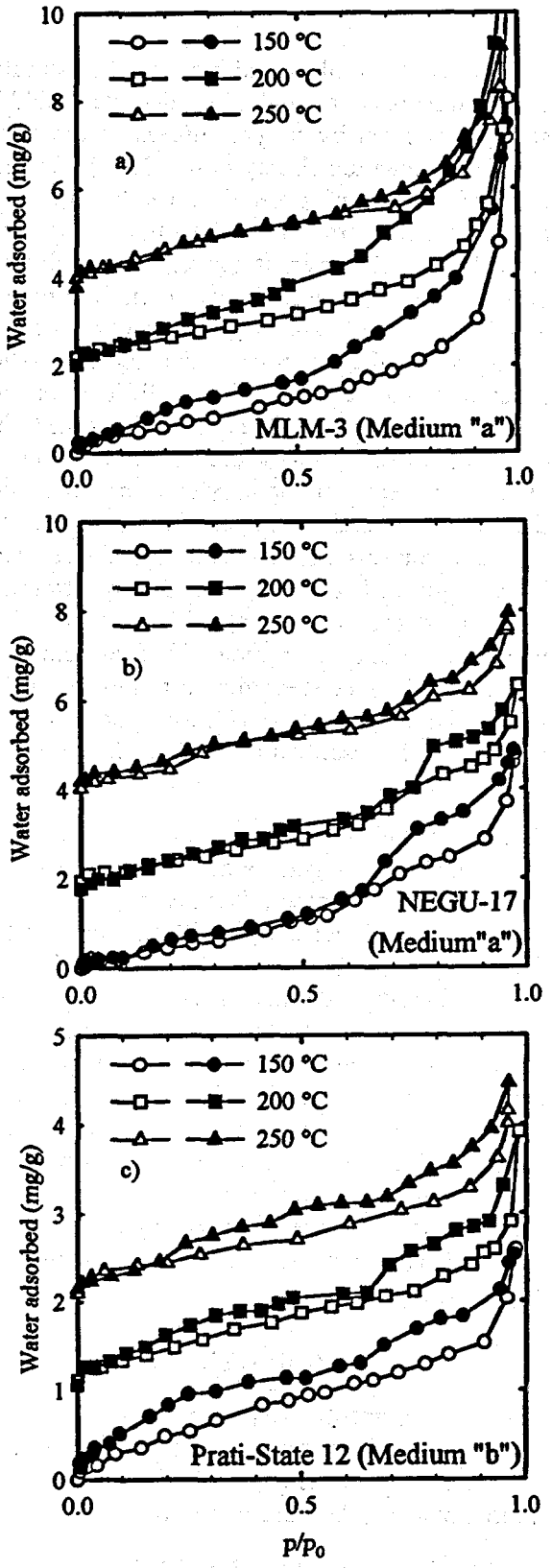

Figure 2. Adsorption and desorption isotherms of water on the medium grain size fractions of the core samples; a) MLM-3, b) NEGU-17, c) Prati-State 12. Offsets of either 1 and 2 mg/g, or 2 and 4 mg/g, were added to the 200 and 250 °C isotherms to prevent overlapping.

and filled symbols represent desorption branches. The following features of physical adsorption of water on the rocks investigated can be seen in Figure 2:

- There is essentially no temperature dependence of the adsorption branches;
- As the temperature increases, the hysteresis loop shrinks in both the amount of the adsorbate and the pressure range (this is most clear in the NEGU-17 isotherms);
- Water adsorption is reversible (the mass of the sample in vacuum after an adsorption-desorption cycle remains the same), but;
- The hysteresis loops persist to very low pressures in the case of MLM-3 and Prati-State 12, while more distinct closure points at an intermediate pressure are present for NEGU-17. The closure points for the 'main' hysteresis loop due to capillary condensation are also visible in MLM-3 and Prati-State 12 isotherms.

While on the adsorption branch the water is largely multilayer adsorbate, in principle all of the excess retention on the desorption branch is due to capillary condensation. This explains why the desorption branch is temperature dependent, while the adsorption branch is nearly temperature independent.

The Kelvin equation accounts for the observed behavior of the hysteresis loop. An analysis of the Kelvin equation indicates that the relation between the relative pressure p/p_0 and the temperature at a constant pore diameter should be approximately linear. The experimentally determined hysteresis loop inception points at 150 °C and 200 °C for NEGU-17 are consistent with corresponding relative pressures calculated from the Kelvin equation. At 250 °C the hysteresis loops are narrow, and the inception points are not well defined. At this temperature the hysteresis is present only on the steep part of the isotherm and it is significantly reduced. (Figure 2). It appears that only a small fraction of the water is adsorbed as capillary condensate at 250 °C, close to the main reservoir temperature at The Geysers.

The causes for the low-pressure hysteresis (Figure 2a and 2c) on very heterogeneous rock samples are difficult to identify with certainty. It has been known (Arnell and McDermott, 1957) that swelling of some sorbents, caused by the presence of adsorbates, can lead to low-temperature hysteresis as new surface sites open up during desorption. Sorbent swelling occurs to a detectable extent even in materials with a rigid structure. Low-pressure hysteresis of water on calcite was observed by Gregg and Gammage (1972) and attributed to the penetration of water deep into molecular-size crevices between adjacent surfaces of the lamellar solid, where it is held by relatively strong forces. Finally, dissolution of the solid in the adsorbent can probably cause both positive and negative hysteresis, depending on whether new adsorption sites are created or destroyed. The components that are most likely responsible for the low-pressure hysteresis observed in the altered graywacke are chlorite and other minerals related to clays, or calcite.

All the nitrogen adsorption isotherms obtained in this work had well defined hysteresis loops closing at $p/p_0 \approx 0.45$, a rather typical value for nitrogen at temperatures close to its boiling point. Figure 3 shows nitrogen adsorption (bold lines) and desorption (regular lines) isotherms for medium grain size samples of the three cores investigated.

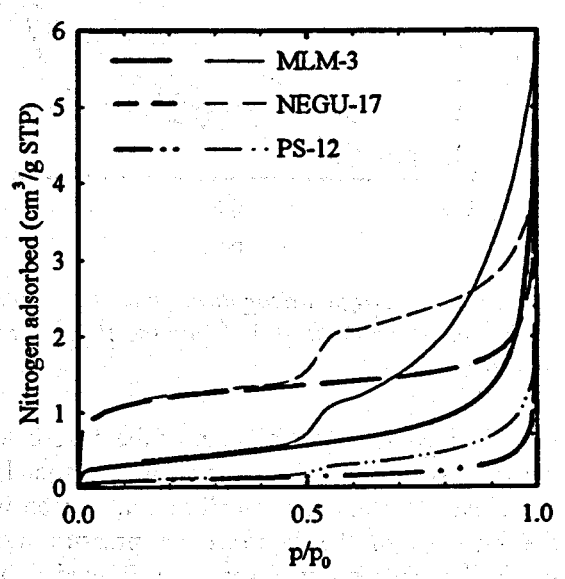

Figure 3. Adsorption and desorption isotherms of nitrogen at 77 K on the medium grain size fractions of the three cores investigated.

The following characteristics of the samples can be seen in Figure 3:

- There are large differences in the amounts adsorbed by the three cores (the ratios MLM-3 :

NEGU-17 : Prati-State 12 at $p/p_0 = 0.4$ are 1 : 2.56 : 0.29; and the BET specific surface areas are 1.31, 4.06, and 0.36 m^2/g, respectively);

- NEGU-17 metagraywacke has the largest specific surface area and its pore area distribution is shifted towards smaller pores compared to the other two cores;
- The MLM-3 metagraywacke adsorbs the largest amount of nitrogen at high pressures, which is likely due to the presence of more macropores.

Figure 4 shows water adsorption isotherms of the three cores (averages of the medium and coarse fractions) at 200 °C. The following characteristics of water adsorption, in contrast to nitrogen adsorption, are evident from a comparison of Figures 3 and 4:

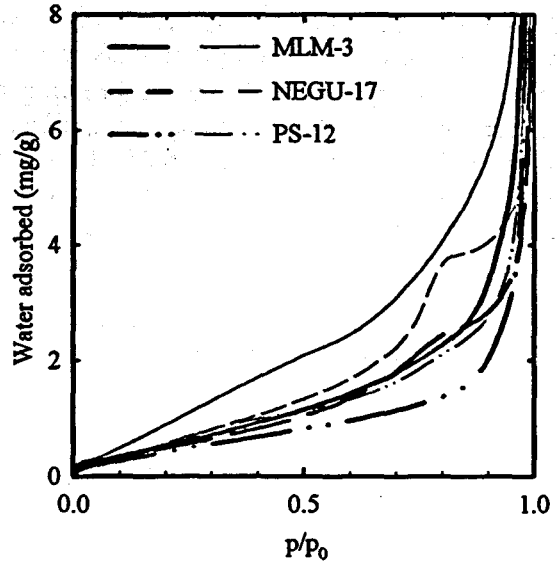

Figure 4. Average adsorption and desorption isotherms of water at 200 °C for the three cores investigated.

- The increase in the amount of the adsorbate in the very low-pressure range, which corresponds to monolayer formation, is small in comparison with the increase in the intermediate pressure range when the subsequent layers are formed. This indicates that solid-fluid interactions are relatively weaker (as compared to the fluid-fluid interactions) for water than for nitrogen. As a consequence, molecular-size pores that are wide enough to admit either N_2 or H_2O molecules, are filled more easily with nitrogen than with water. Water molecules can minimize their energy by forming hydrogen bonds and through strong dipolar interactions between each other. Relatively weak dispersion forces in nitrogen cannot compete with the interactions with the solid surface.
- In contrast to nitrogen adsorption, the amounts of water retained by the three cores at low relative pressures are similar (the ratio MLM-3 : NEGU-17 : Prati-State 12 at $p/p_0 = 0.4$ is 1 : 0.90 : 0.74;
- The NEGU-17 isotherm has a distinctly different shape from the other two isotherms.

Figures 3 and 4 show that the standard BET surface areas cannot be used directly to predict relative capacities of various rocks for water adsorption, even if these rocks are mineralogically similar. There is convincing evidence, obtained by all three methods (high temperature water adsorption, low temperature nitrogen adsorption, and ambient temperature mercury intrusion), indicating that NEGU-17 metagraywacke has significantly more micropores and also fewer very wide macropores than either MLM-3 or Prati-State 12. Pore-volume distributions calculated from both nitrogen and water adsorption isotherms show a distinct difference between NEGU-17 and the other two cores. Average pore diameters (27.2, 6.6, and 28.6 nm for MLM-3, NEGU-17, and Prati-State 12, respectively) calculated from nitrogen adsorption BET surface areas and total pore volumes also support the conclusion that NEGU-17 metagraywacke has a finer pore structure than the other two cores. The Langmuir specific surface area analysis yields even lower average pore diameter for NEGU-17 (4.7 nm).

Both nitrogen adsorption and mercury intrusion results indicated that changes in the pore structure had taken place during the high temperature adsorption experiments. Pore volume distributions showed a shift towards wider pore sizes in NEGU-17 and MLM-3 samples, while Prati-State 12 pore volume distribution remained unchanged. Since the smallest pores are most affected by changes occurring on the surface or by solid dissolution and subsequent deposition, the Prati-State 12 metagraywacke apparently has by far the fewest very narrow pores. Dissolution of the finest crystals and sealing of the finest pores was also indicated by the decreases of 20 to 30 per cent in the BET specific surface areas and increases in the average pore sizes observed for all the cases where such comparisons were made. In a sample of silica gel the fine pore structure was nearly completely destroyed upon exposure to steam, even at 150 °C. The specific surface area decreased from 542 m^2/g

by the BET method, (782 m^2/g by the Langmuir method) to 3.0 m^2/g (BET). This was likely due to the dissolution of SiO_2 in adsorbed water. Similar effects can be expected to occur, to a lesser extent, in reservoir rocks containing silica and other minerals that become increasingly soluble in water at elevated temperatures. Since there is a significant random variability between the samples, obtaining definitive evidence for these changes would require more tests performed on exactly the same aliquots before and after high temperature adsorption measurements.

Total pore volumes (and hence total porosities) are difficult to measure unambiguously by either adsorption or mercury intrusion. The adsorption isotherms of the rock samples were characterized by a steep increase of the amount of water retained with the increase in pressure towards saturation, so that the isotherms were apparently asymptotic to the $p/p_0 = 1$ axis. Such behavior is not universal in porous materials, since often a plateau at high relative pressures is found. The lack of a plateau indicates that the pore volume distribution is relatively even in the upper end of the pore size range, and there is no distinct upper pore size limit. Such shapes of adsorption-desorption isotherms are often observed with aggregates of plate-like particles or sheets giving rise to slit-shaped pores, and they seem to be consistent with porosity caused by fracturing and hydrothermal rock alteration.

The porosity results (8.4, 10.9 and 12.3 % in the sequence NEGU-17, Prati-State 12, and MLM-3) were significantly higher than those reported by Satik *et al.* (1996) for similar materials (up to 5.5 per cent for MLM-3 metagraywacke) or by Gunderson (1990) (1.1 to 5.6 per cent for NEGU-17 core of approximately the same depth as in this work). Since the widest pores are randomly distributed and may have a relatively large volume, total pore volume determinations are subject to a significant random error. On the other hand, the average density of the rocks can be determined fairly accurately (it was 2.75-2.78 g/cm^3 for the samples included in this work, with a maximum error of about 2 per cent). The main difficulty in finding porosities by the mercury intrusion method seems to lie in measuring the total volumes of the porous solids. The differences in mercury intrusion procedures (immersion pressure), sample grain sizes, and random differences between the samples can significantly impact total porosity results.

The differences in adsorption properties between MLM-3, NEGU-17, and Prati-State 12 cores were qualitatively consistent with the differences in mineral compositions (Table 1). Enhanced microporosity of the NEGU-17 samples was concomitant with more than double the content of chlorite and the largest content of organic matter. Chlorite is a mineral related chemically to montmorillonite and other clay minerals, which form, charged molecular layers able to interact with each other and to form stable structures involving water. The strength of such interactions is intermediate between that of dispersion forces and typical chemical bonding. On the other hand, quartz and feldspars, which constitute more than 65 per cent of the MLM-3 and Prati-State 12 samples, but only 45 per cent of the NEGU-17 samples, have more rigid, three-dimensional structures, which do not accommodate water as easily. The highly carbonized organic matter found in the NEGU-17 samples might contribute to the observed microporosity and hydrophobic adsorption, in a manner similar to that observed in water adsorption on charcoal (Gregg and Sing 1982, p. 262). More detailed study focusing on the properties of the constituent minerals could lead to more precise assignments of the contributions to the observed adsorption behavior, which would be useful for predicting adsorption properties of rocks.

ACKNOWLEDGEMENT

Research sponsored by the Office of Geothermal Technology (Office of Energy Efficiency and Renewable Energy), and the Office of Basic Energy Sciences, (Division of Chemical Sciences), US Department of Energy, under contract DE-AC05-96OR22464 at Oak Ridge National Laboratory operated by Lockheed Martin Energy Research Corporation.

REFERENCES

Arnell, J. C. and McDermott, H. L. (1957) "Sorption hysteresis", Proceedings of the Second International Congress on Surface Activity, Vol. 2, pp. 113-121, Butterworths, London.

Barker, B. J., Gulati, M. S., Bryan, M. A. and Riedel, K. L. (1992) "Geysers reservoir performance", Monograph on The Geysers geothermal field, ed. C. Stone, pp. 167-177. Geothermal Resources Council Special Report No. 17.

Bertani, R., Parisi, L., Perini, R. and Tarquini, B. (1996) "High temperature adsorption measurements", Proceedings of the 21st Workshop on Geothermal Reservoir Engineering, pp. 523-529, January 24-26, Stanford University, Stanford, CA.

Brunauer, S., Emmett, P. H. and Teller, E. (1938) "Adsorption of gases in multimolecular layers", J. Am. Chem. Soc., 60, 309-319.

Defay, R., Prigogine, I., Bellemans, A. and Everett, D. H. (1966) Surface tension and adsorption, p. 218, Longmans, London.

Enedy, K. L. (1992) "The role of decline curve analysis at The Geysers", Monograph on The Geysers geothermal field, ed. C. Stone, pp. 197-203. Geothermal Resources Council Special Report No. 17.

Gammage, R. B. and Gregg, S. J. (1972) "The sorption of water vapor by ball-milled calcite", J. Colloid Interface Sci., 38, 118-124.

Gregg, S. J. and Sing, K. S. W. (1982) Adsorption, Surface Area and Porosity, Academic Press, San Diego, CA.

Gruszkiewicz, M. S., Horita, J., Simonson, J. M. and Mesmer, R. E. (1996) "Measurements of water adsorption on The Geysers rocks", Proceedings of the 21st Workshop on Geothermal Reservoir Engineering, pp. 481-487, January 24-26, Stanford University, Stanford, CA.

Gunderson, R. P. (1992) "Porosity of reservoir graywacke at The Geysers", Monograph on The Geysers geothermal field, ed. C. Stone, pp. 89-93. Geothermal Resources Council Special Report No. 17.

Holmes, H. F., Baes Jr., C. F. and. Mesmer, R. E. (1978) "Isopiestic studies of aqueous solutions at elevated temperatures", J. Chem. Thermodynamics, 10, 983-996.

Hsieh, C.-H. and Ramey H. J. Jr. (1978) "An inspection of experimental data on vapor pressure lowering in porous media", Geothermal Resources Council, Transactions, 2, 295-296.

Hulen, J. B., Walters, M. A. and Nielson, D. L. (1991) "Comparison of reservoir and caprock core from the Northwest Geysers steam field, California - implications for development of reservoir porosity", Geothermal Resources Council, Transactions, 15, 11-18.

Hulen, J. B., Nielson, D. L. and Martin, W. (1992) "Early calcite dissolution as a major control on porosity development in The Geysers steam field, California – additional evidence in core from Unocal well NEGU-17", Geothermal Resources Council, Transactions, 16, 167-174.

Hulen, J. B. (1997) Personal communication.

Lippmann, S. C., Strobel, C. J. and Gulati, M. S. (1978) "Reservoir performance of The Geysers field", Geothermics, 7, 209-219.

Pruess, K. and O'Sullivan, M. (1992) "Effects of capillarity and vapor adsorption in the depletion of vapor-dominated geothermal reservoirs", Proceedings of the 17th Workshop on Geothermal Reservoir Engineering, pp. 165-174, January 29-31, Stanford University, Stanford, CA.

Sanyal, S. K., Mezies, A. J., Brown, P. J., Enedy, K. L. and Enedy, S. L. (1992) "A systematic approach to decline curve analysis for The Geysers steam field, California", Monograph on The Geysers geothermal field, ed. C. Stone, pp. 189-196. Geothermal Resources Council Special Report No. 17.

Satik, C., Horne, R. N. (1995) Experimental data published at the Stanford Geothermal Program site on the World Wide Web (http://ekofisk.stanford.edu /geotherm.html).

Satik, C., Walters, M. and Horne, R. M. (1996) "Adsorption characteristics of rocks from vapor-dominated geothermal reservoir at The Geysers, CA", Proceedings of the 21st Workshop on Geothermal Reservoir Engineering, pp. 469-479, January 24-26, Stanford University, Stanford, CA.

Shang, S., Horne, R. N. and Ramey, H. J. (1995) "Water vapor adsorption on geothermal reservoir rocks", Geothermics 24, 523-540.

Chemical Models for Optimizing Geothermal Energy Production

UCSD CHEMICAL GEOLOGY GROUP
Nancy Møller, Principal Investigator; John H. Weare, Co-Principal Investigator
Project Scientists: Jerry P. Greenberg; Zhenhao Duan
Department of Chemistry and Biochemistry
University of California, La Jolla, California, 92093

INTRODUCTION: The ability to predict chemical behavior and heat content as well as to design optimal operating strategies would significantly increase the cost effectiveness of geothermal energy production. Adverse chemical effects, such as scale formation, corrosion and noxious gas emission, which can arise from the manipulation of the high temperature natural fluids driving the energy production process, are expensive to control. Mineral precipitation, for example, can not only damage plant equipment and wells but also significantly decrease the permeability of the formations containing the geothermal fluids, thereby limiting the longevity of the resource itself. Predicting potential chemical problems will become even more important as deeper, higher temperature geothermal systems, with very high development costs, are utilized to meet future energy needs.

To predict the chemistry of geothermal energy production, it is necessary to understand the thermodynamics of the production processes. Unfortunately, the chemical behavior of high temperature brine systems is a very complex function of their composition, temperature and pressure. Since these variables can change significantly during the lifetime of the resource, past experience may not be a reliable guide for future performance. Laboratory simulations are costly and limited to the experimental conditions selected.

The UCSD Chemical Geology Group, with funding from the DOE geothermal program, is constructing computer models to accurately predict the chemical behavior of geothermal brines and their associated phases over wide ranges of composition, temperature and pressure. Our models are based on advanced theoretical developments in physical chemistry which allow description of the thermodynamics of solids, liquids and gases via their free energy. Parameterizing these expressions using experimental data provides a highly reliable representation of the equilibrium properties of complicated natural systems. The parameterization process can be extensive. It involves: finding and assessing the necessary experimental data; developing phenomenological equations which accurately and succinctly summarize these data; correlating the data and equations to evaluate the model parameters; and lastly, validating the parameterized model by comparison with data not used in the parameter evaluation process. However, the benefits of having the data represented by easily used modeling equations are considerable. In addition to interpreting and predicting the thermodynamics of a system under current T,P,X conditions, flexible computer models can easily and quickly simulate behavior under varying T,P,X conditions. Therefore, testing strategies to control unwanted behavior in active operations as well as forecasting the value of

geothermal reservoirs as potential production sites is possible with this approach. Furthermore, the modeling process increases the applicability of many experimental data by providing a means to extrapolate information from limited composition experiments (e.g., boiling data in binary systems) to the more complex situations typical of natural fluids (e.g., boiling in multi-component systems). As we develop more theoretically based phenomenologies, the amount of required data will be reduced and the region of extrapolation increased.

As our models are developed, they are incorporated into interactive software packages that facilitate their application to problems encountered by the geothermal community. Our present technology can be divided into four general modeling approaches. (1) Aqueous solution models, based on the semiempirical electrolyte equations of Pitzer (see Pitzer (1987)), which can be used to predict liquid-solid-gas equilibria in dilute to concentrated brines up to high temperature (250°C). These models are incorporated into the application software package, TEQUIL. (2) Equation of state (EOS) models which can be used to calculate the XPVT properties and vapor-liquid equilibria of natural fluids from subcritical to supercritical temperatures and pressures. These model are incorporated into the GEOFLUIDS application package. (3) First principle models, based on Molecular Dynamics (MD) and Monte Carlo (MC) simulations. These are particularly useful to generate the accurate thermodynamic data needed for developing EOS models which treat conditions that are difficult or impossible to simulate experimentally. (4) Heat content models, incorporating the aqueous solution and EOS technologies, which calculate specific heats and enthalpies for complex liquid-gas mixtures and allow prediction of such information as steam ratios, available heat and work. These models are incorporated into the GEOHEAT application package. Our software packages are available at no cost to the geothermal community to run on PCs and UNIX based computers.

We are also developing an interactive website which will expand the transfer of our technology. Even when summarized by models, the chemistry of geothermal systems is complicated. However, by utilizing the interactive capabilities available over the Web, innovative visualization methods can help users understand the complicated thermodynamic relationships that are responsible for brine behavior. The visualization code we are developing for internet use is being incorporated into a software package, GEOPHASES. A test website is now being prepared which has the TEQUIL application package implemented. A TEQUIL User Manual, accessible from the site, will be available interactively. An example of using this site to solve a problem related to calcite scale formation is being prepared for the upcoming GRC Bulletin.

In the following, a brief explanation of each software package is given. In addition, the application of the packages is illustrated via solutions to problems encountered in the production of geothermal energy.

TEQUIL APPLICATION PACKAGE: Models providing variable temperature (T<300°C) solubilities of scales in brines as a function of brine composition and of the partial pressure of gases coexisting with the solution phase. Such models can be used to predict scaling, gas breakout and brine properties, such as equilibrium concentrations, pH and saturation ratios, as a function of temperature and composition.

Consequently, they can simulate a variety of process conditions, such as reservoir-brine interactions, brine mixing and heating/cooling effects. This modeling approach is targeted for liquid density brines and is based on a careful implementation of the Pitzer electrolyte equations giving the free energy as a function of composition. Temperature variation is incorporated directly into the parameterization. Currently, the TEQUIL package includes our 0-250°C model for calcite and amorphous silica scale and CO_2 exchange and the Harvie-Møller-Weare 25°C model (1984) of the complete seawater system, $Na - K - H - Ca - Mg - Cl - OH - SO_4 - HCO_3 - CO_3 - H_2O - CO_2$. Phase transitions (solid/liquid equilibria) within the carbonate-free seawater system have been modeled from -55 to 25°C (Spencer, Møller and Weare (1990)) and to 250°C (Møller, in prep) as a function of brine composition. Presently, the low temperature model is included in TEQUIL.

To illustrate the application of TEQUIL, we describe below the use of dissolved SiO_2 concentration as a silica geothermometer to estimate the downhole temperatures of geothermal formations. This technique, which is widely used in exploration, depends on the facts that the solubility of quartz is a function of temperature and that the residence time of formation waters is long enough to assume chemical equilibrium.

The stable form of silica in most high temperature formations is quartz. Dissolution of quartz in water, according to the reaction:

$$SiO_2(quartz) + H_2O = H_4SiO_4(aq), \quad (1)$$

yields H_4SiO_4, a very weak acid. Quartz solubility, like that of many minerals, decreases as the temperature is lowered. As a well is produced, the downhole fluid rises to the surface and undergoes a decrease in temperature and pressure. A significant temperature decrease would be expected to cause quartz to precipitate and lower the concentration of H_4SiO_4 in the brine. However, this does not occur for the SiO_2 system because the rate of nucleation and precipitation of quartz is very slow. This feature makes the silica system an attractive candidate as a geothermometer.

The fact that the solubility of quartz is also a function of brine composition can, however, cause important problems. Generally, neutral species are "salted out"; that is, they become less soluble as the salt concentration increases in the solution. This effect can be appreciable for concentrated brines (such as those found in the Salton Sea geothermal area). From the equilibrium relation for the solubility, Eq.(1), the effects of dissolved salt concentration can be expressed in terms of the activity coefficient for the H_4SiO_4 species in the solution. These coefficients can be calculated for a wide range of brine conditions using the TEQUIL software. Results of such calculations are given in Fig. 1. In this figure, the horizontal line represents a hypothetical measured H_4SiO_4 concentration in a geothermal brine. The curves represent the calculated quartz solubility as a function of temperature for different brine compositions: A. in pure water; B. in the low concentration East Mesa brine; C. in the higher concentration Heber brine; and D. in the high concentration Salton Sea brine. From the figure, it can be seen that an error of 86°F would result if the pure water solubility curve was used instead of the Salton Sea curve to relate SiO_2 concentrations in the Salton Sea geothermal area to formation temperatures.

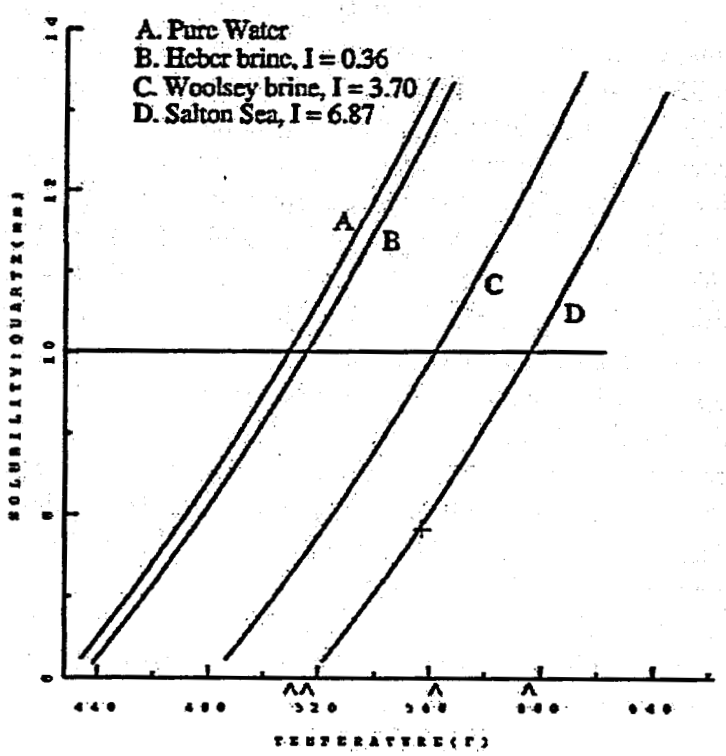

Figure 1: Solubility of amorphous silica in brine.

An additional compositional effect on the silica geothermometer reliabiltiy is the fact that evaporation, caused by the pressure decrease as the brine moves up the well bore to the surface, can increase the concentrations of the dissolved species. This problem can be treated by the GEOHEAT software program and will be discussed below.

GEOFLUIDS APPLICATION PACKAGE: Models for calculating the XPVT properties and salt/liquid/vapor equilibria of brines and other natural fluids from subcritical to supercritical temperatures and pressures. Such models are essential to predict the behavior of geothermal systems undergoing phase separation and density and compositional changes due to significant alterations of temperature and pressure. These conditions can occur during brine extraction (e.g., flashing) and reinjection as well as during the evolution of the resource when brines are cycled through high temperature and pressure regions in the formation.

To build a model of mixture thermodynamics (phase coexistence, miscibility, etc.) for a wide range of composition, temperature and pressure conditions, it was necessary to employ an equation of state (EOS) modeling approach. The phenomenology used in the TEQUIL models (discussed in the last section), which treats liquid density systems, cannot be generalized to arbitrary densities. It is very difficult to incorporate compositional complexity into variable density models. Fortunately, for many problems (XPVT properties, brine flash pressures, etc.) the compositions of geothermal fluids can be well approximated by brines in the system $NaCl-CaCl_2-H_2O-CO_2-CH_4$. In this approximation, the chemistry of 1-1 electrolytes is lumped into the $NaCl$ variable

and $CaCl_2$ is the surrogate for 2-1 electrolytes. The CH_4 and CO_2 species represent the presence of the two major insoluble gases in geothermal fluids.

At present, we have developed a model for the subsystem $NaCl-CO_2-CH_4-H_2O$. This model generalizes the earlier model for the $NaCl - H_2O$ system developed by Anderko and Pitzer (1993) and is related to earlier approach of Dimitrelis and Prausnitz (1986). The development of the EOS is based on the Helmholtz free energy. The system is first idealized as a system of interacting species. The theoretical forms assumed for this "reference system" are then corrected to incorporate the behavior of the real system. The corrections are empirical, but chosen to retain the limiting behavior. The parameters in the resulting equations are evaluated from both PVTX data and phase equilibria data. The detailed equations describing the parameterization of these equation for the $NaCl-H_2O$ are very complicated and are given in Anderko and Pitzer (1993) and Duan, Møller and Weare (1995). In our work, we built on this formulism to add new insoluble species, CO_2 and CH_4, to the model. In principle, we could use our already tested EOS for these species (Duan, Møller and Weare (1992)) but an extensive evaluation of the $NaCl - H_2O$ system led us to the conclusion that the hard sphere and dipolar terms used by Anderko and Pitzer are essential to a reasonable description of the data. To treat mixtures, this forced us to adopt a form similar to the Pitzer EOS for the less polar binaries. We point out that the model is only applicable above 300°C because the $NaCl$ species is assumed to be associated. Our earlier model of the $CO_2 - CH_4 - H_2O$ system, which is included in the GEOFLUIDS package, is applicable to much wider ranges of temperature and pressure (50° to 1000°C and 0 to 1000 bar). GEOFLUIDS also includes our model for the more complex system, $H_2O - CO_2 - CH_4 - N_2 - H_2S - O_2 - H_2$, for application above the critical point of water.

In Fig. 2, the flashing pressures of a geothermal fluid of typical composition calculated by the GEOFLUIDS model as a function of temperature are presented. Because dissolved gases are so insoluble, they make a large contribution to the flashing pressure even at low concentration. We note that for temperatures below 200° C their contribution is much larger than the contribution from the vapor pressure of water. Also note the strong effect of the presence of CH_4 in the brine. Since CH_4 is very insoluble, its contribution to the flashing pressure is large even when its concentration is low.

GEOHEAT APPLICATION PACKAGE: Models calculating the specific heat, heat of solution and enthalpy of complex brine/gas mixtures. They allow the rapid estimation of steam fractions, available heat and work, etc. The estimation of the internal energy content of brines is obviously useful for the geothermal community. Such information is not only necessary to estimate the economic value of the resource but also, as we discuss below, can be an aid in developing models of the processes involved in energy extraction.

Since the models in TEQUIL and GEOFLUIDS are based on the free energy of a system, all other thermodynamic properties, including heat properties, can be derived by the appropriate derivatives. However, in order for this procedure to be successful it is generally necessary to include some heat data in the data base for the parameterization of the free energy. We have developed models of brine and gas phase enthalpies

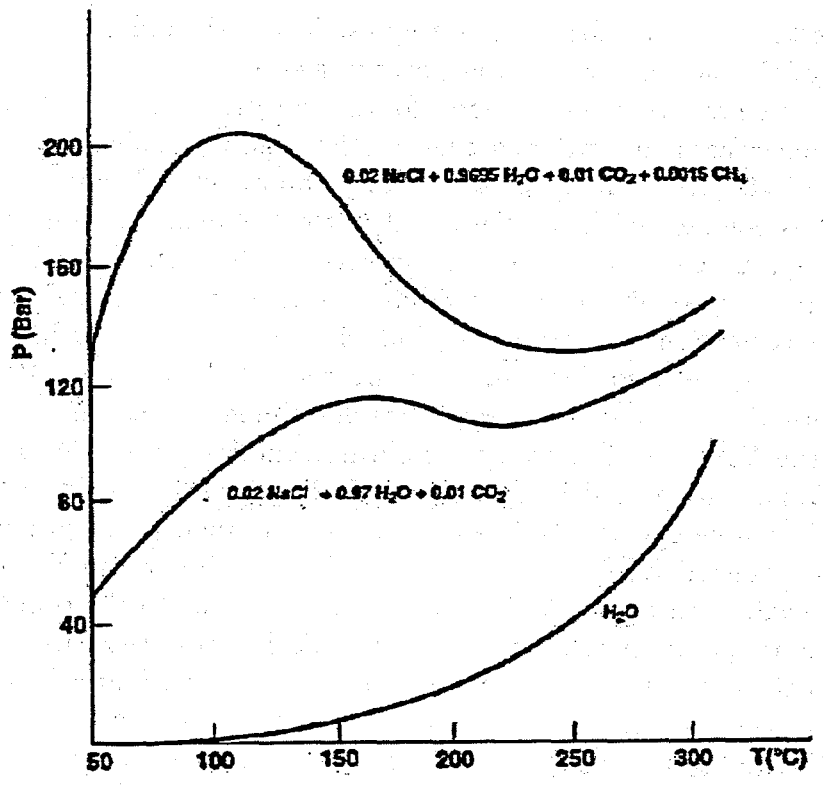

Figure 2: Breakout pressure for geothermal brines.

using this approach. Because the relation between the free energy and the enthalpy is maintained, these models produce consistent predictions of heat properties and other temperature dependent properties related to the free energy (e.g., the solubility of scaling minerals, the temperature dependence of phase coexistence). Although enthalpy models have been developed from our free energy models of the $CO_2 - CH_4 - H_2O$ and $H_2O - CO_2 - CH_4 - N_2 - H_2S - O_2 - H2 - CO - Ar$ systems, presently GEOHEAT models are restricted to the system $NaCl - CO_2 - H_2O$.

In Fig. 3, we have constructed a enthalpy/mol vs. pressure diagram using GEOHEAT for a brine similar in composition to that of the Salton Sea geothermal field. For a multicomponent system such a diagram is dependent on the total composition. In this calculation, we have lumped the entire Salton Sea brine solute composition into the $NaCl$ concentration. For subcritical systems, liquids (lower enthalpy systems) are present on the left of the diagram and gases (higher enthalpy systems) on the right. Considering the 300° C isotherm as an example, we can see that at high pressure the enthalpy is fairly constant with pressure drop. This is because the enthalpy change with pressure in a liquid density system at constant temperature is relatively small. At some pressure, the system will eventually flash and the enthalpy change related to the formation of steam becomes large. For this temperature and composition, flashing occurs at 67 bars, point (a) on the 300°C isotherm. This pressure is a little lower than it would be for pure water (87 bars) because the vapor pressure of the fluid is lowered by the dissolved salt. On the diagram, the two phase region is separated from the

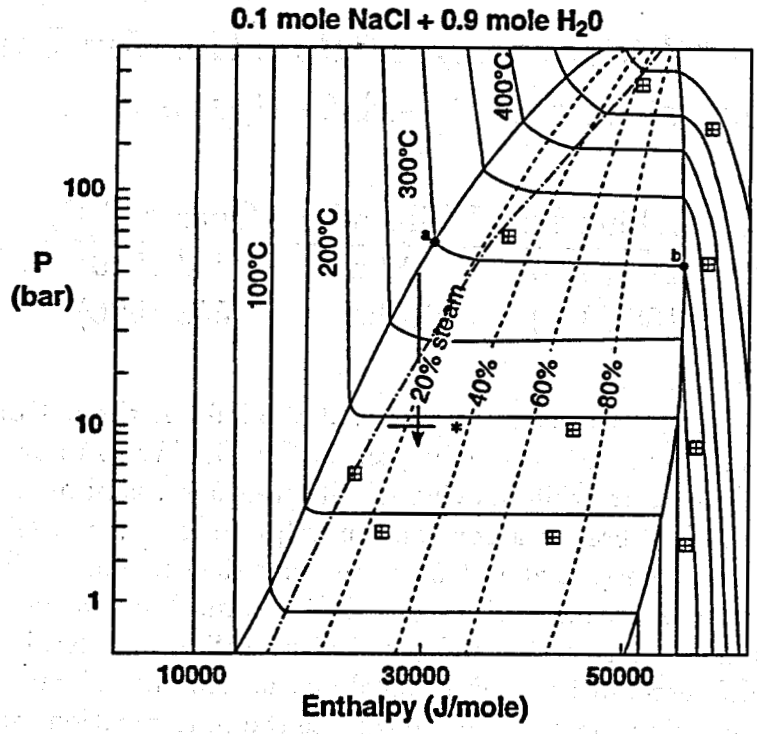

Figure 3: Enthalpy-Pressure diagram for a Salton Sea-like brine.

single phase region by a solid line. Point (a) on the diagram for the 300°C isotherm is the enthalpy of the liquid at the bubble point. As the pressure is lowered below that of point (a), more water is evaporated. Since the composition of the liquid and vapor are changing, the total enthalpy/mol in the coexistence region has curvature. At some point in this system solid $NaCl$ precipitates. When this occurs, the vapor pressure and the solubility (concentration in the liquid phase) of the system are fixed. With continued evaporation, the liquid is then removed from the system along the horizontal line. When the liquid disappears, the pressure again drops at constant T. The enthalpy/mol of the vapor coexisting with the liquid and the solid at 300° C (and along the coexisting liquid/vapor/solid line) is represented on the diagram by point (b).

Fig. 3 also includes mole % steam lines (dashed lines). These lines, which give the steam ratio for a particular isotherm, are especially useful for geothermal applications. All this information may be calculated from the GEOHEAT software.

As an application of the diagram shown in Fig. 3, reconsider Fig. 1. The measured well head brine composition in this figure is represented by the horizontal line. To use the silica geothermometer approach for estimating the downhole temperature, we must be able to reconstruct the downhole brine concentrations. Therefore, we need to correct this well head composition to compensate for the loss of water due to evaporation during production. An interactive process would be required to get a precise answer. Here, we will only look at one cycle. Suppose that the uncorrected composition gives a downhole temperature of 300°C (572°F) from the geothermometer (see Fig. 1). Take that as

Table 1: Steam Separation Properties for Pure Water vs. the NaCl-H_2O System

System	SR	Wellhead T	Wellhead P	Quartz T(F)
Pure Water	0.29	174 (345)	10 bar	453 (510)
Brine (6.87m)	0.23	188 (370)	10 bar	558 (596)

an initial estimate of the temperature and assume that the fluid at the bottom of the well is at the bubble point (point (a) on the diagram in Fig. 3). We can now ask how much a fluid at 300°C evaporates while moving up the well bore, assuming that the motion of the fluid up the well bore is a constant enthalpy process (see the arrow in Fig. 3). Fixing the well head pressure at 10 bar, we see that the constant enthalpy line intersects the 10 bar line at a breakout of roughly 23% steam. We can now use this information to approximately correct the well head composition and recalculate the data of Fig. 1. To simplify here, rather than recalculate the solubility of $SiO_2(quartz)$ for the corrected downhole brine composition, we will use the concentrations at the well head to calculate the H_4SiO_4 activity in the brine. This allows us to use the calculated solubility curves of Fig. 1. Diluting the measured well head concentration of H_4SiO_4 to reflect the loss of water due to evaporation, we recalculate the bottom hole temperature (indicated on Fig. 1 by a cross). Note that the new temperature (558°F) is 38°F less than the first estimate (Table 1, 596 °F).

Recalculated values for important well properties are summarized in Table 1. As expected, the well head steam ratio (SR) at fixed well head pressure is less for the brine than for pure water. This decrease in evaporation is also reflected in the higher well head temperature of the brine.

WEBSITE and the GEOPHASES APPLICATION PACKAGE: This package (under development) provides visualization capabilities to aid in the interpretation of complex gas/liquid/solid phase relations under variable X, T, P conditions.

The calculations that have been reported in Fig's. (1-4) can all be done with the software available from our group via diskettes. We will continue to offer diskette based software. However, as models become more complex their computational load may outgrow the performance of reasonably available personal computers. To address this problem, we are in the process of developing an interactive website that will incorporate the present models as well as provide new functionality (see Fig. 4). By having this software on the internet, updates of the models will immediately be available to users. We hope to obtain a very powerful workstation which will increase performance.

In addition to these capabilities, we are developing a postprocessing package called GEOPHASES (see Table 2), which will compile and process data from the other application packages. The GEOPHASES package automatically calculates phase behavior in multicomponent systems and then constructs the requested phase diagrams for up to three dimensions. Since many points are necessary to define a multidimensional phase

Figure 4:

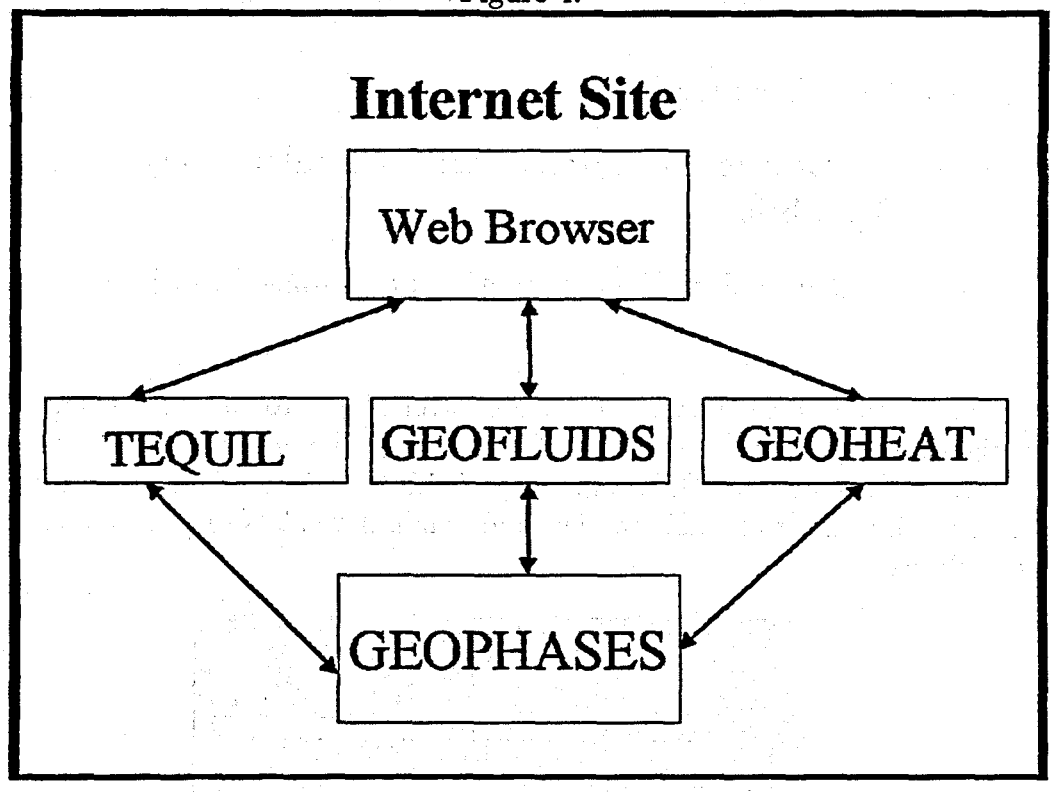

diagram, the computational load can be considerable. Nevertheless, adequate performance can be obtained from a high performance workstation. In Fig. 5, we show a GEOPHASES computed phase diagram for the $Na^+ - K^+ - Mg^{2+} - Cl^- - SO_4^{2-} - H_2O$ 5-component system as a function of temperature. Charge balance implies that there are four degrees of freedom when T and P are fixed. Obviously, the general phase relations for this system cannot be drawn on a three dimensional diagram. However, the dimensionality may be reduced by plotting only certain regions of the diagram. For example, in the Janecke projection shown in Fig. 5 all phases coexist with solid $NaCl$. To construct this figure, the solubility models are used to calculate brine compositions in equilibrium with all the invariant mineral assemblages throughout the 0 to 250°C temperature range. Obtaining this large number of calculated "data" points and then drawing the polythermal phase diagram by hand is a daunting task. GEOPHASES automatizes this process. The GEOPHASES software both directs computations and constructs the appropriate projections. The software is also modular. The raw coexistence data initially calculated may be used by several GEOPHASES scripts and plotting programs. Thus, adding new types of plots (such as the Janecke projection shown in Fig. 5) involves merely writing code to access the calculated data.

More capabilities of GEOPHASES are shown in Fig. 6. The phase diagram for the $CO_2 - H_2O$ system has been constructed using GEOFLUIDS. This system has three degrees of freedom so it can be plotted directly in three dimensions as shown in the figure. For more quantitative interpretation, it is common to plot the data holding one of the variables fixed (for example, T or P as in the shaded regions of the figure).

Table 2: GEOPHASES

- Interactive Tools for Viewing
- Software Package to Automatically Calculate Very Complicated Phase Equilibria
- Reduced Dimensionality Projections of Phase Equilibria

In Fig. 6, the plot is shown via the CosmoPlayer plugin to Netscape Communicator. (Note the control panel at the bottom of the figure.) The browser reads a "VRML" file that is created by the OpenGL component of GEOPHASES. Thus, users merely have to access the internet to be able to view and manipulate plots (e.g., zooming, rotation, and translation).

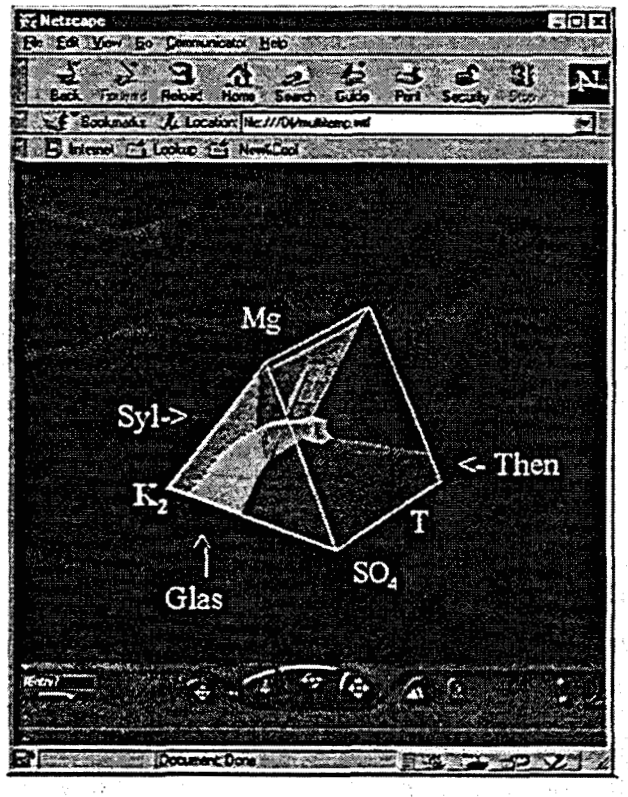

Figure 5:

FUTURE DIRECTIONS: In the future, we plan to expand and advance our modeling and user interface technologies. Communication from the geothermal community is invited in order to best meet its chemical modeling needs.

Some improvements scheduled are to add pressure corrections and more species to the solubility models. We presently have a model for H_2S (gas) exchange in aqueous

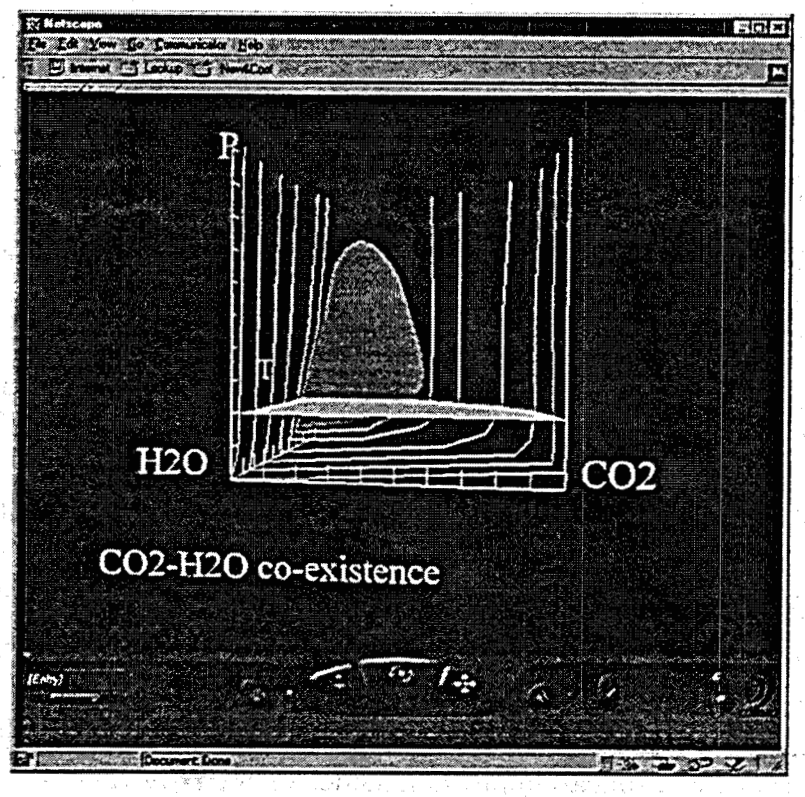

Figure 6:

solution. This model will be generalized to incorporate prediction of sulfide scale and H_2S (gas) emission in multicomponent brines. Inclusion of aluminum species in the seawater models will greatly broaden their application to reservoir studies. The development of accurate chemical models for predicting the behavior of aluminum-bearing scales in geothermal systems is complicated by the many complexation reactions involving aluminum and hydroxide ions. Using the data collected in literature searches we are starting the construction of a preliminary model of aluminum hydrolysis from 0°C to 250°C. Since these reactions vary with pH and salinity, we are using the variable temperature calcite scaling model as a base. Using the formulism of Anderko and Pitzer (1993), we are now adding $CaCl_2$ to the mixture thermodynamic model included in the GEOFLUIDS package. Using this model and the liquid density models present in TEQUIL as well as supercritical models developed with the corresponding states approach (see Duan, Møller and Weare (1996)), the enthalpy models in GEOHEAT will be expanded to treat different regions of T,P space. Also, in the future, internet users will be able to interactively "cut out" data in order to focus on a single plane such as an isotherm or isobar (as illustrated in Fig. 6). Composition variation along coexistence lines will be available directly from the diagram by selecting with the mouse.

REFERENCES:

Anderko, A. and Pitzer K. (1993). Equation of state representation of phase equilibria and volume properties of $NaCl - H_2O$ above 573°K. *Geochim. Cosmochim. Acta.*, 57:1657-1680.

Dimitrelis, D. and Prausnitz, J. (1986). Comparison of two hard-sphere reference systems for perturbation theories for mixtures. *Fluid Phase Equilibria*, 31:1-21.

Duan, Z., Mϕller, N. and Weare, J. (1992). An equation of state for the $CH_4 - CO_2 - H_2O$ system: II. Mixtures from 50 to 1000°C and 0 to 1000 bar. *Geochim. Cosmochim. Acta*, 56:2619-2631.

Duan, Z., Mϕller, N. and Weare, J. (1995). Equation of state for the $NaCl - H_2O - CO_2$ system: Prediction of phase equilibria and volumetric properties. *Geochim. Cosmochim. Acta*, 59:2869-2882.

Duan, Z., Mϕller, N. and Weare, J. (1996). A general equation of state for supercritical fluid mixtures and molecular dynamics simulation for mixture PVTX properties. *Geochim. Cosmochim. Acta*, 60:1209-1216.

Harvie, C. E., Mϕller, N. and Weare, J. H. (1984). The prediction of mineral solubilities in natural waters: the $Na - K - Mg - Ca - H - Cl - SO_4 - OH - HCO_3 - CO_3 - CO_2 - H_2O$ system to high ionic strengths at 25°C. *Geochim. Cosmochim. Acta*, 48:723-751.

Pitzer, K. (1987) *Reviews in Minerology*, chapter 4, "A Thermodynamic Model for Aqueous Solutions of Liquid-like Densities", BookCrafters, Inc., pages 96-142.

Spencer, R. J., Mϕller, N. and Weare, J. H. (1990). The prediction of mineral solubilities in natural waters: a chemical equilibrium model for the $Na - K - Ca - Mg - Cl - SO_4 - H_2O$ system at temperatures below 25° C. *Geochim. Cosmochim. Acta*, 54:575-590.

FRACTURE PERMEABILITY AND IN SITU STRESS IN THE DIXIE VALLEY, NEVADA, GEOTHERMAL RESERVOIR

Stephen Hickman[1], Colleen Barton[2], Mark Zoback[2], Roger Morin[1], Dick Benoit[3], John Sass[1]

[1]U.S. Geological Survey
(650) 329-4807

[2]Stanford University

[3]Oxbow Geothermal Corporation

ABSTRACT

Borehole televiewer, temperature and flowmeter logs and hydraulic fracturing stress measurements conducted in six wells penetrating a geothermal reservoir associated with the Stillwater fault zone in Dixie Valley, Nevada, were used to investigate the relationship between reservoir permeability and the contemporary in situ stress field. Data from wells drilled into productive and nonproductive segments of the Stillwater fault zone indicate that permeability in all wells is dominated by a relatively small number of fractures striking parallel to the local trend of the fault. However, Coulomb failure analysis using these fracture orientations in conjunction with stress orientations and magnitudes suggests that reservoir permeability is high only when individual fractures as well as the overall Stillwater fault zone are optimally oriented and critically stressed for frictional failure.

INTRODUCTION

To evaluate tectonic and geochemical controls on the productivity of a fracture-dominated geothermal reservoir at Dixie Valley, Nevada, we are conducting an integrated study of fracturing, stress, and hydrologic properties in geothermal wells drilled into and near the Stillwater fault zone (Figure 1). This fault is a major, active, range-bounding normal fault located in the western Basin and Range province, Nevada (see Okaya and Thompson, 1985), and comprises the main reservoir for a ~62 MW geothermal electric power plant operated by Oxbow Geothermal Corporation. Although earthquakes have not ruptured this segment of the Stillwater fault in historic times, large (M = 6.8 to 7.7) earthquakes have occurred within the past 80 years along range-bounding faults both to the northeast and southwest of the Dixie Valley Geothermal Field (DVGF), and geologic evidence shows that the Stillwater fault abutting the DVGF experienced two or more faulting episodes (total offset ~9 m) during the past 12,000 years (Wallace and Whitney, 1984).

The principal goal of this study is to define the nature, distribution, and hydraulic properties of fractures associated with the DVGF, and to characterize the manner in which these fractures, and hence the overall reservoir hydrology, are related to the local stress field. This project was initiated in late 1995 with an extensive downhole measurements program conducted in a 2.6-km-deep geothermal production well (well 73B-7) drilled into the Stillwater fault zone by Oxbow Geothermal Corporation (see Hickman et al., 1997). This study has since been expanded to include borehole televiewer logging, temperature/pressure/spinner logging and hydraulic fracturing stress measurements from additional wells within the primary zone of geothermal production (transmissivities on the order of 1 m^2/min) and from wells within a few km of the producing zone that were relatively impermeable and, hence, not commercially viable (transmissivities of about 10^{-4} m^2/min). More detailed presentations of the results from this study can be found in Hickman et al. (1998), Barton et al. (1998) and Morin et al. (1998).

The measurements made in these wells make possible a systematic, comparative study of the effects of in situ stress on fracture permeability along producing and nonproducing segments of the Stillwater fault zone. By comparing and contrasting data from both productive and nonproductive wells, it should be possible to determine if a relationship exists between the contemporary in-situ stress field and reservoir productivity. If so, then these types of data will provide a valuable tool for geothermal reservoir exploration by allowing one to determine which faults or fault segments are likely to be hydraulically conductive in a given stress field. Furthermore, these data would provide critical

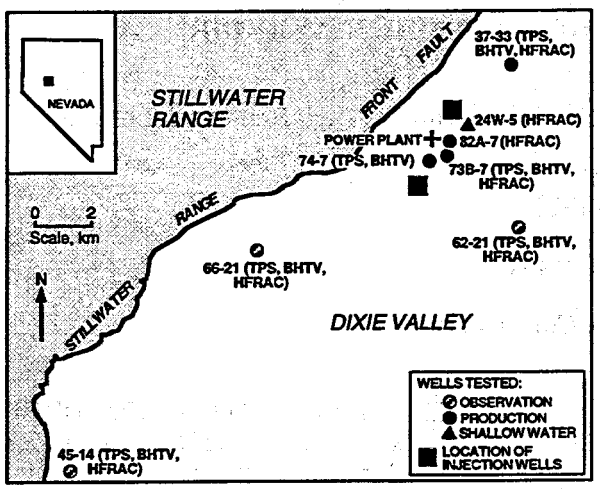

Figure 1. *Map showing geothermal wells in Dixie Valley, Nevada. Injection and production wells penetrated highly permeable portions of the southeast-dipping Stillwater fault zone, whereas observation wells failed to encounter sufficient permeability to be of commercial value. Measurements conducted in these wells are TPS: Temperature/pressure/ spinner logs; BHTV: borehole televiewer logs; HFRAC: and Hydraulic fracturing stress measurements.*

input on decisions related to redrilling of impermeable (i.e., "dry") wells or abandonment of an area or prospect. At some future date, it is also hoped these methods can be used to locate and engineer future production and injection wells and to design enhanced recovery programs (e.g., massive hydraulic fracturing) for less-than-commercial wells within existing geothermal reservoirs.

METHOD

Borehole Televiewer, Spinner Flowmeter and Temperature Logging

The geometry and orientation of natural fractures, drilling-induced tensile fractures and borehole breakouts were determined using borehole televiewer (BHTV) logs. The BHTV is a wireline logging tool that provides a continuous, oriented, ultrasonic image of a borehole wall. The high temperatures in these wells (up to ~240° C) required the use of specialized televiewer tools, owned by Stanford University and the US Geological Survey. These tools were repeatedly calibrated at the surface for orientation and ultrasonic travel times in specially designed calibration tanks and repeat logging runs were used to provide independent checks on the orientations of the images obtained. Data were digitized from the magnetic field tapes and then processed to remove noise, stick-slip effects and other tool-related problems.

Simultaneous temperature, pressure and spinner flowmeter (TPS) logging was used to identify hydraulically conductive fractures and faults in these wells and to determine the rates of fluid flow into or out of these features, both under static conditions and during fluid injection and withdrawal. Local perturbations to well-bore temperature will result from localized fluid flow into or out of the borehole and thus can be detected by precision temperature logging (see Barton et al., 1995). Fractures or faults imaged on the BHTV logs that correlate in depth with these localized temperature perturbations are therefore considered to be hydraulically conductive; multi-pass temperature logs at various production or injection rates were used to assess the persistence of these detected flow horizons. Figures 2a and b show examples of BHTV and temperature gradient logs over the interval 1901 to 1906 m in well 73B-7, where a flow anomaly associated with a permeable fracture at 1903.5 m was detected. In addition, spinner flowmeter and pressure logs were used to identify extremely permeable fractures and faults and to quantitatively determine their permeabilities (see Morin et al., 1998).

Hydraulic Fracturing Stress Measurements

Although hydraulic fracturing stress measurements are typically conducted in short intervals of open hole using inflatable rubber packers, high borehole temperatures precluded the use of packers in these wells. Instead, as discussed by Hickman et al. (1998), the hydraulic fracturing tests in this study were either conducted in short pilot holes during drilling of a new geothermal production well or in an open-hole section of an already drilled and cased well. In the latter case, a TPS log was conducted during the test to identify the depth at which the hydraulic fracture was created. Although necessitated by high borehole temperatures, both types of tests also resulted in more rapid, and hence less expensive, in-situ stress testing than would have been the case had drill-pipe deployed packers been used.

Pressures and flow rates were measured at the surface and pressures were also recorded using a quartz pressure gauge suspended a few meters above the test interval. Following initiation of the hydraulic fracture, the magnitude of the minimum horizontal principal stress,

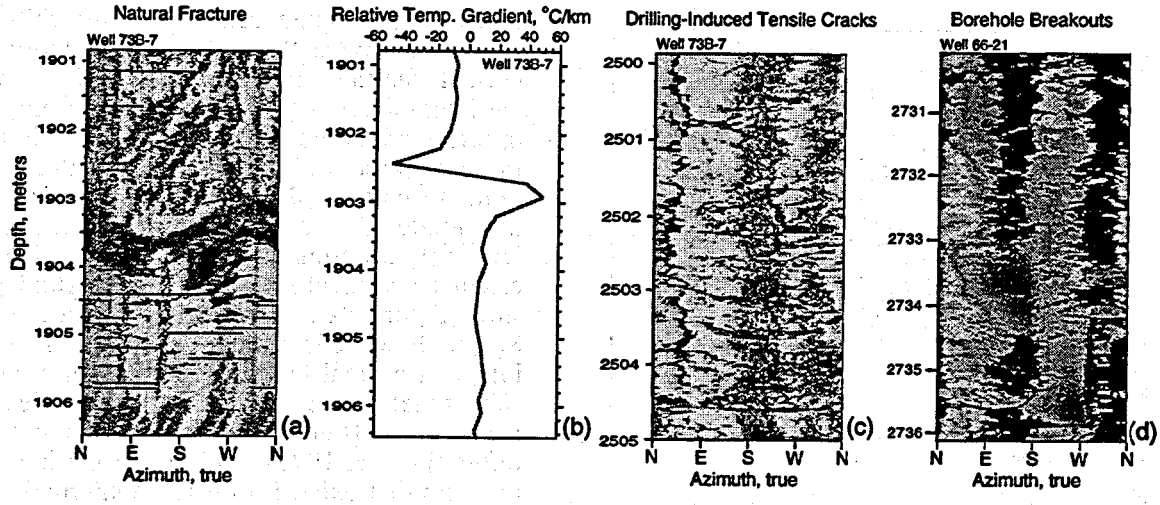

Figure 2. *(a) BHTV image from well 73B-7, oriented relative to true North, showing a large fracture zone (sinusoid) intersecting the borehole at 1903.5 m and (b) relative temperature gradient (i.e., difference between the instantaneous and average gradients) over the same interval. (c) BHTV log from well 73B-7 showing drilling-induced (cooling) fractures, imaged as undulating vertical features occurring on diametrically opposed sides of the borehole and aligned in a northeast-southwest direction. (d) BHTV log from well 66-21 showing the development of stress-induced breakouts (discontinuous dark bands) on diametrically opposed sides of the borehole.*

S_{hmin}, was determined from stable instantaneous shut-in and pumping pressures recorded during multiple pressurization cycles. BHTV logs showed that the tested intervals contained numerous preexisting fractures (both natural and drilling-induced) at a variety of orientations (see below and Barton et al., 1998). Thus, it was not possible to directly measure the magnitude of the maximum horizontal principal stress, S_{Hmax}, in these tests. Rather, as discussed below, bounds to the magnitude of S_{Hmax} were obtained using estimates of compressive rock strength and the presence or absence of borehole breakouts. Breakouts result from compressive rock failure in response to the concentration of stresses at the borehole wall (see Moos and Zoback, 1990),

The vertical (overburden) stress, S_V, was calculated using geophysical density logs conducted in the test wells, or nearby wells, in conjunction with rock densities measured on surface samples obtained from Dixie Valley (Okaya and Thompson, 1985). In-situ fluid pressure, P_p, was estimated by integrating the equation of state for water for the appropriate geothermal gradient and using the pre-production reservoir water table.

RESULTS AND DISCUSSION

We have conducted BHTV and TPS logs and hydraulic fracturing stress measurements in a total of eight wells at Dixie Valley (Figure 1). With the exception of a 550-m-deep water well drilled ~1 km northeast of well 73B-7 (well 24W-5) and a 3.4-km-deep observation well (62-21) drilled toward the center of Dixie Valley, all of these wells penetrate the Stillwater fault zone at depths of 2 to 3 km. Four of these wells (73B-7, 82A-7, 74-7 and 37-33) penetrated the highly permeable (i.e., producing) segment of the fault zone constituting the main geothermal reservoir. The other two wells (66-21 and 45-14), which failed to encounter enough permeability to be viable production wells, penetrated segments of the Stillwater fault located approximately 8 and 20 km southwest of the main reservoir.

Producing Fault Segment

Televiewer logs from wells penetrating the highly permeable (i.e., producing) segment of the Stillwater fault zone revealed extensive drilling-induced tensile fractures (e.g., Figure 2c). As discussed by Moos and Zoback (1990), these tensile fractures result from the superposition of the ambient in-situ stresses and thermal stresses induced by circulation of relatively cold drilling fluids at the borehole wall. These tensile fractures indicate that the direction of the minimum horizontal principal stress, S_{hmin}, adjacent to the main geothermal reservoir is about S55°E ± 15°. As the Stillwater fault at this location dips S45°E at ~53°, it is thus nearly at the optimal orientation for normal faulting in the current stress field (Figure 3).

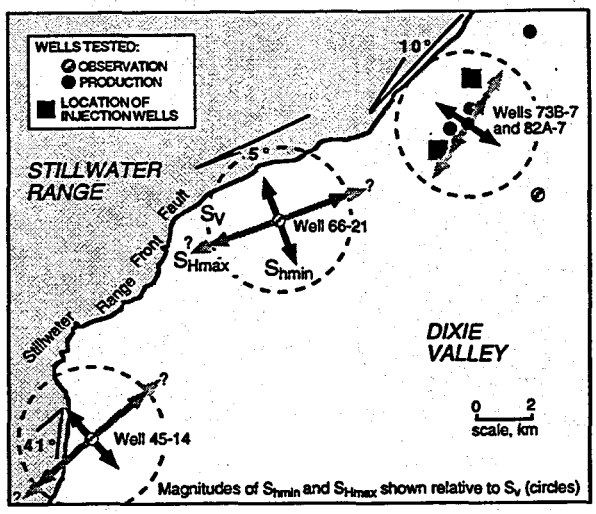

Figure 3. *Orientations and relative magnitudes of the least horizontal principal stress, S_{hmin}, and the greatest horizontal principal stress, S_{Hmax}, at Dixie Valley. The length of each arrow is proportional to the magnitude of the corresponding stress, normalized to the magnitude of the vertical stress S_V (dashed circle) appropriate for that well and test depth. Lower and upper bounds on S_{Hmax}, determined through analysis of conditions for breakout formation (see Figure 4), are depicted as dark and light gray arrows, respectively. Stresses shown for wells 73B-7 and 82A-7 are average values from three measurements at 1.7 to 2.5 km depth. Also shown is the extent (in degrees) to which the Stillwater fault is locally deviated from the optimal orientation for normal faulting.*

Analysis of hydraulic fracturing tests from the deep geothermal production wells 73B-7 and 82A-7, together with the shallow water well 24W-5, shows that the magnitude of S_{hmin} is very low relative to the calculated vertical stress, with S_{hmin}/S_V ranging from 0.45 to 0.62 at depths of 0.4–2.5 km (Figure 4a). Stress measurements made near the bottoms of wells 73B-7 and 82A-7 indicate that S_{hmin}/S_V reaches its lowest values of 0.45 to 0.51 within a few hundred meters of the Stillwater fault zone. As shown in Hickman et al. (1998), the deepest stress measurement in well 37-33 yielded S_{hmin} magnitudes comparable to those observed in the other producing wells, with an S_{hmin}/S_V value of 0.46 at a depth of 2.63 km. Upper bounds to the magnitude of S_{Hmax}, obtained using estimates of the compressive strength of rocks encountered and the observed absence of borehole breakouts in these wells indicate a normal faulting stress regime (i.e., $S_{Hmax} < S_v$; see Figure 4a and Hickman et al., 1998).

Since the producing segment of the Stillwater fault is nearly at the optimal orientation for normal faulting, the stress magnitudes from the hydraulic fracturing tests can be analyzed in terms of the potential for slip on this fault. In accordance with the Coulomb failure criterion, we calculated the critical range of S_{hmin} magnitudes for frictional failure (i.e., normal faulting) on optimally oriented faults given the calculated vertical stress and in-situ fluid pressure (Figure 4a). This analysis indicates that S_{hmin} in these wells is close to that predicted for incipient normal faulting on the Stillwater and subparallel faults, using laboratory measurements of coefficients of friction of 0.6 to 1.0 (after Byerlee, 1978) and the formation fluid pressure that existed prior to geothermal reservoir production. Similar results were obtained from the northernmost production well 37-33 and the "background" well 62-21 (not shown), indicating that the near-failure stress state adjacent to the permeable segment of the Stillwater fault zone is relatively homogeneous.

Televiewer data recorded in these wells show pervasive macroscopic fractures with a wide range of orientations throughout the logged intervals. Although fractures imaged in the BHTV logs from the permeable wells 73B-7, 74-7 and 37-33 exhibit considerable scatter in orientation, they generally strike between north and east, with shallow to moderate dips (15 to 70°) toward the southeast (Figure 5, left column). These fractures tend to become steeper and larger in apparent aperture with depth.

The orientations of hydraulically conductive fractures identified on the basis of temperature anomalies are distinct from the overall fracture population, and are near-optimally oriented for normal faulting in the measured stress field (Figure 5, right column). In particular, analysis of TPS logs under flowing conditions indicates that production within the DVGF is dominated by only a few fractures: typically between 3 and 6 fractures in any given well. We found that the permeability of these fractures is extremely high, ranging from about 2 to 5 x 10^{-11} m^2 (i.e., 20 to 50 Darcies), and that these fractures are oriented nearly parallel to the local trend of the Stillwater Fault (see Hickman et al., 1997; Barton et al., 1998).

Using the stress orientations and magnitudes measured in these wells together with fracture orientations obtained from the BHTV logs, we then calculated the shear and normal stress on each of the fracture planes and used the Cou-

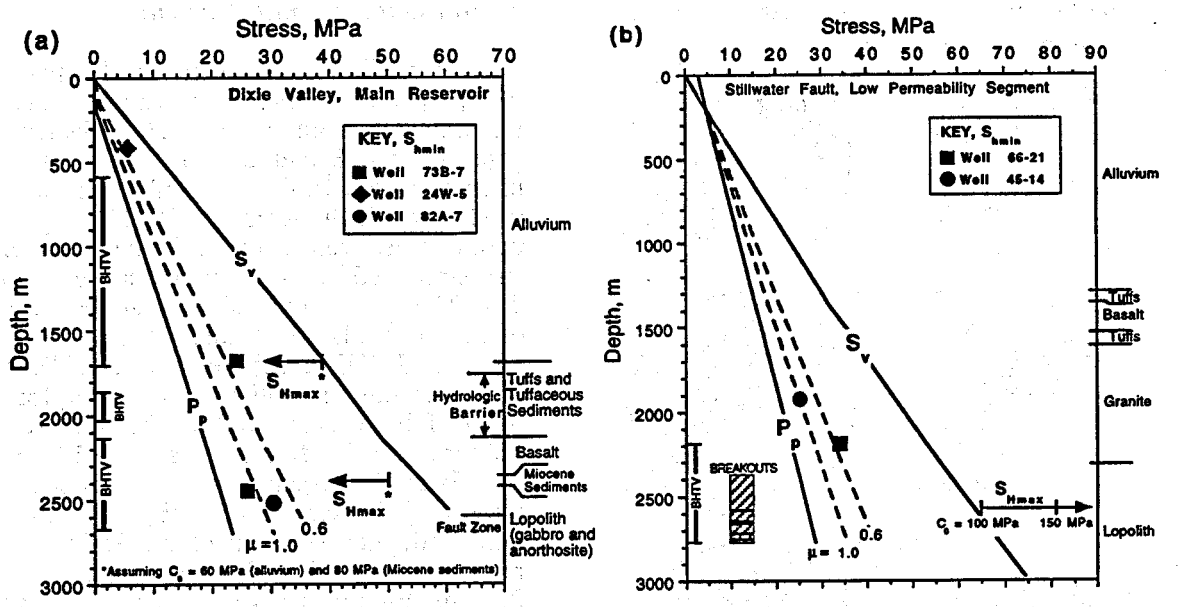

Figure 4. *(a) Stress magnitudes from wells adjacent to the highly permeable segment of the Stillwater fault. Upper bounds to S_{Hmax} in well 73B-7 were determined from the absence of borehole breakouts, using indicated values for the compressive rock strength C_o. The dashed lines indicate the range of S_{hmin} at which frictional failure would be expected on optimally oriented faults for coefficients of friction of 0.6 to 1.0. (b) Same as Figure a, but for wells adjacent to the relatively impermeable segment of the Stillwater fault. The lithology, S_V, P_p, BHTV coverage and breakout distribution shown are from well 66-21; although the frictional failure lines are drawn for well 66-21, they are also accurate for well 45-14 to within 2%. Breakouts were either discontinuous (hachured pattern) or continuous (solid lines). Lower bounds to S_{Hmax} were obtained using a breakout initiation criteria and estimates of C_o, only bounds from well 66-21 are shown.*

lomb failure criterion to determine whether or not each plane was a potentially active fault. Based upon laboratory measurements of the frictional strength of prefractured rock (Byerlee, 1978), we assumed that fractures with a ratio of shear to normal stress ≥ 0.6 are optimally oriented to the stress field for frictional failure. This analysis was performed on both hydraulically conductive fractures and on a control population of non-hydraulically conductive fractures extracted from the total fracture population.

The results of this analysis are illustrated in Figures 6a and b for well 73B-7. As indicated by the Coulomb failure lines for μ=0.6 and μ=1.0, most of the hydraulically conductive fractures in this well are critically stressed, potentially active faults in frictional equilibrium with the current stress field. In contrast, the majority of fractures not associated with temperature anomalies (i.e., non-hydraulically conductive) lie below the Coulomb failure lines and therefore do not appear to be critically stressed shear fractures (Figure 6b). Furthermore, the highly permeable fractures identified from the TPS logs (i.e., large-scale flow anomalies) are subparallel to the local orientation of the Stillwater fault zone and are thus also critically stressed for failure (Figure 6a). This analysis indicates that the hydraulically conductive fractures observed in these wells are—like the Stillwater fault itself—critically stressed, potentially active shear planes in the current north-northwest extensional stress regime at Dixie Valley. Nearly identical results were obtained for the other production wells 74-7 and 37-33 (Barton et al., 1998)

Permeability reduction and the establishment of fault seals would be expected along the productive segment of the Stillwater fault, given the high reservoir temperatures (~220 to 250° C at 2.3 to 3.0 km); surface observations of hydrothermal alteration, mineralization, and pressure-solution deformation within and adjacent to the fault zone (e.g., Seront et al., 1997); and thermal evidence for upward transport of hydrothermal fluids within the fault zone (Benoit, 1996; Williams et al., 1997). In particular, analyses of fluid samples recovered from the Stillwater fault zone prior to reservoir production by Oxbow Geothermal Corporation indicate a decrease in silica concentration of about 120 ppm as these fluids

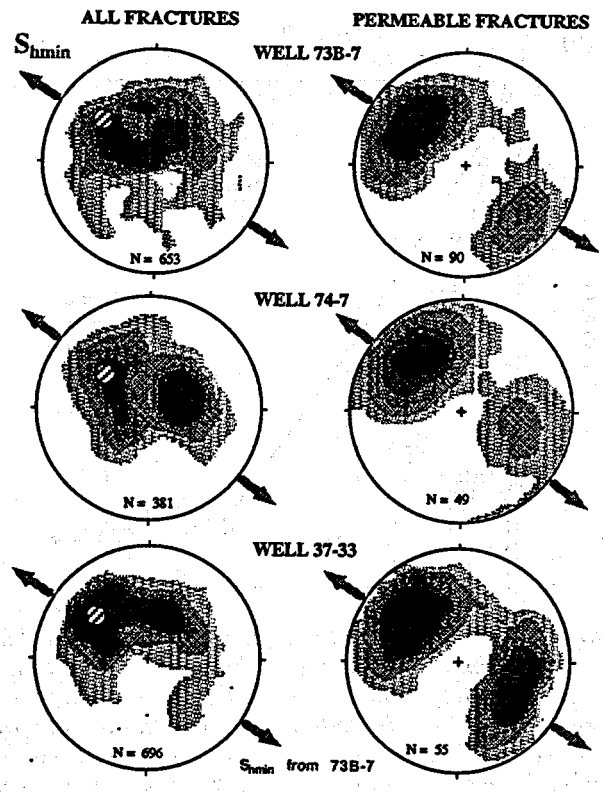

Figure 5. *Kamb contours of poles to fracture planes for geothermal production wells in Dixie Valley for all fractures (left column) and permeable fractures only (right column). In these plots (after Kamb, 1959), the density of shading is proportional to the number of poles per unit area on a lower hemisphere projection, normalized to the total fracture count, N. Hachured circles represent poles to the local trend of the Stillwater fault adjacent to each well. Arrows indicate the orientation of S_{hmin} measured in each well, except for well 37-33 in which we used the S_{hmin} orientation from nearby well 73B-7 (see Hickman et al., 1998).*

ascend from 3.0 to 2.3 km. This loss of silica can be expected to seal fractures within the Stillwater fault zone over geological time scales, thereby reducing the high overall fault-zone permeability. However, the observation that the permeability of fractures within and adjacent to the highly productive segment of the Stillwater fault zone is quite high (see Morin et al., 1998) and that these fractures are favorably aligned and critically stressed for normal faulting in the current stress field (e.g., Figures 5 and 6) suggests that dilatancy associated with ongoing fault slip in response to high differential stresses (i.e., $S_V - S_{hmin}$) is sufficient to counteract the expected permeability reduction.

Non-Producing Fault Segment

Similar data were collected in the two wells (66-21 and 45-14) penetrating relatively impermeable segments of the Stillwater fault zone, located 8 and 20 km southwest of the main reservoir. Unlike the wells adjacent to the productive fault segment, BHTV logs from both of these wells showed the development of stress-induced borehole breakouts (e.g., Figure 2d). These breakouts show that the direction of S_{hmin} in wells 66-21 and 45-14 is S20°E ± 15° and S41°E ± 12°, respectively. Thus, the Stillwater fault is optimally oriented for frictional failure near well 66-21 but severely missoriented for failure at site 45-14 (Figure 3). Hydraulic fracturing tests conducted in these wells indicate that S_{hmin}/S_V adjacent to the non-producing segment of the Stillwater fault ranges from 0.55 to 0.64 at depths of 1.9 to 2.2 km (Figure 4b), which is higher than the values of 0.45 to 0.51 observed immediately above the Stillwater fault zone in producing wells to the northeast (i.e., at depths of 2.4 to 2.6 km; see Figure 4a).

Interestingly, fluid pressures in wells 66-21 and 45-14 are artesian, in contrast to the subhdydrostatic pressures encountered within the main geothermal reservoir. Coulomb failure analysis, taking account of these elevated fluid pressures and the appropriate rock densities, indicates that the magnitude of S_{hmin} in well 66-21 is not low enough to induce frictional failure, even on optimally oriented faults (Figure 4b). Thus, at this site, the Stillwater and subparallel faults are optimally oriented—but not critically stressed—for normal faulting. In contrast, Coulomb failure analysis indicates that the S_{hmin} magnitude measured in well 45-14 is low enough to result in incipient frictional failure on optimally oriented normal faults (Figure 4b).

The observation that breakouts were present in these relatively impermeable wells, but absent in wells drilled into the productive main reservoir, suggests a significant increase in the magnitude of S_{Hmax} going from the producing to nonproducing segments of the fault (see Hickman et al., 1998). We used theoretical analyses of the conditions necessary for breakout initiation (e.g., Moos and Zoback, 1990) to place lower bounds on the magnitude of S_{Hmax} in wells 66-21 and 45-14. In so doing, we extrapolated our measurements of S_{hmin} magnitudes in these wells to the depths over which breakouts were observed (assuming constant S_{hmin}/S_V; see Figure 4b) and used estimates of the compressive strength of rocks

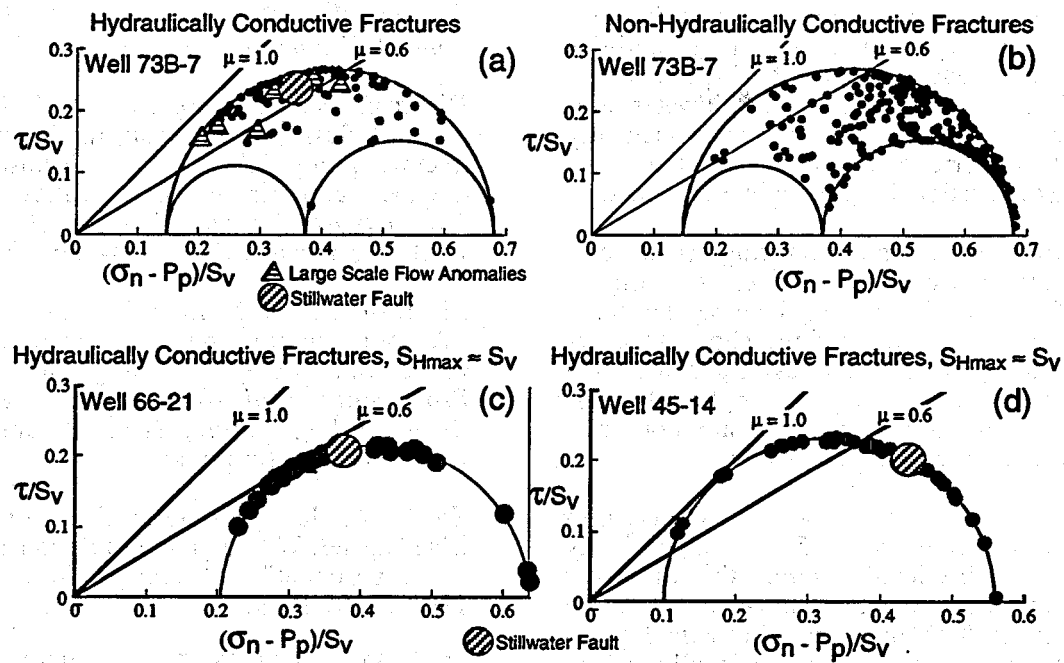

Figure 6. *Shear stress versus effective normal stress, normalized to S_v, for (a) hydraulically conductive and (b) non-hydraulically conductive fractures in well 73B-7. Stresses on the Stillwater Fault adjacent to this well and on fractures primarily responsible for geothermal production (large scale flow anomalies) are also shown. Coulomb failure lines are drawn for coefficients of friction of 0.6 and 1.0. (c), (d) Same as Figure a, but for hydraulically conductive fractures encountered in non-producing wells 66-21 and 45-14, calculated assuming $S_{Hmax} = S_v$.*

encountered at these depths. In this manner, we determined that the magnitude of S_{Hmax} in these non-productive wells is greater than S_v (Figure 4b). This is in marked contrast to wells penetrating the permeable main reservoir, where S_{Hmax} is less than S_v (Figure 4a).

BHTV logs conducted in wells 66-21 and 45-14 revealed extensive natural fracturing, with the dominant fracture set in each well striking parallel to the local trend of the Stillwater fault (Barton et al., 1998). Analysis of TPS and precision temperature logs acquired in these wells under naturally flowing conditions and during injection indicates that hydraulically conductive fractures along the non-producing segment of the Stillwater fault have much lower permeabilities and are fewer in number than observed in wells 74-7 and 73B-7 (Morin et al., 1998). Coulomb failure analysis performed on individual hydraulically conductive fractures from the non-producing well 66-21 indicate that neither these fractures nor the nearby Stillwater fault zone are critically stressed for frictional failure (i.e., these fractures and the Stillwater fault lie below the μ = 0.6 failure line in Figure 6c). Similar analysis for well 45-14 indicates that some—but not all—of the hydraulically conductive fractures in this well are critically stressed for frictional failure (Figure 6d). However, the combined effects of an increase in S_{Hmax} magnitudes relative to S_v (when compared to the producing fault segment) and the extreme misorientation of the Stillwater fault zone with respect to the principal stress directions near well 45-14 (Figure 3), leads to a decrease in the proximity of the Stillwater fault zone itself to Coulomb failure (Figure 6d). These observations suggests that a necessary condition for high reservoir permeability is that both the local state of stress and the orientation of the Stillwater fault zone be such that the fault zone itself is critically stressed for frictional failure.

CONCLUSIONS

We have collected and analyzed fracture and fluid flow data from wells both within and outside the producing geothermal reservoir at Dixie Valley. Data from wellbore imaging and flow tests in wells outside the producing field that are not sufficiently hydraulically connected to the reservoir to be of commercial value provide both the necessary control group of fracture populations and an opportunity to test the concepts proposed in this study on a regional, whole-reservoir scale.

Results of our analysis indicate that fracture zones with high measured permeabilities within the producing segment of the fault are parallel to the local trend of the Stillwater fault and are optimally oriented and critically stressed for frictional failure in the east-southeast extensional stress regime at the site.

In contrast, in the nonproducing (i.e., relatively impermeable) well 66-21 the higher ratio of S_{hmin} to S_v acts to decrease the shear stress available to drive fault slip. Thus, although many of the fractures at this site (like the Stillwater fault itself) are optimally oriented for normal faulting they are not critically stressed for frictional failure.

Although some of the fractures observed in the nonproducing well 45-14 are critically stressed for frictional failure, the Stillwater fault itself is frictionally stable. This is due to the relatively high maximum horizontal principal stress magnitude and the locally severe missorientation of the Stillwater fault zone for normal faulting, which appear to dominate the overall potential for fluid flow at this location.

ACKNOWLEDGMENTS

This work was supported by the DOE Geothermal Technologies Program, under contract DE-FG07-96ID13463 and M600115. However, any opinions, findings, conclusions, or recommendations expressed herein are those of the authors and do not necessarily reflect the views of the DOE. Additional support was provided by the Earthquake Hazards Reduction Program of the U.S. Geological Survey.

REFERENCES

Barton, C., M.D. Zoback and D. Moos, "Fluid flow along potentially active faults in crystalline rock", *Geology*, v. 23, p. 683-686, 1995.

Barton, C., S. Hickman, R. Morin, M.D. Zoback, and R. Benoit, "Reservoir-scale fracture permeability in the Dixie Valley, Nevada, geothermal field", *Proceedings 23rd Workshop on Geothermal Reservoir Engineering*, Stanford Univ., Stanford, CA, 1998 (in press).

Benoit, W., Injection of geothermal fluid in Nevada as typified by the Dixie Valley project, in *Deep Injection Disposal of Hazardous and Industrial Wastes*, J. Apps and C. Tsang (eds.), Academic Press, San Diego, p. 449-464, 1996.

Byerlee, J.D., "Friction of rocks", *Pure and Applied Geophysics*, v. 116, p. 615-629, 1978.

Hickman, S., C. Barton, M.D. Zoback, R. Morin, J. Sass, and R. Benoit, In situ stress and fracture permeability in a fault-hosted geothermal reservoir at Dixie Valley, Nevada, *Transactions Geothermal Resources Council*, v. 21, Burlingame, CA, p.181-189, 1997.

Hickman, S., M.D. Zoback, and R. Benoit, "Tectonic controls on reservoir permeability in the Dixie Valley, Nevada, geothermal field, *Proceedings 23rd Workshop on Geothermal Reservoir Engineering*, Stanford Univ., Stanford, CA, 1998 (in press).

Kamb, W., "Ice petrofabric observations from Blue Glacier, Washington, in relation to theory and experiment", *J. Geophys. Res.*, v. 64, p. 1891-1910, 1959.

Moos, D., and M. D. Zoback, "Utilization of observations of well bore failure to constrain the orientation and magnitude of crustal stresses: Application to continental, Deep Sea Drilling Project, and Ocean Drilling Program boreholes," *J. Geophys. Res.*, v. 95, p. 9305-9325, 1990.

Morin, R., S. Hickman, C. Barton, A. Shapiro, W. Benoit, and J. Sass, "Hydrologic properties of the Dixie Valley, Nevada, geothermal reservoir from well-test analyses," *Proceedings 23rd Workshop on Geothermal Reservoir Engineering*, Stanford Univ., Stanford, CA, 1998 (in press).

Okaya, D.A., and G. Thompson, "Geometry of Cenozoic extensional faulting: Dixie Valley, Nevada," *Tectonics*, v. 4, p. 107-125, 1985.

Seront, B., T.-F. Wong, J. Caine, C. Forster, and J. Fredrich, "Laboratory characterization of hydromechanical properties of a seismogenic normal fault system", *Journal of Structural Geology*, 1998 (in press).

Wallace, R., and R. Whitney, "Late Quaternary history of the Stillwater seismic gap, Nevada," *Bulletin of the Seismological Society of America*, v. 74, p. 301-314, 1984.

Williams, C., J. Sass, and F. Grubb, "Thermal signature of subsurface fluid flow in the Dixie Valley geothermal field, Nevada, *Proceedings 22nd Workshop on Geothermal Reservoir Engineering*, Stanford Univ., Stanford, CA, p. 161-168, 1997.

Laboratory Studies of Geysers Rock and Impacts on Exploration

Brian Bonner
Jeffery Roberts
Alfred Duba
Paul Kasameyer
Lawrence Livermore National Laboratory
(925) 422-7080

ABSTRACT

Measurements of the geophysical properties of recovered core from The Geysers have yielded new data for electrical resistivity and ultrasonic velocities. Large changes in electrical resistivity are caused by boiling of pore fluid entrained in matrix rock, although the increase at the boiling transition is not abrupt as predicted by bulk thermodynamics. Instead, the change is gradual and controlled by high capillary forces due to microporosity in the matrix rock. Resistivity and ultrasonic velocity show a characteristic small change with confining pressure. This indicates that microscopic hydrothermal deposits, which begin lithification at grain contacts, stiffen the rock matrix. These measurements improve understanding of several processes, particularly boiling of pore fluid, hydrothermal reactions, and the effect of depth, that in part control geophysical properties measured in field surveys. Measurements such as these are aimed at developing improved geophysical methods for detecting regions of high hydraulic conductivity in the subsurface and for following reservoir maturation during production.

BACKGROUND

Fundamental studies of the geophysical properties of core have been rare because of the inherent difficulties and resulting high costs for recovering core from geothermal areas. The successful recovery of a long continuous core from The Geysers Scientific Corehole, SB-15D in the central Geysers, CA, provided an opportunity to measure the electrical and seismic properties of the metashale and metagraywacke sequence sampled by coring. Tests conducted on this core have provided valuable data for understanding the processes that control the geophysical response of geothermal rocks.

In particular, measurements of the electrical resistivity of rock during boiling of the pore fluid indicate the potential and limitations of field electrical methods for detecting two-phase fluid *in situ*. Measurements of ultrasonic velocities at pressure by Boitnott and Boyd[1] show that the seismic properties of matrix rock depend only slightly on lithology and fluid content, suggesting that field data are disproportionately influenced by large-scale features such as fractures and rubbleized zones.

EXPERIMENTAL TECHNIQUE

Electrical measurements were conducted inside an externally heated high-pressure vessel with independent control of confining and pore pressure. It was possible to reach the full range of reservoir pressures with this system. Experimental temperatures were sufficient to cause boiling at pressure, but were limited to ~150°C by stability of the insulating jackets used to confine the samples. A similar system operating at room temperature was used by Boitnott and Boyd[1] for ultrasonic measurements. Detailed descriptions of the apparatus and procedures are beyond the scope of this report, but can be found in Roberts et al.[2] and Boitnott and Boyd[1].

RESULTS

A brief summary of experimental results will be given here to illustrate unique aspects of the data particularly relevant to exploration. Detailed results are given by Roberts et al.[2] Resistivity for a metashale sample from 919 ft in SB-15D is plotted in Figure 1 for a constant confining pressure of 50 bars (5 MPa = 725 psi) and temperature of 147°C. A pore pressure gradient increasing with time was applied to the sample by lowering downstream pressure while maintaining upstream pressure at 15 bars. Measurements of the thermodynamic properties for brines of the composition used here indicate that boiling should occur when the pressure is reduced to 4.4 bars, a value not very different than that for pure water. If the brine entrained in the sample flashed to steam, a sharp increase in resistivity should occur at this pressure. Instead, a gradual increase in resistivity occurs as the downstream pressure decreases, consistent with boiling occurring first in the largest pores followed by boiling in successively smaller pores. Estimates of the capillary pressures in the sample using pore diameters determined by mercury injection suggest that local forces in the pores are large enough to retard boiling.

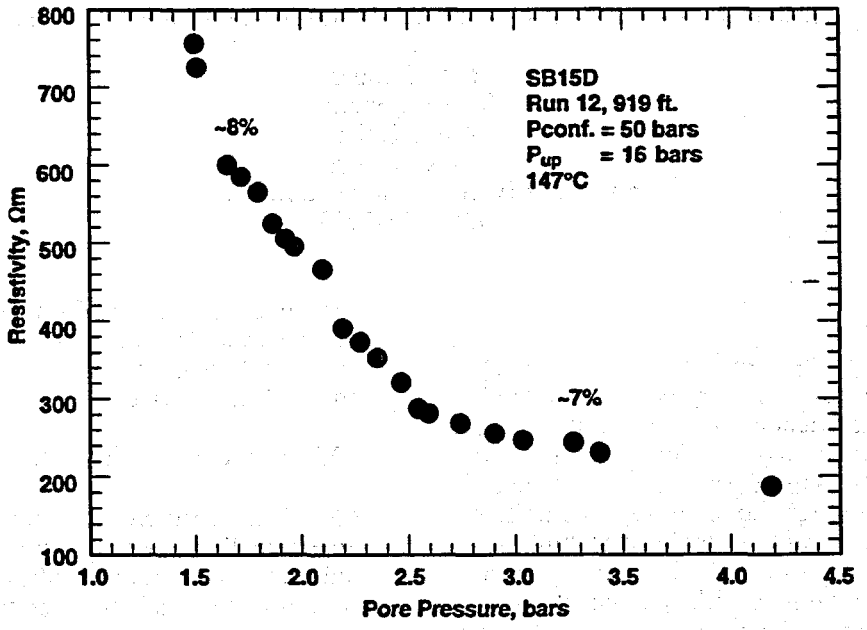

Figure 1. Resistivity as a function of downstream pore pressure at 147°C for a metashale from SB-15D. The percentages on the plot are estimates of the vapor saturation derived independently from measured pore size distribution and estimates of capillary pressure for a pore of a given size.

A numerical simulation of the experimental configuration for resistivity measurements was performed by M. Shook of INEL (Shook, personal communication, 1997) to aid in interpretation of this result and to plan further experiments. The results of a simulation using the TETRAD code are shown in Figure 2. The input parameters were 0.03 porosity, 1 nD permeability, and a maximum capillary pressure of 300 bar (30,000 kPa). A plug of appropriate geometry was subjected to a 14-bar pore pressure gradient, and the simulation was run for 14 days. At the end of the simulation, 20% of the core nearest the downstream boundary contained two-phase fluid in the pore space, and the vapor saturation was 90% at the downstream boundary. Although the saturation profile in the two-phase region depends critically on the capillary pressure relation chosen as input, the simulation is broadly consistent with the laboratory observations of electrical resistivity.

Ultrasonic data from Boitnott and Boyd[1] are summarized in Figure 3, and show several significant features. Velocities are quite high for quartz-rich sedimentary rock. In all cases, the change with confining pressure, which corresponds approximately to 3 km depth, is strikingly small when compared with the response of typical crustal rocks. The increase in compressional velocity, Vp, with fluid saturation is notably small. This is in part explained by the decrease in shear velocity, Vs, with fluid saturation. This softening of the shear response is particularly strong in the metashale and has been shown to increase with increasing clay content[1,3]. It appears that rock chemical–water interactions occur at the grain scale in hydrothermal alteration products that cement the rock matrix. Additional measurements in the laboratory at seismic frequencies indicate that the softening also occurs in the hertz frequency range.

DISCUSSION

Measurements of electrical resistivity at high temperature and pressure were made to determine properties relevant to the matrix rock at reservoir conditions. Resistivity of the rock is dominated by changes in the properties of the pore fluid. Measurements of electrical resistivity for rocks from The Geysers at temperature and pressures close to reservoir conditions indicate that small electrical resistivity increases are caused by changes in confining pressure; larger decreases in electrical resistivity occur with decreasing temperature when the pore fluid is liquid. Large changes in rock resistivity with pore fluid temperature suggest that relatively cool fluid could be followed into zones of high fluid conductivity underground with a high-

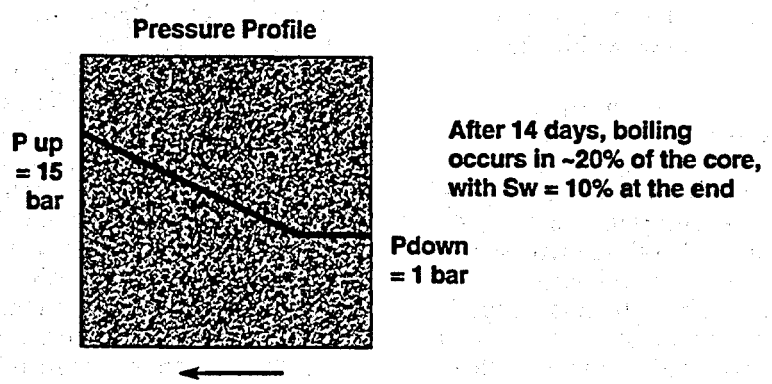

Parameters for TETRAD simulation	
Porosity	0.03
Permeability	1 nanodarcy (10^–21 m^2)
Max. capillary pressure	300 bar (30,000 kPa)

$P_c = 30{,}000\ (1\text{-}Sw)^2$

Figure 2. Input parameters and results of a numerical simulation of the experimental configuration used for resistivity experiments. See text for details.

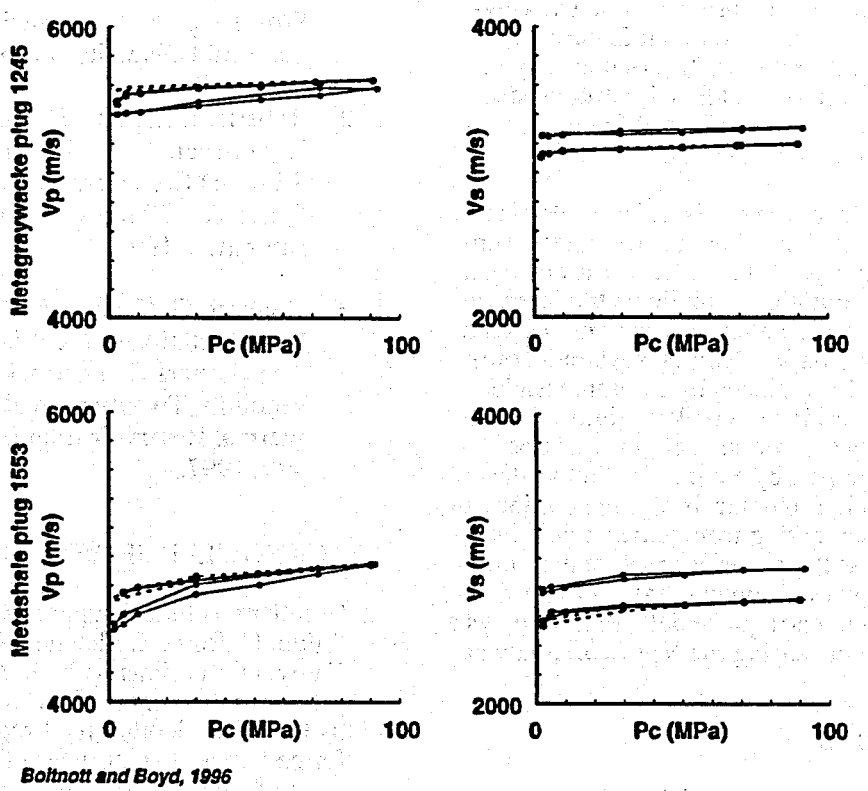

Figure 3. Ultrasonic velocities for metashale and metagraywacke from SB-15D. Note small increases with pressure, which are equivalent to ~3 km depth in the reservoir.

temperature EM logging tool as a method to map major conducting fractures within the reservoir.

The most dramatic resistivity changes are associated with boiling of pore fluid. Resistivity increases gradually as pore fluid entrained in progressively smaller pores flashes to steam. Both decreasing temperature and boiling increase resistivity, so care must be taken in interpreting low-resistivity anomalies. Nonetheless, properly interpreted field resistivity measurements should be useful in locating two-phase regions, such as developing steam caps in liquid-dominated systems and in monitoring reservoir maturation in vapor-dominated systems such as The Geysers.

Laboratory measurements of ultrasonic velocities by Boitnott and colleagues have pointed out the importance of hydrothermal interactions on the seismic properties. High velocities and the lack of pressure dependence indicate that the beginning of lithification at grain contacts has reduced compliant microporosity at these sites, stiffening the rock elastic response. The lack of pressure dependence has important implications for interpretation of field seismic data. Since field velocities are relatively low and change with depth (pressure), large-scale features not present in the intact plugs disproportionately control the field seismic properties at The Geysers. These large-scale compliant features are clearly important for hydraulic conductivity in the reservoir. Boitnott and Boyd[1] introduced a model to analyze how matrix and fracture properties interact on the field scale.

Geochemical alteration on the microscale also makes rocks from The Geysers structurally sensitive to aqueous pore fluids. Decreases in shear velocity with saturation complicate the interpretation of Vp/Vs anomalies observed in the field. In all porous media Vp decreases when incompressible liquid is replaced by a compressible gas phase, decreasing the bulk modulus. For rocks from The Geysers this effect might be compensated in part by a reduction in the shear modulus, which also controls Vp. In addition, an increase in Vs resulting from geochemical interaction occurs as the material desaturates. Boitnott and Kirkpatrick[3] convincingly argue, from analysis of microearthquake data, that Vs plays a the major role in causing the Vp/Vs anomaly at The Geysers.

CONCLUSIONS

Laboratory measurements of the seismic and electrical properties of rocks from geothermal areas are beginning to yield a consistent picture of the effects of the hydrothermal environment. Geochemical alteration at the microscale is reflected in the electrical and seismic properties. For matrix rocks from The Geysers alteration tends to diminish differences in lithology. Lack of pressure dependence in ultrasonic velocities for Geysers rocks suggest that field seismic properties, particularly the depth dependence, are controlled by large-scale features. Although such features are not present in plug samples, they are critically important for hydraulic conductivity. When the pore fluid is liquid, temperature controls rock resistivity. It should be possible to design borehole surveys to follow cooler fluids, such as injectate, into regions of high permeability. Resistivity measurements show that boiling occurs over a range of pressure or temperature in a material with fine porosity such as matrix rock from The Geysers. Since electrical resistivity depends on vapor saturation during progressive boiling, it may be possible to monitor reservoir maturation with field data.

REFERENCES

1. Boitnott, G. N. and P. J. Boyd, "Permeability, Electrical Impedance, and Acoustic Velocities on Reservoir Rocks from The Geysers Geothermal Field," pp. 343-350, Proceedings, Twenty-first Workshop on Geothermal Reservoir Engineering, Stanford University, 1996.

2. Roberts, J. J., A. G. Duba, B. P. Bonner, and P. Kasameyer, "Resistivity During Boiling in the SB-15-D Core from The Geysers Geothermal Field: The Effects of Capillarity," Geothermics, submitted, 1997.

3. Boitnott, G. N. and Ann Kirkpatrick, "Interpretation of Field Seismic Tomography at The Geysers Geothermal Field, California," Proceedings, Twenty-second Workshop on Geothermal Reservoir Engineering, Stanford University, 1997.

ACKNOWLEDGEMENTS

Excellent technical support was provided by W. Ralph, C. Boro, S. Fletcher, A. Bradley, and T. Carey. Discussions with G. Boitnott contributed greatly to this report. This work was sponsored by the DOE Geothermal Program and was performed under the auspices of the U.S. Department of Energy Office of Basic Energy Sciences by Lawrence Livermore National Laboratory under Contract W-7405-ENG-48.

Concurrent Session 4:

Energy Conversion Technology

Investigation of Innovative Cycles using Mixed Working Fluids

Desikan Bharathan
Vahab Hassani
National Renewable Energy Laboratory
(303) 384-7464

Abstract

For medium-temperature geothermal resources, use of mixed working fluids in subcritical power cycles is investigated. This paper presents a progress report on the ongoing work at NREL.

Introduction

Many of the hydrothermal high-temperature reservoirs are already in use for power generation in the United States. However, low- and medium-temperature reservoirs are numerous; many are accessible closer to the ground. To expand their use, there is a need for substantial reduction in cost, especially in the cost related to energy conversion equipment.

The United States Department of Energy (US DOE) has embarked on a concerted research and development effort at the National Renewable Energy Laboratory (NREL) with the goal of reducing the cost of energy conversion systems. During fiscal year 1997, researchers at NREL began a task to explore and assess innovative power cycle configurations. By design, NREL limited the selection of cycles to those that can use non-azeotropic mixed working fluids. NREL's efforts have been focused on the adaptability of these innovative cycle arrangements that are practical and that have the potential to achieve cost reduction. Results presented in this paper summarize a subset of the progress made in our investigations.

Scope and limitations

The overall scope of the investigation has remained fairly broad. Choices related to the selection of the power cycle, working fluids, operating pressures, fluid compositions, flow splits, heating and cooling arrangements are numerous. However, in this paper, we will limit our discussions to subcritical "binary" cycles, which use hydrocarbon working fluids. We conducted all cycle analyses using the commercially available software ASPEN™. We further made the following assumptions:

- o brine resource temperature, 335°F
- o minimum brine outlet temperature, 160°F
- o vaporizer pinch point ΔT, 10°F,
- o condenser is air cooled,
- o ambient air temperature, 50°F,
- o an air temperature rise of 15°F,
- o condenser pinch point ΔT, 15°F,
- o turbine isentropic efficiency, 72%
- o pump efficiency, 65%;

Pressure losses through the various components are ignored; for hydrocarbons vapor superheating is considered not necessary. These assumptions were adopted to allow the results of this study to be readily applicable to realistic operating power systems in the industry.

An ideal cycle

Figure 1 illustrates an ideal cycle in a T-S diagram where the working fluid heating and cooling curves match the corresponding brine cooling and the air heating curves, respectively. Such ideal cycles have been analyzed, among others, by Ibrahim, et. al. [1991]. Our analyses, following Ibrahim, indicates that the maximum power yield from such a cycle per unit brine mass flow (or the brine effectiveness) is 11.3 Wh/lb. This value represents the high limit which can used to compare the relative merits of various proposed practical schemes.

Practical working fluids and their properties

The ideal cycles use an "ideal" working fluid, the characteristics of which cannot be realized in practice. Commonly used fluids in the binary cycles include hydrocarbons, ammonia, and water. Figure

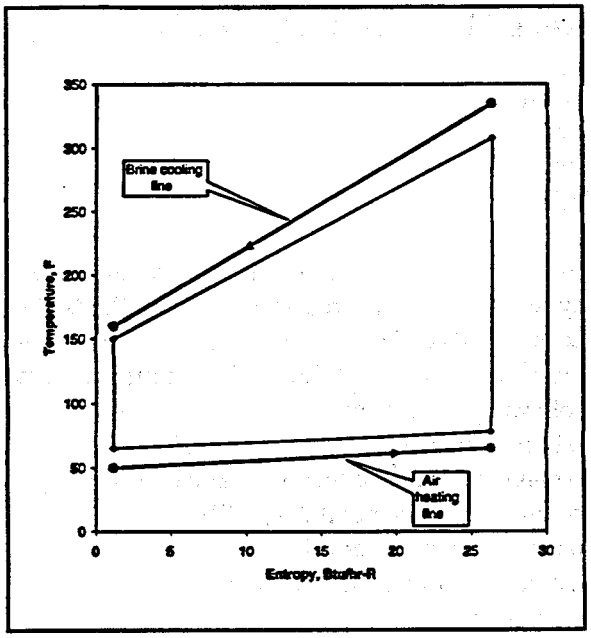

Figure 1. An illustration of an ideal cycle in a Temperature vs Entropy diagram

2 illustrates the variation of saturation pressure with temperature for a select list of candidates for the working fluid. Likely vaporizer temperature ranges from 160°F to 260°F, as indicated by dotted vertical lines. Atmospheric pressure as well as a high pressure practical limit of 500 psia are also indicated as horizontal dashed lines in this figure. As expected, ammonia and propane yield the highest saturation pressures over the range of indicated boiler temperatures. For iC_5 and iC_6, the condenser pressure at a temperature of 65°F is subatmospheric. For water, both the boiler and condenser pressures are likely to be subatmospheric. Pure fluids offer only a few discrete choices for optimum high and low pressures for the cycle.

With mixed working fluids, such as NH_3 and water, an entire range of cycle high pressures are possible (approximately from 30 psia to 500 psia), by varying the mixture concentration. The concentration also allows one to select a most suitable condenser pressure as well. For mixtures of hydrocarbons, such as iC_4 (isobutane) and iC_5 (isopentane), subatmospheric pressures in all parts of the cycle should be avoided for safety considerations. The following results of the cycle analyses indicate how optimal high and low pressures may be chosen by the designer.

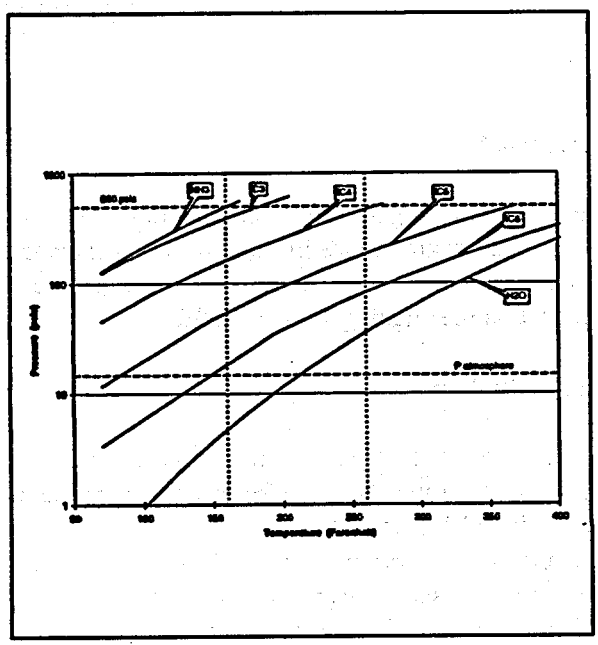

Figure 2. Saturation pressures for a few common working fluids

Rankine cycle with pure fluids

Consistent with the stated assumptions, we analyzed the Rankine cycle that uses pure iC_4 and pure iC_5. For these hydrocarbons, vapor from the evaporator was not superheated.

For pure iC_4, Figure 3 shows the variation of brine effectiveness and the saturation temperature as functions of vaporizer pressure. The brine effectiveness generally increases with increasing cycle maximum pressure. We note that the highest effectiveness of 6.6 Wh/lb is obtained at a vaporizer pressure of nearly 475 psia. Above 500 psia, the cycle becomes supercritical and is beyond the focus of the current analyses. The saturation temperature increases in concert with the vaporizer pressure, as dictated by the property of iC_4. For all cases shown in this figure, the condenser pressure was nearly 40 psia.

Similar variations for pure iC_5 are shown in Figure 4. In this figure, we note that the maximum cycle pressure varies from 80 psia to 180 psia. The variation of the brine outlet temperature is also shown. A maximum for brine effectiveness of 6.75 occurs at a vaporizer pressure of nearly 140 psia. For all vaporizer pressures, the condenser for iC_5 operates at a subatmospheric pressure of about 11 psia.

We note from the previous two figures that the vaporizer pressure for the pure fluid must be fixed at specific values for achieving the maximum brine effectiveness. For iC_5, the condenser operation at a subatmospheric pressure is not recommended for safety reasons.

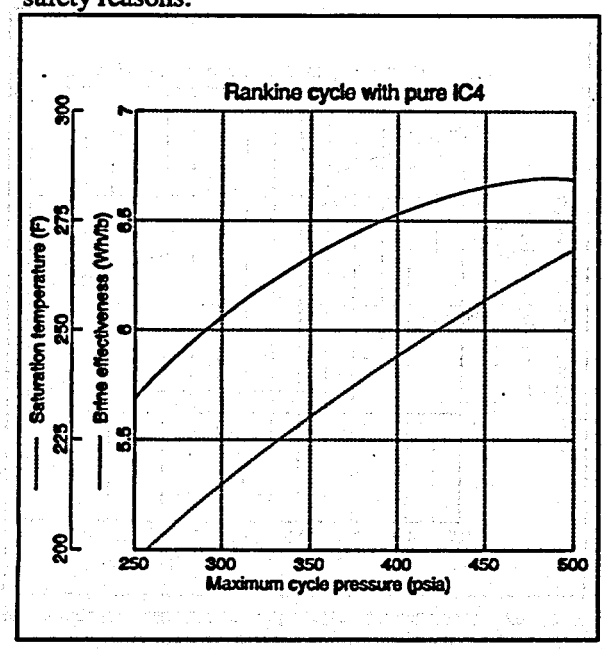

Figure 3. Brine effectiveness and vaporizer saturation temperature as functions of vaporizer pressure

Rankine cycle with mixed fluids

A Rankine cycle that uses a mixed working fluid allows a wider range of choice for the maximum cycle pressure. Usually the pressure range available for the designer runs from a low (namely, the saturation pressure of the heavy component of the mixture) to a high (the saturation pressure of the light component) at any given temperature. Such an option arises because the composition of the mixture can be varied by the designer. We investigated a Rankine cycle that uses a mixture of iC_4 and iC_5.

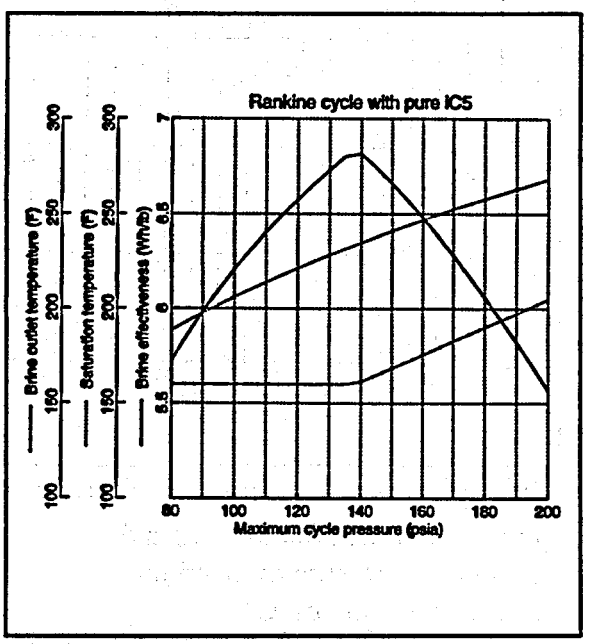

Figure 4. Brine effectiveness and vaporizer saturation temperature as functions of vaporizer pressure

For the illustrated analyses, we chose a maximum cycle pressure of 275 psia (which falls within a 300 psig limit for the use of Sch. 40 flanges and fittings). The composition of the mixture was allowed to vary from 20% iC_4 to 100% iC_4. During evaporation and condensation of the mixture, the heating and cooling the working fluid is assumed to be carried out in a countercurrent flow arrangement. Such an arrangement allows the vapor to rise in temperature between the bubble point and the dew point as the vapor fraction of the mixture increases.

Figure 5 shows the results of the analyses. In this figure the brine effectiveness and the condenser pressure are plotted as functions of isobutane mass fraction. Over the range of mass fraction shown, the condenser pressure remains above the atmospheric pressure and increases with increasing iC_4 concentration. A maximum brine effectiveness of nearly 6.4 Wh/lb occurs at a concentration of about 0.5.

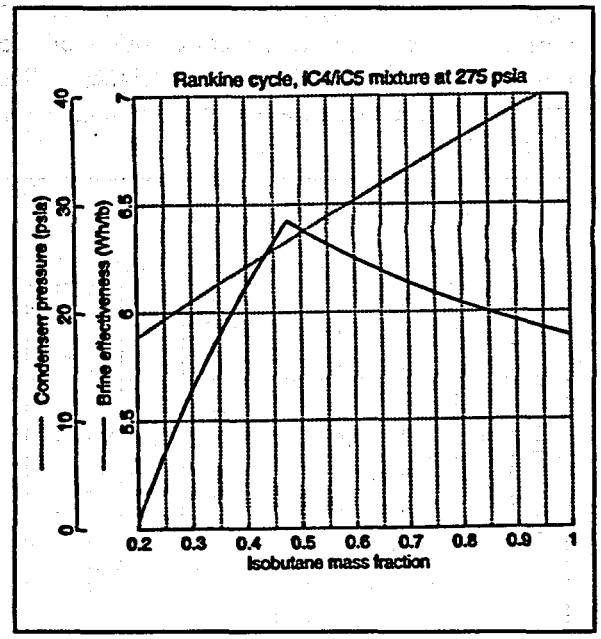

Figure 5. Brine effectiveness and condenser pressure as functions of concentration of iC4

Accompanying Figure 6 shows the variations of the bubble point and dew point of the working fluid mixture and the brine outlet temperature for this cycle. The brine outlet temperature decreases with in-creasing iC_4 concentration and attains the design goal of 160°F at a concentration of 0.5. The difference between the dew point and the bubble point for the mixture attains a value of about 10°F at this concentration. The results of the analyses shown in figures 5 and 6 assume that the vapor leaving the vaporizer can attain the dew point temperature corresponding to the basic mixture concentration. However, on account of the changing flow regime in the vaporizer, heating of the vapor to this dew point may not be realized in a practical countercurrent heat exchanger.

To model a realistic countercurrent heat exchange scheme for mixed working fluids, we limited the vapor fraction of the exiting working fluid mixture to 15%. This arrangement requires the heated liquid that remains behind after vapor separation to be recirculated through the vaporizer. With such a pump-around scheme, we reanalyzed the Rankine cycle with the stated pinch point assumptions.

The results of this analyses is shown in figure 7. Condenser operating pressure and the brine effectiveness are plotted once again as functions of the iC_4 concentration. From this figure, we find that the maximum brine effectiveness of about 6.2 Wh/lb occurs at a higher iC_4 concentration of slightly over 60%. We find that this maximum is less than that obtained in the previous case. This reduced brine effectiveness occurs because we are unable to take advantage of the temperature difference between the bubble and dew points for the mixture in a realistic scheme.

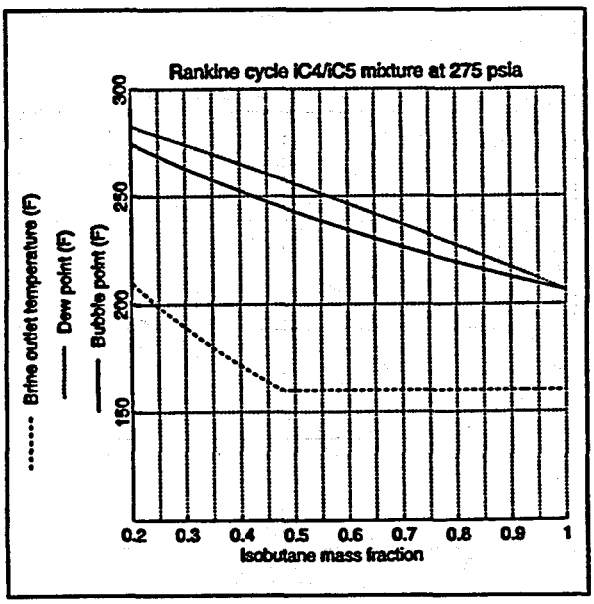

Figure 6. Brine effectiveness and condenser pressure as functions of iC4 concentration for Rankine cycle

In the ongoing work at NREL, researchers will attempt to capture the potential gain that may be possible here through new designs for countercurrent heat exchanger schemes.

Maloney-Robertson cycle

Figure 8 shows a schematic diagram of a Maloney-Robertson (M-R) cycle that uses a mixed working fluid [Maloney & Robertson, 1953]. This cycle can

be classified as the absorption cycle, and was originally studied for use of ammonia/water mixture. The working fluid mixture is partially vaporized in a boiler. The vapor is separated, superheated if necessary, and is then expanded through a turbine to produce power. The effluent liquid from the separator exchanges heat with the incoming boiler feed. It then is expanded through a liquid turbine to extract more power (This is a variation from the original M-R cycle, which uses a pressure reducing valve here). Finally, this liquid is mixed with the turbine exhaust vapor to lower the condenser operating pressure. The vapor/liquid mixture is then condensed, in this case, in an air-cooled condenser.

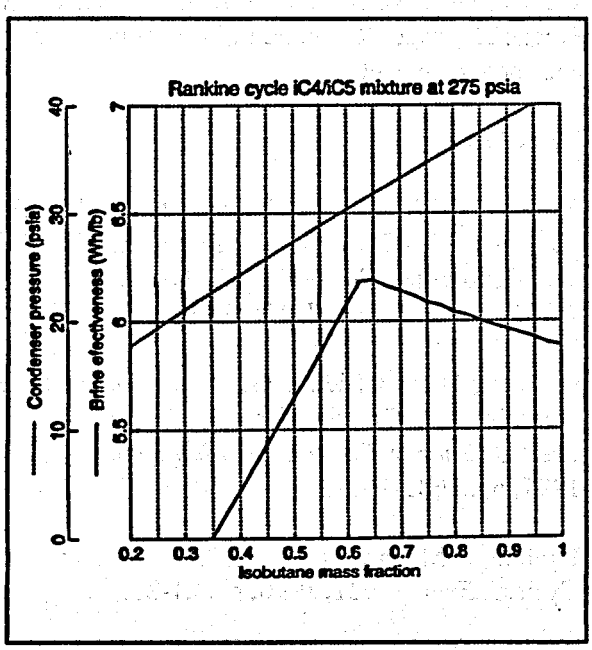

Figure 7. Brine effectiveness and condenser pressure as functions of iC4 concentration for Rankine cycle with a reboiler

We studied the potential for the M-R cycle, using iC_4/iC_5 mixtures. Once again, to model a realistic countercurrent heat exchange scheme for mixed working fluids, we limited the vapor fraction of the exiting working fluid mixture to 15%. The results of this analysis, conducted at a chosen cycle maximum pressure of 275 psia, are shown in Figure 9. Brine effectiveness, mixture bubble-point temperature, and the brine outlet temperature are plotted as functions of the mixture iC_4 concentration. The brine effectiveness varies from a low of 2 to a high of 3 as the iC_4 concentration is increased. The brine outlet temperature decreases from about 280°F down to 180°F with increasing iC_4 concentration . The bubble point temperature shows a similar trend and stays approximately 10°F higher.

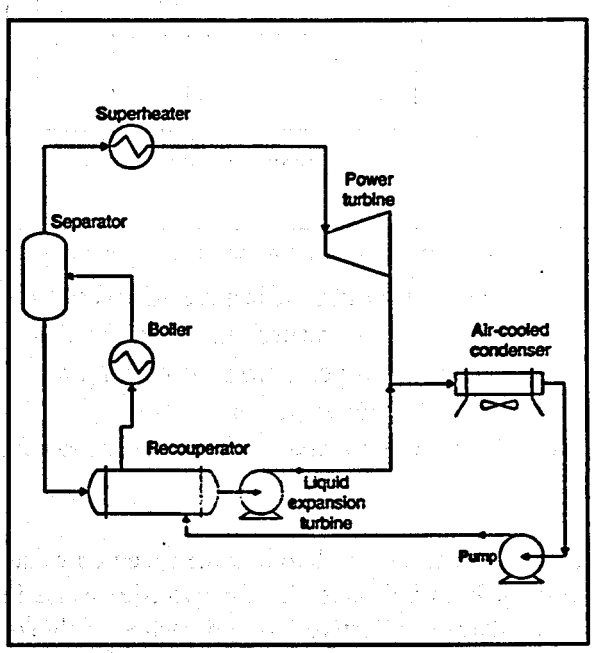

Figure 8. A schematic diagram for the Maloney-Robertson cycle

We find that the brine effectiveness for this cycle is substantially lower than that for the corresponding Rankine cycle. The reasons behind the lower values are that 1) the heat exchange occurring in the recuperator adds additional losses to the cycle, 2) because the feed is heated by recuperation, the brine outlet temperature remains high, and 3) the pumping the large volume of liquid back and forth between the low and high pressures consumes parasitic power.

If the required brine outlet temperature must be reached, one may use two MR cycles in series (i.e. one below another) and limit the brine

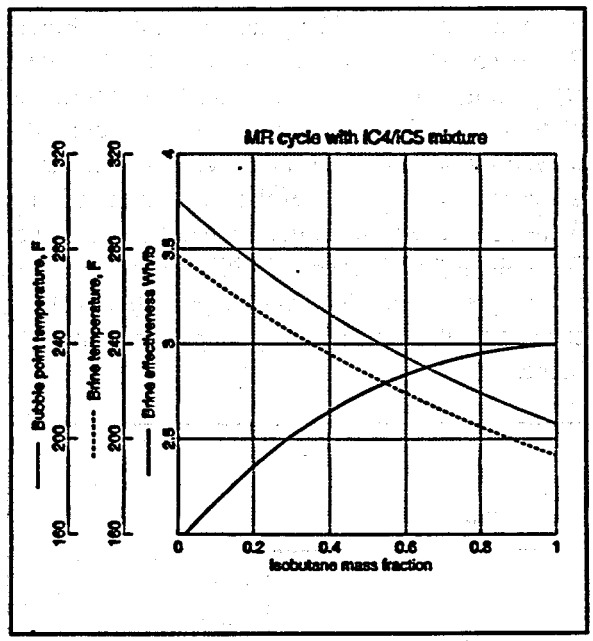

Figure 9. Variations of brine effectiveness brine outlet temperature, and mixture bubble-point temperature as functions of mixture iC4 concentration

temperature drop in each to half the specified value. Our analysis indicates that for two MR cycles in series, the brine effectiveness approaches a value of 5. The MR cycle performance may be improved by increasing the performance of the recuperator, and seeking a higher efficiency for the feed liquid pump. However, we find that the MR cycle, as configured, does not offer any significant potential for increased brine effectiveness than the simple Rankine cycle.

Summary and Conclusions

Mixed working fluids have the potential to offer more design flexibility in a binary cycle than pure fluids, without a significant improvement or penalty on the brine effectiveness. This flexibility arises with respect to a designer's choices for the boiler and condenser pressures. This study presented results for mixtures of isobutane and isopentane. A Rankine cycle using a mixed this mixture yields a higher brine utilization that the Maloney Robertson cycle. The M-R cycle's performance suffers because a large amount of liquid is pumped back and forth between the high and low pressure regions of the cycle.

Continuing work

Ongoing work at NREL sponsored by the US DOE will investigate other candidate mixtures for the working fluid, more advanced components , and other variations in the processes, with the goal of reducing the cost of power production from medium-temperature geothermal resources.

Acknowledgements

We would like to thank our Geothermal Technology Program Manager Raymond LaSala for his support and encouragement.

References

Ibrahim, O.M., S.A. Klein, and J.W. Mitchell, "Optimum Heat Power Cycles for Specified Boundary Conditions," *Journal of Engineering for Gas Turbines and Power*, V113, 1991, pp. 514-521.

Desideri, U. and Bidini, G., "Study of Possible Optimisation Criteria for Geothermal Power Plants," *Energy Conversion Management*, V38, 1997, pp. 1681-1691.

Ibrahim, O.M. and S.A. Klein, "Absorption Power Cycles," *Energy*, v21, 1996, pp. 21-27.

Maloney, J.D. and R.C. Robertson, "Thermodynamic Study of Ammonia Water Heat Power Cycles," Oak Ridge National Laboratory, Report CF-53-8-43, Oak Ridge, TN, August 1953.

PROGRESS ON COMMERCIALIZATION OF THE BIPHASE GEOTHERMAL TURBINE

Don Cerini, Ken Wiberg, Walter Studhalter, Lance Hays
Douglas Energy Company
Placentia, California
(714) 524-3338

INTRODUCTION

The Biphase turbine is a turbine which generates power from high pressure mixtures of gases and liquids for which energy previously has been wasted in flashing and pressure letdown processes. It has been commercialized for refrigeration and the first commercial oil and gas unit will be operated this month. Douglas Energy Company is currently conducting a project to demonstrate a commercial Biphase geothermal turbine at the Cerro Prieto geothermal field of the Comisión Federal de Electricidad (CFE). The project is supported by a U.S. Department of Energy Cooperative Funding Agreement; a California Energy Commission cost shared loan grant; an E&Co project loan; technical and facility assistance by CFE. and Douglas Energy Company internal funding.

The project was initiated by the DOE in September 1993 in response to Solicitation No. DE-PS02-92CH10516. Cooperative Funding Agreements were awarded at that time to Douglas Energy Co. and to Exergy Inc. for a Kalina Cycle demonstration.

In September 1994 Douglas Energy Co. completed a successful demonstration of a subscale Biphase turbine at the Coso Hot Springs field of California Energy Company, reference 1. California Energy Company provided a geothermal well and site. The inlet quality to the subscale Biphase turbine was varied from zero (0) to one (1). The unit was successfully operated for 700 hours of testing, during which the performance was measured and agreed well with that predicted by existing two-phase nozzle and turbine codes at Douglas Energy Company, reference 2.

The site for a full size unit was provided by CFE, who agreed to purchase the generated power for a two-year period. In July 1997, installation was completed for the full size Biphase turbine unit, rated at 1.1 megawatt. In addition, installation was completed for the balance of plant for a back pressure steam turbine rated at 3.2 megawatts. The steam turbine will use the high pressure steam provided by the Biphase turbine to generate the additional power. The power plant installation is shown in Figure 1.

This paper reports the results of operations of the Biphase turbine during the startup period and the current status and future plans for the project.

OPERATIONAL HISTORY AND PROJECT STATUS

The flow schematic for the completed Biphase turbine power plant is provided in Figure 2. Startup was initiated in July 1997. After a period of electrical calibration and modifications to the power metering equipment to meet CFE standards, the Biphase turbine was synchronized with the CFE commercial grid on August 8, 1997. The unit was initially operated with steam from the CFE separator to enable synchronization and checkout of the protective relays, instrumentation and trip circuits.

The results were successful and on August 18 two-phase well flow was introduced to the Biphase turbine. The unit operated smoothly for a period of about five hours after which rapid increases in bearing vibration levels (from 2 mils to 11 mils) were measured.

Examination of the turbine showed a buildup of solids on the diffuser side of the separator rotor (only) which eventually led to contact and rubbing of the diffuser inlet, causing the high vibration levels.

Several startup periods ensued during which several means were tried to overcome the solids buildup including: extended pre-operational steam blow cleaning of the piping, moderate pressure water jet fluidization of the solids and small two-phase nozzle jet fluidization of the solids.

These various methods enabled full two-phase wellhead operation for short periods of time. The operation enabled the generation of a complete "punch list" for the facility and initial two-phase performance data.

Private funding sources are currently being applied to implement the "punch list" and solve the solids problem. After the Biphase turbine is operated for 2000 hours, the back pressure steam turbine will be installed and operated.

RESULTS TO DATE

Perhaps the most rewarding results thus far has been the generation of power for the CFE grid from the complete wellhead flow at 610 psia. The geothermal well of the installation, No. 103, has experienced a decline in wellhead pressure and enthalpy during the period of design and construction. Figure 3 shows the history of the decline. The power production potential from that well alone has declined accordingly. In order to generate the full 1.1 megawatt potential of the Biphase turbine, the flow from a nearby well, No. E-15, will need to be added to the flow from No. 103.

The decline in enthalpy has produced a lower steam inlet quality than the design. This has resulted in a nozzle which is substantially underexpanded at the present conditions.

A test series was completed to measure the power generation from the well and compare the results to the power predicted by the design codes. Figure 4 shows the results. At the lower pressure points the inlet pressure to the turbine was varied by bypassing a portion of the flow and dropping the pressure through the inlet valves. At the high pressure points the complete two-phase well flow was provided to the turbine. The calculated curve uses the CFE measured wellhead enthalpy for No. 103 and the actual Biphase turbine geometry and design codes.

With a correction for underexpansion losses, the data agree well with the predicted power at full well flow. At full well flow the generated power of .81 megawatts is within 10% of the predicted power.

Currenty the power generated by the central steam turbine from the steam from well No. 103 is 5.87 megawatts. When the Biphase turbine generated at full flow the total was 6.55 megawatts, a 12% increase. (Addition of the back pressure steam turbine at the current well conditions will add another 1.97 megawatts to give a total of 8.17 megawatts for a 39% increase.)

The efficiency (electric power generated divided by isentropic enthalpy difference) of the Biphase turbine at full wellhead flow was measured to be 33%. The shaft power efficiency would be 35% based on the quoted generator efficiency of 95%. If the expansion ratio of the nozzles were modified to account for the new well conditions, the efficiency would be 41%.

A total of 23 startup and shutdowns and 73 running hours were logged during startup operations. The water lubricated silicon carbide bearings performed well and were unaffected by the thermal transients. In the absence of solids rubbing the diffuser, the vibration levels were in the 2-3 mil range with two-phase flow. A photograph of the bearings after these startup cycles is shown in Figure 5. No wear or cracking is discernible.

An analysis of the solids is provided in Table 1. It is unknown whether the source of solids is mechanical or whether the solids are forming in the nozzle expansion. The nozzle side of the rotary separator, Figure 6, is free of deposits or erosion, suggesting that the high momentum of the nozzle flow keeps the solids fluidized. The diffuser side, as shown in Figure 6, had deposits due to the centrifugal separation. Attempts to fluidize the solids with moderate pressure (1000 psi) hydroblast nozzles as shown and with small two-phase nozzles improved operation, but was not completely successful.

A two-prong attack on the solids problem is planned: a side-stream test of additives and pH modification in the event the solids are formed by dissolution and high pressure hydroblast nozzles (5000 psi) to periodically provide the same momentum as the main two-phase nozzles to fluidize the solids enabling them to exit with the diffuser flow. Scanning electron microscope photographs of the solids showed the majority to be in the 2-3 micron size range. At that size, mechanical fluidization should be effective. Figure 7 is a schematic of the solids test system to be installed.

SUMMARY

Operation of the Biphase turbine with two-phase well flow at 610 psia during startup was in close agreement with off-design predictions. The maximum power generated for the CFE grid was .81 megawatts, within 10% of the design code prediction.

Work is proceeding on a solution to the solids problem and on completing the startup "punch list" items. The pacing item to date has been financial rather than technical constraints. With the addition of private funding, demonstration of the Biphase turbine and installation and operation of the back pressure steam turbine is planned for 1998.

REFERENCES

1. Studhalter, W., Cerini, D., Hays, L., "Demonstration of an Advanced Biphase Turbine at Coso Hot Springs", DOE Project Review, San Francisco, April, 1995.

2. Studhalter, W., "Biphase Geothermal Turbine,Topical Report No. Q2", U.S. Department of Energy Contract DE-FC3b-93CH10590, Placentia, CA, February, 1996.

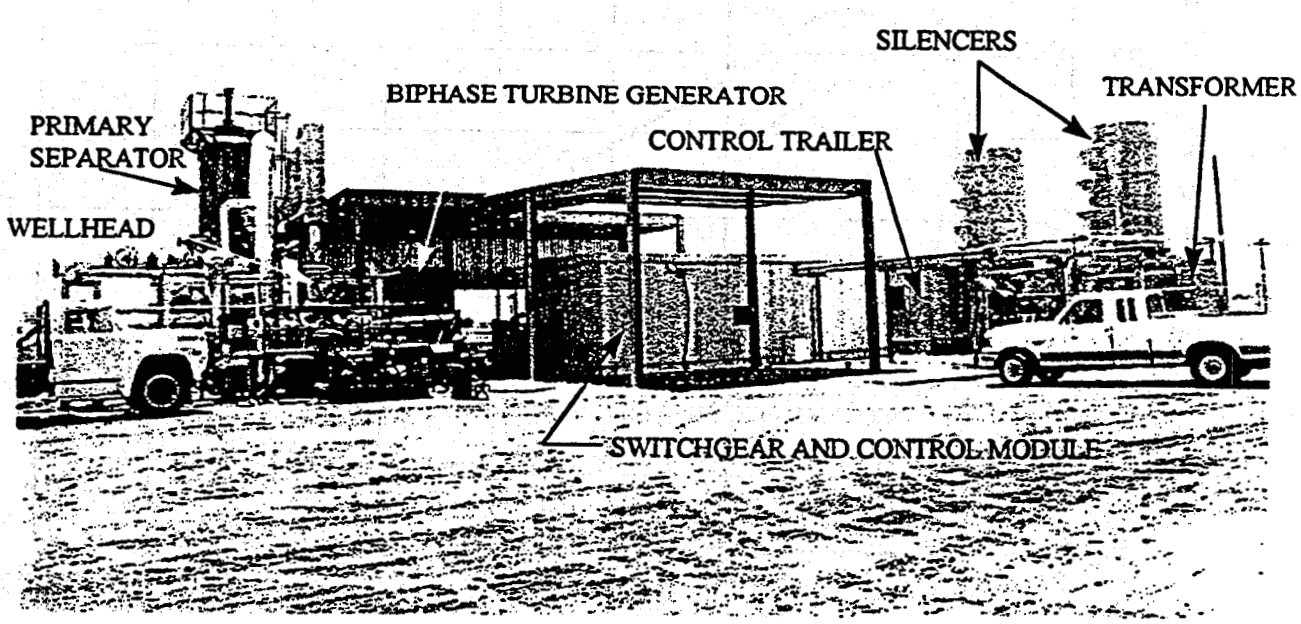

Figure 1. Biphase Power Plant at Cerro Prieto.

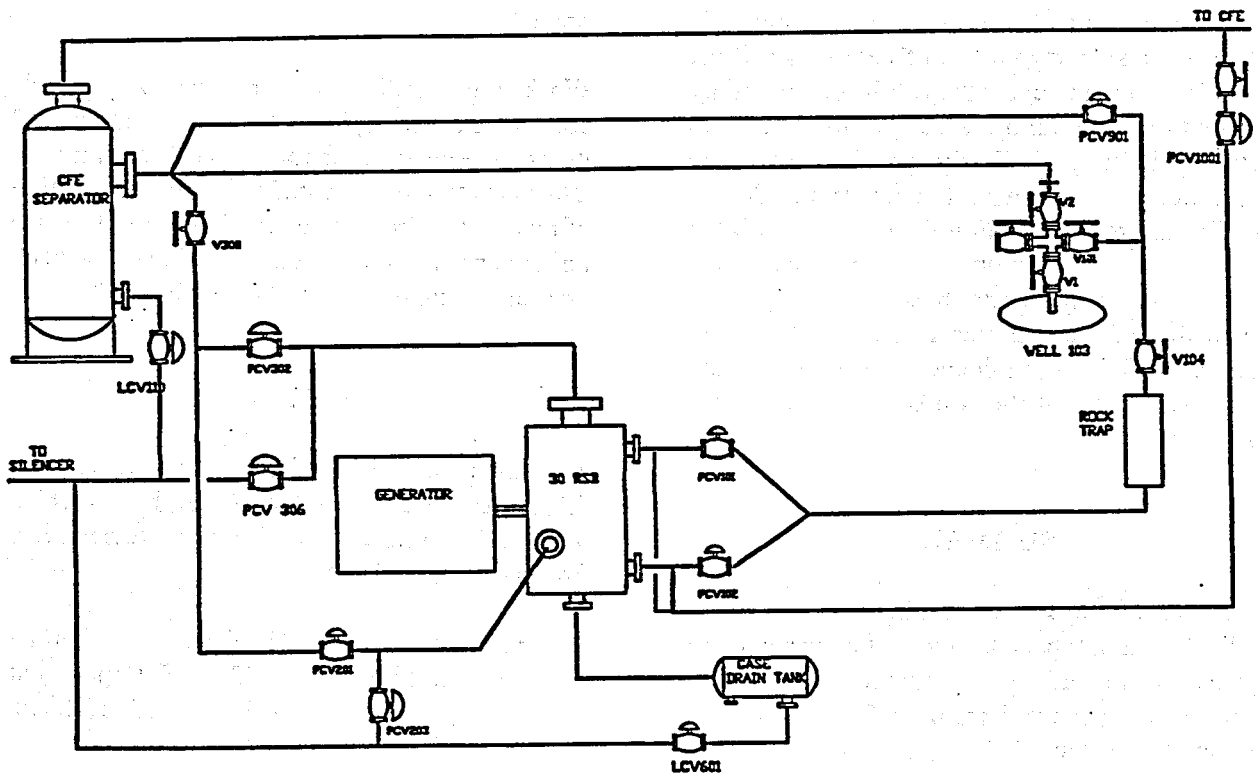

Figure 2. Flow Schemataic for Existing Biphase Turbine Installation.

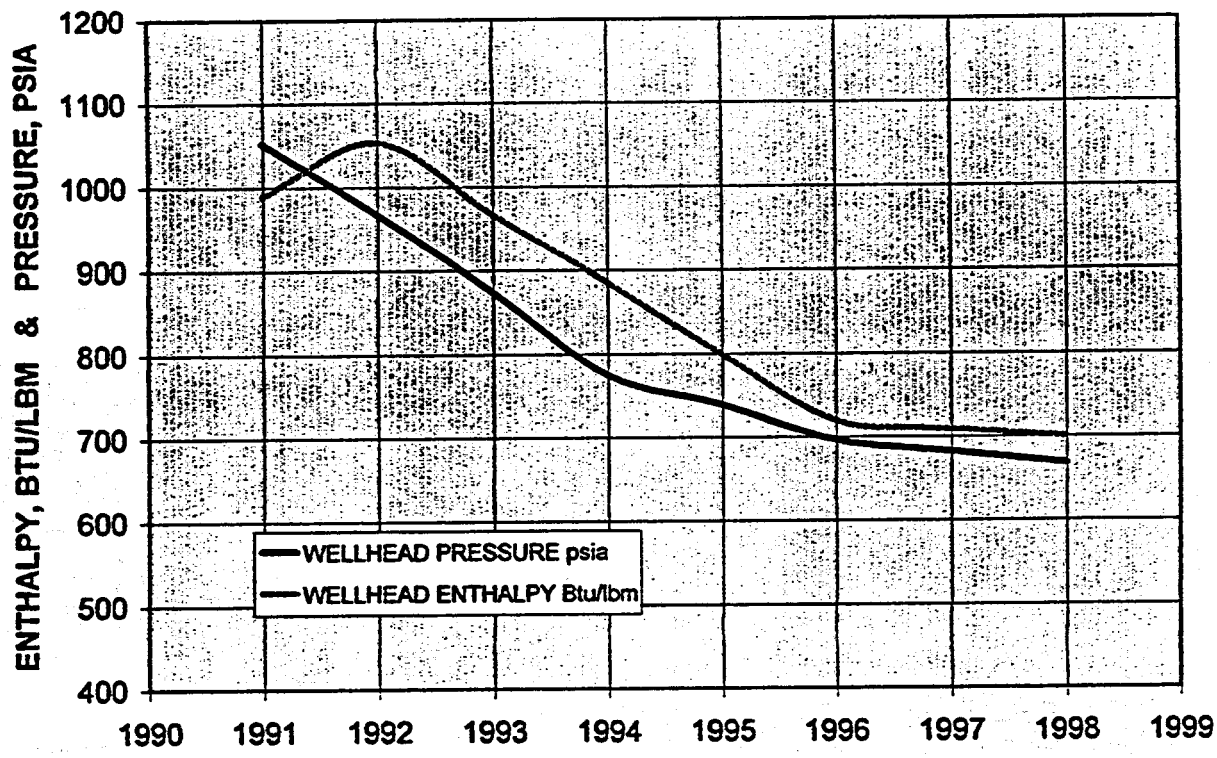

Figure 3. Wellhead Enthalpy and Pressure Variation with Time for Well No. 103.

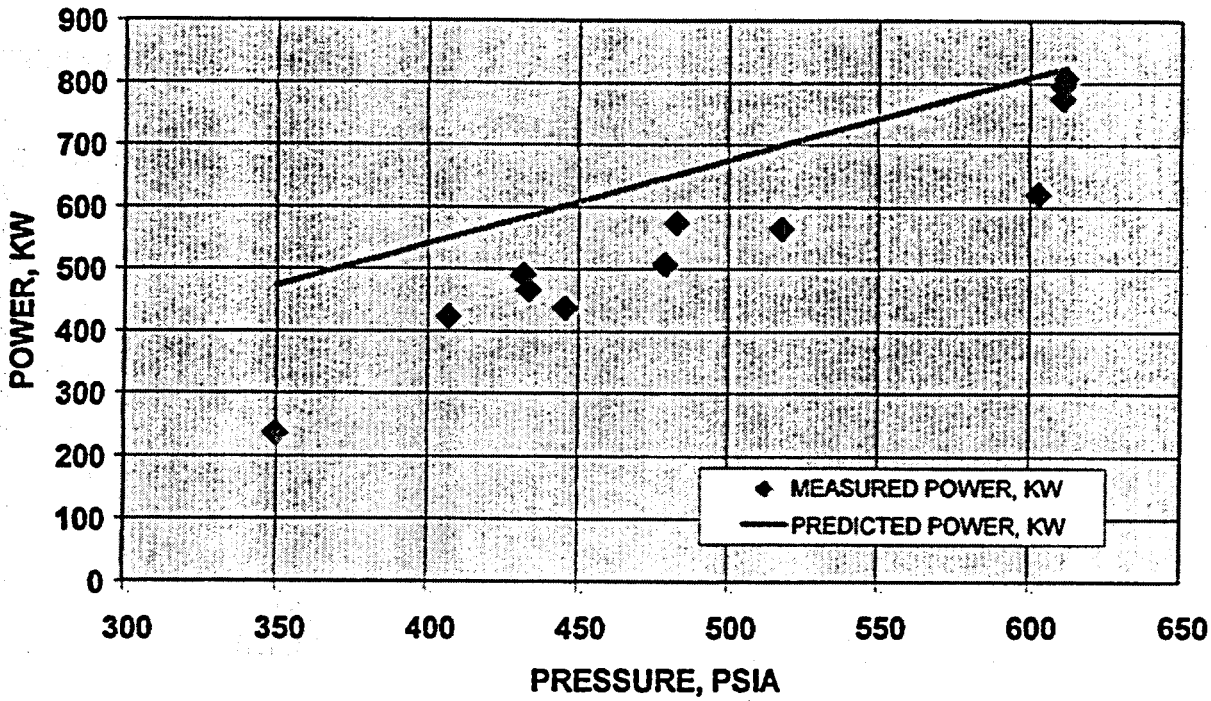

Figure 4. Measured and Predicted Power Variation with Inlet Pressure.

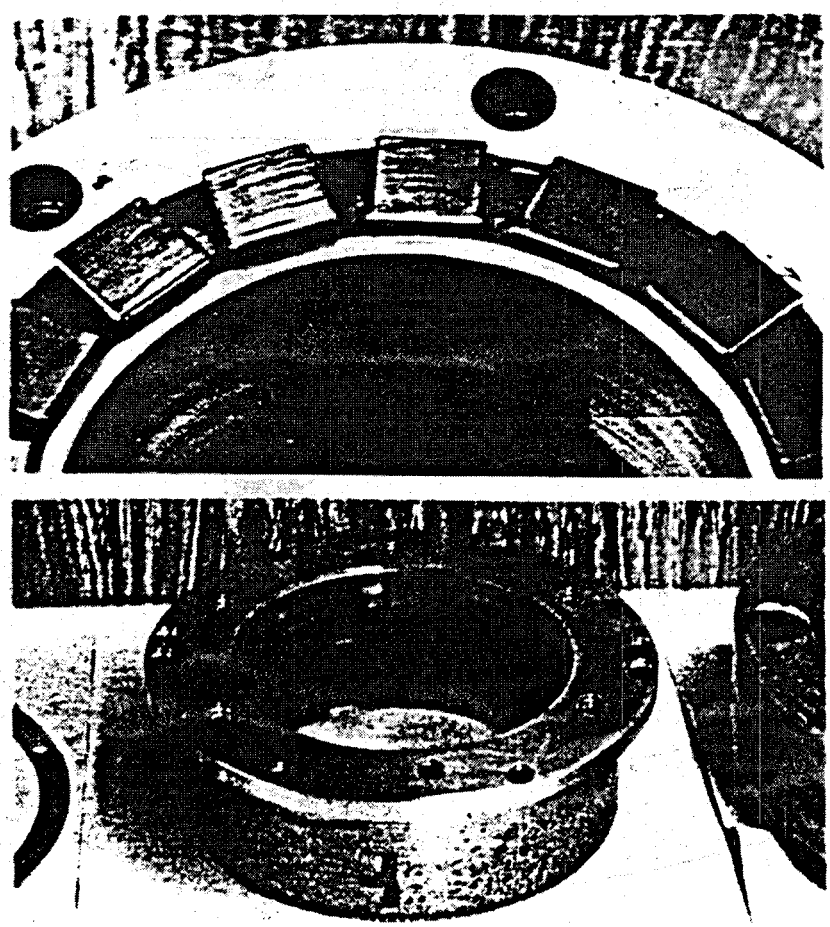

Figure 5. Silicon Carbide Thrust and Radial Bearing Pads after Initial Operation.

Table 1. Composition of Solids Removed from Biphase Turbine Rim

X-ray Diffraction Analyses

Mineral Name	Formula	Approx. wt. %
Magnetite	Fe_3O_4	>60
Hematite	Fe_2O_3	5
Goethite	FeOOH	5
Pyrite	FeS_2	8
Chalcopyrite	$CuFeS_2$	5
Sulfur	S_8	<5
Melanterite	$FeSO_4.7H_2O$	<3
Quartz	SiO_2	6
Unidentified	?	<5

X-ray Fluorescence Analyses

Analyte	Wt. %
Fe_3O_4, Fe_2O_3, FeOOH	74.7
FeS_2	7.9
$CuFeS_2$	4.7
PbS	0.4
ZnS	0.8
S_8	2.6
$FeSO_4.7H_2O$	1.5
SiO_2	6.6
MnO	0.2
$(Na,K,Ca,Mg)Al_2SiO_4$	0.7
Cr	0.03
Ni	0.03
Mo	0.02
TiO_2	0.06
TOTAL	100.24

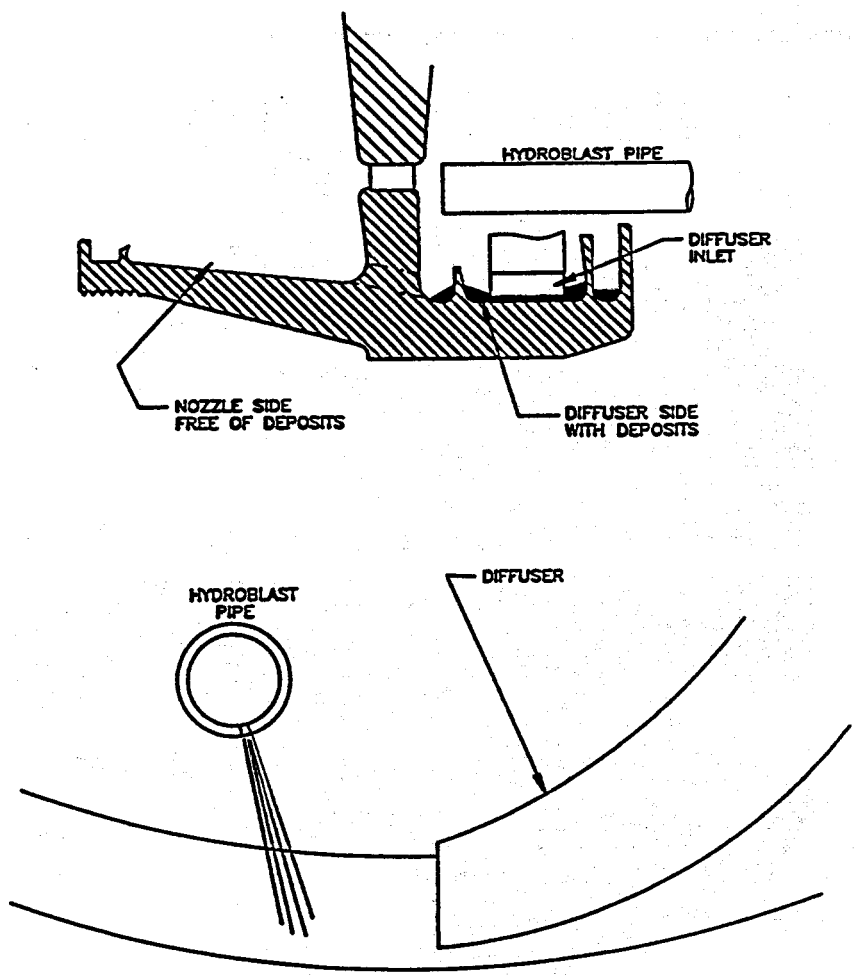

Figure 6. Schematic of Deposits and Use of Hydroblast Nozzles to Fluidize.

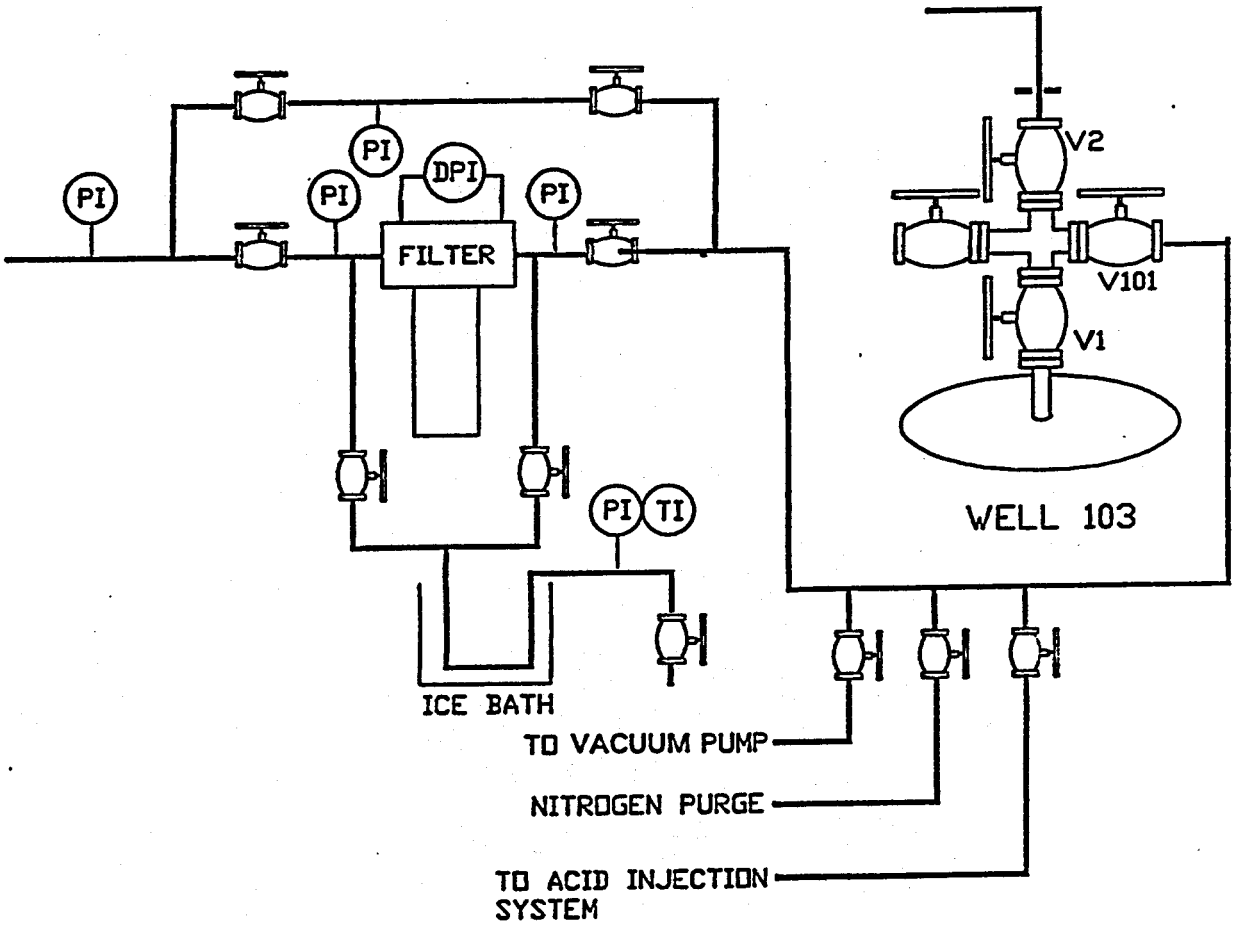

Figure 7. Wellhead Solids Control Test System.

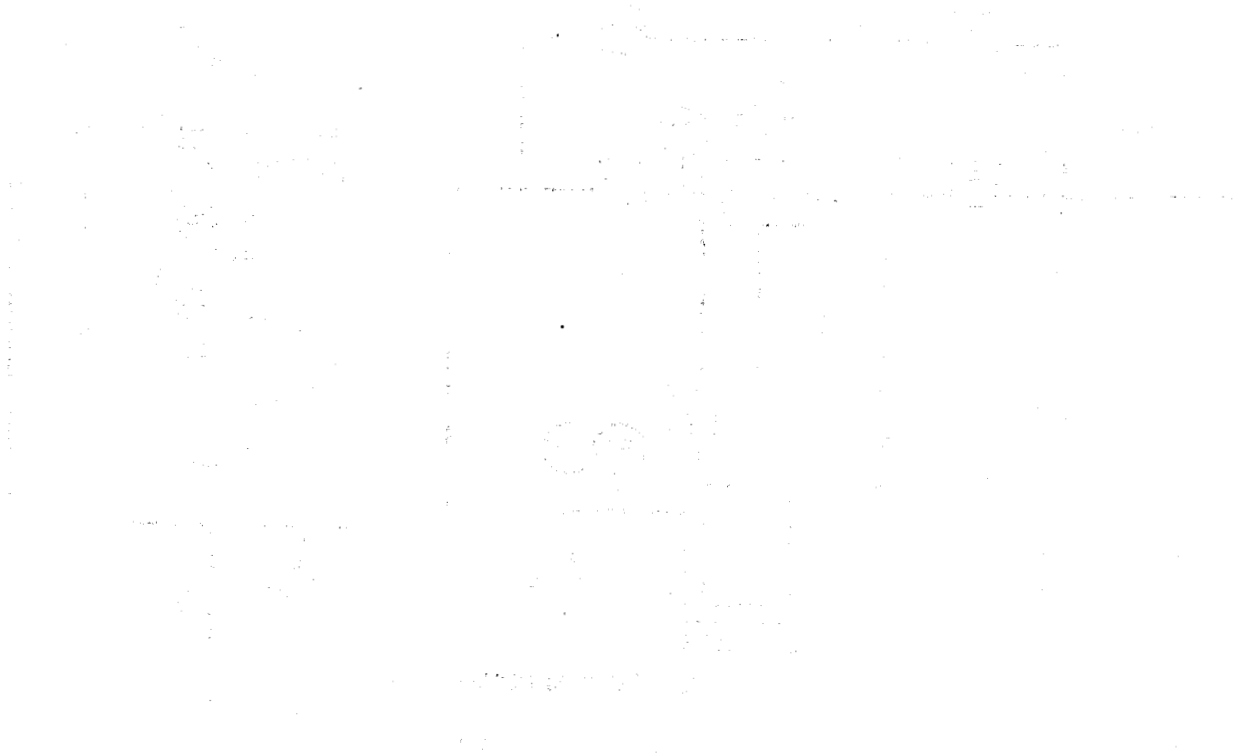

Kalina Demonstration Project at Steamboat Springs

Hank Leibowitz

Exergy, Inc.

Background

- Exergy Awarded $7.2 Million Grant By DOE in 1994
- 12.5 MW KCS11 Binary
- "demonstrate economic benefits of improved electrical power generation systems for geothermal applications."
- Sierra Pacific Cancels LOI To Purchase Power

Background (continued)

- Exergy/WPI (Affiliate of FWC) Propose to Complete Project As 5.5 MW KCS11 Binary
- Objective: Modularization
- Power Used "Inside the Fence" – No PPA Required
- Start 12/1/97; On-Line Estimated By 5/99

Status

- Preliminary Engineering Complete
- Major Equipment Quotes Received
  - Turbine
  - Heat Exchangers
  - Air Cooler
- EPC Price Due Mid-April

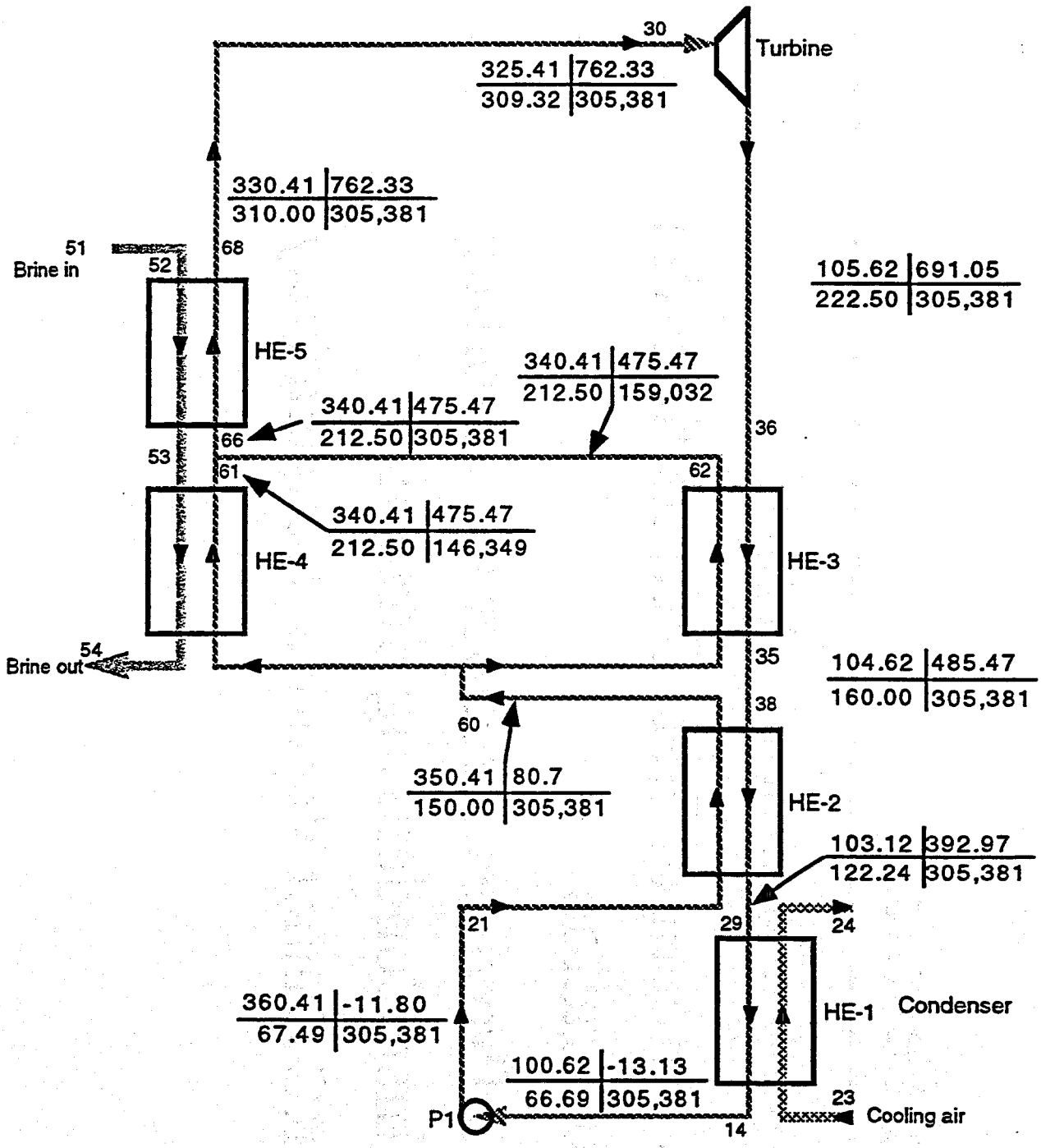

LEGEND

Working solution

Brine

Cooling water air

P (psi) | H (Btu/lb)

T (°F) | Flow (lb/hr)

Kalina Cycle

CONCEPTUAL FLOW DIAGRAM
SYSTEM 11

KCS11

Design Features

- 83 Percent Ammonia-Water
- 38.5 Percent of Heat Acquisition Via Recuperation
- HE-3 Provides Recuperative Boiling Against Condensing Stream
  - ORC Cannot Vaporize Recuperatively

Design Features (continued)

- HE-1 (Air Condenser)
  - Multi-Pass, Multi-Row
  - Variable Temperature Condensation
  - Smaller, Less Expensive
- Turbine Generator
  - "Steam Turbine" Design
  - Multi-Stage Axial
  - High Efficiency, Low Cost

Vapor Turbine Cross Section

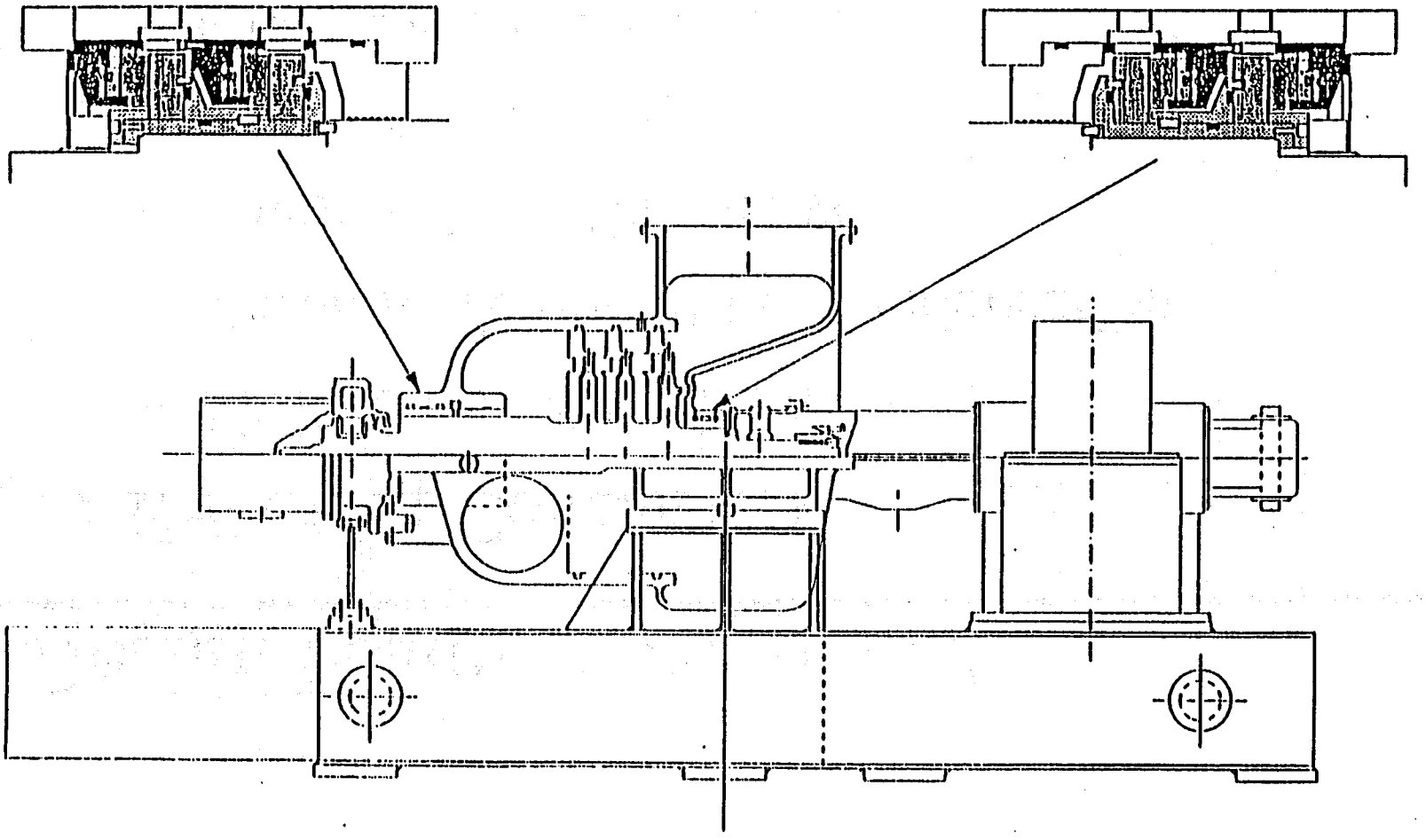

Temperature Profile In HE-1

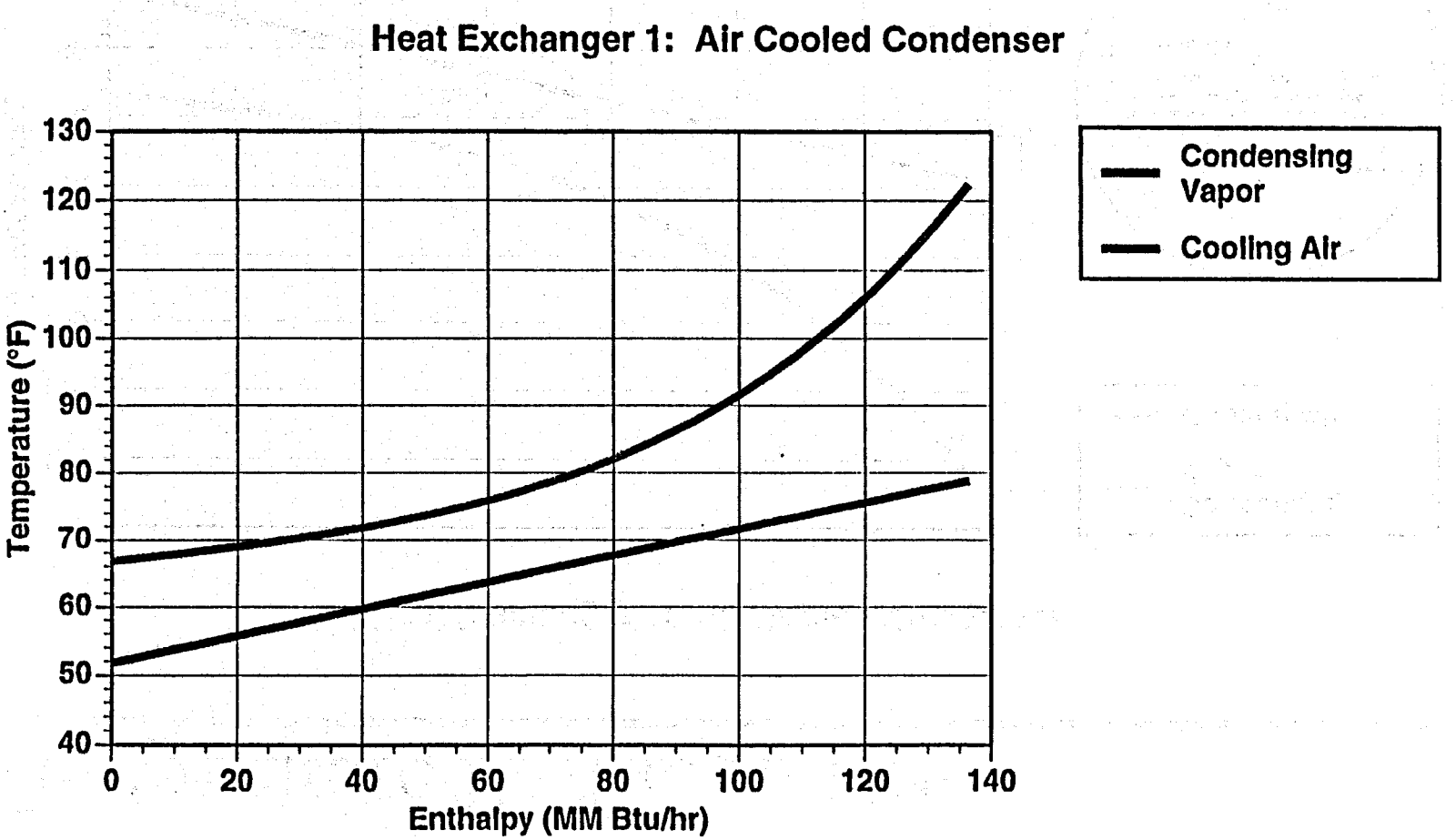

Temperature Profile In HE-1

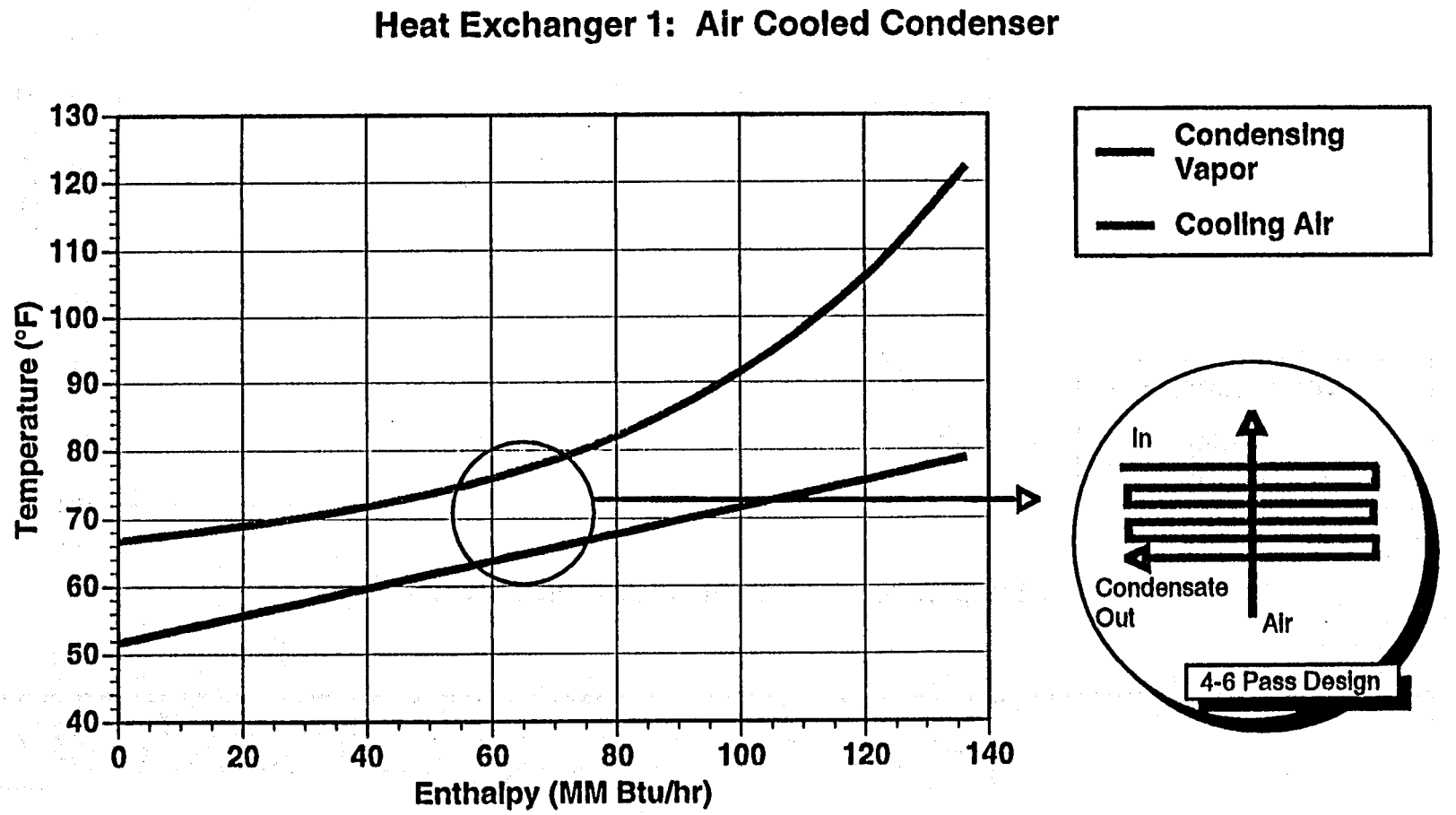

Temperature Profile in HE-2

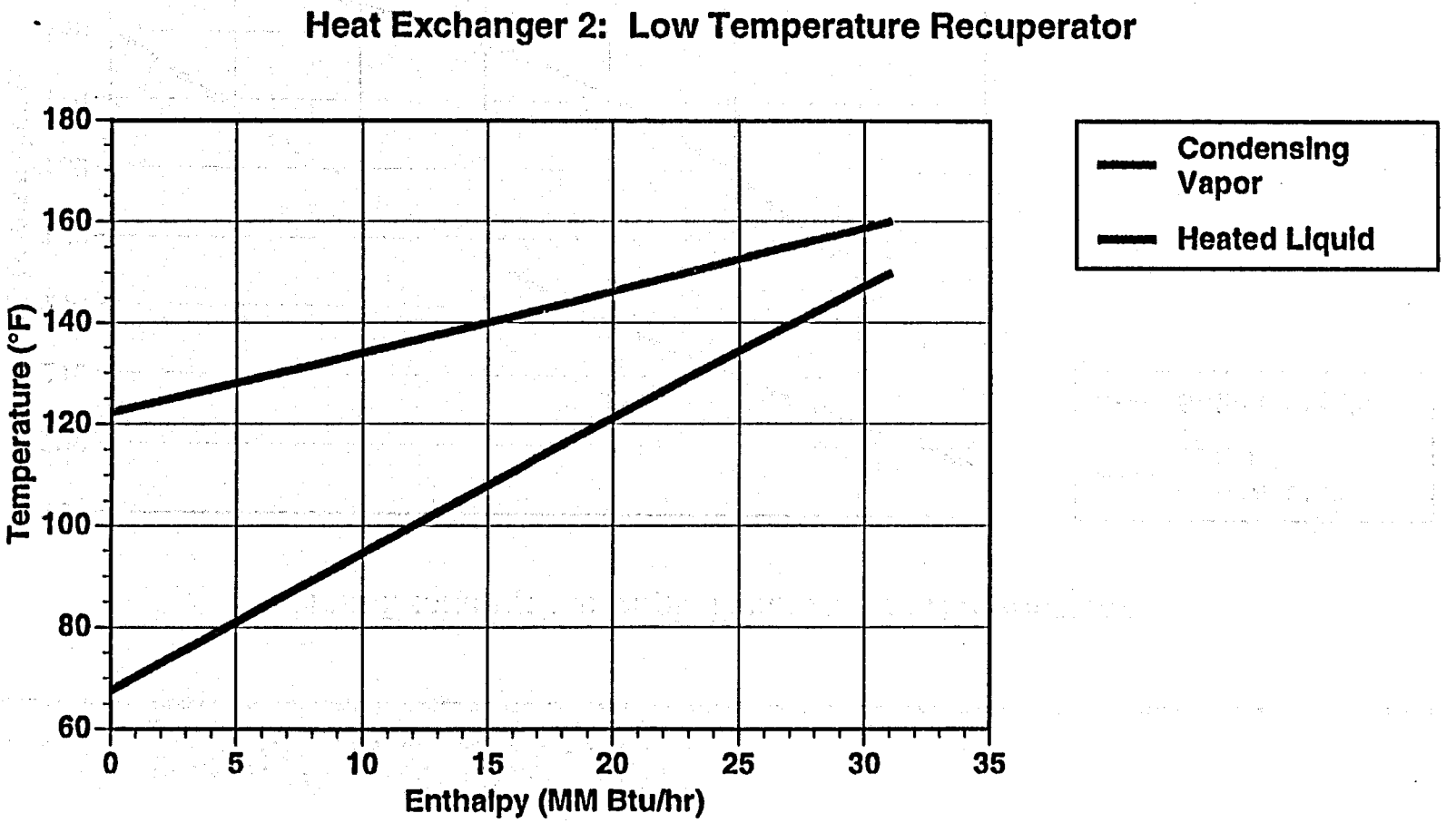

Temperature Profile in HE-3

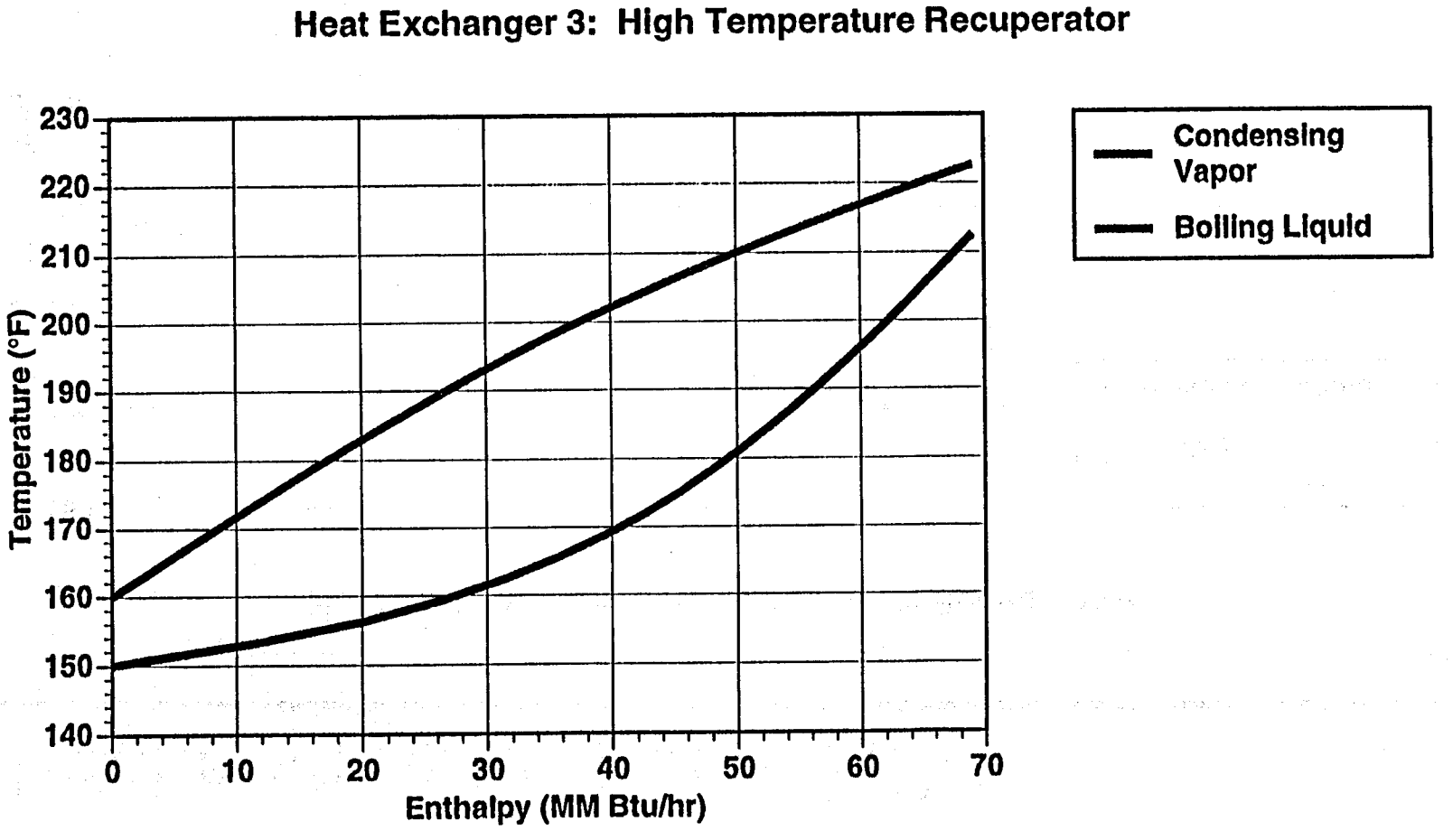

Temperature Profile in HE-4

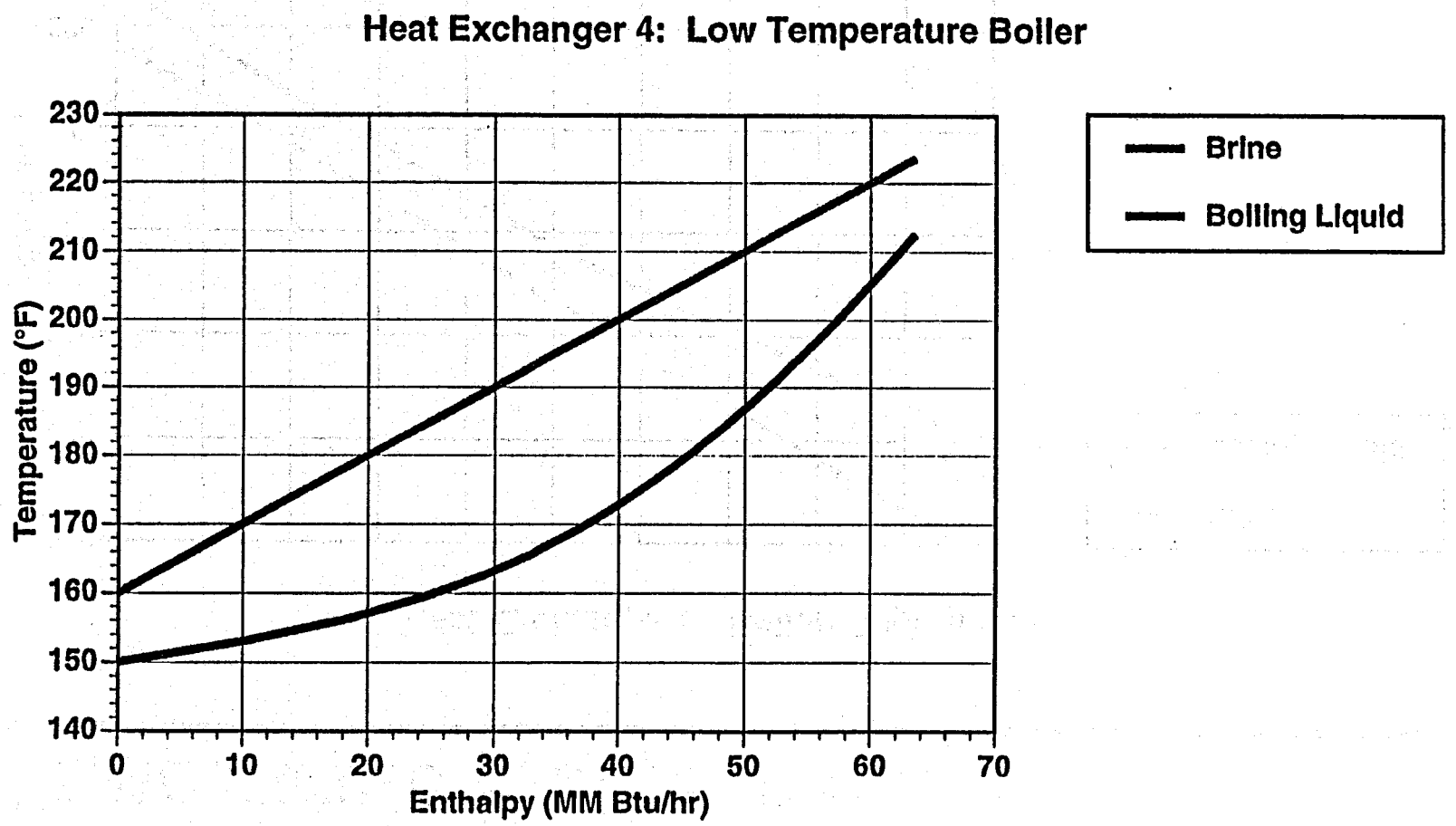

Temperature Profile in HE-5

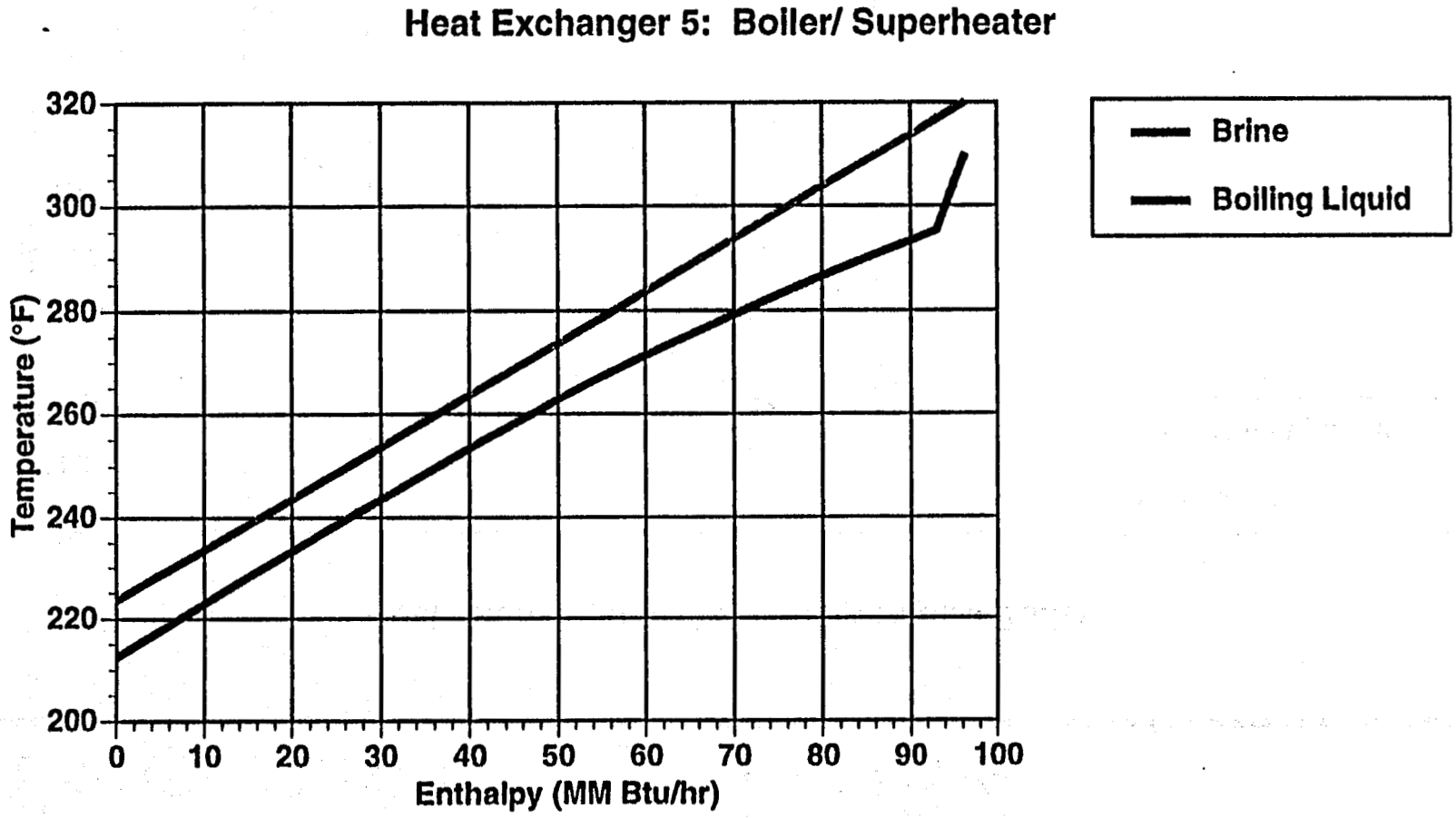

Temperature Profile in Heat Acquisition

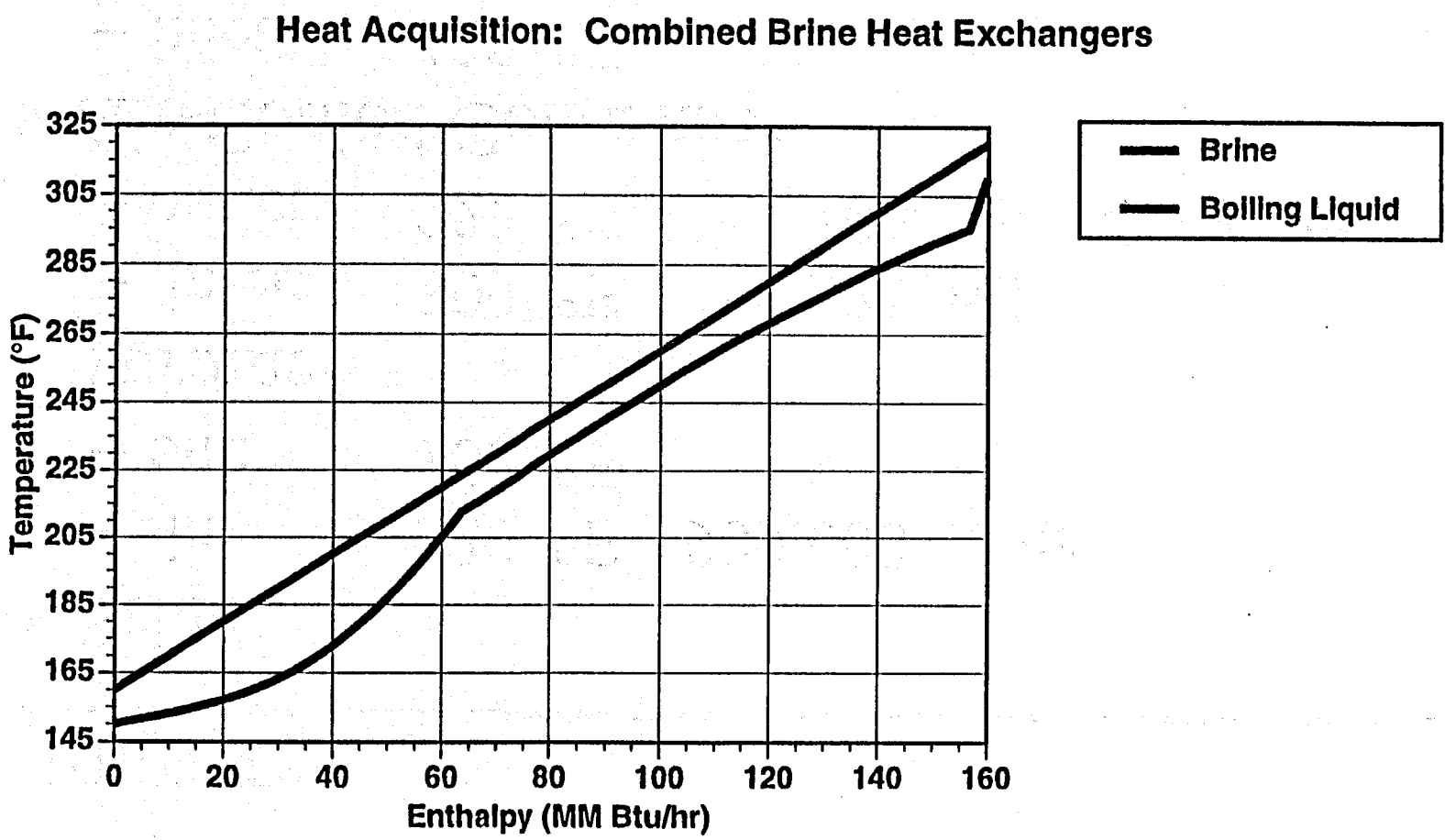

Summary

- Brine
  - in: 320 °F 909,000 lb/hr
  - out: 160 °F
- Turbine
  - inlet: 309 °F 325 psi
  - outlet: 222 °F 106 psi 4.5 % wet
- Air-Cooled Condenser
  - inlet: 122 °F
  - outlet: 67 °F
  - air inlet: 52 °F
  - air outlet: 79 °F

Summary (continued)

- Generator Output: 6,064 kW
- Net Plant Output: 5,215 kW
- Second Law Efficiency: 52.4 %
- Brine Utilization: 6.07 W-hr/lb

KCS11 Comparison Study

	Vale, Oregon 330°F / 161°F 7,660,000 lb/hr	Surprise Valley 377°F / 171°F 5,060,000 lb/hr	Thermo Hot Springs 265°F / 150°F 10,070,000 lb/hr	Raft River 300°F / 150°F 7,660,000 lb/hr
Ben Holt ORC				
kWh/1,000 lb	5.76	7.35	2.44	4.04
KCS11				
MW net	53.27	48.69	32.95	40.42
kWh/1,000 lb	6.95	9.62	3.27	5.27
Improvement (%)	**20.6**	**30.9**	**34.0**	**30.4**

FIELD TESTING OF HEAT EXCHANGER TUBE COATINGS

Keith Gawlik
National Renewable Energy Laboratory
(303) 384-7515

Toshifumi Sugama, Ronald Webster, and Walter Reams
Brookhaven National Laboratory
(516) 344-4029

Abstract

In order to reduce the capital cost of geothermal power plant heat exchange equipment and the maintenance cost associated with fouling, the National Renewable Energy Laboratory has been conducting tests of polymer-based liner systems developed by Brookhaven National Laboratory. These liner systems protect low-cost carbon steel tubing from corrosion and are formulated to reduce the rate of fouling. Preliminary field test data of the latest liner systems show a fouling rate reduction of 20% compared to previous liner formulations. New substrates used between the polymer liner and tube are expected to improve the liner-to-tube bond and enhance durability during cleaning operations.

Introduction

Corrosion, erosion, and fouling by scale deposits are critical issues for brine-wetted heat exchanger tubes in geothermal power plants in the Salton Sea reservoir. Replacing these tubes is very costly and time consuming. At present, titanium alloys and stainless steels are commonly used in shell and tube heat exchangers for their corrosion resistance. These materials have no special anti-fouling properties. These metals are considerably more expensive and have much lower thermal conductivities than copper and carbon steel. The capital cost of these large heat exchangers would be considerably reduced if an inexpensive tube made of carbon steel could be coated with a thermally conductive material that provides corrosion resistance equal to high-grade alloy steels. Thus, the development of corrosion/erosion/fouling-resistant coating and lining systems for carbon steel-based tubes is the subject of ongoing investigations at Brookhaven National Laboratory (BNL) and the National Renewable Energy Laboratory (NREL).

In 1987, BNL developed a silicon carbide (SiC) grit-filled polymer liner that provided a corrosion protective barrier and excellent thermal conductivity for heat exchanger tubes used in geothermal environments at temperatures up to 150°C (Fontana et al., 1987). The overall heat transfer coefficient of the SiC/polymer-lined tubes was only 9% less than that of expensive stainless steel (AL-6XN) tubes commonly used in geothermal power plants (Hassani and Hoo, 1995). The polymer matrix that bound the thermally conductive SiC grit into a coherent mass was composed of a trimethylolpropane trimethacrylate-cross linked styrene/methyl methacrylate (ST-TMP) copolymer network.

However, a major drawback of this lining material was that the polymer surfaces suffered hot brine-induced oxidation, forming a functional carboxylate group (Sugama, 1997). This group preferentially reacted with Ba^{++} ions present in the geothermal brines, to form Ba-complexed carboxylate hydrolysates. The oxidation not only caused the disintegration of the highly cross-linked polymer binder, but also promoted the deposition of geothermal brine-induced scale on the surface of the SiC-filled polymer liner. The strongly bonded Ba-carboxylate hydrolysates formed at the interface between the liner and the scale produces a scale that is difficult to remove.

Accordingly, a primary criterion for polymeric materials used in the coatings and liners at temperatures ranging from 90° to 110°C is resistance to the oxidation reaction with brine, thereby minimizing the rate of scale deposition. To achieve this goal, two polymeric materials— antioxidant (PDA)-modified ST-TMP and polyphenylenesulfide (PPS)—were evaluated for use as corrosion- and fouling-resistant liners and coatings.

In addition, it has been found that the surface modification of metals can improve the adherence of liners and coatings to the steel substrates and can reduce the rate of corrosion and wear of the steels (Sugama and Carciello, 1992). To this end, a zinc phosphate (Zn.Ph) ceramic precoating is deposited directly on the steel surfaces for use as an interfacial tailoring and modification material.

The coatings systems have been evaluated in the laboratory and are currently under test in the field. In the laboratory, the coatings were tested on carbon steel coupons in a low pH, hyper-saline brine in a laboratory setting and found to have improved oxidation resistance compared to previously used coatings. After the laboratory evaluation, the coatings were put into service as carbon steel tube liners in brine-wetted heat exchangers at the Hoch power plant in the Salton Sea Geothermal Area. They are installed in an apparatus that was originally built by Idaho National Engineering Laboratory (INEL) and used for testing BNL's liner systems in the early 1990s. More information on this apparatus is at a later point in this paper. The field evaluation consists of testing the tubes for 45 days in a highly aggressive brine environment. At this time, the tests are 78% completed. The current results from the test apparatus show that the antioxidant has been effective in reducing the fouling rate of the tubes by 20%.

Properties of polymers and coatings

Information on the thermal characteristics of ST-TMP, PDA-modified ST-TMP, and PPS polymers was obtained using the combined techniques of thermogravimetric analysis (TGA) and differential scanning calorimetry (DSC) in air. The results of these tests are given in Table 1.

Table 1. *Thermal Properties of Polymers*

System	Type	Melting Point, °C	Crystallization point on cooling, °C	Onset temperature of decomposition, °C
ST-TMP	Thermoset	–	–	270
PDA-modified ST-TMP	Thermoset	–	–	230
PPS	Thermo-plastic	280	202	380

The two polymer systems, ST-TMP and PDA-modified ST-TMP, are thermoset materials composed of a cross-linked polymer network structure, so that they do not have melt characteristics. In contrast, the PPS polymer is a thermoplastic; i.e., it can be remelted many times as a recyclable polymer. The major characteristic of PPS is the molecular orientation caused by chain extension at its melting point of 280°C. This orientation causes the crystallization of molten polymer during the cooling, and has a crystalline point at 202°C. This semi-crystalline PPS polymer has excellent thermal stability, as indicted by the fact that the onset of thermal decomposition begins around 380°C. In contrast, the thermal decomposition of the ST-TMP and PDA-modified ST-TMP polymers start near 270°C and 230°C, respectively. The overall appearance of the coated steel panels (7- by 7-cm) after exposure for up to 21 days in low pH, hyper saline brine (1 wt% H_2SO_4, 13 wt% NaCl, and 86 wt% water) at 200°C was examined to determine the hydrothermal stability and ability of the coating films to protect the underlying steel against corrosion (Table 2).

Table 2. *Visual Observation of Coating Films as a Function of Exposure Time at 200°C*

Coating System	Exposure time, day			
	1	3	14	21
ST-TMP/Zn.Ph/steel	good	good	good	good
PDA-ST-TMP/Zn.Ph/steel	good	good	good	good
PPS/ steel	good	blister	peels	–
PPS/Zn.Ph/steel	good	good	good	good

All of the coatings, except the PPS/steel system, exhibited no visual signs of delamination and damage after 21 days of exposure. The underlying steel in the "good" cases showed no corrosive attack at all. When the PPS coating was deposited directly to the steel substrate, in the absence of the Zn.Ph precoating, blistering was observed after only 3 days of exposure. Extending the exposure time to 14 days caused the film to peel from the steel substrate. These results indicated that the Zn.Ph precoating contributes significantly to improving the durability of the bond at the interfaces between the coating and the steel substrate, and in providing increased

protection of the steel against corrosion during exposure to a wet, harsh environment. X-ray photoelectron spectroscopy (XPS) analysis for 0-, 3-, 14-, and 21-day exposures was conducted to determine the degree of the oxidation of the coatings. Figure 1 illustrates the changes in the atomic ratio of oxygen/carbon (O/C) for the coating surfaces before and after exposure in an autoclave to low pH, hyper saline brine at 200°C.

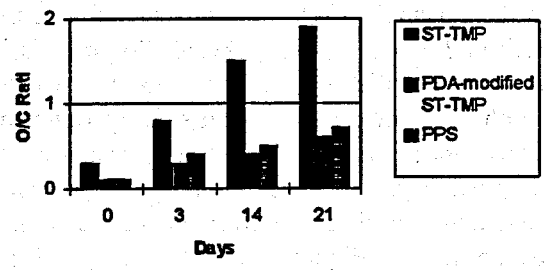

Figure 1. *Changes in O/C ratio for ST-TMP, PDA-modified ST-TMP, and PPS polymer surfaces as a function of exposure time in low pH, hyper saline brine at 200°C.*

As is illustrated, the O/C ratio for the ST-TMP coating increased with exposure time. The O/C ratio for the ST-TMP system after 21 days of exposure was determined to be 1.8, indicating that the polymer suffered oxidation damage in the hot brine. An O/C ratio under 1.0 is considered acceptable. In contrast, the addition of the PDA antioxidant to the ST-TMP system acted to greatly inhibit the degree of oxidation. As illustrated by the O/C ratio of 0.6 measured after 21 days of exposure. As expected, the PPS surfaces also displayed excellent resistance to oxidation.

Fabrication of HX tubes for field evaluation

A total of eight HX tubes were fabricated using 6.0 m (19 ft. 8 in.) lengths of 2.54 cm (1 in.) OD by 1.24 mm (0.049 in.) wall carbon steel tubing. A 5.1 cm (2 in.) long AL-6XN stub was welded to each end of the tube to provide the safe end connection to the tubesheet. This produced a tube with an overall length of 6.09 m (20 ft.), 6.04 m (19 ft. 10 in.) of which was lined or coated. The first 2.54 cm (1 in.) of each stub was left unlined in order to provide a location for roller expanding the safe end to the tubesheet. Presented in Table 3 is a summary of the tubes fabricated for field evaluation and the locations of the tubes within the test skids.

Table 3. *HX tube liners and coatings selected for field evaluation at the Hoch power plant.*

Leg	Test Skid A
1	PDA-modified ST-TMP/SiC
2	PDA-modified ST-TMP/SiC
3	ZP/PDA-modified ST-TMP/SiC
4	ZP/PPS
Leg	**Test Skid B**
1	ST-TMP/SiC
2	ST-TMP/SiC
3	ZP/ST-TMP/SiC
4	ZP/PPS/SiC

A combination of techniques was used to apply the various coatings. Common to all applications was careful preparation of the tube interior through degreasing and sandblasting. The Zn.Ph coating is applied using a "fill and drain" technique. The tube is coated by attaching a valve to one end of the tube and then inserting it into a vertically oriented furnace. The coating solution is poured into the tube from the top and then drained from the bottom once the coating process has been completed. The PPS and PPS/SiC coatings are also applied using the "fill and drain" technique. The PPS system consists of two layers of PPS while the PPS/SiC system consists of one layer of PPS and a top layer of SiC-filled PPS. The ST-TMP/SiC and PDA-modified ST-TMP/SiC liners are centrifugally cast inside the tubing. Details of the application techniques are in the Appendix.

The formulations of PPS/SiC and ST-TMP are detailed in Table 4. The ST-TMP/SiC and PDA-modified ST-TMP/SiC systems are polymer composite systems consisting of 18 wt% monomer and 82 wt% SiC grit. The formulation of the PDA-modified ST-TMP monomer system is identical to that of the ST-TMP monomer system with the exception that 0.1 wt% antioxidant is added to the system.

Table 4. *Compositions of PPS/SiC and ST-TMP.*

Composition of the PPS/SiC slurry
45 wt% isopropyl alcohol
36 wt% PPS
18 wt% SiC
1 wt% surfactant
Composition of the ST-TMP monomer system
53 wt% styrene-polystyrene mixture
35.4 wt% TMP
4.8 wt% poly(methyl methacrylate)
4.8 wt% ambient and high temperature initiators
1 wt% silane coupling agent
1 wt% promoter

Field Test Results

The eight tubes were put into service at the Heat Exchanger Test Skid, located at CalEnergy Operating Company's Hoch plant in the Salton Sea Geothermal Area. This area is known for its aggressive brines with high suspended solids content. The test skid consists of two parallel sets of four 6.1 m (20 ft.) long counterflow heat exchangers. Each heat exchanger consists of one lined, 2.54 cm (1 in.) OD tube surrounded by a shell made of 3.81 cm (1.5 in.) schedule 80 pipe. Brine from the clarifier tank flows through the tubes, which are cooled on the shell side by water in a closed loop system. The heat exchangers are plumbed so that brine and cooling water flow in countercurrent directions from one heat exchanger to the next. Figure 2 is a depiction of this apparatus.

The brine is supplied from the clarifier tank at 110°C (230°F) and pumped to the test skid with a single pump. Flow rates through the two sets of heat exchangers are sensed with magnetic

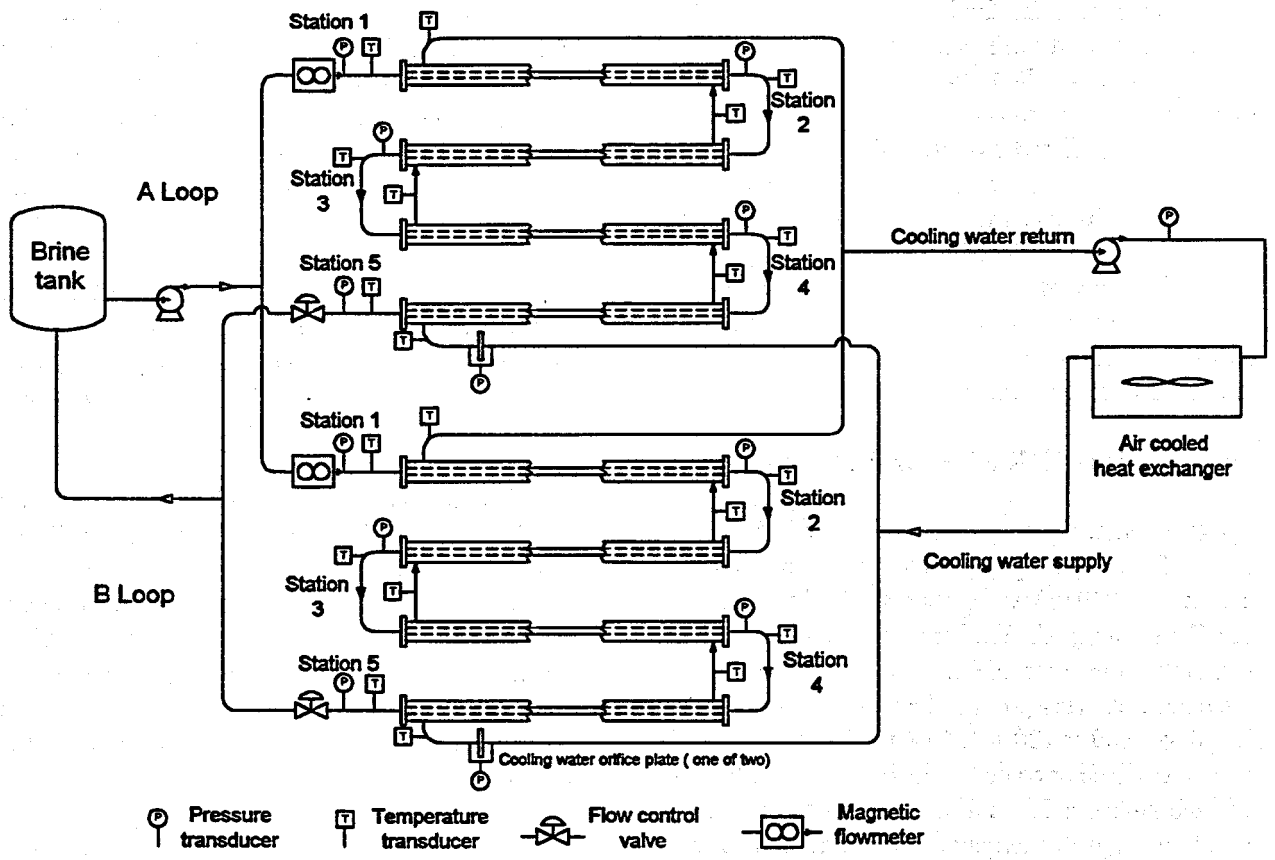

Figure 2. *Schematic of the Heat Exchanger Test Skid.*

flowmeters and controlled by globe valves at the exit of each loop through individual proportional-integral-derivative control systems. Total dissolved solids levels are approximately 250,000 entering the skid.

The current test period started in September 1997. The test duration is 45 days. From the results of previous tests, this length of time was considered sufficient to evaluate liner performance. The tubes in one loop now have 840 hours of test time, and the tubes in the other loop have an additional 100 hours. The difference is due to temporary loss of brine flow in one loop when a tube on that side of the rig completely plugged near one of its ends.

The tests were started with a flowrate of 0.63 liters/sec (10 gpm) through each loop. As the tubes scaled, it became increasingly difficult to maintain this flowrate. When the brine flowrates dropped below 0.06 liters/sec (1 gpm) on each side, the rig was shut down to remove heavy accumulations of scale, which often formed at the entrances and exits of the tubes.

The apparatus has been periodically shut down for other maintenance as well. The brine pump impeller and the brine piping upstream and downstream of the heat exchangers have been hydroblasted and mechanically cleaned numerous times. The welds between the AL-6XN safe ends and the carbon steel tubing on two tube assemblies cracked and developed leaks. This led to failure of the cooling system expansion tank. The cracking was apparently due to rough handling during tube installation and the location of the safe end welds too close to an area where roller expansion was performed. The tubes were repaired and returned to service. Delays in completing the test program were also due to failure of the phone line to the data acquisition system and scheduled plant shutdowns. In response to problems with sticking of the brine valves in earlier tests, a scheme was developed to stroke the brine valves through their complete range of motion every three hours. This has been effective in preventing valve sticking.

The brine flowrates through the two loops, designated A and B, are shown in the following two figures. These data are for periods in which both the brine and coolant systems were operating normally. The data do not show a smooth transition from a nominal 0.63 liters/sec (10 gpm) flowrate to a reduced flow because there was a period of operation when the brine was flowing, but no cooling water was available. The data from this period were not used.

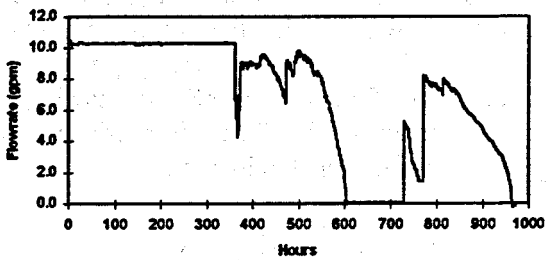

Figure 3. *Brine flow on the A side of the apparatus.*

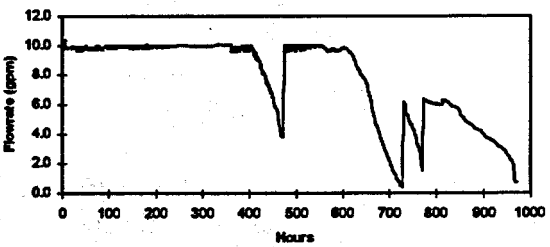

Figure 4. *Brine flow on the B side of the apparatus.*

As seen in the plots, the A side experienced a prolonged down period when one of the tubes on that side plugged completely. The B side remained open, however, and brine continued to flow through the apparatus. The jumps from a low to high brine flow represent occasions when the apparatus was taken out of service to clean the pump impeller and remove restrictions in the tubes or brine piping.

The heat exchangers are instrumented to provide data on the pressure drop through the tubes, temperature change of the brine and cooling water through each heat exchanger, and brine and cooling water flowrates. With this information, one can calculate how the resistance to heat flow through the lined tube increases as scale forms in the interior. This additional resistance to heat flow is defined as the fouling coefficient, or

$$R_f = \frac{r_2}{r_4}\left[\frac{1}{U_0} - \frac{1}{h_0} - \frac{r_4}{r_1}\frac{1}{h_i}\right] - \frac{r_2}{k_{steel}}\ln\left(\frac{r_4}{r_3}\right) - \frac{r_2}{k_{liner}}\ln\left(\frac{r_3}{r_2}\right)$$

where r_1 is the inner radius of scale buildup; r_2, inner radius of the liner; r_3, the inner radius of the tube; r_4, the outer radius of the tube; h_i, the tube interior heat transfer coefficient; h_o, the heat transfer coefficient on the tube exterior; U_0, the overall heat transfer coefficient from brine to water; k_{steel}, the thermal conductivity of the carbon steel tube; and k_{liner}, the thermal conductivity of the liner system. The geometry is illustrated in Figure 5.

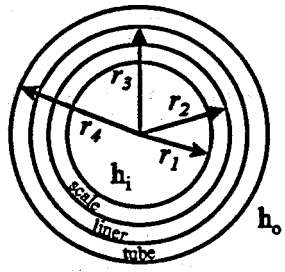

Figure 5. *Definition of system used in R_f eqn.*

The values of the heat transfer coefficients are determined from well-known correlations. The overall heat transfer coefficient was calculated from the data at the beginning of the test. The conductivity of the carbon steel was taken from handbook data and of the liner, from the test data at the beginning of the run when the tubes were clean. The thicknesses of the liners were determined from x-ray photographs of the tubes before they were installed in the apparatus.

Preliminary results show a reduction in fouling due to the presence of the antioxidant. The fouling coefficients for one of the PDA-modifiied ST-TMP/SiC-lined tubes and a plain ST-TMP/SiC-lined tube are shown in Figure 6. It should be noted that this plot does not represent continuous data collection. There were many periods when the brine flow was lost or became so low that the calculation of R_f became highly inaccurate.

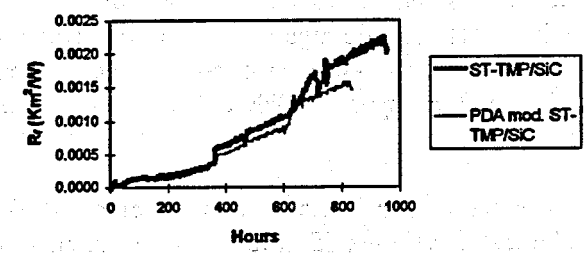

Figure 6. *Performance of the ST-TMP/SiC-based liners.*

The jump in R_f at the 630 hour point is due to a period when brine was stagnant in the tube after that side of the apparatus plugged. Note that there are about 100 more hours of operating time on the ST-TMP/SiC tube because it was installed on the side of the apparatus that maintained brine flow after the A side plugged.

In comparing the two tubes at a point when they both have the same amount of operating time, one sees that the use of antioxidant results in a reduction of fouling of approximately 20%. At the 600 hour point, for instance, the tube with antioxidant has a fouling coefficient of 0.000833 Km^2/W. At the same time, the tube without antioxidant has a fouling coefficient of 0.001058 Km^2/W. The use of antioxidant at this point has reduced fouling by 21%.

There is also available a side-by-side comparison of PDA-modified and plain ST-TMP/SiC liners applied over the Zn.Ph coating. The purpose of the Zn.Ph coating is to increase the liner-to-tube bond strength, and its effectiveness will be tested when the tubes are hydroblasted clean at the end of the test period. It has no effect on the fouling rate. But comparison of these results confirms the effectiveness of the PDA addition. In Figure 7 are shown the fouling coefficients for the PDA-modified ST-TMP/SiC liner and the ST-TMP/SiC liner, both applied over the Zn.Ph coating. As for the liner systems that do not include the Zn.Ph coating, there is an approximately 20% reduction in fouling when the antioxidant is used.

The fouling rate of the PPS-based systems is affected by the addition of SiC. Shown in Figure 8 are the fouling rates for the PPS and PPS/SiC liners, both applied over Zn.Ph.

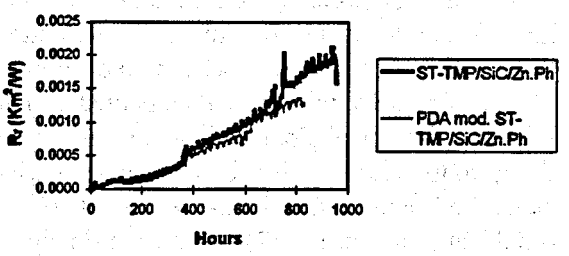

Figure 7. *Performance of the ST-TMP/SiC-based liners applied over Zn.Ph.*

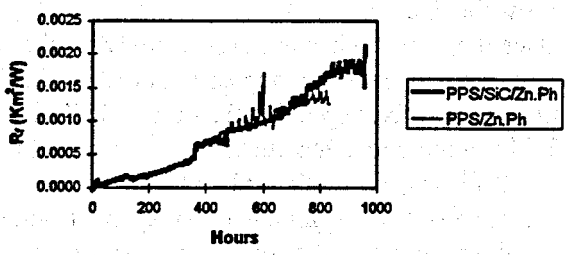

Figure 8. *Performance of PPS-based liners.*

At the 800 hour point, the PPS liner has a fouling coefficient 13% less than the PPS/SiC liner.

The use of SiC in PPS greatly enhances heat transfer through the coating, however. Initially, when the tubes were clean, the overall heat transfer coefficient for the PPS/SiC-lined tube was 55% greater than the PPS-lined tube. This is due to a 92% greater thermal conductivity of PPS/SiC over PPS. If a PPS-based system is considered, the thermal advantages of SiC will have to be weighed against the fouling rate. This is essentially a comparison of initial capital cost—primarily a function of heat exchanger size if the tube material is fixed—to maintenance costs during operation.

The PPS liner is currently fouled to the same level as the PDA-modified ST-TMP/SiC liner. In Figure 9 are shown the results for PDA-modified ST-TMP/SiC and for PPS, both applied over a Zn.Ph coating. The fouling rates of the liners at the beginning and end of the test period are similar. There is some difference between the two in the period between the time the skid was temporarily shut down due to the failure of the expansion tank and the point when the flow stopped in this loop. It appears likely that the fouling at the end of the test program will be comparable between the two. This result will be similar to the laboratory coupon tests on oxidation of these two materials and help to show the dependence of fouling rate on surface oxidation.

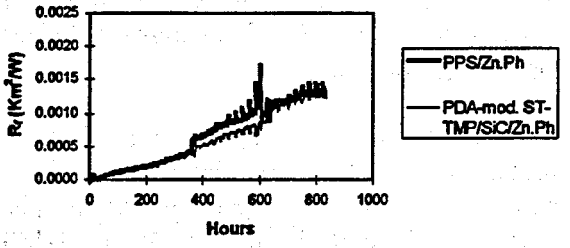

Figure 9. *Comparisons between two liners with antioxidant properties.*

The tests are only 78% complete. At the completion of the tests, scheduled to occur in April, 1998, a thorough evaluation of all aspects of the thermal, chemical, and mechanical behavior of the liner systems in heat exchanger use will be made.

Conclusions

Preliminary results show that the addition of PDA to the ST-TMP/SiC liner system has significantly reduced that system's rate of fouling in a highly aggressive brine environment. The PPS and PDA-modified ST-TMP/SiC liners, two systems with demonstrated oxidation-resistant properties in the coupon tests, are currently fouled at the same level, which is low relative to the plain ST-TMP/SiC. The effectiveness of the Zn.Ph substrate is yet to be determined since the fouling tests are not finished and the liner-to-tube bond strength will be evaluated when the tube is hydroblasted. The PPS-based systems show that the addition of SiC tends to increase the fouling rate, but the PPS/SiC composite has the advantage of higher thermal conductivity.

References

Fontana, J., Reams, W., and Chang, H., "Potential polymer concrete heat exchanger tubes for corrosion environments," in The Production, Performance & Potential of Polymers in Concrete (Staynes, B., Editor), Brighton Polytechnic, 180-193, 1987.

Hassani, V. and Hoo, E., "Results of field testing on heat exchangers with polymer concrete lining," National Renewable Energy Laboratory Technical Report, November 1995.

Sugama, T., "Interfaces between geothermal brine-induced scales and SiC-filled polymer linings," Geothermic, (in press).

Sugama, T., and Carciello, N.R., "Corrosion protection of steel and bond durability at polyphenylenesulfide-to-anhydrous zinc phosphate interfaces," J. Appl. Polym. Sci., 45, 1291-1301, 1992.

Appendix

In general, the steps in the coating process were as follows: (1) degrease the interior surface of the tube, (2) sandblast the interior surface of the tube, (3) apply the Zn.Ph ceramic precoating, if required, and (4) apply the ST-TMP/SiC, PPS, or PPS/SiC coating system.

The application of the Zn.Ph coating is performed in the following manner: (1) insert the tube into the vertical furnace, (2) preheat the tube to 80°C, (3) preheat the Zn.Ph solution to 80°C, (4) fill the tube with the Zn.Ph solution and maintain the filled tube at a temperature of 80°C±5° for 30 min., (5) drain the solution from the tube and wash the interior with water which has been preheated to 80°C, (6) bake the Zn.Ph-treated tube at 125°C for 1 hr. to prepare the anhydrous Zn.Ph coating.

The application process for the PPS-based liners is as follows: (1) insert the tube into the vertical furnace, (2) coat the interior of the tube by filling it with a slurry of 50 wt% PPS, 49 wt% isopropyl alcohol, and 1 wt% surfactant, (3) drain the slurry from the tube, (4) allow the slurry-coated tube to stand for 1 hr to allow the alcohol to evaporate, (5) preheat the tube to 125°C drive off any remaining alcohol then raise the temperature of the tube to 320°C and maintain it at this level for 3 hr to cure and crosslink the PPS, (6) allow the tube to cool to room temperature and then repeat the process to apply a second coat of PPS or a top coat of the SiC-filled PPS.

The application procedure for the ST-TMP/SiC liners is as follows: (1) The tube is inserted into the spinning assembly and locked into position. The monomer/SiC mixture is then poured into the tube and distributed along its length using a screed designed to uniformly distribute enough material along the length of the tube to produce a 0.76 mm (0.030-in.) thick liner. (2) The tube is slowly rotated to allow the mix to fully coat the interior surface. The drive motor speed is then gradually increased to 600 rpm and the tube is spun for 4 hr to compact the liner against the tubing and to allow the liner mixture to take its initial set. (3) Once the spinning has been completed the tube is post-cured using a two-step curing process. The first step involves spinning the tube at 80°C for 2.5 hr in order to complete the initial curing of the liner. This is accomplished by placing an enclosure over the spinning assembly and heating the air space within the enclosure. The tube is then removed from the spinning assembly and placed inside a curing chamber where it is cured a second time at a temperature of 175°C for 4 hr.

GEOTHERMAL HEAT PUMP GROUTING MATERIALS

Marita Allan
Brookhaven National Laboratory
(516) 344-3060

ABSTRACT

The thermal conductivity of cementitious grouts has been investigated in order to determine suitability of these materials for grouting vertical boreholes used with geothermal heat pumps. The roles of mix variables such as water/cement ratio, sand/cement ratio and superplasticizer dosage were measured. The cement-sand grouts were also tested for rheological characteristics, bleeding, permeability, bond to HDPE pipe, shrinkage, coefficient of thermal expansion, exotherm, durability and environmental impact. This paper summarizes the thermal conductivity, permeability, bonding and exotherm data for selected cementitious grouts. The theoretical reduction in bore length that could be achieved with the BNL-developed cement-sand grouts is examined. Finally, the FY 98 research and field trials are discussed.

INTRODUCTION

Key to the successful widespread use of geothermal heat pumps is reduction of installation costs. One way of tackling this is decreasing drilling costs by reducing the required bore length. This, in turn, can be achieved by increasing the thermal conductivity of grout used to seal the annulus between the borehole and heat exchanger loop. The grout provides a heat transfer medium between the U-loop and surrounding formation, controls groundwater movement and prevents contamination of water supply.

Properly designed and mixed cementitious grouts have potential for use as GHP grouts and may prove superior in thermal properties, long term performance and overall economics than bentonite grouts in current use. Cementitious grouts are relatively inexpensive, safe and easy to work with, comprising readily available materials and have a long history of use in geotechnical and civil engineering applications.

This project involves characterization of cement-silica sand grouts for thermal conductivity and other properties pertinent to backfilling vertical boreholes for GHPs. Cost analysis and calculations of the reduction in heat exchanger length that can theoretically be achieved with such grouts are being performed by the University of Alabama. Experimental work focuses on optimization of grout formulations in order to improve thermal conductivity while meeting requirements for mixing and pumping with conventional equipment, permeability, shrinkage, bonding to U-loop, durability, ease of handling, durability and economics. This paper describes some of the major results to date. Further details of the research, including testing for other properties such as rheology, shrinkage, durability, environmental impact and coefficient of thermal expansion, can be found in the FY 97 Progress Report (Allan, 1997).

EXPERIMENTAL PROCEDURE

Materials

The grouts delineated as having potentially suitable characteristics for GHP applications consist of Type I cement (ASTM C 150), silica sand, water and superplasticizer. Work in FY 97 also examined sulphate resistant cements and the use of fly ash (FA) and ground granulated blast furnace slag (BFS) as partial replacement for Type I cement in some of the grout formulations. These supplementary cementing materials are recognized for their ability to enhance durability in adverse environments (e.g., aggressive groundwater), reduce heat of hydration and reduce cost. The fly ash conformed to ASTM C 618 Class F. This is a low calcium fly ash produced from combustion of bituminous coal. The blast furnace slag was ASTM C 989 Grade 100.

The superplasticizer (SP) used was a sulfonated naphthalene type with a solids content of 42% by mass and was supplied by Master Builders Technologies (Rheobuild 1000). This chemical admixture functions as a dispersant and increases grout fluidity. Thus, superplasticizer allowed the water content of the grout to be reduced while maintaining pumpability. The aim was to keep the water/cementitious material ratio (w/c) as low

as possible in order to improve thermal properties, reduce permeability, and increase durability.

Silica sand was chosen as a particulate filler to increase thermal conductivity of the cementitious grouts. This decision was based on previous data that showed the efficacy of sand for improving thermal properties (Allan and Kavanaugh, 1998), ready availability, low cost, compatibility with grout mixing and placement equipment and ease of use. Different gradations of sand were evaluated in FY 97. Of these, sand conforming to the gradation suggested by ACI Committee 304 (Grading 1) gave the best combined performance. The ratio of sand to cementitious material (s/c) by mass for grouts discussed in this paper was varied from 2.0 to 2.5. Comparisons were made with neat cement grouts (i.e., no sand added).

A small proportion of Wyoming bentonite (sodium montmorillonite) was added to some of the cementitious grouts to reduce bleeding, promote full-volume set, and improve sand carrying capacity (i.e., reduce settling). However, use of bentonite was later discontinued in order to simplify the grout mix.

The cementitious grouts were intended to be mixable and pumpable with conventional grouting equipment. The mix proportions of some of the neat cement (Mixes 1 to 3) and cement-sand grouts covered in this paper are given in Table 1. The terms w/c, s/c and SP/c refer to water/cementitious materials ratio by mass, sand/cementitious material ratio by mass and superplasticizer dosage in ml/kg cementitious material, respectively. Mix 5 has a s/c value corresponding to two 100 lb bags of sand added for one 94 lb bag of cement. This ratio was chosen for ease of field mixing.

Table 1. Mix Proportions of Selected Grouts

Mix No.	w/c	s/c	SP/c (ml/kg)
1	0.4	0	20
2	0.6	0	0
3	0.8	0	0
4	0.5	2	20
5	0.55	2.13	15
6	0.6	2.5	10
7 (40% BFS)	0.6	2.5	10
8 (40% FA)	0.6	2.5	10
9	0.75	2	0

Mixes 7 and 8 contain blast furnace slag and fly ash at a cement replacement level of 40%, respectively.

Thermal Conductivity Measurements

The cementitious grouts were cast as blocks 75 mm x 125 mm x 25 mm. Three specimens per batch were cast. The blocks were sealed to prevent evaporation, demoulded after 24 hours and placed in a water bath to cure. The hardened grouts were tested for thermal conductivity at an age of 14 days. The grouts were then dried in an oven at 40°C over a period of seven days, allowed to cool, and re-tested to determine the effect of loss of moisture.

Thermal conductivity was measured using a Shotherm QTM-D2 Thermal Conductivity Meter. This meter uses the hot wire method to calculate the thermal conductivity, λ. The hot wire test is a transient method and therefore overcomes the problem of moisture migration and subsequent decrease in thermal conductivity that would occur with a steady state method. Further details of the test method are available in the FY 97 Progress Report (Allan, 1997). Three measurements per specimen were made.

Permeability

The water permeability (hydraulic conductivity) of the grouts under saturated conditions was measured in a flexible wall triaxial cell permeameter on cylindrical specimens. The experimental set up followed that given in ASTM D 5084-90. Two series of permeability tests have been performed to date. The first series was on bulk grouts. The second series was on an annulus of grout cast around an axial length of 1 in. ID (1.3 in. OD) HDPE Driscopipe® 5300 (Phillips 66). Since the permeameter was originally set up for 76 mm diameter cylinders, it was not possible to place two lengths of pipe in the specimens. All specimens were insulated for 24 hours after casting so that thermal effects similar to those which may occur in a borehole were simulated. Specimens were demoulded after 24 hours and cured for 28 days in a water bath. The ends of the pipe were plugged before conducting permeability tests so that water would flow either through the grout or between the grout-pipe interface. This indicated how permeability of the grout-pipe system may be influenced by grout

shrinkage. Three specimens per batch were tested.

Bond Strength

The relative bond strength of selected grouts to HDPE was measured by push out tests. An annulus of grout was cast around an axial length of 1 in. ID (1.3 in. OD) HDPE Driscopipe® 5300 (Phillips 66). Mixes 1, 6, 7, and 8 were tested. The specimens were placed in a Geotest compression tester with modified platens so that the pipe could be pushed out. Movement of the pipe was monitored with a dial gauge and LVDT. The load required to push the pipe out 0.04 in. (1 mm) was recorded. Bond strength was calculated as the load divided by the surface area of the embedded pipe. Six specimens per grout batch were tested.

Temperature versus Time

Concerns have been expressed about the elevated temperatures generated during cement hydration and how this may effect bonding between the cementitious grout and U-loop. Thermal expansion and contraction of the U-loop would occur as the grout temperature increases and subsequently decreases. In order to investigate this issue, the temperature versus time was monitored for simulated boreholes. Tubes were grouted to determine temperature-time profiles and also check for grout pumpability and uniformity of grouting. The tests involved grouting 102 mm inner diameter 6 m long insulated Schedule 40 PVC tubes that contained an axial length of 25.4 mm (1 in) ID (33.0 mm/1.3 in. OD) HDPE Driscopipe® 5300. The insulation was 25 mm thick fibreglass. Thermocouples were embedded in the grout and temperature versus time was monitored with a data logger. One of the tubes was filled with Mix 6 and the other with Mix 7 (slag-modified). The grouts were mixed in a ChemGrout CG-550P paddle mixer and pumped with a piston pump. The temperatures at the grout set time and at the peak of the exotherm were measured. The grouted tubes were later sectioned to examine the microstructure of the grout/pipe interface and the uniformity of grouting throughout the length of the tube.

RESULTS AND DISCUSSION

Thermal Conductivity

The thermal conductivities in saturated and dry conditions of selected different neat cement and cement-sand grouts are compared in Figure 1. The mix numbers are those given in Table 1. The error bars indicate the standard deviation.

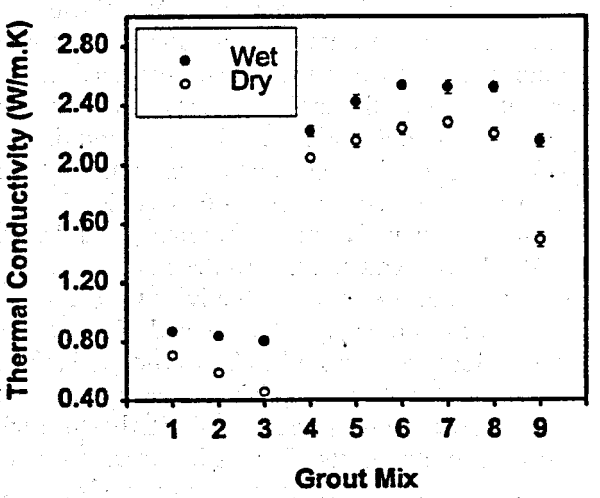

Figure 1. Thermal conductivity of different grouts.

The figure shows that thermal conductivity of neat cement grouts increases with decreasing w/c. When the amount of water in the original mix exceeds that required for hydration of cement the excess can be evaporated, thus leaving pores in the hardened grout. High w/c grouts will have greater porosity and lower thermal conductivity than low w/c grouts. The neat cement grout with w/c = 0.8 (Mix 3) showed a significant decrease in mean thermal conductivity of 43.2% on oven drying. Comparison with the superplasticized grout with w/c = 0.4 (Mix 1) demonstrated that the percentage decrease in thermal conductivity on drying was reduced to 18.7% by lowering w/c.

Addition of sand increases the thermal conductivity substantially. The retention of conductivity under drying conditions is also improved and this is beneficial when heat is rejected into the borehole or in arid environments. Loss of conductivity for the cement-sand grouts with w/c = 0.5 to 0.6 and s/c = 2 to 2.5 ranged from 8.1 to 11.5%. Mix 9 (w/c = 0.75, s/c = 2) underwent a decrease in thermal conductivity of

31%. Therefore, this grout, while having a reasonable conductivity in the saturated state, would not perform well if moisture is lost. Selected grouts that had been oven dried were re-saturated and the thermal conductivity was re-measured. It was found that the thermal conductivity returned to its original value. Therefore, the decrease in conductivity on drying of the cement-sand grouts is reversible.

The results can be compared with those for bentonite-based grouts. High solids bentonite grouts that are in current use for backfilling boreholes have thermal conductivities ranging from 0.65 to 0.90 W/m.K (Remund and Lund, 1993). Thermally enhanced bentonite has an increased conductivity of 1.46 W/m.K due to addition of quartzite sand (Remund and Lund, 1993). These values refer to the moist state and significant decreases in conductivity for bentonite grouts occur on drying (Allan and Kavanaugh, 1998). Heat transfer studies by Braud (1991) and Braud and McNamara (1989) have shown that neat cement grout performs similarly to high solids bentonite grouts. This is in agreement with the relatively low thermal conductivity of the neat cement grouts tested in this work.

Permeability

The results of bulk versus bonded permeabilities are compared graphically in Figures 2 and 3. The permeability data in Figure 2 demonstrate that increasing w/c from 0.4 (Mix 1) to 0.8 (Mix 2) causes an order of magnitude increase in neat cement grout permeability. A dramatic increase in permeability for the grout-pipe specimens is observed for the high w/c of 0.8. This is attributed to a higher permeability pathway at the pipe interface which was confirmed by microstructure studies. For the cement-sand grouts in Figure 3, the value of w/c also controls permeability of the bulk grouts. Fly ash and blast furnace slag have slight effects on permeability. The results show that addition of sand to the grout decreases the permeability of the grout-pipe interface as compared to the neat cement grouts. The permeability of grout-pipe specimens for Mixes 5 and 9 have not been measured. Despite the increase in permeability associated with imperfect bonding, the values are below 10^{-7} cm/s, which is the recommended value for GHP grouts (Eckhart, 1991).

The permeameter is currently undergoing modification to accept 102 mm diameter specimens that will contain two lengths of HDPE pipe. This will give a better representation of the permeability of a grouted borehole. The effect of thermal cycling on the bond permeability will be investigated.

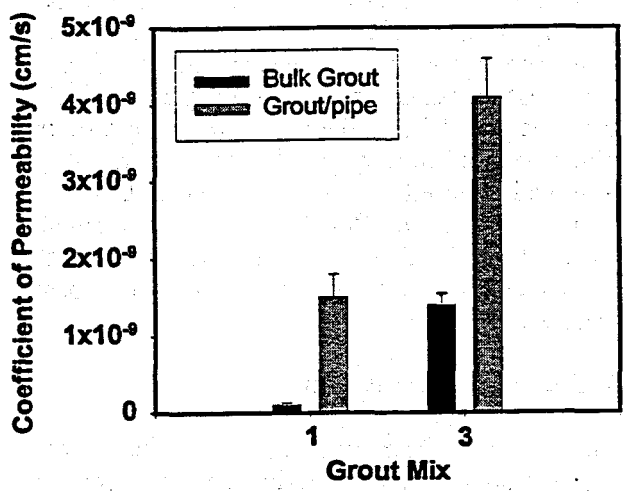

Figure 2. Permeability of neat cement grouts.

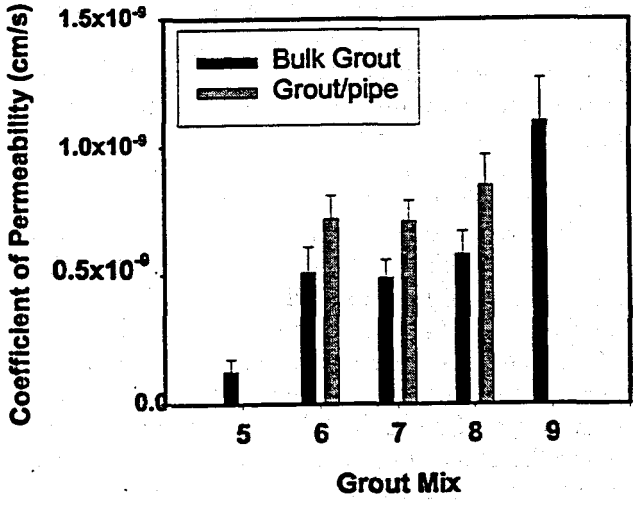

Figure 3. Permeability of cement-sand grouts.

Bond Strength

The results of the bond strength tests are presented in Figure 4. The average and standard deviation for six specimens are given. Relatively high shrinkage of superplasticized neat cement results in very low bond strength. Neat cement

grout will also have a higher exotherm than a cement-sand grout and this will result in greater expansion of embedded HDPE pipe during curing. The bond strengths for Mixes 6 and 7 were virtually the same, despite the lower exotherm of the slag-modified grout. The fly ash-modified grout (Mix 8) had a significantly lower bond strength and this is attributed to higher shrinkage

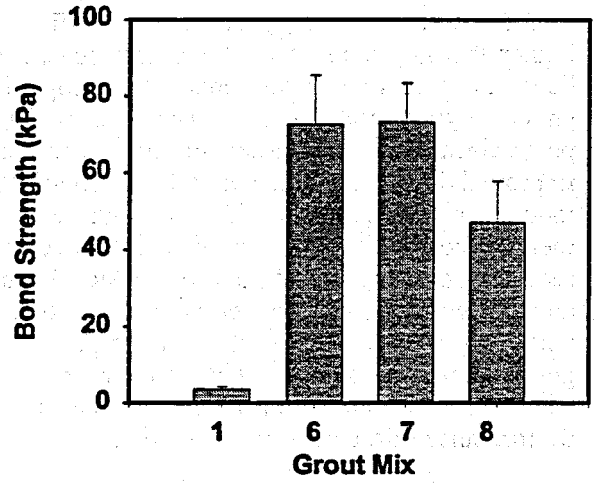

Figure 4. Bond strengths for neat cement and cement-sand grouts.

Temperature versus Time

Temperature versus time data was obtained for the grout cast in the insulated 6 m x 102 mm PVC tubes. The peak temperature was 51.2°C for Mix 6 and this occurred at an elapsed time of 12 hours and 20 minutes. The set time of this grout was 8 hours and the corresponding temperature at this time was 32°C. For the slag-modified grout (Mix 7) the peak temperature was 36.7°C at 17 hours and 46 minutes after completion of grouting. The set time was 9 hours at which time the temperature was 25.3°C.

The circumferential coefficient of thermal expansion for the HDPE pipe used is 1.1 x 10^{-4}/°C. This can be used to calculate the expansion of the pipe at the set time of the grout. Subsequent cooling of the grout could possibly contribute to imperfect bonding at the grout/pipe interface. The change in circumference of the pipe at 32°C is 0.176 mm and the diameter change is 0.056 mm. For the slag-modified grout, the circumference and diameter changes at the set time are 0.095 and 0.03 mm, respectively. The assumption that the pipe and grout are at the same temperature is a simplification. Hence, the calculated expansions represent maximums for the studied system. Thermal expansion of the grout has been neglected in the calculations.

Microstructure of Grout/Pipe Interface

Specimens used in the permeability tests were sectioned and viewed under an optical microscope at 50 x magnification to examine the integrity of the grout bond to HDPE. In addition, the 6 m x 102 mm tubes were sectioned for analysis. For the 76 mm diameter permeability specimens it was found that those grouts without sand had the greatest gaps at the grout-pipe interface. Mix 1 had a gap of 0.02 to 0.4 mm. Such gaps would increase contact resistance and be detrimental to overall heat transfer. Addition of sand to the grouts was found to improve the bond integrity and this concurs with the permeability and bond strength results. Mix 6 exhibited regions where grout was intimately bonded to the pipe. Some discontinuous gaps 0.02 mm wide were observed. Similar observations were made for the sanded slag-modified grout (Mix 7). Hence, reduction of the exotherm by addition of slag to the mix did not improve bonding. This is attributed to the higher early shrinkage of the slag-modified grout (Allan, 1997) which counterbalances the benefit of decreasing temperature and subsequent expansion of embedded HDPE pipe. The sanded fly-ash modified grout (Mix 8) had a continuous gap at the interface around 0.02 - 0.2 mm wide, in addition to some voids.

The sections cut from the 102 mm diameter insulated tubes grouted with Mixes 6 and 7 showed gaps 0.06 - 0.075 mm wide at the interface, which is greater than that observed on the smaller permeability test specimens. The increased gap width is probably due the higher exotherm experienced in the tubes than in the 76 mm diameter cylinders.

Bore Length Design and Grout Costs

The required bore length depends in part on the thermal conductivity of the backfill grout. A team of Mechanical Engineering students (Daniel Suggs, Shane Peek and Jeff Rimel) at the University of Alabama conducted bore length calculations for different grout thermal

conductivities, formation geologies and building load. Bore length design software developed by Prof. S. Kavanaugh (University of Alabama) was used. Calculations were based on a 4 in. diameter bore with a single U-tube. The analysis assumed that the buildings were located in Tuscaloosa, AL and the heating and cooling loads were as follows:

- Residential heating and cooling load: 3 tons
- Commercial heating and cooling load: 10.5 tons
- School heating and cooling load: 75 tons

The results of the required bore length calculations for grouts with thermal conductivities of 1.46 (thermally enhanced bentonite) and 2.42 W/m.K (Mix 5) are presented in Table 2. The material costs for grouting the borehole are included and assume 51 gallons of grout per 100 lineal feet and no loss to the formation. The estimated cost of Mix 5 is $0.626/gallon based on prices of $5.15/94 lb bag of cement, $3.00/100 lb bag of sand and $5.25/gallon of superplasticizer. The cost may vary with freight charges. A price of $0.80/gallon has been assumed for thermally enhanced bentonite. The specific gravities of the thermally enhanced bentonite and Mix 5 are 1.64 and 2.18, respectively. The drilling costs for the different lengths of boreholes can also be included in the cost calculations and will vary with geology and size of the job. A conservative estimate would be $3/ft. Other studies of bore length design are reported in Allan and Kavanaugh (1998).

FY 98 ACTIVITIES

In FY 98 it is planned to conduct two field demonstrations using Mix 5 in collaboration with Oklahoma State University and Sandia National Laboratories. In-situ thermal conductivity measurements will be performed and compared with laboratory data. Heat pump performance will be monitored over heating and cooling seasons. The field demonstration will enable quantitative comparison of the selected cement-sand grout with conventional grouts under actual working conditions. Specifications for mixing the grout will be developed. Further studies of bonding of cementitious grouts to U-tube will be conducted, including analysis of the effect thermal cycling. Freeze-thaw durability tests will be completed. Collaboration with the University of Alabama to measure thermal resistance per unit length for different grouts is ongoing. The costs associated with prepackaging the dry materials for the cement-sand grouts to simplify field mixing will be investigated.

CONCLUSIONS

Superplasticized cement-silica sand grouts have thermal conductivities in the range of 2.161 to 2.531 W/m.K for sand/cement ratios by mass of 2 to 2.5. Cement-sand grouts have significantly higher thermal conductivity than neat cement or bentonite grouts and retain conductive properties under drying conditions. The grouts have permeabilities of the order of 10^{-10} cm/s and improved bonding characteristics to HDPE U-loop over neat cements. The improvements in thermal conductivity are predicted to decrease required bore length, and therefore reduce drilling and materials costs associated with installation of vertically oriented heat exchangers for geothermal heat pumps. The forthcoming field trials will provide information on the in-situ performance of the cement-sand grouts.

ACKNOWLEDGMENT

Thanks are due to Mr. Lew Pratsch of the Department of Energy/Office of Geothermal Technologies for support of this work..

REFERENCES

ACI 304.1R, "Guide for the Use of Preplaced Aggregate Concrete for Structural and Mass Concrete Applications", American Concrete Institute Materials Journal, V. 88, No. 6, pp. 650-668, 1991.

M.L. Allan, "Thermal Conductivity of Cementitious Grouts for Geothermal Heat Pumps", BNL 65129, November, 1997.

M.L. Allan and S.P. Kavanaugh, "Thermal Conductivity of Cementitious Grouts and Impact on Heat Exchanger Length Design for Geothermal Heat Pumps", Submitted to International Journal of HVAC&R Research, 1998.

H.J. Braud, "Grout Effect in Vertical Heat Pump Bores", Proceedings of International Energy Agency Ground Coupled Heat Pump Conference, 1991.

H.J. Braud and S. McNamara, "Enhancement of Heat Transfer to Earth in Ground Coupled Heat Pump Bores, ASAE/CSAE Meeting, Quebec, 1989.

F. Eckhart, "Grouting Procedures for Ground-Source Heat Pump Systems", Oklahoma State University, Ground Source Heat Pump Publications, 1991.

C.P. Remund and J.T. Lund, "Thermal Enhancement of Bentonite Grouts for Vertical GSHP Systems in Heat Pumps and Refrigeration Systems", K.R. Den Braven and V. Mei (Eds.), ASME, 29, pp 95-106, 1993.

Table 2. Bore length and cost calculations for different grout thermal conductivities

Type	Grout λ = 1.46 W/m.K		Grout λ = 2.42 W/m.K	
	Bore Length (ft)	Grout Cost ($)	Bore Length (ft)	Grout Cost ($)
Residential				
Igneous	700	286	600	191
Metamorphic	720	294	620	198
Sedimentary	720	294	630	201
Commercial				
Igneous	2470	1008	2270	725
Metamorphic	2540	1036	2330	744
Sedimentary	2550	1040	2340	747
School				
Igneous	17910	7307	15480	4942
Metamorphic	18370	7495	15940	5089
Sedimentary	18430	7519	16000	5108

ON-LINE H_2S MONITORING USING NEAR-INFRARED TUNABLE DIODE LASER SPECTROSCOPY

J. K. Partin and C. L. Jeffery
Lockheed Martin Idaho Technologies Company
Idaho National Environmental and Engineering Laboratory
Idaho Falls, Idaho 83415-2211

ABSTRACT

The purpose of this project is to evaluate and demonstrate the technique of frequency-modulated, tunable diode laser spectroscopy for the monitoring of H_2S gas in geothermal plant emissions. The geothermal power industry has an interest in the development of real-time techniques for monitoring these emissions, since improved measurement capabilities could lead to considerable cost savings through the optimization of the chemicals used for abatement.

There are several locations throughout the plant at which this measurement could be performed. They vary from the main stream line which operates at a temperature of about 350 ^{0}F (175 ^{0}C) and a pressure of 100 psig to the cooling stack with a temperature of 80-100 ^{0}F (27-38 ^{0}C) at ambient pressure. Gas concentrations range from 0.1 ppm to 1000's of ppms. The technical goal of this effort was to perform a series of scoping experiments to determine the effect of elevated pressure, temperature and water vapor on the sensitivity of this spectroscopic technique for the detection of H_2S. The results of these experiments are presented, and the deployment options and system designs are discussed.

INTRODUCTION

The goal of this project is to develop and demonstrate a real-time detection system for monitoring H_2S gas in geothermal plants. The system is based upon the use of near-infrared diode laser technology which offers several advantages for geothermal emission and process control operations. For this application, there is a fortuitous coincidence between the standard communication laser diode at 1.55 microns and the H_2S combination absorption band at 1.578. The communication diode is easily temperature-shifted by the amount needed to access this absorption line. The spectral resolution of the diode laser is on the order of 1 GHz. This extremely narrow source linewidth reduces potential signal contributions from interferents, such as water vapor or carbon dioxide, which can limit the sensitivity and accuracy of other types of measurements. The output from these lasers can easily be propagated over standard fused silica optical fibers. This allows for the configuration of a system in which the sensitive optical and electronic components can be located in an environmentally-controlled area, and also allows multiplexing of signals so that a single device could be used to make a number of remote measurements.

The ability to perform real-time H_2S stack monitoring could result in several benefits, including improved air quality monitoring and compliance. A significant dollar savings could also be realized through the optimization of chemical usage, primarily iron chelates. Iron chelate is added to the circulating water to react with dissolved H_2S to form elemental sulfur. H_2S fluctuations in the incoming steam require most plants to target iron feed to obtain 75% of allowable emissions. Accurate real time stack emission monitoring would allow lower iron chelate concentrations to obtain 90% of allowable emissions. This 15% improvement could result in an annual savings of about $65-75 K/plant.

There are several locations within the plant at which this measurement could be made. They vary in environmental conditions from the main steam line which operates at a temperature of 350°F (175°C) and a pressure of 100 psig to the cooling stack with a temperature of 80-100 °F (27-38 °C) at ambient pressure. H_2S concentrations in these locations vary from 0.1 ppm to 1000's of ppms. In order to establish the optimal plant location and design configuration for the monitor, a series of scoping experiments have been conducted to determine the effect of pressure, temperature and water vapor on the sensitivity of proposed spectroscopic technique. This report presents the results of these experiments; and in addition, discusses various deployment options and system design concepts.

BACKGROUND

From discussions with plant personnel, several locations were identified and prioritized as possible positions for siting a gas monitoring system. In addition to H_2S, there is also some interest in extending the measurement capability to other species. The possible applications and priorities are summarized in Table 1.

APPROACH

The monitor is based upon the use of solid-state diode lasers and frequency modulation techniques. The GaAs diode lasers used emit light in the 0.7 to the 2.7 micron region of the electromagnetic spectrum. This region contains the overtone and combination absorption bands of a number of species of industrial interest, including H_2S, HCl and CH_4. A particular diode device can be tuned over a small range to match the absorption line by changing its applied current and temperature.

For the measurements, the injection current of the diode is sinusoidally (frequency) modulated. As illustrated in Figure 1, when this laser beam is directed through a sample cell or gas plume containing an absorbing gas, part of the laser frequency modulation is converted into an amplitude modulation (Risis et al., 1993). In frequency space the modulated laser beam consists of a carrier frequency, which is the emission frequency of the laser, and side bands displaced from the carrier by integral multiples of the modulation frequency. When this light impinges upon a photodetector, each side band mixes with the carrier to give a signal at the modulation frequency.

CHEMICAL SPECIES	MEASUREMENT LOCATION	PRIORITY
H_2S	Cooling Tower Fan Stack	High
H_2S	Main Steam Line	High
H_2S	Untreated Vent Gas	Medium
O_2	Untreated Vent Gas	Medium
HCl	Main Steam Line	Medium
SO_2	Treated Vent Gas	Low
O_2	Treated Vent Gas	Low
CH_4	Main Steam Line	Low
H_2S	Treated Vent Gas	Low
H_2	Main Steam Line	Low

Table 1. Geothermal Plant Gas Monitoring Applications.

Since the sidebands are equal and opposite in phase the two signals generated by the mixing process cancel unless their relative amplitudes and phases are altered in the measurement process. For trace gas detection, this alteration is arranged by adjusting the laser emission and modulation frequencies so that a strong line of the molecular species of interest overlaps one of the sidebands.

The advantage of this technique is that the measurement can be performed where the intensity noise in the laser is a minimum; and therefore, very high signal-to-noise measurements are possible. Under laboratory conditions, absorbances as low as 10^{-7} are possible (Silver et al., 1992).

One practical difficulty in achieving this sensitivity in industrial applications is due to the requirement that the modulation frequency, and corresponding detector bandwidth, be on the order of the linewidth of the species to be detected and measured. For atmospherically broadened (10GHz) lines, this is readily accomplished using two-tone modulation techniques in which a pair of closely spaced frequencies are used to modulate the laser. The detector output is then demodulated at the difference frequency. This technique permits high-modulation frequencies matched to pressure-broadened lines using modest bandwidth detectors (Cooper and Warren, 1987; Janik, et al., 1986). For example, a two-tone technique could be employed that modulated the laser at 10,000,000,000 Hz and 10,001,000,000 Hz and consequently performed the demodulation and detection at 1 MHz.

While frequency-modulated detection schemes have proven very sensitive under low pressure and atmospheric conditions, the additional line broadening that occurs under conditions of high pressure and elevated temperature can significantly limit the effectiveness of the technique. Scattering from condensate and other particulate may also reduce the signal transmission to unusable levels. The goal of this study was to evaluate the response of an near infrared, tunable diode spectrometer under these types of conditions. This data is then used in determining which plant locations are optimal for deployment and developing conceptual designs for a field device.

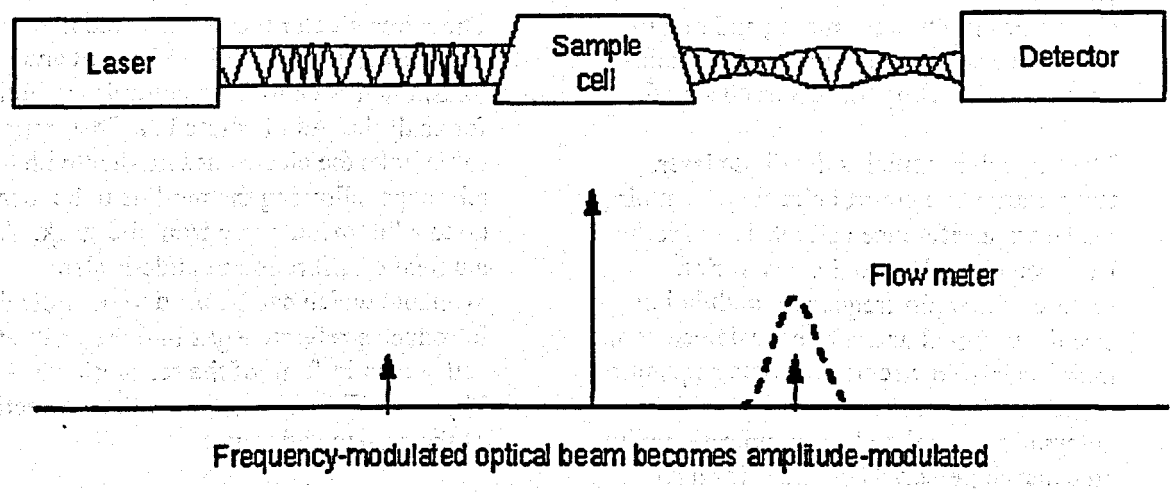

Figure 1. Frequency-Modulated Spectroscopy Concept.

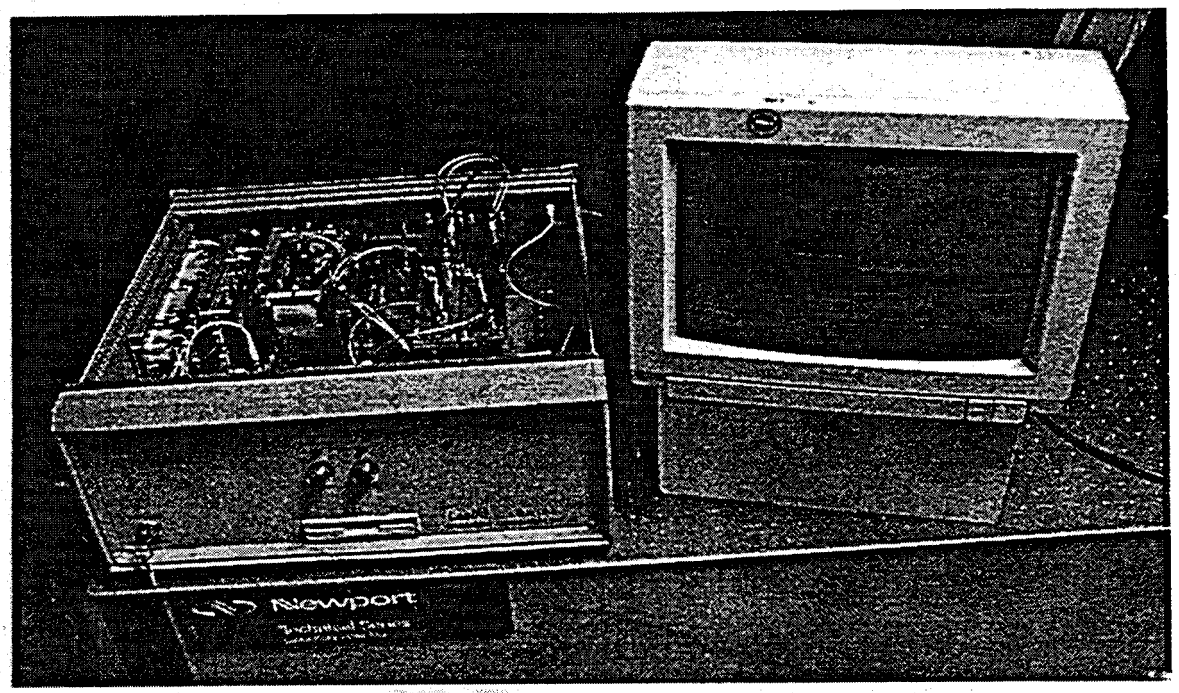

Figure 2. Photograph of the LasIR Instrument and Display Module.

EXPERIMENTAL

The components, shown in Figure 2 and 3, of the frequency-modulated, diode laser spectroscopy system were procured from Unisearch Associates. These included a distributed feedback laser diode which emits radiation at 1.578 microns, a small telescope and retroreflector assembly, and an electronics module for tuning and modulating the laser probe signal and demodulating and detecting the absorbed signal.

The controller contains the diode laser, temperature and control circuitry for tuning the laser; a reference cell used to lock the laser wavelength onto the absorption feature; the radio frequency modulation circuitry; signal and reference detectors and their associated circuitry; a data acquisition board; and an on-board computer for automatic control and communication with an external personal computer for data logging and display purposes. This system is packaged into a 46 (L) X 22 (H) X 45 (W) centimeter size module (LaSIR Operation Manual, 1997).

The probe signal is transmitted by a small telescope and retroreflector assembly, shown schematically in Figure 2, which can be mounted onto the emission stack. The telescope collimates the light and directs it to a retroreflector located across the stack. The retroreflector then returns the light to the telescope, where it is refocused and transmitted back to the electronics module for analysis. As illustrated , a fiber optic cable links the electronics module with the telescope, allowing the module to be located up to a kilometer away from the stack. An automatic calibration module is also available which can be used to periodically introduce a reference gas into the calibration cell shown in front of the retroreflector in Figure 3. This allows for on-line correction of the system calibration.

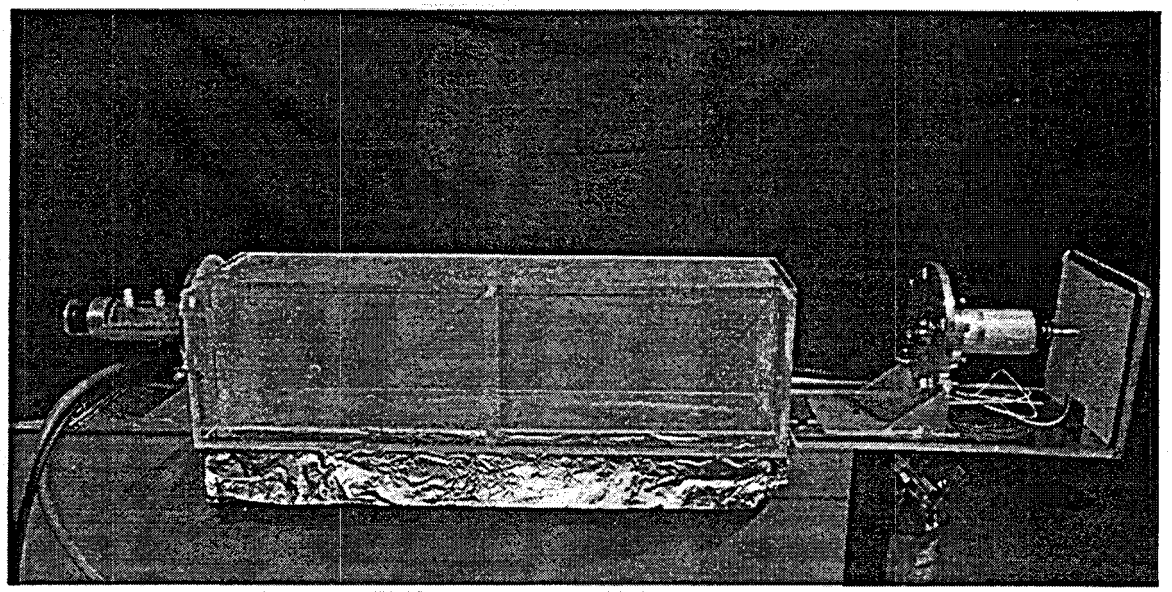

Figure 3. LasIR Telescope and Retroreflector Assembly Shown in Experimental Set-Up for Condensate Measurements.

For the experiments, a stainless steel test cell, 80 centimeters in length and 2.54 centimeters in diameter, was configured with sapphire windows. The cell was designed to be placed in a clam shell furnace for operation at high temperature; and in addition, could be pressurized to at least 7 atmospheres (100 psig). The laser radiation was collimated into a narrow beam by a grin lens, propagated through the cell, and detected at the opposite end using a germanium detector. The LasIR system was used to control and modulate the beam, as well as to demodulate and analyze the signals.

A separate fixture, a 100 centimeters (L) X 35 centimeters (W) X 35 centimeters (H) dimension plexiglass box, was configured with access holes to accommodate the telescope and retroreflector assembly for use in the tests to evaluate the response of the device in the presence of condensate. For this work, the 10 centimeter calibration cell was filled with 5000 ppm H_2S in nitrogen gas. Heated vapor from a boiling flask of water was then introduced into the containment box and the effect on the existing signal was observed. A picture of this set-up is shown in Figure 3.

RESULTS

The sensitivity and detectivity of the device was evaluated by filling the calibration cell with various mixtures (550 and 5000 ppm in nitrogen) of H_2S from calibration cylinders and observing the standard deviation in the signal. An example of a plot of this type of data is present in Figure 4.

A detection limit on the order of 25 ppm-m was readily obtainable with the device. Extrapolating over the 8 meter diameter of the stack, it should be possible to detect H_2S at a level of 1-2 ppm in a signal retro-reflected across the stack. Some signal noise modulation due to optical feedback into the laser diode was observed in the signals. It is speculated that by improving the optical isolation in the system this noise could be reduced and the detection limit improved. The measurement precision was found to be on the order of +/- 5% of full scale, and a stability of +/- 10% of the calibration signal per hour was observed in the tests.

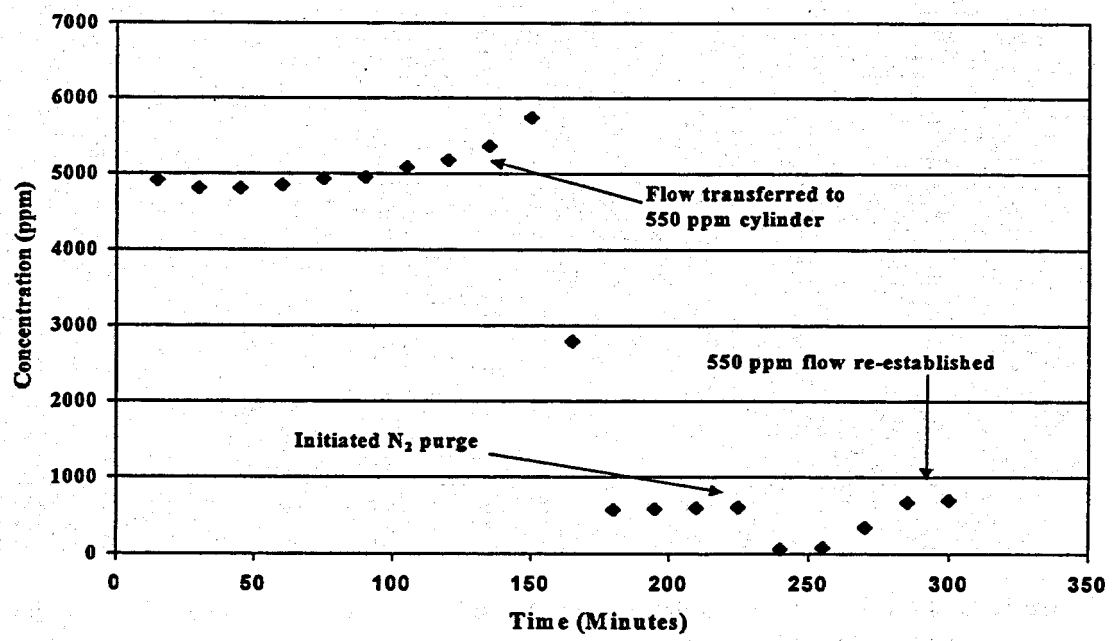

Figure 4. H_2S Detection Test.

The response of the system to changes in pressure is presented in Figure 5. For this plot, the stainless steel cell was filled with 5000 ppm H_2S gas to various pressures. These plots indicate that the measurement is quite sensitive to changes in pressure, exhibiting a 50% decrease in signal for every 1/3 atmosphere increase in pressure. The poor response of the instrument at high pressure is not unexpected since the analytical technique, to a first approximation, measures the derivative of the absorption line. As noted in Figure 5, the absorption line broadens in response to increases in pressure; and therefore, the slope (derivative) of the line decreases, along with the measurement sensitivity. The sloping background observed in this data is due to an etalon effect. This effect occurs because the windows in the stainless steel cell were not angled relative to the propagating beam, resulting in the generation of a broad interference fringe that is detected by the device as a change in intensity. Fortunately, it was possible to largely mitigate this effect using a quadratic suppression technique. In this technique, a quadratic function of the form, $y = a + bx + cx^2$ is fitted to the signal and reference spectra. The spectra are then divided by the fitted functions, effectively removing the baseline and making the function more symmetric prior to the analysis step.

The device exhibited much less sensitivity to changes in temperature. Signal changes of less than 25% are observed over a temperature range of 40^0 F (20^0C) to 230^0 F (110^0 C). Experiments with water vapor indicated that the device was effective at excluding the contribution of water vapor in the signal, but a marked decrease in signal-to-noise was observed as droplets formed which were comparable to the size of the wavelength of the light, i.e. the device did not function well in fog. In the tests, the device was able to function with reasonable signal-to-noise after a loss of up to 80% of the initial signal.

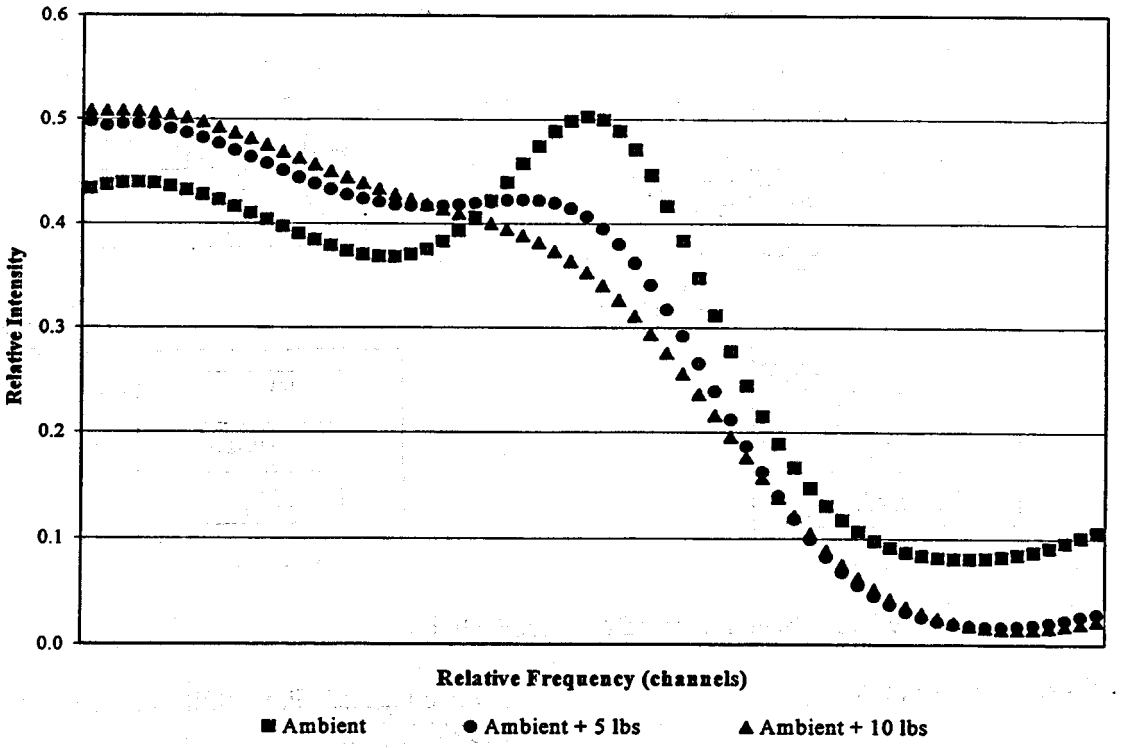

Figure 5. Change in Absorption Signature as a Function of Pressure.

CONCLUSIONS

The technique shows good promise for use as a stack monitor. For this application, the laser signal would be propagated via an optical fiber to a telescope located on the stack near the fan circulation for appropriate mixing to prevent condensate or fog formation. A retroreflector would be placed on the stack opposite the telescope assembly and used to redirect the laser signal back across the stack and into the fiber optic for transmission to the detection and data logging electronics.

In view of the pressure and temperature sensitivity, it is apparent that direct sampling of the stream will not be effective for locations such as the main steam line. However, it would also be possible to use the technique for real-time monitoring in these locations, using a side-stream in which a portion of the stream is circulated through a long-pass optical cell. The use of this configuration allows for the conditioning of the stream to a reasonable temperature and pressure prior to introducing the vapor sample into the cell for measurement.

The use of the long-pass cell might also be considered if there is too much condensate to make a measurement in the stack via the open path measurement. In this scenario, the sample could be collected by installing a perforated tube across a chord of the stack. The vapor would then be pulled into the long pass cell for measurement. (An additional water trap could be placed in the line, if needed, to eliminate droplets.) This configuration could also be used to increase the measurement sensitivity. If the cell is evacuated at a rate that causes a small pressure drop in the cell, then the line broadening effect is reduced and the spectroscopic technique is more sensitive to the sharper absorption feature. These deployment options are shown schematically in Figure 6.

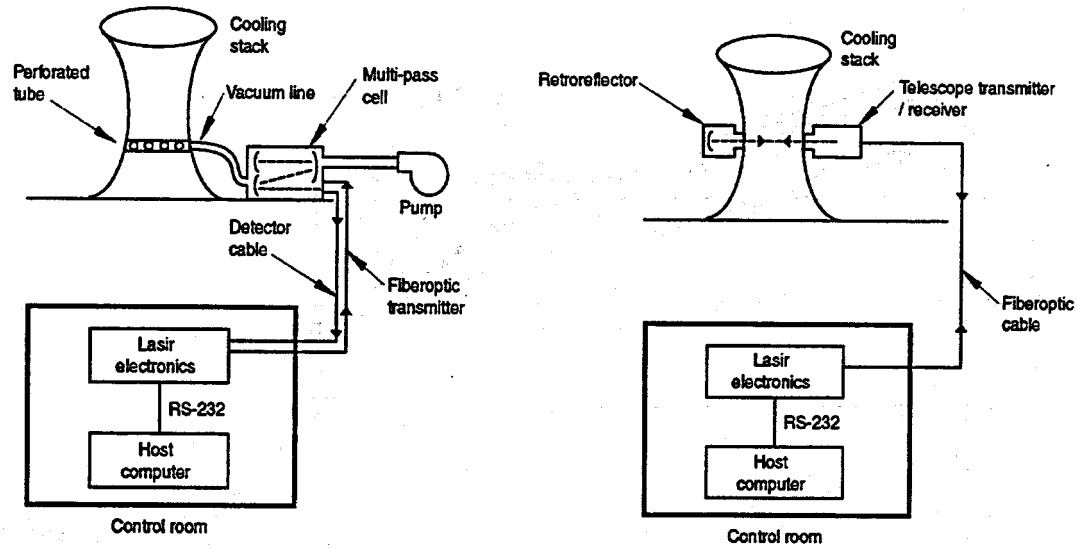

Figure 6. Tunable Diode Spectrometer Deployment Options.

ACKNOWLEDGMENTS

This work is supported by the U.S. Department of Energy, Assistant Secretary for Energy Efficiency and Renewable Energy, under DOE Operations Office Contract DE-AC07-94-ID13223.

REFERENCES

Cooper, D. E. and R. E. Warren, "Frequency Modulation Spectroscopy with Lead-Salt Lasers: A Comparison of Single-Tone and Two-Tone Techniques", App. Opt., *26*, 3726-3732, 1987.

Janik, G. R., C. B. Carlisle, and T. F. Gallagher, "Two-Tone Frequency-Modulation Spectroscopy", J. Opt. Soc. Am. B, *3*, p. 1070-1074, 1986.

LasIR Operation Manual, Unisearch Associates Inc., 96 Bradwick Drive, Concord, Ontario. 1997.

Risis, H. , D. Cooper, C. Carlisle, L. Carr, and J. Van der Laan, "Frequency Modulation Spectroscopy with Tunable Diode Lasers," Proc. SPIE, *2112*, 12-18, 1993.

Silver, J. A., "Frequency-Modulation Spectroscopy for Trace Species Detection: Theory and Comparison Among Experimental Methods," App. Opt., *31*, 707-717, 1992.

BIOCORROSION STUDIES AT GEOTHERMAL PLANTS

P. A. Pryfogle and J. L. Renner
Idaho National Engineering and Environmental Laboratory
(208) 526-0373

ABSTRACT

The status of a project investigating the role microbiologically-influenced corrosion (MIC) plays in the degradation of critical components in geothermal power plants is described. The research involves the integration of established sampling and analysis procedures with new analytical techniques to predict the on-set and severity of MIC in plant subsystems. The data from this study will be used to more accurately determine the benefit of various treatment alternatives.

INTRODUCTION

Biofouling occurs when planktonic microorganisms present in industrial process fluids deposit and attach to surfaces. Upon attachment these cells divide, increase in number, and may produce polysaccharides, or other extracellular polymeric materials. These materials are commonly referred to as biofilms. Biofilms act to stabilize and protect the microbial community, allowing the introduction of organisms and the subsequent formation of a more complex structure. This growth and accumulation of biomass may impact operations by reducing heat transfer within condensers, increasing drag within pipes, and producing hydrodynamic resistance across filters. In addition, these organisms may possess different metabolic capabilities including enzymatic interactions, utilization of nutrients, and resistance to environmental perturbations. The complex interactions of organisms within the biofilm can lead to the development of micro-habitats producing aerobic and anaerobic sites. These sites may have pronounced effects on surface chemistry, which is of particular importance in dealing with metallic substrates. Aerobic organisms, such as heterotrophic bacteria, are capable of scavenging oxygen for their growth, resulting in low or depleted oxygen zones. Loss, or decreased availability, of oxygen to the metal may result in the degeneration of the metal oxide layer that serves as a barrier of resistance to corrosive activity. Anaerobic sites can facilitate the growth of fermentors and hydrogen-utilizing bacteria whose acidic fermentation products can initiate metal solubilization. The biofilm and bacteria may alter the electrochemical nature of the metal surface, creating micro-cathodic or anodic sites that may enhance corrosion (Videla, 1996).

This work focuses on an investigation of microbially influenced corrosion (MIC) in geothermal power facilities. Corrosion is of particular concern in these systems due to the harsh conditions at which they operate. MIC has occurred in some components, including the tube sheets in the condensers, as illustrated in Figure 1. Materials from the tube sheets have been analyzed and found to contain sulfate and nitrogen-reducing bacteria. Generally, any systems which are not drained are vulnerable to MIC. In addition to the cost of repairing or replacing components, and the associated shutdown costs, a considerable amount of money is spent on the purchase of corrosion control products. It is estimated that on the order of $50K per year is expended on products for controlling MIC at some plant sites.

The technical goals of this effort are to develop a more detailed understanding of the development and extent of MIC at geothermal power production facilities. A particular difficulty in the assessment and control of this type of corrosion is related to the inability to distinguish damage caused by microorganisms from that produced by direct chemical means. In particular, there are no reliable on-line techniques to recognize and predict the on-set of MIC. Currently, treatments are applied at the plants either on a predefined schedule, or on an as-needed basis corresponding to visual evidence of microbial growth. Therefore, there is potential for over- or under-treatment of the

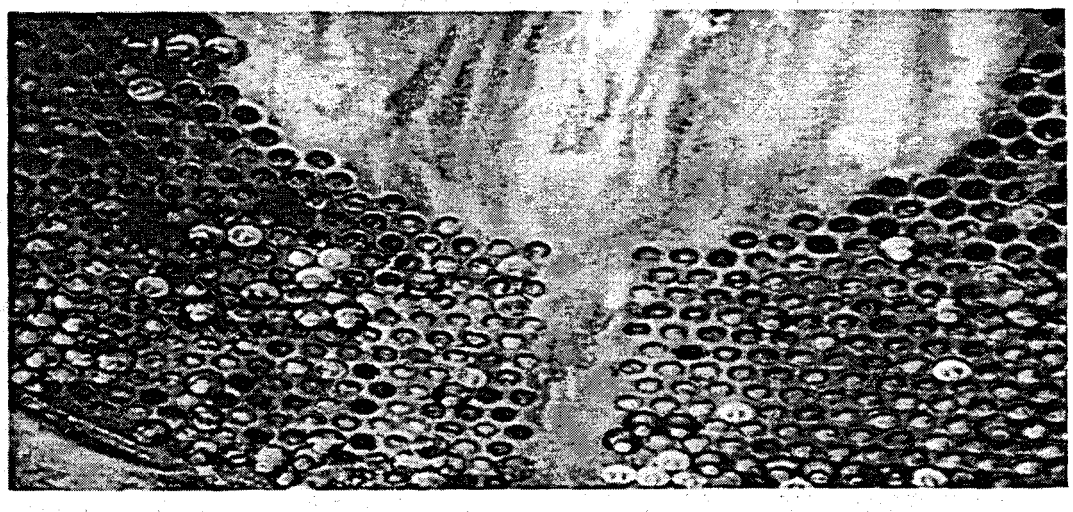

Figure 1. Corrosion on Tube-Sheet Facing Inside a Condenser.

problem. This effort is evaluating analytical techniques which may be used to estimate and partition corrosion between microbial and other sources; and in addition, examining the feasibility of using these techniques in the development of diagnostic tools to measure and sample biofouling *in-situ* in critical components. The ultimate goal of the work is to support the geothermal industry in identifying the most economical methods to prevent biocorrosion.

APPROACH

This investigation involves the integration of established sampling and analysis procedures with new analytical techniques to predict the on-set and severity of MIC in plant subsystems. This section describes a number of measurement approaches for accessing MIC at the geothermal plants and their relative advantages and disadvantages in identifying and mitigating problems at these facilities (Kearns and Little, 1994).

The most commonly used method for evaluating MIC is to determine the relative abundance, or ***most probable number (MPN)***, of the bacteria known to contribute to the degradation of materials. This method consists of making replicate dilutions of an environmental sample in into selective media. Typically, the specific growth media are designed to test for the presence of heterotrophic bacteria, sulfate-reducing bacteria (SRB's), acid-formers and others, such as de-nitrifying bacteria, which may be of importance in particular environments. The inoculated media are incubated for a period of approximately 28 days, and statistical analyses are then performed to determine cell populations from growth patterns in serial dilutions of sample vials.

This technique is very sensitive and is particularly useful for applications in which the growth kinetics is highly variable. (In these cases, the long incubation period allows the presence of slowly growing organisms to be counted.) It is also preferred in cases where the microorganisms of interest produce some identifying product of metabolism. For example when SRB's are introduced into a sodium lactate solution containing an iron substrate, the sulfate is reduced to sulfide which reacts with the iron to form black ferrous oxides which are easily visualized. The disadvantage of the technique is that the results may not accurately represent the microbial community contributing to the problem. First, the analyses require a planktonic sample, which may not accurately represent the makeup of the biofilm community. The susceptibility of planktonic organisms to biocides differs markedly from those protected by a biofilm; and therefore, treatment assessments relying totally on this type of analysis may be misleading.

Second, the selective media are, by definition, preferential to some bacterial species and may not support all the types present. Finally, the biggest disadvantage is with the long incubation period. Conditions in a plant environment may change significantly between the identification of the problem and the application of a treatment.

Metal coupon studies are also frequently utilized to estimate the effects of corrosion within industrial operating systems. In these studies, a coupon of the same type metal used in the system component is weighed and deployed in the plant environment. The samples are then collected after exposure and analyzed for evidence of biofouling or corrosion. An individual sample may then be re-weighed and depth profiles performed to determine the degree of physical deterioration. Other more detailed surface analyses are required to determine if MIC has occurred. A typical scheme involves staining the coupon and performing sessile bacterial counts; conducting surface analyses with scanning electron microscopy (SEM), energy dispersive x-ray spectroscopy (EDS), and Auger electron spectroscopy (AES) to confirm the presence of a biofilm and identify corrosion products; and using other techniques, such as confocal scanning laser microscopy (CSLM) for detailed visualization of the physical properties of the biofilm.

The advantage of this type of approach is that it provides a means of collecting data under realistic conditions, since the composition of the metal coupons are chosen to match those of the system components and the exposure is typically performed in a side stream of the plant sub-system so that the operating environmental parameters are closely matched. As described, a large amount of data can be derived from a detailed analysis of the coupon; and in particular, the relative extent and rate of corrosion can be estimated.

Unfortunately, considerable handling and processing of the coupon is required to obtain this data. Many of the analyses are quite time-consuming and require the use of expensive analytical instrumentation. These analyses also do not unambiguously distinguish between chemical and biological types of corrosion. Again, there is a considerable delay between the sample deployment, retrieval and evaluation of the problem.

Several indirect methods may also be used to track changes in plant conditions that could indicate increased biological activity and biofouling problems. For example, ***total organic carbon (TOC)***, can be used to determine the level of biological activity in a system component, particularly if the component can be isolated as a subsystem of a linear flow process, such as a condenser. Dissolved carbon in aquatic systems may be divided into inorganic and organic compounds. These carbon compounds can serve as substrates for biological metabolism and may provide an indication of the degree of eutrophication.

The technique requires that a sample be collected and injected into an analyzer where it is acidified to release the dissolved inorganic carbon (CO_2). The gas is then purged from a reaction vessel into an analytical chamber where an infrared absorption measurement is used to determine the CO_2 concentration. The sample is then activated with a chemical oxidant and heated to 100^0C to oxidize the organic carbon fraction in the sample. This fraction is purged and analyzed, resulting in a calculation of the dissolved organic component. These two fractions, the organic and inorganic carbon, are added to obtain the total carbon for the sample. This data, collected over time, could provide an early indication of increased microbial activity and biofilm formation.

This analysis could be operated in an on-line sampling mode. The technique uses a small sample volume, and the analysis can be completed within minutes of sample injection. The drawback of the technique is that it does not provide a specific analysis of the carbon and, as all indirect methods, must be correlated with other process parameters to be meaningful.

Biological productivity in process streams can also be performed by an analysis of the *adenosine triphosphate (ATP)* content. ATP is a high-energy molecule generated by living cells to perform metabolic functions. It is considered a conservative compound which is reduced upon cell lysis and death. Therefore, it can be used as a measure of the active, or living cells, in an aquatic system. Because it is produced by all cells, it can also serve as a means of estimating the concentration of living biomass in a sample. For the analysis, a sample aliquot is collected and placed in a dark chamber containing a photomultiplier detector. A cell-lysing compound is added to the sample, along with a buffer compound, to prevent the rapid decay of the released ATP. A second compound (luciferin-luciferase reagent) is added which reacts with the free ATP, emitting photons, which are detected by the photomultiplier. The intensity of the emitted light can be correlated to the amount of living biomass in the sample.

ATP analysis can also be performed as an on-line sampling procedure. However, it can not specify the types of microorganisms present, and can be sensitive to sulfide and some types of biocides, which may quench the reaction. Successful data interpretation is dependent upon tying the measurement to other operational parameters.

Electrochemical measurements have been widely used to use detect and characterize corrosion. Metal corrosion is, by definition, an electrochemical oxidation/reduction process that can be influenced by the physical, chemical and biological properties of the surrounding environment. In particular, bacteria within biofilms are capable of changing the type and concentration of ions, pH, dissolved oxygen level, flow velocity and the buffering capacity at the metal/solution interface, thereby influencing the corrosion resistance of components (Mansfield and Little, 1991).

The most widely used field technique of this type is based upon the measurement of *electrical resistance,* sometimes referred to as *zero resistance ammetery (ZRA)*. In this technique, a metallic strip is inserted into the process medium and its electrical resistance is monitored with time. The electrical resistance of the probe is inversely proportional to the cross-sectional area and directly proportional to temperature. Therefore, at constant temperature, the corrosion will cause the metallic strip to suffer a decrease in cross-sectional area, and as a result, an increase in resistance. The strip is sampled over a period of time and the average corrosion rate is extrapolated from the difference in resistance between two readings.

Electrochemical noise analysis (ENA) has also been applied in the field to detect the on-set of corrosion. ENA measures the fluctuations of current or potential as a function of time or experimental conditions. For the measurement, two identical samples are placed in the process solution and connected to a digital multimeter controlled by a computer. Amplitude and frequency changes in the noise spectrum are induced by various corrosion processes.

Both ZRA and ENA have been used as on-line monitoring devices. The principle disadvantages of these techniques are that the data is often difficult to interpret; localized corrosion can be masked by changes in the stream environment; and most importantly for this project, the standard measurement configurations of these devices do not readily allow the partitioning between the abiotic and biotic contributions to the corrosion of the substrate.

In order to overcome this last drawback, a split-cell arrangement is being investigated for differentiating MIC from other types of corrosive activity on metals exposed to geothermal fluids. The technique, developed by Brenda Little, et. al., uses a double cell arrangement in which one of the cells contains the metal sample of interest, the process fluid, and bacteria. The other cell is sterilized and the process fluid is filtered to prevent bacterial contamination. The cells, shown in Figure 2, share a common internal pathway connected to semi-permeable membrane that permits the exchange of ions, but again will not allow the passage of bacteria into the sterile side. The cells contain working electrodes that are

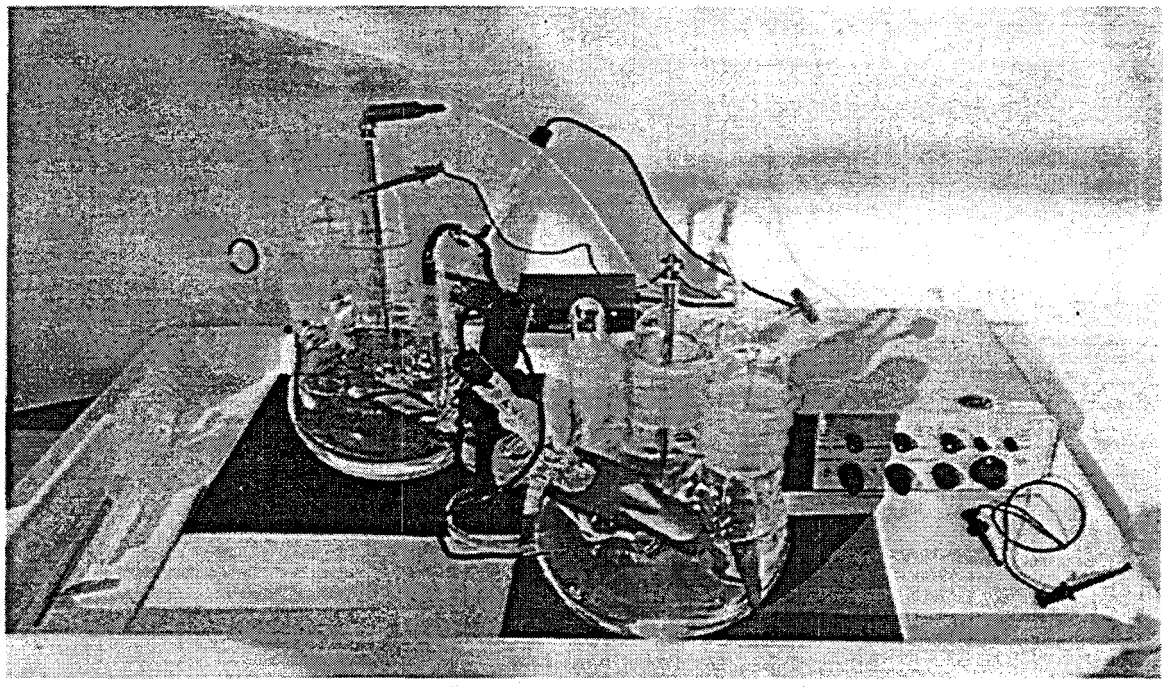

Figure 2. Electrochemical Cells for Measuring MIC Activity.

connected externally through a zero potential potentiostat and calomel reference electrodes. When bacterial corrosion occurs, a change in potential is induced between the working and reference electrode. This change unbalances the zero potential between the two cells and is detected as a current (Gerchakov, et al., 1986).

These devices have been used successfully as laboratory research tools. This project is investigating design modifications which would allow the devices to be deployed as on-line monitors in geothermal plants. In addition to implementing a more compact, rugged packaging that can realistically sample the stream; other technical challenges include maintaining sufficient stability and abiotic/biotic partitioning for long-term field operation.

DATA COLLECTION AND ANALYSIS

Initial efforts have concentrated on developing baseline data on MIC for the Geysers site. The basin is approximately 35 miles across, measuring from the northwest to the southeast corner. While the geothermal source is common to all locations, there are differences in the steam character that can impact MIC. Therefore, a series of sites, including facilities operated by Calpine, Pacific Gas and Electric (PG&E) and the Northern California Power Agency (NCPA), were selected for seasonal sampling and analysis of microbial activity.

To date, samples from six field stations have been collected on three occasions, and most probable number (MPN) analyses performed. The sampling periods provide seasonal indicators for the early summer, fall and winter. The MPN data was collected and analyzed using commercially-available sampling kits obtained from Sherry Laboratories, Tulsa, Oklahoma, which could detect the presence of heterotrophic, de-nitrifying, sulfate-reducing and acid-producing bacteria. (While sulfate-reducers, or SRB's, are the type most commonly associated with MIC, the current practice is to look at the overall community structure and relate the findings to the conditions present at the point of sampling.) In this study, the samples were collected from the in-flow

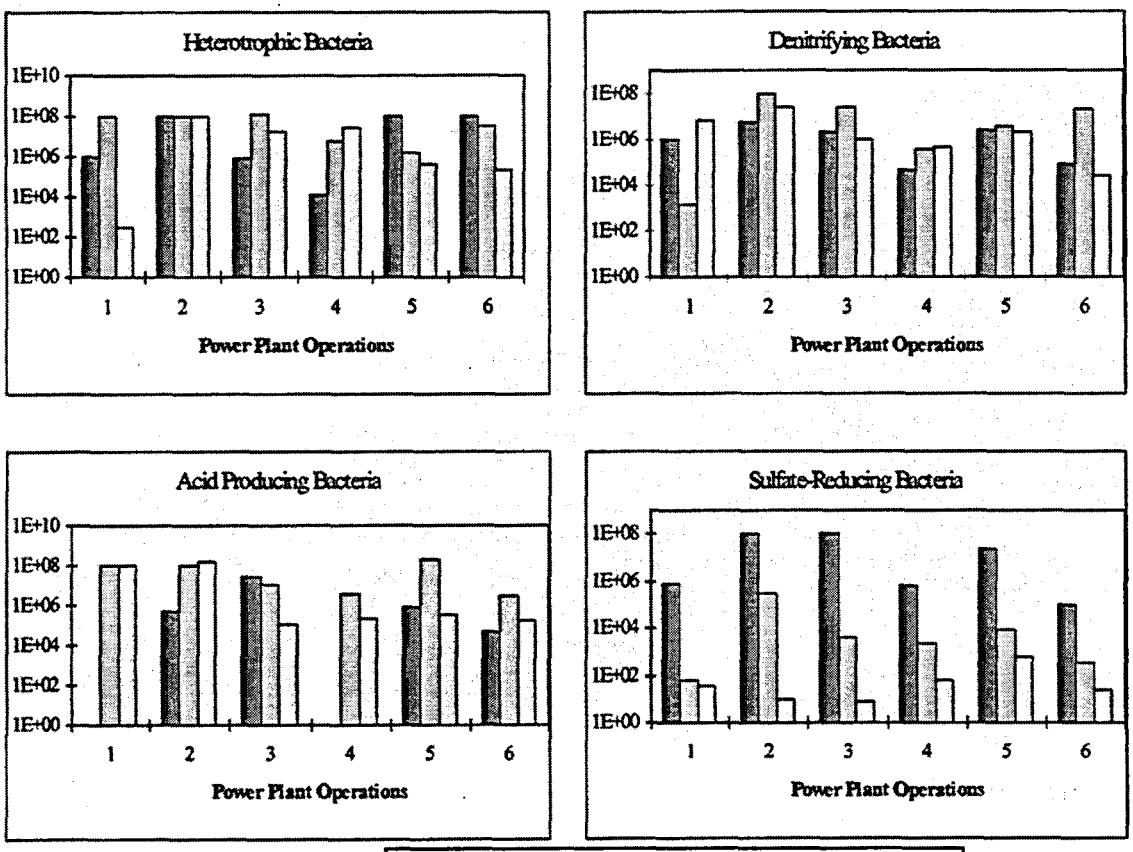

Figure 3. MPN Out-Flow Data.

and out-flow lines to the steam condensers. One milliliter (mL) of the sample was injected into a vial containing 9 mL of media. The media was mixed well, and then 1 mL was withdrawn form that bottle and added to the next in the series. This procedure resulted in a 1 to 10 dilution factor for the series, which was carried out into eight vials and replicated five times. Bacterial growth or activity, observed in the diluted samples, was used for the MPN calculations.

The MPN out-flow data is presented in Figure 3. The effluent samples were generally determined to have higher densities of bacteria than those taken from water flowing into the condensers. MPN numbers are seen to vary both as a function of location and season. There were high numbers of heterotrophic bacteria detected. In general, numbers exceeding 10^6 cells/mL are indicative of potential biofouling and/or MIC problems. Three of the plant operations consistently had higher numbers of all bacterial types than other operations, which incidentally reported fewer corrosion problems. SRB numbers were generally low but did show seasonal variances with the highest numbers observed during the summer sampling. This drop was unique to the SRB data.

Total organic carbon (TOC) analyses were also performed on samples collected from the six Geysers power stations over the same sampling periods. As Figure 4 illustrates, there was considerable variability in the levels of dissolved carbon in the samples. These values represent total carbon (TC) measurements in water flowing into the condensers at the six plants. There is a general trend for both dissolved inorganic and organic carbon to increase along the northwest to southeast stations gradient. There were also higher TC values detected in the influent streams than in the effluent streams. While some of the loss might be associated with heating, and therefore reduced capacity for dissolved gases such as CO_2, in most cases the same trend was observed

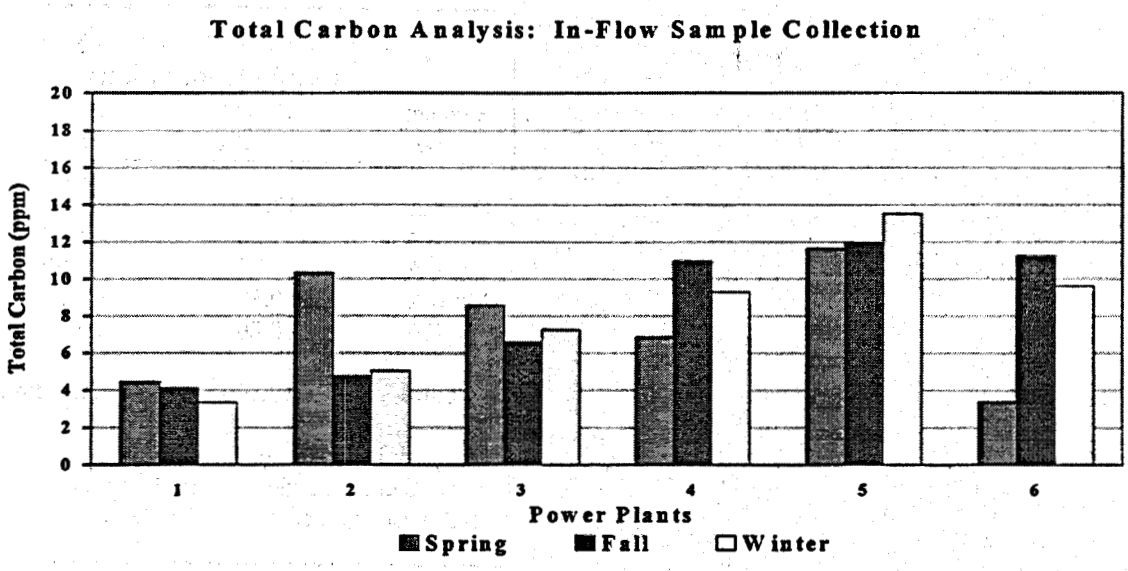

Figure 4. Total Carbon (TC) for the Geysers Plants, Influent Condenser Streams.

for the TOC values as well. This type of result, correlated with other data, could indicate biofouling within the condenser. That is, there was a loss of carbon in the condenser, and one possible explanation of where the carbon has gone is into the growth of biomass. Stations with the higher MPN values also tended to show high TC values in their influent water. Specific points of correlation are being compared with operational data to determine their significance.

Brief coupon studies have also been conducted at three facilities. For these studies, various alloys of steel, including A105 carbon steel, 304L and 316 stainless, were purchased from Metals Samples Company in Munford, Alabama and deployed at the plants. Sets were pulled after two, four, and six-week exposures. They were placed in an isolation package, filled to the top with process water before closure, and sent to our laboratory for analyses. The principle goals of this work were to determine what levels of activity could be expected for a typical exposure and to determine which analysis techniques are the most productive for elucidating differences in microbially and chemically induced corrosion.

An example is presented in Figure 5, in which energy dispersive x-ray spectroscopy (EDS) was used to determine the relative composition of materials on the surface of one of the exposed substrates. The coupon shows visual indication of a film (section 1), and an analysis of the underlying area detected various corrosion products. Unfortunately, this analysis is not capable of detecting atoms of low proton structure; and therefore, it could not be unambiguously determined that the film was biological in nature, and caused the underlying corrosion. (A new environmental SEM recently ordered by our laboratory will allow this determination.)

FUTURE WORK

As noted in the previous section, the ability to identify and detect corrosion of biological origin is not a straightforward process. Even sophisticated surface analyses may result in ambiguous results. The ability to successfully detect and predict the on-set of microbial corrosion depends upon the ability to correlate data with various operational parameters. An essential element for performing this correlation is the development of instrumentation, such as the split-cell electrochemical device, that will indicate in a realistic time frame when microbial activity is occurring.

Standardless EDS Analysis
(XPP Quantitation)

Element & Line	Weight Percent	Atomic Percent*
O KA	18.34	43.57
Si KA	1.20	1.62
Cr KA	1.23	0.90
Mn KA	0.37	0.26
Fe KA	78.86	53.66
Total	**100.00**	**Iterations 9**

Accelerating Voltage	20 Kev
Beam Sample Angle	90 Degrees
X-Ray Emergence Angle	35 Degrees

Figure 5. SEM/BSE (back-scatter electron) Micrograph of Biofilm on Metal Coupon

ACKNOWLEDGEMENTS

The authors would like to thank the personnel at PG&E, Calpine and NCPA for their support of our sampling program. In particular, we would like to thank Walt Southall (PG&E), Milt Rhine (PG&E), Murray Grande (NCPA), Charlotte Dorrity (Calpine), Diane Tullos (Calpine), Jacob Rudisill (Calpine) and other plant personnel for their patience and support of this effort. This work is supported by U.S. Department of Energy, Assistant Secretary for Energy Efficiency and Renewable Energy, under DOE Operations Office Contract DE-AC07-94-ID13223.

REFERENCES

Gerchakov, S.M., B.J. Little, and P.Wagner, "Probing Microbiologically Induced Corrosion," Corrosion, *42*, pp. 689-692.

Kearns, Jeffery and Brenda Little, Editors, Microbiologically Influenced Corrosion Testing, Proceedings of ASTM Symposium, Miami, Florida, Nov. 16-17, 1992, ASTM STP *1232*, 1994.

Mansfield, Florian and Brenda Little, "A Technical Review of Electrochemical Techniques Applied to Microbiologically Influenced Corrosion," Corrosion Science, *32*, pp. 247-272, 1991.

Videla, Hector A., Manual of Biocorrosion, Lewis Publishers, Boca Raton, Florida, 1996.

BIOCHEMICAL PROCESSES FOR GEOTHERMAL BRINE TREATMENT

Eugene T. Premuzic
Brookhaven National Laboratory
Department of Applied Science
(516) 344-2893

ABSTRACT

As part of the DOE Geothermal Energy Program the BNL's Advanced Biochemical Processes for Geothermal Brines (ABPGB) project is aimed at the development of cost-efficient and environmentally acceptable technologies for the disposal of geothermal wastes. Extensive chemical studies of high and low salinity brines and precipitates have indicated that in addition to trace quantities of regulated substances, e.g., toxic metals such as arsenic and mercury, there are significant concentrations of valuable metals, including gold, silver and platinum, all present in a solid matrix. Further chemical and physical studies of the silica product have also shown that the produced silica is a valuable material with commercial potential. A combined biochemical and chemical technology is being developed which (1) solubilizes, separates, and removes environmentally regulated constituents in geothermal precipitates and brines (2) generates an amorphos silica product which may be used as feedstock for the production of revenue generating materials, (3) recover economically valuable trace metals and salts. Geothermal power resources which utilize low salinity brines and use the Stretford process for hydrogen sulfide abetment generate a contaminated sulfur cake. Combined technology converts such sulfur to a commercial grade sulfur, suitable for agricultural use. The R&D activities at BNL are conducted jointly with industrial parties in an effort focused on field applications.

BACKGROUND

Research and development strategy at BNL has focussed on cost-efficient processing of geothermal brines and sludges (Premuzic et al., 1996, 1997). This R&D effort led to the exploration of environmentally acceptable and cost efficient technologies, which more recently, evolved into recycling and conversion technologies for the treatment of geothermal sludges and brines, summarized in Figure 1. This

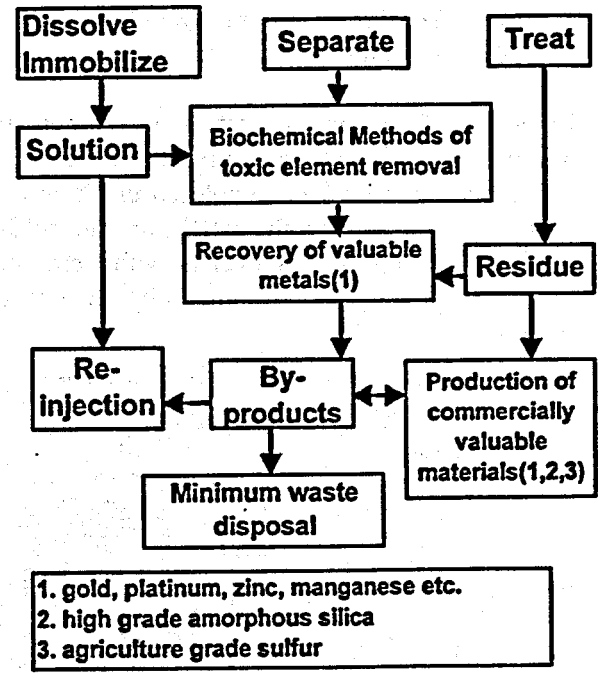

Figure 1. MRP's and MRB's treatment options

figure also introduces a new terminology, namely, "Geothermal Mineral Rich Precipitates (MRPs), rather than "Geothermal Sludges", and similarly, "Geothermal Mineral Rich Brines (MRBs). Using this strategy, a process (Figure 2) for high salinity brines has been developed. In this process, the brine is treated for metal recovery, while the silica rich precipitate, i.e., the MRP "cake" becomes the feedstock for the production of amorphous silica. A significant modification of this process is being developed for the treatment of the by-product generated from low salinity geothermal resources. The byproduct, a contaminated sulfur residue produced in the Stretford hydrogen sulfide abatement process, is treated first biochemically and then sublimed. The overall process is summarized in the block diagram shown in

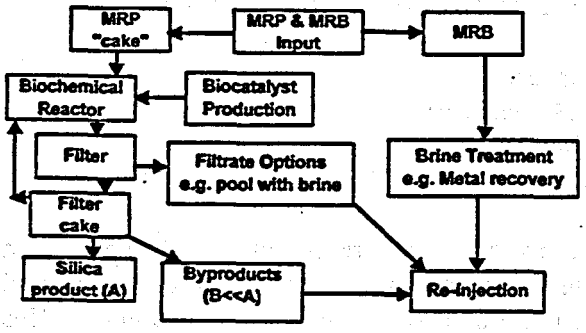

Figure 2. Total Processing of Geothermal Sludges and Brines

Figure 3. The end product is a commercial, agricultural grade sulfur. Currently, conceptual process designs are being explored in which by-products from either the MRP or the sulfur process will be fully recycled with zero, or, minimum yields of environmentally acceptable wastes.

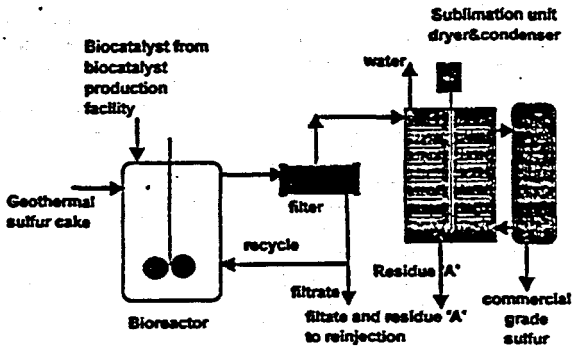

Figure 3. The Sulfur Cake Process

RECENT ACTIVITIES

The process for the treatment of mineral rich precipitates (MRPs) leading to the production of amorphous silica is being developed jointly with CalEnergy Company, Inc., and is schematically summarized in Figure 4. The process yields amorphous silica in a quantity which is about one half of the original highly pigmented MRP feedstock. The dissolved "impurities" present in the liquid phase are reinjected. Biochemical treatment followed by chemical treatment applied at different concentrations and temperatures, leads to the production of a silica product with varying degrees of pigmentation. In the chemical composition of this product the major contribution

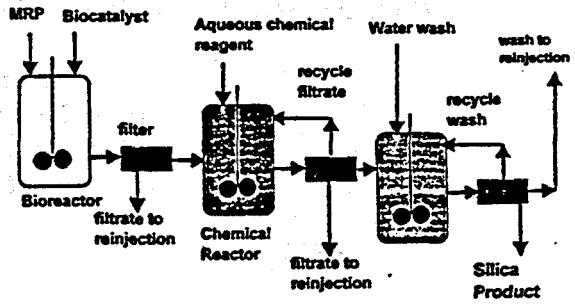

Figure 4. Treatment of Mineral Rich Precipitates

to pigmentation is iron. Results of an inductively-coupled-plasma-mass spectrometric analysis (ICP-MS) of untreated and treated MRP with two different biocatalysts, BNL-3-25 and BNL-3-23 followed by chemical treatment R-1 are shown in Figure 5. The actual pigmentation is due to different chemical species of the responsible metals. For example, iron, the predominant metal present, under processing conditions appears in several forms, as shown in Table 1. The "effect" of the other metals, present in subtrace quantities, on the quality of the end product, is being investigated. For this purpose the use of BNL's Synchrotron Light Source (NSLS) in combination with other technologies is being explored (Bajt et al., 1994).

Under appropriate processing conditions the extent and the rates of depigmentation, expressed in terms of iron, are fast and efficient as shown in Figure 6a & b. There are several uses for the silica products. For example, the BNL silica product can be incorporated into acrylic wall

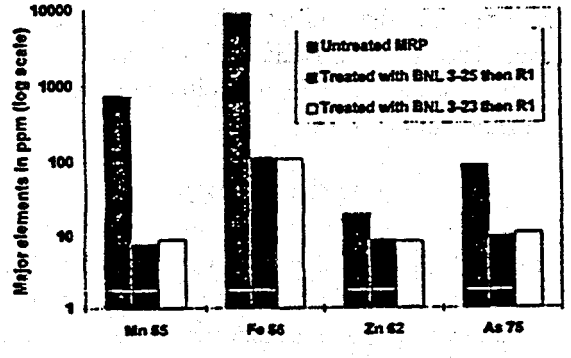

Figure 5. Reagent R1 Treatment of Biotreated MRP

Table 1. Species of Iron Pigments

- FeO(OH) hydrous ferric oxide is brown
- Fe_3O_4 is a mixture of Fe(II)-Fe(III) oxide and is black
- α-Fe_2O_3 is red brown
- Fe(III) chloride·$6H_2O$ is yellow
- Fe(II) chloride·$8H_2O$ is colorless
- Fe(II) chloride·$6H_2O$ and Fe(II)Chloride·$4H_20$ are pale green
- Iron(II) and Iron(III) sulfides are black

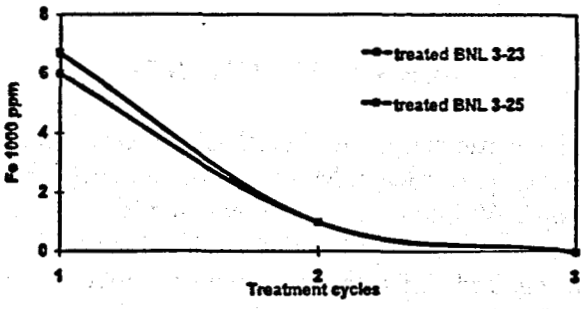

Figure 6a. Silica Production: ICP-MS Analysis of Iron Concentration of Biotreated MRP as Function of R1 Chemical Treatment Cycles

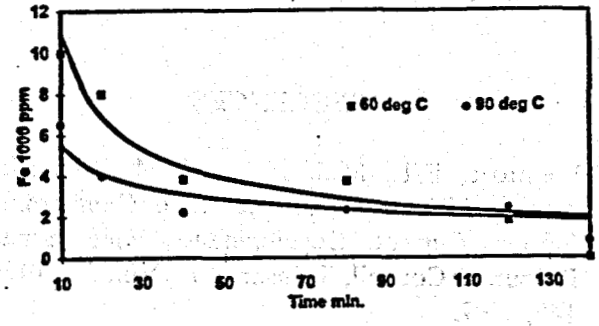

Figure 6b. Reaction Rate vs. Temperature Iron Removal

paints. When compared to a commercial material, the produced silica rates very favorably with the commercial product, as shown in Table 2.

Table 2. Comparison of the Geothermal MRP Silica Product Produced in the BNL Process with Commercially Available Amorphous Silica

The geothermal MRP product was comparable to the commercial product in the following areas

Ease of dispersion
Viscosity stability
pH stability
Package stability
freeze-thaw resistance
reflectance
contrast ratio
pencil hardness
sheen
burnishing
ease of application

The geothermal MRP product was inferior only in scrubbing resistance while it had a superior opacity (whiteness) of 97% as opposed to the commercial products 94%

The process for the treatment of the sulfur cake derived from the Stretford hydrogen sulfide abatement technology is being developed jointly by BNL and CET International, Inc. A recent economic analysis of the MRP and the sulfur process is summarized in Table 3.

At BNL, metal recovery options continue to be actively explored. Experimental data remain consistent and support the view that the aqueous phase produced by ABPGB process should be pooled with the post heat exchanger brines, processed for metal recovery, and the remaining aqueous phase reinjected. Currently several different biosorbants are being tested. The overall selectivity of biosorbants is shown in Figure 7. Specific selectivity of the biosorbants used is further demonstrated by adsorption of platinum and gold at pH 1 and 100°C, as shown in Table 4. While the recovery of valuable trace metals from dilute solutions using biosorbants is very promising, further evaluation studies are needed. At the present time the quality of biosorbants varies from preparation to preparation. However, based on the results generated thus far and discussions with biosorbant producers, this disadvantage may be resolved.

Table 3. Economic Summary

Mineral Rich Precipitate (MRP): Silica Recovery Process

Capital cost $7 million dollars
Operating expenses $6 million/yr
Revenues:
$6 million/yr saving from disposal
$6 million/yr sale of silica
$6 million/yr pretax profit
55% yearly return on investment

Stretford H2S Abatement Technology: The Sulfur Cake Process

Capital cost $700 thousand
Operating expenses $331 thousand/yr
Revenues:
$164 thousand/yr saving from disposal
$190 thousand/yr sale of sulfur
$23 thousand/yr pretax profit
11% yearly return on investment

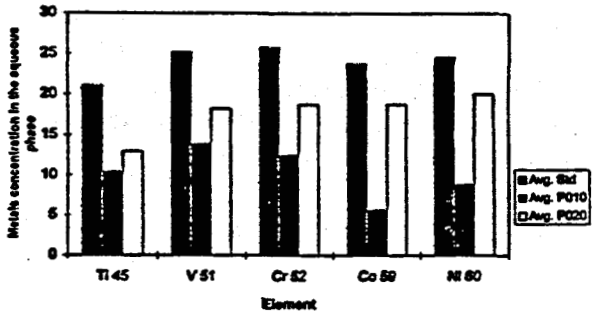

Figure 7. Selective Biosorption of Metals Dissolved in the Aqueous Phase

Table 4. Analysis of Brine Liquid for Platinum and Gold Using Different Biosorbents at pH 1 and 100°C

Sample	Standard Pt (ppm)	Standard Au(ppm)	% Uptake of Pt	%Uptake of Au
Before Biosorption	5.04	0.335		
Biosorbent P010	2.42		52	
Biosorbent P020		0.195		42
Biosorbent P030	4.79	0.063	5	81
Biosorbent P040	1.36		73	
Biosorbent P051	1.9		62	

CONCLUSIONS

1. A combination of biochemical and chemical processes has led to the design of a cost efficient technology for the treatment of geothermal metal rich precipitates (MRPs) and metal rich brines (MRBs).

2. Combined processes utilize fully recycling options.

3. The emerging technology is environmentally attractive and yields commercially viable products.

4. Collaborations with industry enables a full development and field application of the emerging technology.

ACKNOWLEDGMENTS

The participation of the BNL's Research and Development team, M.S. Lin, M. Bohenek, G.J. Topé, W. Zhou, L. Shelenkova, and R. Wilke is fully acknowledged and their invaluable input recognized. This work has been supported by the U.S. Department of Energy, Office of Conservation and Renewable Energy, Geothermal Technology Division, Washington, DC, under Contract No. AM-35-10. We also with to acknowledge Ray LaSala, the U.S. DOE Program Manager for continuous interest and encouragement.

REFERENCES

Premuzic, E.T., M.S. Lin, and M. Bohenek, Advanced Biochemical Processes for Geothermal Brines: Current Developments, Geothermal Resources Council, Transactions, Vol. 21, 145-149, 1997.

Premuzic, E.T., M.S. Lin, and H. Lian. Geothermal Brines and Sludges: A New Resource, Proceedings of SWEMP 96, Cagliari, Italy, Fourth International Conference, Vol. 2, 1019-1025, 1996.

Bajt, S., S.R. Sutton, and J.S. Delaney. X-ray Microprobe Analysis of Iron Oxidation States in Silicates and Oxides Using X-ray Adsorption Near Edge Structure (XANES), Geochimica & Comochemica Acta Vol. 58 (23), 5209-5214, 1994.

Concurrent Session 5:

Drilling Technology

Wireless Telemetry Tools

Douglas S. Drumheller
Geothermal Research Department
Sandia National Laboratories
(505) 844-8920
dsdrumh@sandia.gov

The routine operations of drilling, completion, and production are essentially done blind. When we drill into the earth to extract hot geothermal fluids, we depend heavily on the art and experience of the operator and very little on hard information. For many years we have had sensors that can measure this information in relatively cool wells, and in recent years with the advances of high-temperature electronics, sensors are becoming available for geothermal applications. However, the real trick is not just to measure these parameters but to get this information from miles underground, where it is measured, back to the surface. In the past, few commercial options have been available to people who really want to know what's going on down there. These options have high costs and severe limitations. A new low-cost alternative will be entering the commercial market soon that will allow communication between the surface and the production zone via sound waves propagating in the production tubing of the well. Development of this tool was jointly sponsored by the Office of Fossil Energy through the Natural Gas and Oil Technology Partnership Program and the Office of Geothermal Technologies through the Sandia Geothermal Technology Program. It is a low-temperature tool primarily designed for telemetry of data in oil and gas wells. Based upon our success with this design and the expanding availability of high-temperature electronics, we are now developing a prototype for telemetry of data in geothermal drilling projects.

The low-temperature wireless telemetry tool has been licensed to Baker Oil Tools for general use in all of their production and completion operations. They envision numerous applications in monitoring environmental parameters in production zones as well as applications to assist in the installation and operation of many different types of downhole equipment. The wireless telemetry tool has no mechanical moving parts and its operation does not require any contact with well fluids. Rather it transmits data up to 15,000 feet by generating acoustic tones in either drillpipe, coiled tubing, or production tubing. These signals are picked up by a sensitive accelerometer strapped to the tubing at the surface. Signal processing allows us to interpret the data even in the presence of rig and pump noise. Our experience also shows that when this tool is deployed only a few thousand feet into the well, its signal is audible above high noise levels, even to the ears of people who are working on the rig floor.

We show the prototype with its cover removed. This exposes, from top to bottom, the transducer element, its tuning coil, the microprocessor-controlled power amplifier, and the battery pack. This tool has the capability to produce more than 10-W of acoustic energy with less than 50-W of electrical energy. Quiescent power between transmissions is negligible. While the tool can

transmit any data you wish to give it, the prototype is configured to transmit measurements of its own acoustic signal strength, several system voltages, and the temperature. It has been successfully fielded several times, and even though it was not designed for drilling, it has successfully drilled out a 70-foot cement plug at the bottom of an 11,000-foot gas well.

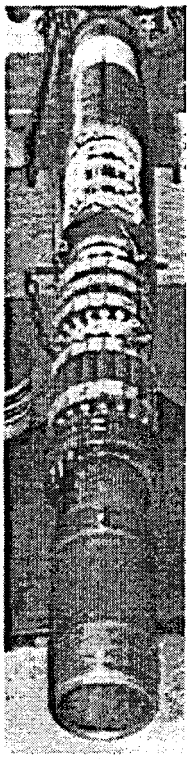

The virtue of the wireless telemetry tool is that it is primarily electronic while being mechanically simple. For example, the only threaded part in the design is the case, which is not shown in the figure. Traditionally, people have held the view that electronics are unreliable. However, in modern consumer electronics, it's not the integrated circuits that wear out, it's the mechanical push buttons. Driven by the aircraft industry over the past few years, manufacturers have developed new high-temperature circuit components. Today the high-temperature circuit components to build this tool are available. We are developing a high-temperature prototype for geothermal drilling. It's operating temperature will be 200 °C, and it will survive 300 °C. Its maximum range will be 10,000 feet, and it will be housed in 4.75-inch drill collar. The prototype will measure fluid pressure and temperature, which can be used to estimate fluid levels in the annulus during production zone drilling with loss of circulation. This will provide a direct indication of the production potential of the well. Field tests are scheduled to begin in 1999.

References

D. S. Drumheller, "Acoustical telemetry in a drill string using inverse distortion and echo suppression", U. S. Patent No. 5,128,901, 1991.

D. S. Drumheller, "Electromechanical transducer for acoustic telemetry system", U. S. Patent No. 5,222,049, 1991.

D. S. Drumheller, "Analog circuit for controlling acoustic transducer arrays", U. S. Patent No. 5,056,067, 1991.

D. S. Drumheller and D. D. Scott, "Digital circuit for echo and noise suppression in a drill string", U. S. Patent No. 5,274,606, 1991.

D. S. Drumheller, "Acoustic transducer", U. S. Patent No. 5,703,836, 1997.

D. S. Drumheller, "Acoustical properties of drill strings", J. Acoustical Society of America, 85:1048--1064, 1989.

D. S. Drumheller, "Attenuation of sound waves in drill strings", J. Acoustical Society of America, 94:2387--2396, 1993.

D. S. Drumheller and S. D. Knudsen, "The propagation of sound waves in drill strings", J. Acoustical Society of America, 97:2116--2125, 1995.

D. S. Drumheller, "Coupled extensional and bending motion in

elastic waveguides", Wave Motion, 17:319--327, 1993.

A. Bedford and D. S. Drumheller, **Introduction to Elastic Wave Propagation**, Wiley, New York, 1994, ISBN 047193884X (1994) and ISBN 0471967009 (1996).

D. S. Drumheller, **Introduction to Wave Propagation in Nonlinear Solids and Fluids**, Cambridge University Press, Cambridge, 1998, ISBN 0521583136 (hard cover) and ISBN 0521587468 (soft cover).

S. D. Knudsen D. S. Drumheller and L. E. Mendez, "Wireless telemetry for well production applications", SPE Journal. In review.

A NEW APPROACH TO DRILL BITS - THE MINI-DISC™ CUTTER BIT

James E. Friant
Excavation Engineering Associates, Inc., Seattle, WA

1.0 INTRODUCTION

In 1908 Howard Hughes patented his unique twin rolling cone drill bit. Each cone, shaped to provide a near true rolling action as the bit rotated, had multiple sharp edges. Even in soft rock formations, Howard's bit made the previous designs of down hole tools, which pounded or scraped at the hole bottom, obsolete virtually overnight. The oil and gas industry grew at a phenomenal rate with much credit going to the roller cone bit.

The Hughes Tool Company and various other upstart manufacturers, continued to develop and improve the roller cone bit. In the early 30's a third cone was added. Improvements in bearings, seals, lubricants and abrasion resistant materials followed, resulting in today's sophisticated tri-cone bit. Much improved to be sure, but still based on Howard's concept.

When the Atomic Energy Commission began drilling deep test holes at the Nevada test site in the early 1960's, the oil drilling industry provided the technology. As shaft size increased, bits grew to as large as 14 ft diameter and the drill rigs grew in proportion. Tapered roller cone cutters, standards of the oil drilling industry, were adapted for big hole drilling as well; mill tooth cones for softer formations and carbide button "strawberry" cutters for harder rock.

Quite independently from the drilling industry, another technology was developing; the single disc rolling cutter. Some turn-of-the-century trials with disc cutters can be found in the tunneling history books, but the real beginnings started in 1956 when James Robbins, placed disc cutters on a small Tunnel Boring Machine (TBM). On a Toronto sewer job, in moderately hard rock, this TBM set the astonishing record of 105 ft of advance in a single day. From then on, The Robbins Company grew to dominate the market. By 1980, every company in the TBM field had all converted to large saddle mounted single disc cutters.

In the early days, there was more art than science in the use of disc cutters. Cutters seemed to work pretty well when they cut in concentric circles spaced at about 3.0 inches. The cutting action was not well understood, and the industry was dominated by small but dedicated companies who had little funding for R&D.

As far as cutters were concerned, the basic observation was made that the harder they were pushed, the deeper they sank into the rock, and the machines penetrated faster. As a result, cutter capacity went from 20,000 lbs on a 12 inch cutter, to 40,000 lbs on a 15.5

inch cutter to 60,000 lbs on a 17 inch cutter and now 75,000 lbs is claimed for 19 and 20 inch cutters. Onward and upward, always increasing in size and weight as larger and larger bearings were needed. What the manufacturers in the "capacity war" did not recognize was that each time performance was enhanced by greater load capacity, the increase in cutter diameter offset a portion of the advantage. By the time cutter diameter reached 19 and 20 inches, the advantage of increased load capacity was almost completely offset by diameter increase.

2.0 TWO TECHNOLOGIES MEET IN BIG HOLE DRILLING

In 1979, as part of the Chicago Tunnel and Reservoir Project (TARP), the plan to drill hundreds of drop shafts to direct storm water into the huge underground water storage caverns was in the hands of contractors. The majority of these shafts were 99 inches diameter, and blasting in the heart of Chicago was forbidden.

The contractors involved were from the heavy construction industry, and had little exposure to big hole drilling. When they went to look at the huge enlarged oil drilling derricks operating at the Nevada site, they realized the impossibility of using this equipment in an urban environment. At many Chicago sites, no more than 1/4 acre was available and some sites would consist of two barges.

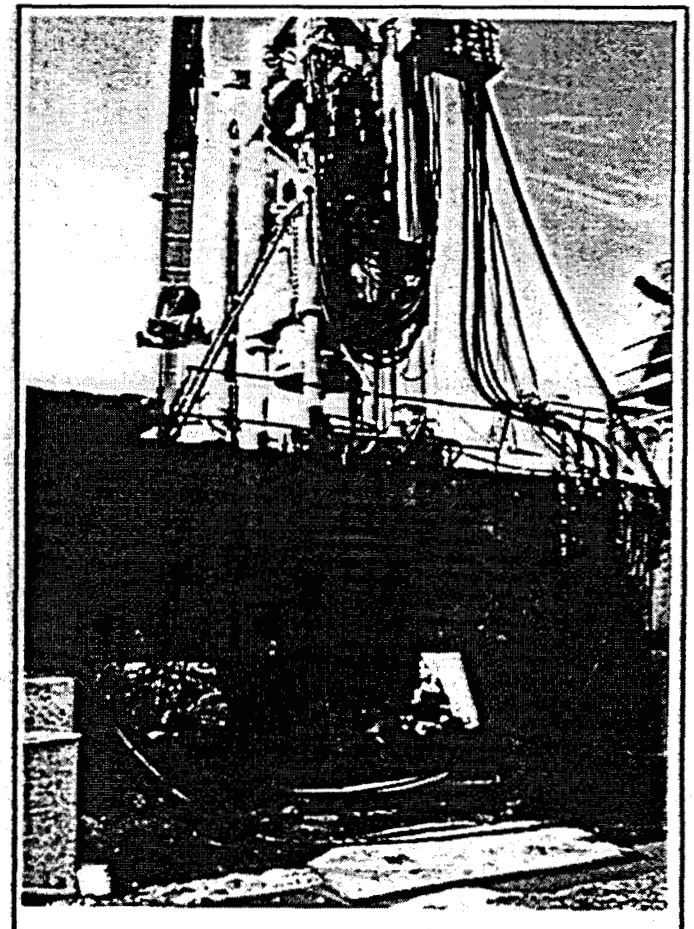

Figure 1
121 BR Drill Rig

Opportunity from Dilemma

From the Chicago problem, the opportunity arose to step away from traditional big hole drilling technology and find alternate ways to operate. The Robbins Company, already involved in the TARP project through building TBMs, and well known to the heavy civil constructors, captured orders to build two powerful hydraulic rigs. These drill rigs were based on compact raise drill design; units specifically designed to operate in cramped

underground mining environments. The largest of the two, the 121BR had a lifting capability of 1.25 M lbs and a torque of 365,000 ft-lbs up to 6 rpm. This rig is shown on site in Chicago in Figure 1.

The rig high torque at low speed and lift capability were designed with disc cutters in mind. Initially the client insisted on using more traditional cutters. These were two-row carbide insert cutters. However, they used standard disc cutter saddle mounts. Progress was slow on the first two shafts, but on the third shaft, the button cutters were replaced with single disc cutters. The performance comparison in hard Limestone is shown below.

	RPM	Torque	WOB	Penetration
Insert bit	6	300,000 ft-lbs	300,000 lbs	1.5 ft/hr
Disc bit	6	150,000 ft-lbs	250,000 lbs	3.0 ft/hr

The next hundred shafts were drilled with disc equipped cutterheads. The best performance in the first series was 7 ft/hr with the best shaft averaging 4.14 ft/hr. A typical Chicago 99 inch disc drill "bit" is shown in Figure 2.

Not long after this experience, Zeni Drilling Company, Morgantown WV, broke from tradition and tried a disc equipped cutterhead. This company and an off shoot company, North American Drillers, now use disc cutters exclusively and dominate the mine shaft drilling business. Don Zeni once summed up the reason for using discs with traditional directness, *"One, they go fast, and two, they're cheap".*

Figures 3 and 4 show the contrast between a roller cone big hole bit and a Zeni disc head.

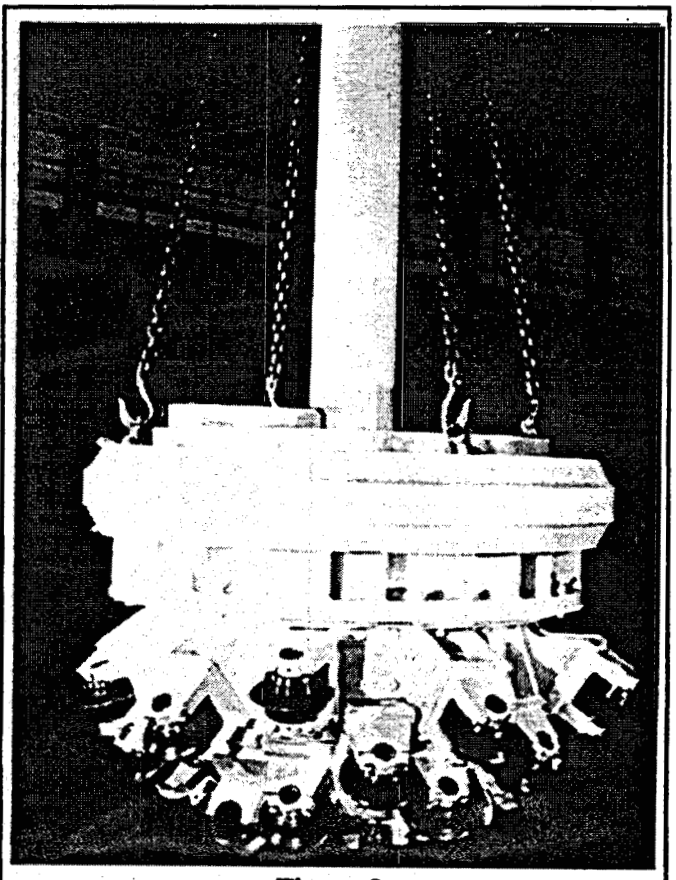

Figure 2
99 Inch Drill Bit

3.0 THE SCIENCE OF DISC CUTTERS

Scientific analysis of rock excavation physics was undertaken in 1975 at the Colorado School of Mines Laboratory and continues today. This well equipped laboratory has machinery which utilizes full scale cutters, drill bits and even small TBM cutterheads. By recording rock characteristics, cutter types, dimensions and operating parameters, patterns were observed. Eventually a computer model was created describing the disc cutter function. To achieve the lowest specific energy of excavation, the objective is to form the highest proportion of rock chips and pieces and the minimum of sand and powder. This concept is illustrated by the curve of Energy vs. Particle Size shown in Figure 5.

The reason for the high performance of the disc cutter in rock excavation then became obvious; they

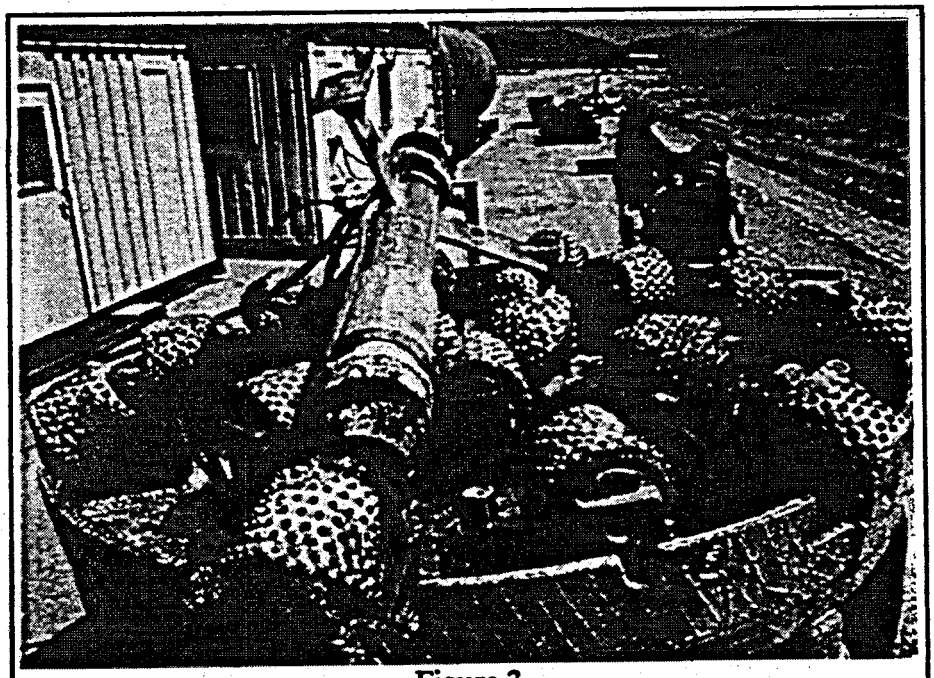

Figure 3
A Roller Cone Big Hole Bit

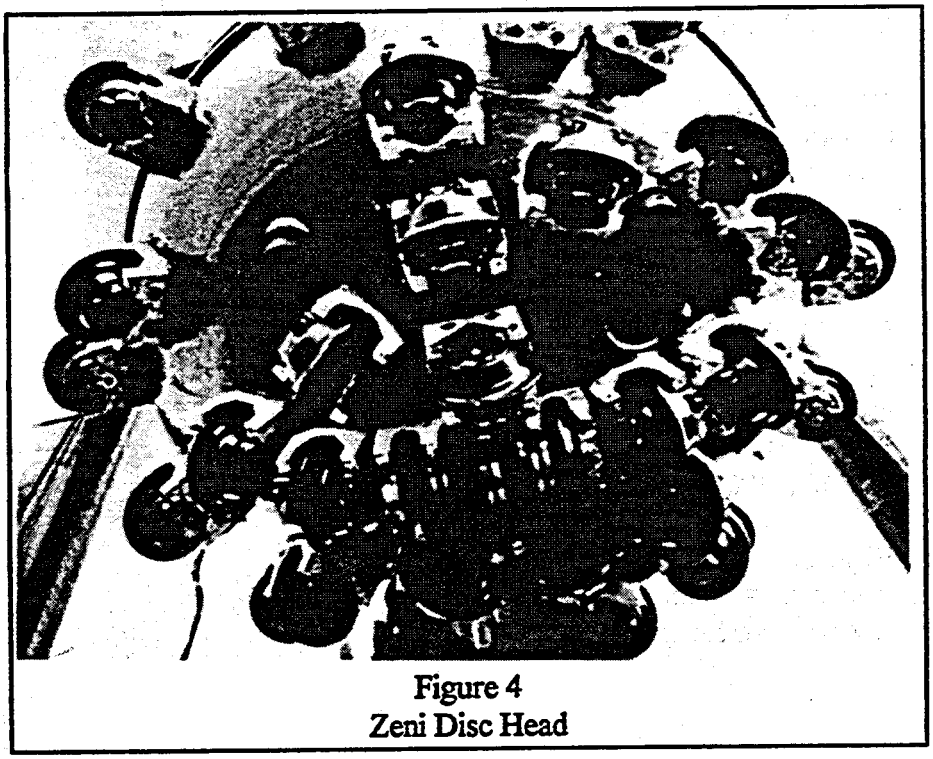

Figure 4
Zeni Disc Head

produce larger average particle sizes than other cutter types. For a given amount of power available, they will excavate more rock volume.

4.0 THE CONCEPT OF MINI-DISC™ CUTTERS

The incentive for designing a small disc cutter started by using the predictive computer program. This showed that the two most effective ways of improving performance, which could be controlled by the designer, were cutter diameter and blade width.

Until recently, the smallest production single discs were 15.5 and 14 inches diameter, while the smallest special order discs were 12 inches. But even the 12 inch cutters, with their large saddle mounts occupy too much cutterhead "real estate" to use effectively on small diameter cutterheads.

To take advantage of the disc type cutter on small cutterheads and drill bits, much smaller cutter diameters were needed and much less space had to be taken up with the mounting structure. Plus the cutter needed a rugged structure to absorb the tremendous punishment of rock excavation.

To solve the "real estate" problem, cantilever mounted cutters were a must. With cantilever cutters, cutter kerfs can be close or far apart as desired, and can be positioned on the head wherever needed to minimize out-of-balance forces. To provide a rugged cutter design, the center shaft with respect to the cutter diameter had to be large. Traditional double row tapered bearings were not satisfactory because their radial

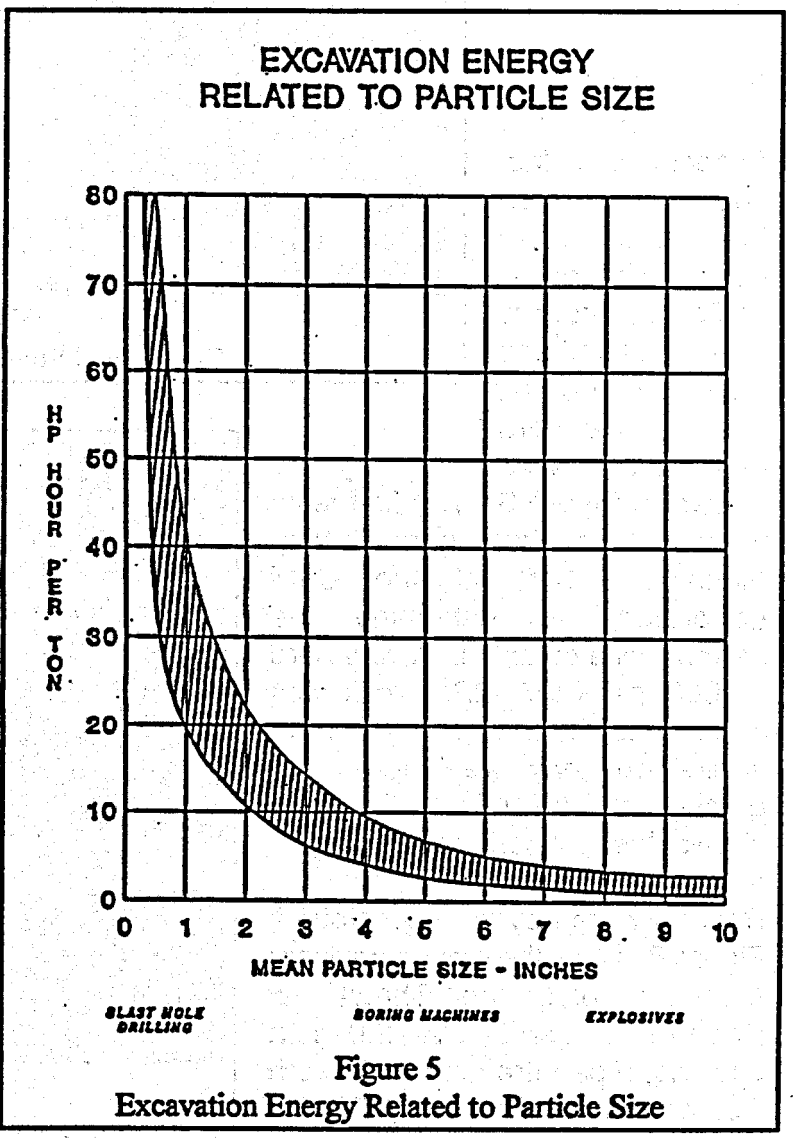

Figure 5
Excavation Energy Related to Particle Size

dimensions are large compared with the load they can carry. Either shaft size or cutter blade size would be compromised. A new approach to bearing structure was taken.

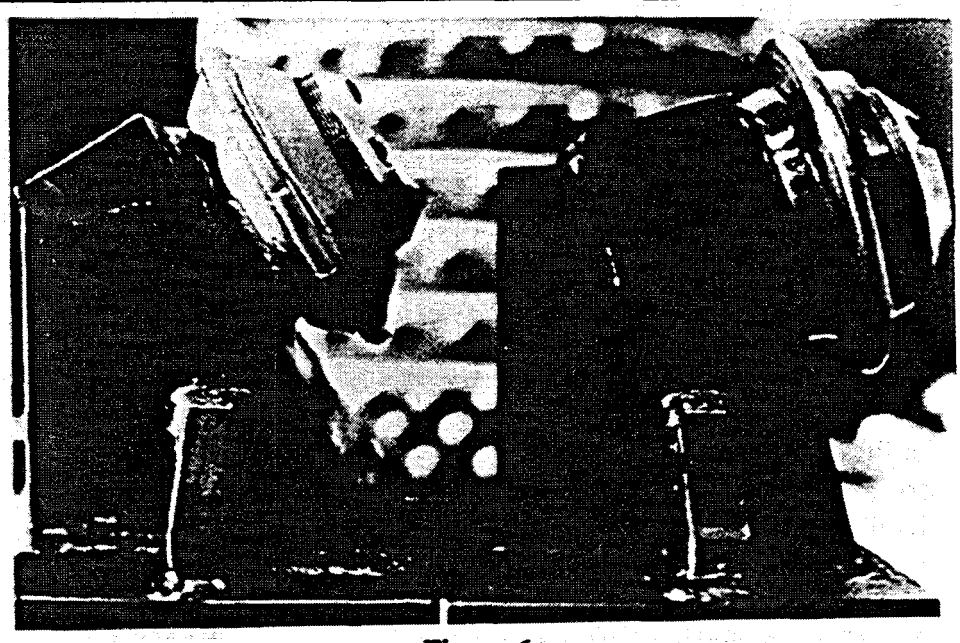

Figure 6
Carbide and Steel, 5 Inch Disc Cutters

Excavation Engineering Associates, Inc. decided to take on the small disc design challenge. Prototype cutters were designed and built in both an all steel and a hard metal insert version. They are shown in Figure 6. The first tests were run on the Linear Cutting Machine (LCM) at the CSM Laboratory to determine the performance potential. A very hard 43,000 psi (297 MPa) rock was chosen as the first test sample to shake out any weaknesses as quickly as possible. Figure 7 shows this test series underway.

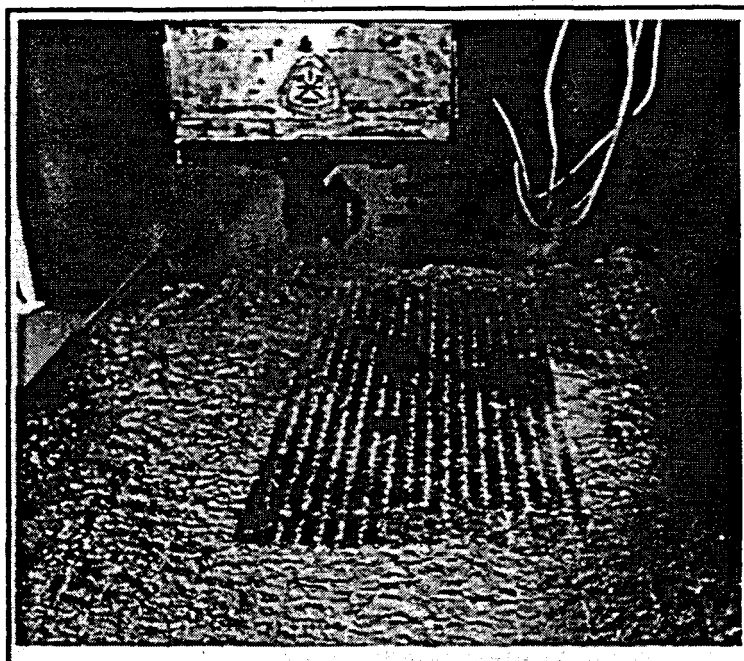

Figure 7
Linear Cutter Fixture, 5 Inch Disc Cutter

Results were beyond expectation. Figure 8 shows the most significant summary plot, the Thrust vs. Penetration curve. At 2.0 inch spacing, a penetration of .125 inch was achieved with only 11,700 lbs of thrust. To put this achievement into perspective, a standard 17 inch TBM cutter requires over 60,000 lbs to achieve this penetration in the same rock.

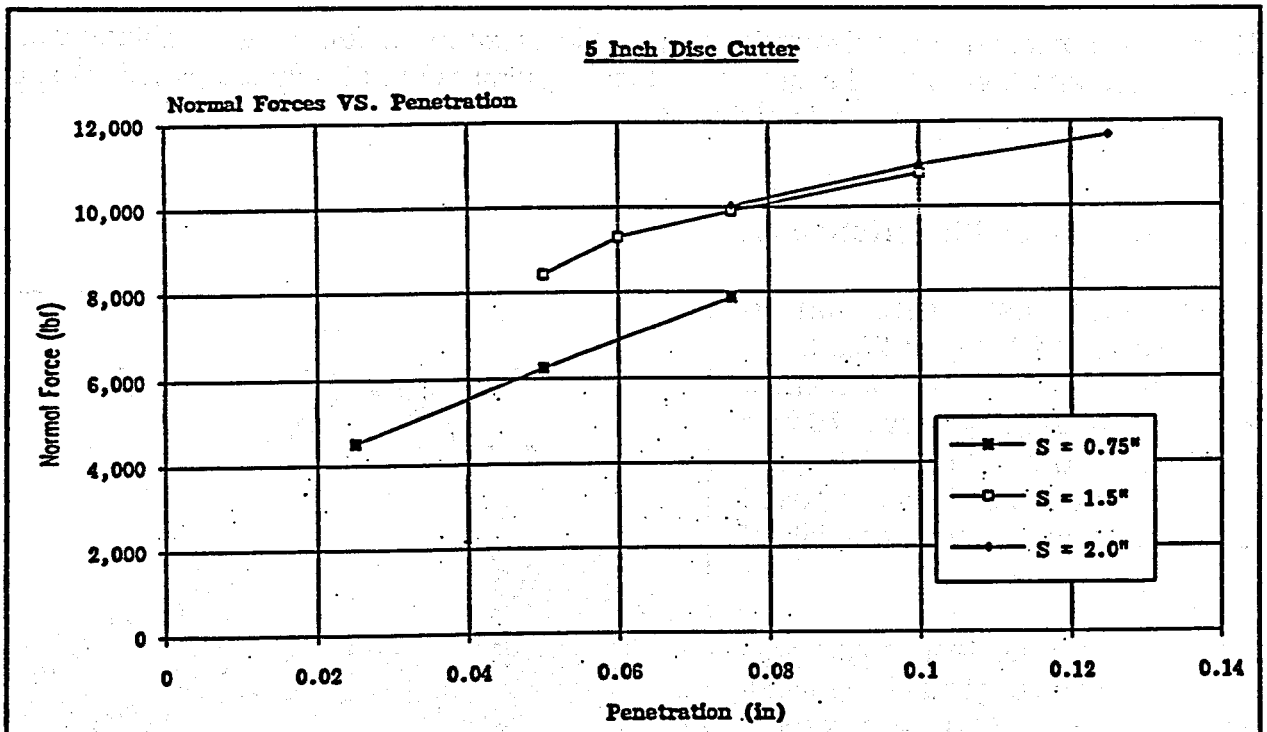

Figure 8
Linear Cutting Test Results, 43,000 psi Rock Sample

Also, the specific energy measured at 2.0 inch spacing was only 6.9 to 8.5 hp-hr/ton. This was far superior to the best multi-row or button type cutters tested. To gage these results, compare these figures to field tests of a 9 3/4 carbide insert roller cone drill bit which required 80 hp-hr/ton in aged concrete and 120 hp-hr/ton in Basalt.

The cutters were extensively tested, two carbide designs, four all steel designs of different sizes, various angles and in at least four different rock types. Full scale tests were run on a 32 inch diameter cutterhead. Undoubtedly, one of the most thorough series of tests conducted by CSM's Laboratory.

5.0 MINI-DISC™ DRILL BITS

The first drill bit experiments utilized a 5.0 inch Mini-disc™ cutter because a great deal of backlog data was available; data from the LCM tests and from a 32 inch cutterhead. A 13 1/8 inch bit diameter for the first tests was selected using six each, 5.0 inch Mini-discs™ Figure 9 is a photograph of the bit.

The cutter profile was set up such that the widest spacing between any two cutters was 1.5 inches. The azimuth of each cutter was established by a computer balance program.

Using the computer three-dimensional dynamic balance model, cutter positions were exchanged and then moved slightly to achieve minimum out-of-balance (whirling) and, minimum moment about the axis of the bit.

5.1 13 1/8 Inch Bit Performance

Performance tests were run in 10,000 psi Limestone and 25,000 psi Welded Tuff. A maximum penetration rate of just over 70 ft/hr was achieved with both rock types. This appeared to be a limit imposed by the cuttings removal capability of the bit.

Obvious from the test results was the significance of good bit cleaning. At a constant 7,500 ft-lbs torque, penetration rate increased from 28 to 72 ft/hr when water flushing was used. And at a constant 55,000 lbs of thrust, penetration rate increased from 37 to 72 ft/hr when water flushing was employed.

Specific energy of excavation achieved was 15 to 19 hp-hr/ton. As mentioned earlier, this compares with the 80 to 120 hp-hr/ton experienced with standard carbide tri-cone bits.

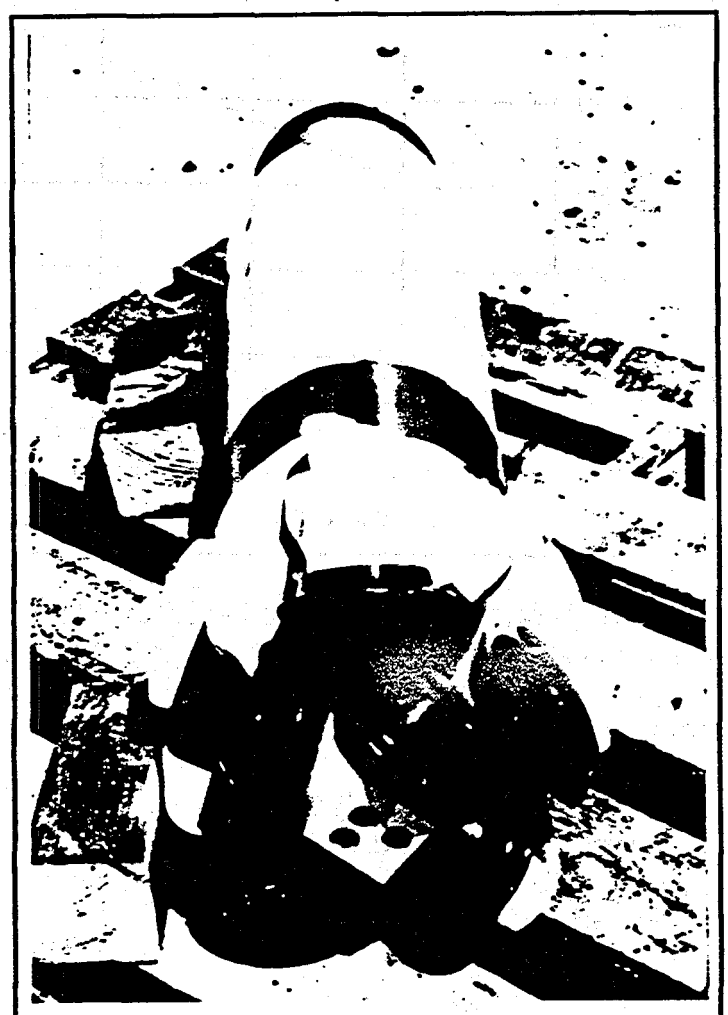

Figure 9
13 1/8 Inch Diameter Drill Bit

5.2 The 7 7/8 Inch Mini-Disc™ Bit Performance

The 7 7/8 inch bit configuration was established as using five each, 3.25 inch diameter disc cutters. Maximum spacing between cutter kerfs was only 0.9 inches. Unlike the 13 1/8 inch bit, outside cutters for this bit were bolted onto the perimeter of the bit, using wedge shaped pedestals fitting into tapered slots. This configuration was chosen for ease of assembly and because more open space around the bit was available for the cuttings to escape. Only the center cutter pedestal was permanently welded in place. The bit body

was equipped with a 4 1/2 inch "standard" API thread. Fluid passages were drilled into the bit body to direct water or mud to the face.

Two 7 7/8 inch drill bits were built; the first was used for atmospheric testing at the CSM Laboratory. The second bit was equipped with high pressure passages and jetting nozzles and used for tests in a pressurized chamber with Bentonite and silica sand mud as the circulation fluid. The 7 7/8 inch bit is shown in Figure 10.

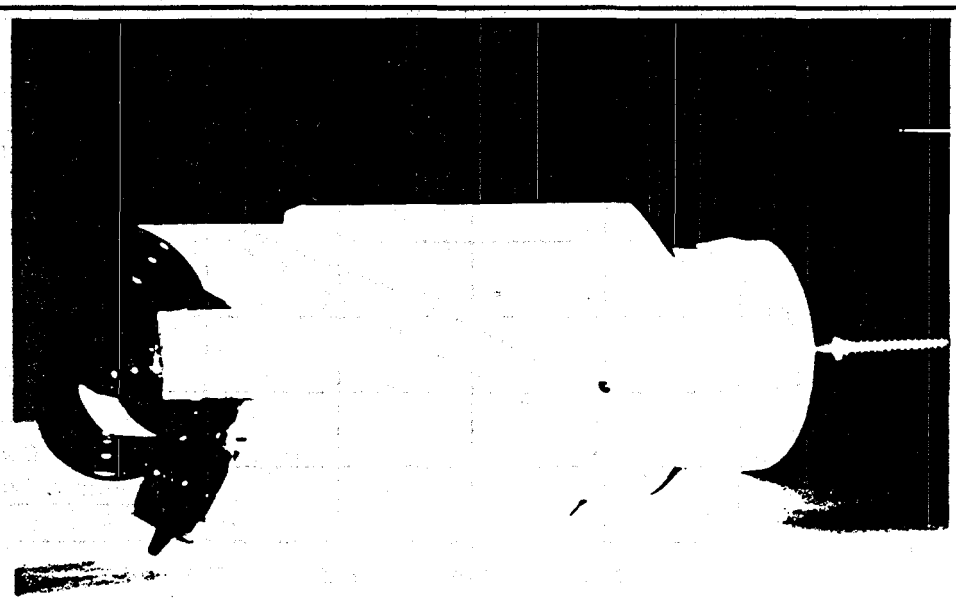

Figure 10
7 7/8 Inch Drill Bit

In the CSM Laboratory, penetration rates of up to 126 ft/hr were obtained with 32,000 lbs thrust. Pressure was atmospheric water flushing was used at a rate of about 30 gpm, and rotary speed was 57-60 rpm. Torque required was only 2,500 ft-lbs. Interestingly, there was little performance difference between the 10,000 psi Indiana Limestone and the 25,000 Welded Tuff. The top penetration rate in either rock, however, was probably governed by the geometry of the cutter. Since at maximum penetration rate, the cutter was indenting the rock about 0.4 inches, the cutter was literally rolling on the hub. Under these circumstances, further increases in penetration rate could be obtained by increasing rpm, but not by additional bit weight.

Figure 11 shows the test results in terms of WOB vs Penetration Rate and Torque vs Penetration Rate.

5.3 7 7/8 Inch Bit Testing at Simulated Depth

The second bit was equipped with flow passages and nozzles to permit a mud flow rate of about 260 gpm at a nozzle pressure drop of 570 psi. This unit was tested in a test rig that includes a chamber that can be pressurized to about 3,000 psi. Samples of Welded

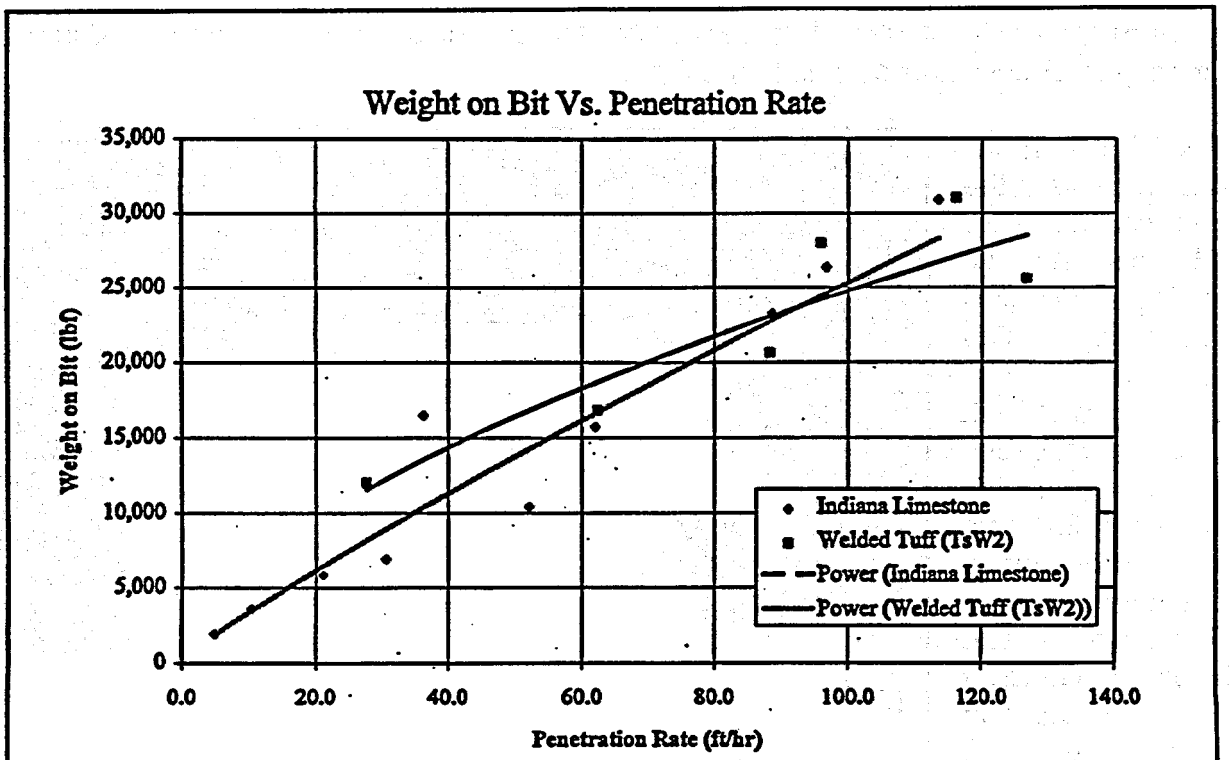

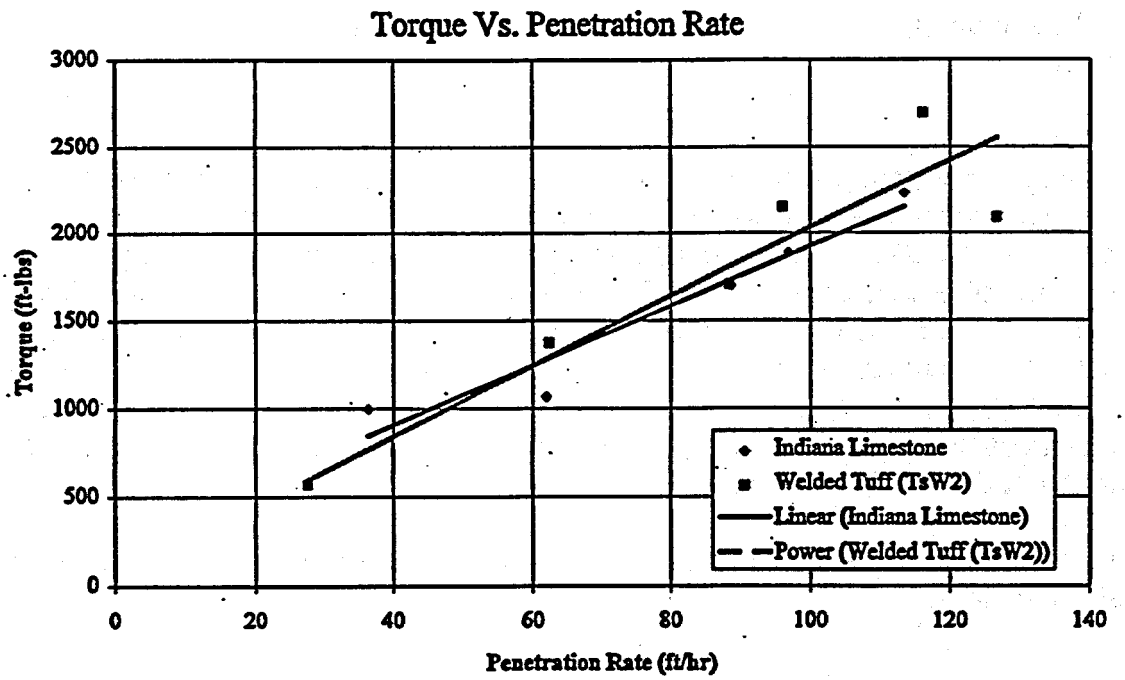

Figure 11
7 7/8 Inch Bit Performance - Atmospheric Pressure

Tuff and Indiana Limestone were used so direct comparisons could be made with the previous atmospheric tests.

A great deal of data was obtained, including a comparative run in the Limestone with a standard tri-cone bit.

To make sense of the data, in which every parameter was a variable, multiple regression analyses were conducted. Logarithmic regression curves showed the closest correlation to actual data. Correlation was between 91 and 94%.

Figure 12a shows the fall-off in performance with pressure in Welded Tuff. While dramatic degradation was observed with the Disc-bit, a standard tri-cone bit was adversely affected as well. In fact, under similar conditions and at the highest pressure tested, the Disc-bit still drilled about 20% faster than the standard bit. Figure 12b shows ROP vs WOB.

This data also illustrates the importance of increasing WOB as pressure (depth) increases. 20,000 lbs WOB at atmospheric produced 65 ft/hr, 20,000 lbs WOB at depth produced only 5 ft/hr. Increasing WOB from 20,000 lbs to 30,000 lbs virtually doubled penetration rate.

17 1/2 INCH MINI-DISC™ DRILL BIT

The 17 1/2 inch drill bit is one of the more common bit sizes for the top section of oil and gas wells, for pilot holes and for geothermal drilling. In these applications, hard rock is often encountered causing short life for all types of drag or fixed tool type drill bits.

For the initial tests, the 17 1/2 inch bit was drilled with two alternate water or mud circulation schemes. Figure 13 shows the bit and looking closely, both fluid injection systems can be seen. The brass fittings on the individual pedestals are the high pressure jets, aimed at the tracks of the center five cutters. The large hole at the center of the bit is the port for low pressure circulation.

With conventional bits, large amounts of "Hydraulic Horsepower" are consumed with high pressure jets. These help to scrub the cuttings off the rock face. With disc cutters, however, the rock breaking mechanism is actually a tensile failure and chips literally fly off the face. Thus the jetting action needed for standard bits may be redundant for a Disc-bit. Test constants were water circulation at 280 gpm and rotation speed as close to 50 rpm as possible.

Figures 14 and 15 show the test results in terms of Advance vs WOB and Advance vs Torque, respectively.

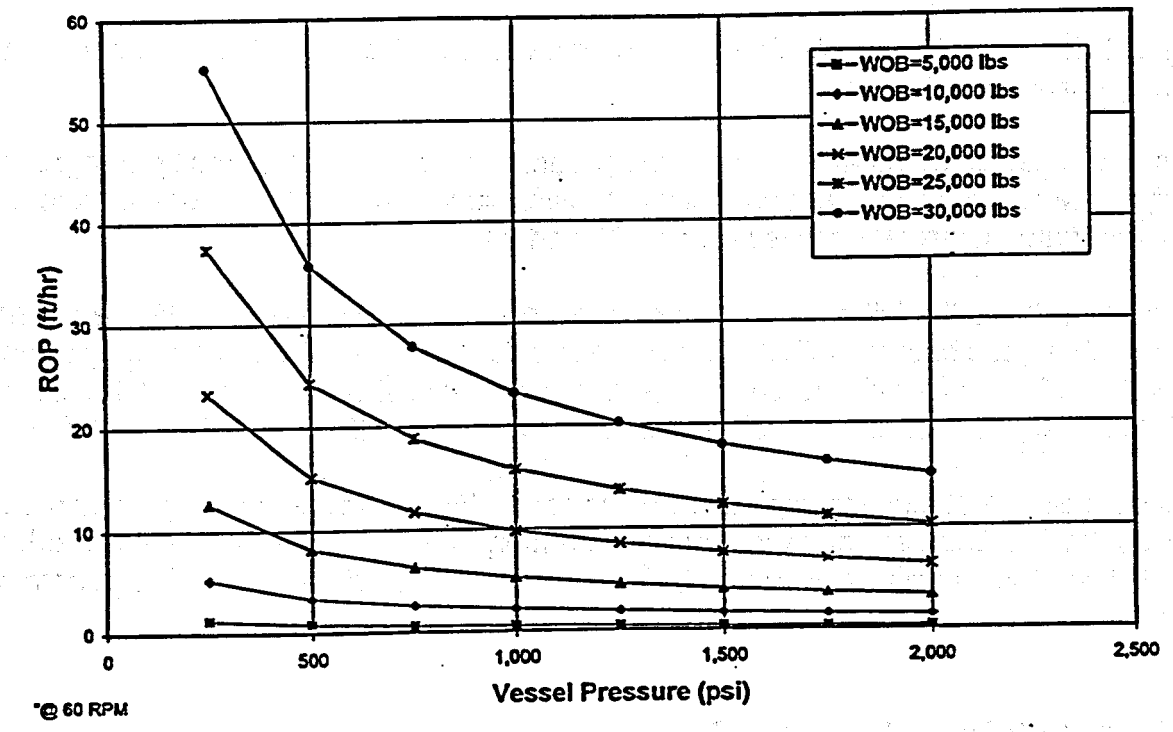

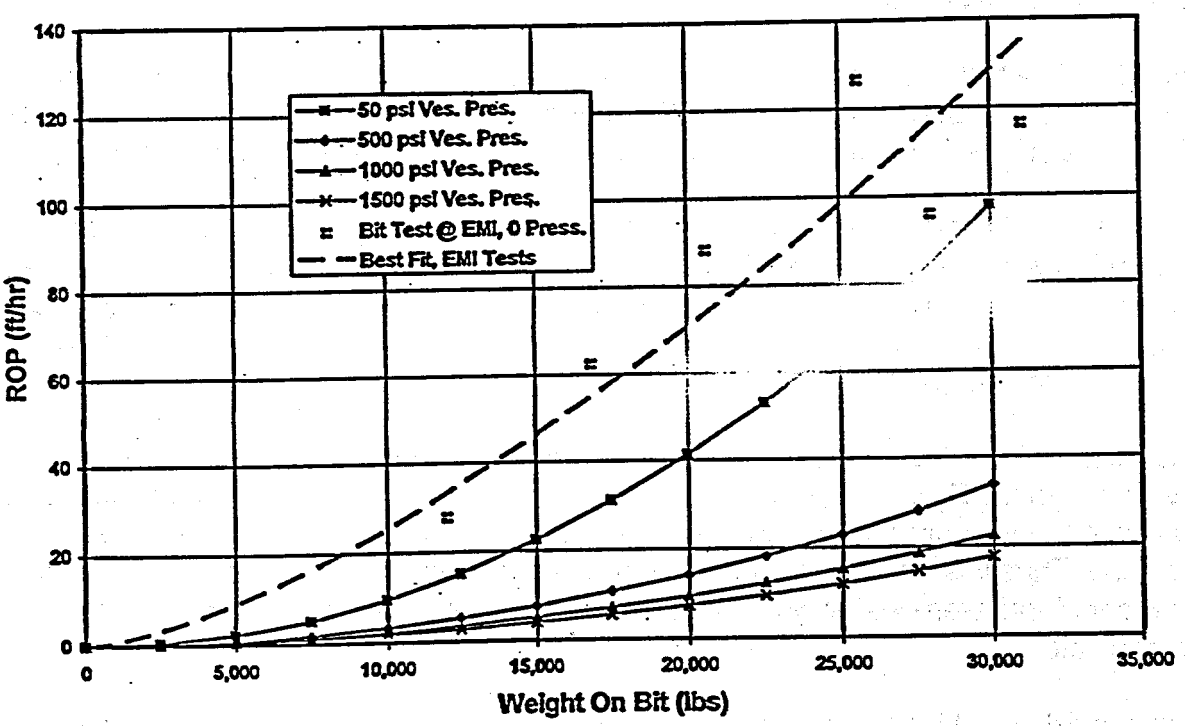

Figure 12
Bit Performance Under Mud Pressure in Welded Tuff

a. A maximum penetration rate of 326 ft/hr was attained at 52,540 lbs of thrust.

b. Multiple jets at 2,100 psi and a single centered, low pressure inlet produced identical performance; example 250 ft/hr at 45,500 lbs thrust. Torque was also essentially identical at 7,250 ft-lbs.

By virtue of the above, the design, placement of cutters and balance of the bit were validated.

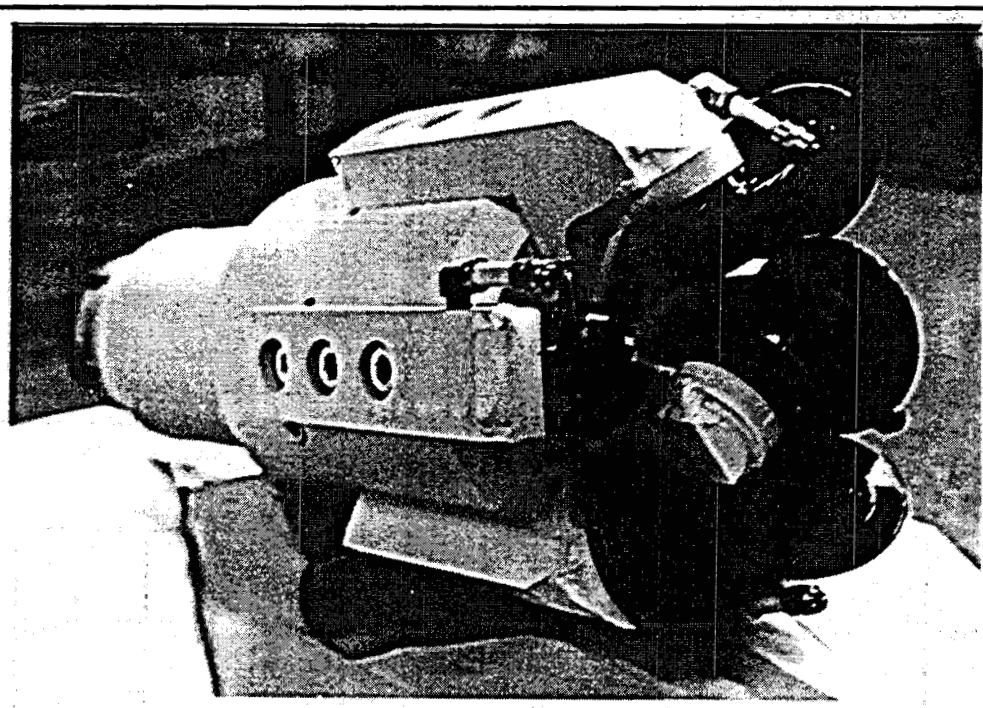

Figure 13
17 1/2 Inch Mini-disc™ Drill Bit

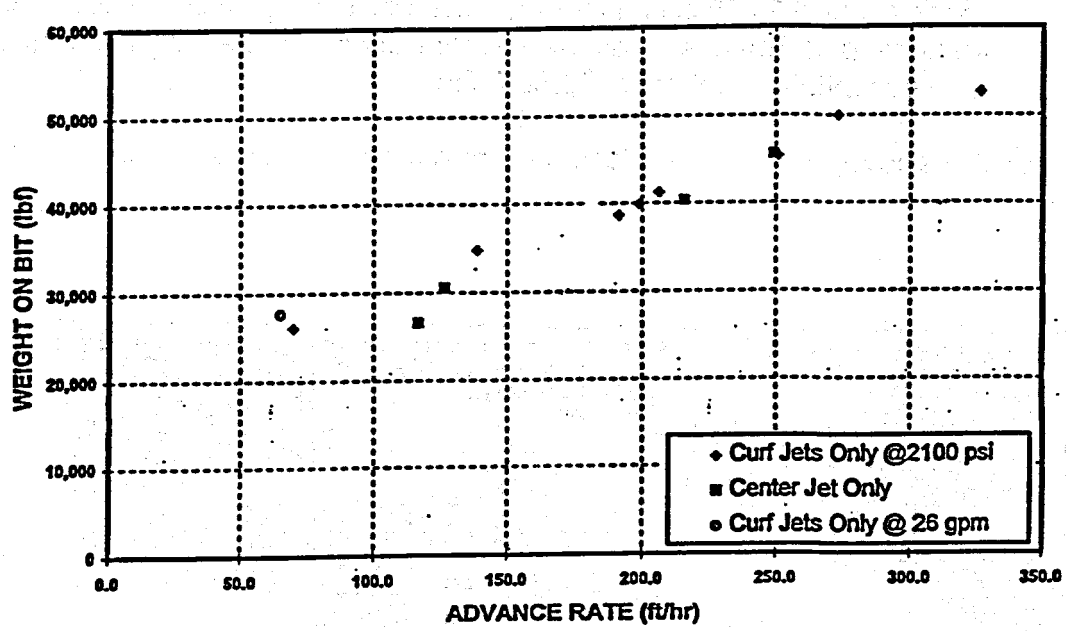

Figure 14
Weight on Bit (thrust) vs Penetration Rate

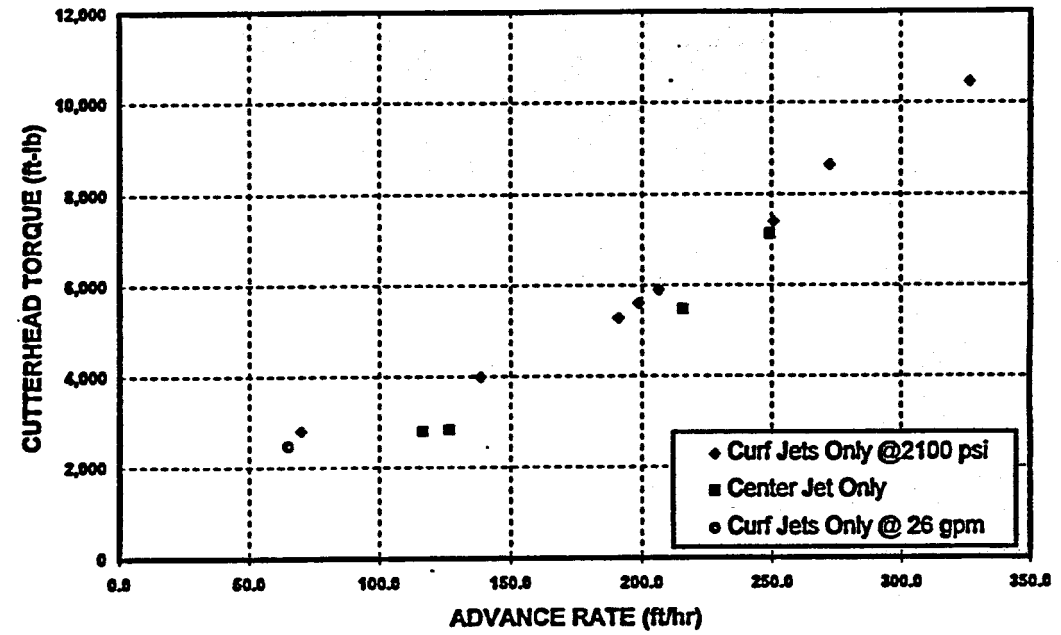

Figure 15
Torque vs Penetration Rate

FUTURE OF THE MINI-DISC™ BIT

At this point, the developers feel there is little left to discover by laboratory testing and simulation. It is probably one of the most tested products of its type, prior to release for field use. Structure, bearing, seal, lubrication. Life and performance have all been pushed to their limits in the laboratory. As this article is written, the first bits for use in the field have been shipped. We trust our extensive development work will be justified.

FOOT NOTES:

The author, James E. Friant, is President of Excavation Engineering Associates, Inc., of Seattle, Washington. He can be contacted by phone 206 248-7388, FAX 206 244-7994, or E-mail: FRIANTJIM@aol.com. Mr. Friant is also a Research Professor at Colorado School of Mines where much of the test work was done with the able support of Dr. Ozdemir and his capable staff. Mr. Friant has been active in the field of mechanical excavation for more than 30 years.

The Mini-disc™ cutters, and certain features of the drill bits and cutterheads described here are protected under U. S. And foreign patents. Mini-disc™ is a registered trade name.

The 7 7/8 inch bit testing described here was sponsored by, and is presented through the courtesy of the Gas Research Institute, Chicago, IL.

The 17 1/2 inch bit testing described here was sponsored by and is presented through the courtesy of the NADET Institute of MIT, Boston, MA.

Concurrent Session 6:

Direct Use and Geothermal Heat Pump Technology

DIRECT-USE PROJECTS AT THE GEO-HEAT CENTER

Dr. John W. Lund, P.E.
Geo-Heat Center
Oregon Institute of Technology
Klamath Falls, OR 97601

ABSTRACT

The Geo-Heat Center staff provides technical assistance to those actively involved in geothermal projects, conducts direct-heat applied research and distributes information by means of technical report, papers at conferences and through the Internet. The technical assistance program provided responses to 761 requests in 1997, a 30% increase over 1996. Recent research reports completed by Center staff include: "A Comprehensive Geothermal Greenhouse Developer Package" and "Well Pumping in Commercial Groundwater Heat Pump Systems." The staff have also completed the revision of the Geothermal Direct-Use Engineering and Design Guidebook and have participated in writing a manual on "Ground-Source Heat Pumps - Design of Geothermal Systems for Commercial and Institutional Buildings," a newsletter "Outside the Loop" written for geothermal heat pump designers and installers, and the Quarterly Bulletin with recent issues devoted to geothermal use in South Dakota and equipment. Future work include research on "Model Construction Specifications for Geothermal Wells and Well Equipment" and "A Comprehensive Aquaculture Developer's Package."

BACKGROUND AND STATUS

The Geo-Heat Center, established in 1975 at Oregon Institute of Technology, conducts research, provides technical assistance and distributes general information on a wide range of applications in the area of geothermal energy. This program, the only one of its kind in the nation, provides rapid response, unbiased information to designers, developers and owners of systems ranging from geothermal heat pumps, through direct use, to small-scale power generation projects.

The main thrusts of the Center are to conduct direct-heat applied research and development, and to provide assistance to stimulate utilization of the nation's large low-to-moderate temperature (<20° to 150°C) geothermal resource base. Research and development tasks are conceived carefully to address current industry needs in the areas of cost containment, equipment performance and application, and system design.

The technical assistance program, designed to augment, not compete with private engineering firms and developers, offers technical support for system design, equipment selection and troubleshooting for geothermal systems. This program places the unique technical expertise of the Center's staff at the disposal of potential developers and designers around the country.

A major obstacle to wider use of geothermal energy is lack of awareness. The Center's outreach program addresses this issue with a variety of information sources. Through the publication of a Quarterly Bulletin (2,000 subscribers), handbooks, software, Internet website (http://www.oit.edu/~geoheat), a dedicated geothermal technical library (5,300

volumes), and many professional papers and technical reports, a broad spectrum of information is available to the public. Staff activity with professional groups such as GRC, IGA, and ASHRAE greatly enhances technology transfer efforts.

TECHNICAL ASSISTANCE PROGRAM

The Geo-Heat Center staff provides assistance to those actively involved in geothermal development. Geothermal projects are allocated a limited number of man-hours (usually eight hours per project unless prior approval for additional hours are received from USDOE) for analysis. Engineering and economic assistance has been provided to a broad range of clients, from the homeowner interested in geothermal space heating and municipalities engaged in geothermal district heating projects, to industrial concerns adapting geothermal resources to meet their process energy needs. With the advent of the Internet, we also get many requests from grade school, junior high and high school students to assist them in writing papers, preparing for debates and building projects associated with geothermal energy.

A summary of activity for the 1997 calendar year as compared to previous years is as follows: in 1997 we had a total of 761 requests for information or assistance as compared with 583 for 1996, 350 for 1995, 331 for 1994 and 348 for 1993. These requests have doubled since we went online with our website in February of 1996. We went from an average of 86 requests per quarter up through the first quarter of 1996 to 178 per quarter after that time. About half of the current requests and responses are now done by e-mail and approximately 15% are of international origin.

A breakdown of requests relative to applications for 1997 calendar years are geothermal heat pumps (30%), general (22%), resource/wells (12%), space heating/cooling (7%), equipment (7%), greenhouses (5%), aquaculture (4%), district heating (4%), electric power (4%), resorts/spas (3%), industrial (2%) and snow melt (<1%). A comparison of the activities between 1996 and 1997 is shown in Figures 1 and 2.

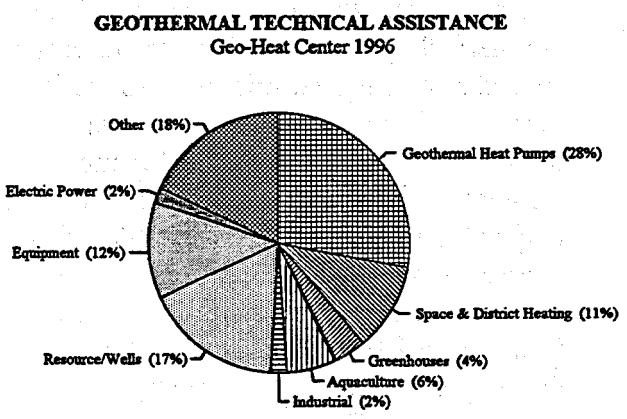

Figure 1. Geothermal technical assistance 1996.

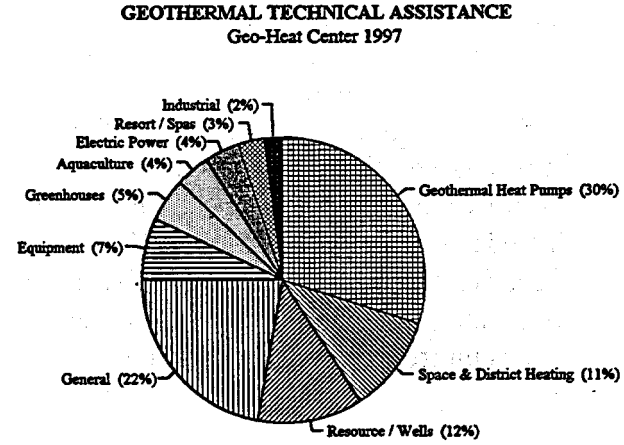

Figure 2. Geothermal technical assistance 1997.

RECENT RESEARCH PROJECTS

A Comprehensive Geothermal Greenhouse Developer Package (Rafferty and Boyd, 1997)

The package of information is intended to provide background information for developers of geothermal greenhouses. The material is divided into seven sections covering such issues as crop culture and prices, operating costs for greenhouses, heating system design, vendors and a list of other sources of information.

Section 1 - Crop Market Prices contains recent wholesale price information for some typical vegetable and flower crops grown in greenhouses. Both national and regional prices are included along with an indication of seasonal variations for some crops. Sources for current price information are provided at the end of the section. An example of season average prices for four common greenhouse vegetables are as follows:

	Season Average Price $/cwt			
Vegetable	1992	1993	1994	1995
Tomatoes	35.80	31.70	27.50	26.00
Bell Peppers	26.80	30.20	29.60	31.10
Head Lettuce	12.50	16.00	13.30	23.10
Cucumbers	19.10	18.00	16.00	16.70

Section 2 - Greenhouse Operating Costs outlines ranges of costs for a typical operation such as labor, utilities, plant stock and mortgage components. Cost ranges for structure construction are also provided. The total greenhouse costs (including greenhouse and operating equipment) range from $11.34 to $14.24/ft^2 of greenhouse, with an average price of $12.65ft^2. The construction costs alone were in the $7.30 to $8.05/ft^2 range with an average of $7.44/ft^2.

Section 3 - Crop Culture Information provides abbreviated culture information for some typical vegetables and flower crops. Such issues as temperature requirements, CO_2, lighting and disease issues are covered. For each species, an extensive list of additional information sources are provided. Detailed information is provided on tomatoes, cucumbers, hydroponic lettuce, carnations and roses.

Section 4 - Greenhouse Heating Systems consists of recently updated *Chapter 15 - Greenhouses* from the Geothermal Direct-Use Engineering and Design Guidebook. It covers the design and performance of various heating equipment commonly used in geothermal greenhouses. The topic of peaking with conventional fuel is also covered. Construction material of glass, plastic film and fiberglass are discussed and heating systems using finned pipe, standard unit heaters, low-temperature unit heaters, fan coil units, soil heating and bare tube are also covered in detail using sample design calculations.

Section 5 - Greenhouse Heating Equipment Selection Spreadsheet is the supporting information and documentation for a spreadsheet based on Section 4. Included are: screens covering the selection and cost of six types of geothermal greenhouse heating systems. This material is intended for use by engineers and those very familiar with the design of heating systems.

Section 6 - Vendor Information provides a list of vendors for components of geothermal systems, and greenhouse structures and equipment. These include the name and address for greenhouse supplies, hydroponic systems, greenhouse manufacturers and suppliers, plant materials--seeds and plants, well pumps, variable-speed drives, plate heat exchangers, piping and space heating equipment.

Section 7 - Other Information Services provides an extensive list of sources for information on greenhouse operation including state extension agencies, and USDA state offices.

Well Pumping in Commercial Groundwater Heat Pump Systems (Rafferty, 1997)

Key to efficient well pumping design is the consideration of three major power consuming components of commercial groundwater heat pump systems: well pump, heat pumps and building loop pump. Careful consideration of the interaction between these components and their impact upon system performance is necessary in order to minimize operating costs for the building owner.

The research considered well pump head analysis, well pump power requirements, optimum water flow requirements for the loop pump and comparison of ground-coupled heat pump system performance.

Well pump head in a groundwater heat pump (GWHP) application consists of three major components: lift, surface requirements and injection head. The vertical distance between the pumping level and the ground surface constitutes the "lift" portion of the well pump head. Surface head loss includes the losses in piping, the isolation heat exchanger and associated fittings and accessories. The report discusses the use of injection for disposal and how to calculate the injection pressure. If the water level remains below ground level at design flow conditions, there is no additional well pump head associated with injection.

Well pump power requirement is a function of flow, head and efficiency. Based on an overall well pump (and motor) efficiency of 60%, well pump power consumption varies from <50 W/ton (@ 1 gpm/ton and 100 ft head) to nearly 375 W/ton (@ 3 gpm/ton and 400 ft head)--[14 W/kW (@ 1 L/min/kW and 30 m head) to nearly 107 W/kW (@ 3 L/min/kW and 120 m head)].

Avoidance of excessive well pump power lies in a design procedure which rests upon total system performance rather than simply heat pump unit performance.

Optimum system performance is obtained when the power consumption of the well pump, loop pump and heat pumps is minimized through careful design. At a given loop flow rate, heat pump performance is largely a function of loop water temperature. In most GWHP applications, the groundwater flow will be less than the building loop flow for optimum design. Information on total system performance for three water temperatures (50, 60 and 70°F)(10, 16 and 21°C) at various well pump heads and flows were developed to show the designer that he has some latitude in loop flow selection. Figure 3 shows example curves for cooling duty with 60°F (16°C) groundwater.

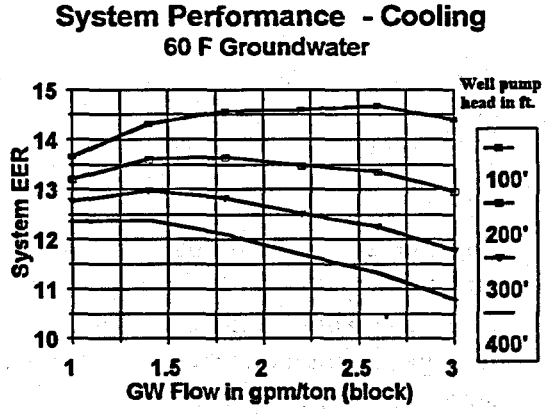

Figure 3. Well pump requirements as a function of flow and pump head.

Properly designed groundwater heat pump systems are characterized by peak load

performance comparable to, or in some cases superior to, ground-coupled systems. To achieve this performance, it is necessary to select the groundwater flow with total system performance in mind. In addition, the flow should be based upon peak block load and not installed capacity.

RECENT PUBLICATIONS

Guidebook

"Geothermal Direct-Use Engineering and Design Guidebook" - 3rd edition (Lund, Lienau and Lunis, editors, 1998). This is an update of the popular direct-use guidebook, last published in 1991. All of the 19 chapters have been revised based on technical assistance experience at the Geo-Heat Center and reflecting current trends in the industry. The 470-page book covers material on Lessons Learned, Nature of Geothermal Resources, Exploration for Direct-Heat Resources, Geothermal Fluid Sampling Techniques, Drilling and Well Construction, Well Testing and Reservoir Evaluation, Materials Selection Guidelines, Well Pumps, Piping, Heat Exchangers, Space Heating Equipment, Absorption Refrigeration, Greenhouses, Aquaculture, Industrial Applications, Engineering Cost Analysis, Regulatory and Commercial Aspects, and Environmental Consideration. The Guidebook, with contributions for 14 authors, is mainly written for designers and engineers involved in direct-use projects. The Guidebook can be ordered from the Geo-Heat Center.

Geothermal Heat Pumps

"Ground-Source Heat Pumps - Design of Geothermal Systems for Commercial and Institutional Buildings" (Kavanaugh and Rafferty, 1998). This 167-page monograph, co-authored by Kevin Rafferty of the Geo-Heat Center, includes an Introduction, and topics on Heat Pump Units, Vertical Ground Heat Exchanger Design, Design of Ground Heat Exchangers, Pumps and Piping, Groundwater Heat Pumps, Surface Water Heat Pumps, and Economics of GSHP Systems. The other author, Stephen Kavanaugh is at the University of Alabama. The publication is available from ASHRAE.

Outside the Loop Newsletter

Volume 1, Number 1 of a newsletter, "Outside the Loop," written for the geothermal heat pump designers and installers, was issued in January 1998. This 8-page newsletter, written by Kevin Rafferty and Stephen Kavanaugh, is available free of charge from either the Geo-Heat Center or the University of Alabama. The primary purpose of this publication is to assist engineers in finding the tools and information needed to design larger ground-source heat pump (GSHP) systems. The newsletter also includes a listing of publications, meeting schedules, and other sources that are of interest on GSHP designers. It is funded in part by the Geothermal Heat Pump Consortium.

Quarterly Bulletin

The last two issues of the Geo-Heat Center Quarterly Bulletin were each devoted to a single topic:

1. Vol. 18, No. 4 (December 1997) describes geothermal energy projects in South Dakota, including articles on the geology of the Madison aquifer, district heating systems in Philip and Midland, large heat pump systems in Pierre, and the spa and pool community of Hot Springs.

2. Vol. 19, No. 1 (March 1998) is devoted to geothermal direct-use equipment and includes a general overview article, and specific articles on well pumps, piping, heat exchangers, space heating equipment and absorption refrigeration. The last five articles are abbreviated versions of the chapters in the Guidebook.

FUTURE WORK

The Geo-Heat Center staff are presently working on two publications that will assist developers of geothermal direct-use projects. They will be available later this year and are titled:

1. "Model Construction Specifications for Geothermal Wells and Well Equipment" by K. Rafferty, and

2. "A Comprehensive Aquaculture Developer's Package" by K. Rafferty and T. Boyd.

Geothermal Heat Pumps: 1998

Market Mobilization Mid-Point

John D. Geyer

John Geyer & Associates, Inc.

DOE Geothermal Program Review

Berkeley, CA

April 2, 1998

Who <u>are</u> those guys?

and . . .

What are they doing with *our* name?

Or (more to the point) . . . .

WHAT are they doing in *our program*?

- - *" What ?"* - -

"Geothermal Heat Pumps" (marketers)

aka

"Ground-Coupled Heat Pumps" (engineers)

aka

"Water-Source Heat Pumps" (manufacturers)

aka

"Closed-Loop Heat Pumps" (contractors)

aka

"GeoExchange"

- - *" Why ? "* - -

Electric Industry Restructuring

Administration Energy & Env. Goals

"Efficient" and "Green" Energy Appetites

Absence of Commercial Alternatives

Imbalance of Supply and Demand

6-12

- - *"Who?"* - -

Geothermal Heat Pump Consortium, Inc.

290 Utilities

13 National Organizations

22 GHP Manufacturers

955 Other Mfgrs. & Trade Allies

52 International Organizations

(As of Jan. 22, 1998)

- - *GHPC Sponsors* - -

US DOE, Geothermal Program

+

US Environmental Protection Agency

+

Utility Organizations

+

GHP Industry Members

Energy Flow of HVAC Systems

Energy Mix	Thermal Equiv. Into Power Plant	G & T Losses	Input to Heat'g Appl.	Thermal End Use
Fossil + Air HP	17.0 kWh thermal	12.0 kWh thermal	5.0 kWh electric	10.0 kWh thermal
Fossil + Oil Furnace	14.6 kWh thermal = 1.6 kWh th + 13.0 kWh th	2.6 kWh thermal = 1.1 kWh th + 1.5 kWh th	0.5 elec + 11.5 th = 0.5 kWh electric + 11.5 kWh thermal	10.0 kWh thermal
Fossil + Geo HP	9.0 kWh thermal	6.3 kWh thermal	2.7 kWh electric	10.0 kWh thermal
CC Gas + Geo HP	7.0 kWh thermal	4.3 kWh thermal	2.7 kWh electric	10.0 kWh thermal

- - Low Demand - -

Summer

Date: 9/4/96
High Temp: 87 ° F
Dew Point 69 ° F

ACVAV School Ave. ——— (Gas Heat)
WCVAV School Ave. —o—o— (Gas Heat)
GHPC School Ave. - - - - - - (All Electric)

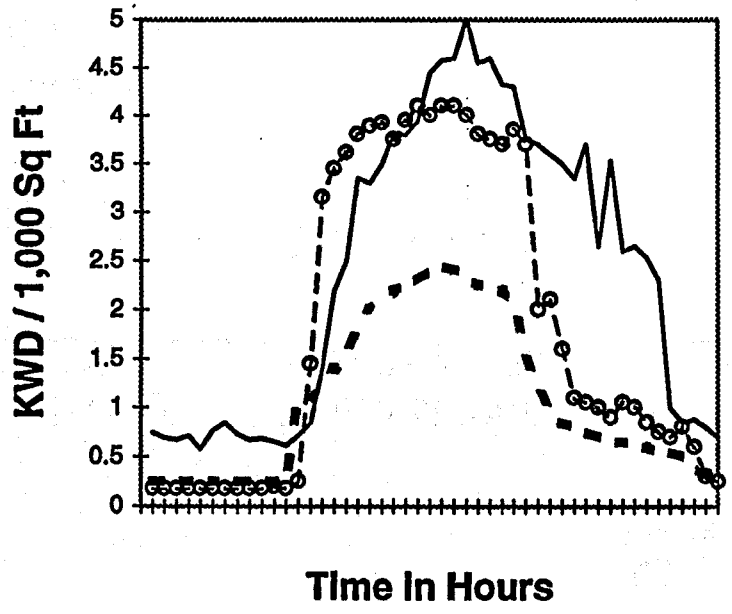

Winter

Date: 1/10/97
High Temp: + 2 ° F
Dew Point - 12 ° F

ACVAV School Ave. ———
WCVAV School Ave. —o—o—
GHPC School Ave. - - - - - -

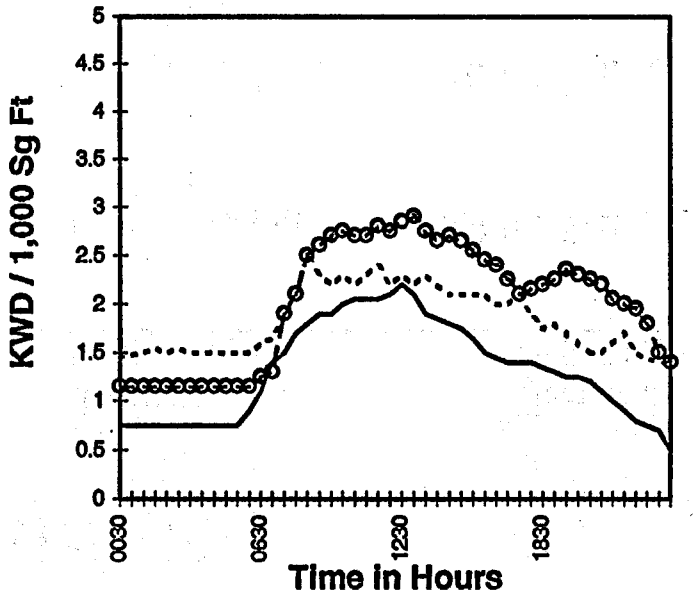

New Schools Energy Cost

Total Annual Energy Costs for 4 New Elementary Schools, '95/'96 (Electrical & Natural Gas)

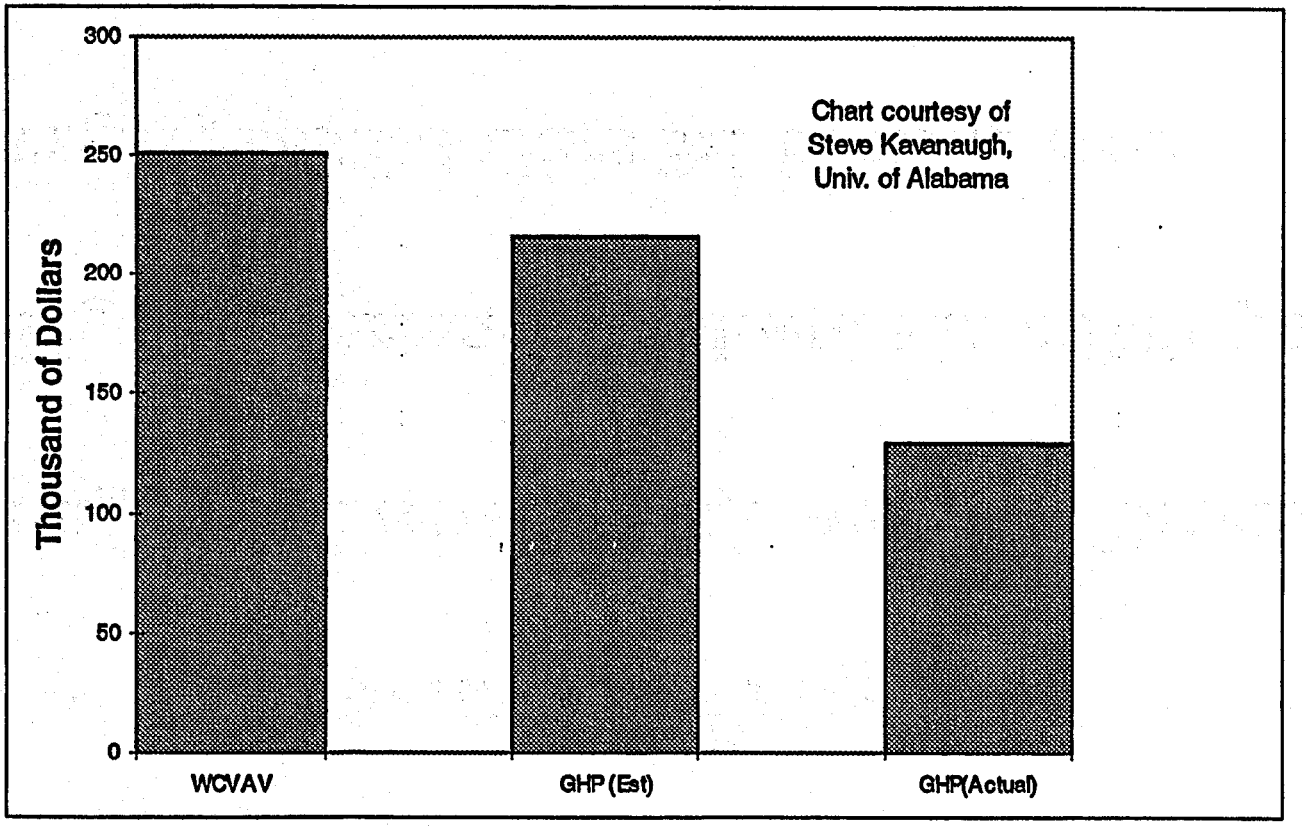

6 - 17

- - *Works In Progress* - -

- **Building Public Awareness, Interest & Demand**
- **Earning Geothermal prominence in public policy**
- **Leveraging DOE dollars 3:1 in same year**
- **New $3 Billion market in less than 10 years (300:1)**

6 - 18

- - *Outlook (for next 3 Years)* - -

- **New Energy Product Development Prototype**
- **Value Standard for Energy Service**
- **Customer and Supplier Choice**
- **Mass Market Emergence**
- **Geothermal Prominence in Energy Market**

- - *How Can This Be ? - -*

No comparable or market-ready alternatives which:

- **Perform as promised & better than alternatives;**
- **Benefit both end-user and supplier;**
- **Yield effects big enough to matter;**
- **Integrate risks, costs and benefits; and**
- **Justify cost payment by users.**

6 - 20

In short,

Geothermal Heat Pumps work . . . now,

Except for:

Industry Infrastructure Gaps,

Consumer Confidence, and

Cost Containment in Immature Markets

These are GHPC's focal points.

6-21

- - *1998 "Snapshot"* - -

Program Mid-Point

Subscription & Resources Established

Public Awareness Growing

Industry consolidating

20 % to 30 % Growth in 1997

Growth Accelerating

"Threatened" Opposition Forming

Concurrent Session 7:

Enhanced Geothermal Systems Workshop

Workshop on "Dual-Use Technologies" for Hydrothermal and Advanced Geothermal Reservoirs

Dan Entingh

Enhanced Geothermal Systems R&D Management Project
Princeton Economic Research, Inc.
Rockville, Maryland

Abstract

DOE's new R&D sub-program to conduct R&D to develop hot dry rock and other sub-hydrothermal geothermal energy production technologies has been refocussed and renamed "Enhanced Geothermal Systems" (EGS). The new industry-based R&D management team led a workshop at Geothermal Program Review XVI to identify "Dual-Use" R&D thrusts: research that would benefit both EGS and hydrothermal-based systems. This paper reports some of the results from the workshop.

Introduction

The workshop was one of the kick off events for new approaches to managing Enhanced Geothermal Resources research. It was conducted on April 2, 1998.

"Enhanced Geothermal Systems" is a new term coined by the geothermal industry and now used by the Department of Energy to encompass resources and technologies that range from Hot Dry Rock at the difficult end of the resource scale and through very marginal hydrothermal resources at the easier end of the scale. Workshop participants were asked to identify issues for study of Hydrothermal/Hot-Dry-Rock Dual-Use Technologies and major criteria under which R&D proposals might be accepted as "dual-use" R&D projects. We have defined "Dual-Use" projects as R&D projects whose expected results will benefit both near-term geothermal hydrothermal commercial projects (e.g., through cost-reduction) and longer-term hot dry rock or other "advanced" geothermal resource projects (e.g., through contributions to resolving some longstanding technical barriers.)

The practical implication of the "dual-use" concept is that some of the OGT R&D projects that are proposed due to their short-term benefit to industry, might be granted additional or expedited funding from the Advanced Reservoirs part of the OGT budget, if they also appear to offer promise of hastening the development of HDR systems. If Dual-Use is to be a useful concept and approach, it has to be defined as a R&D management and selection process, with groups of analysts, R&D performers, R&D managers, looking at both the hydrothermal and the EGS sides of the fence.

The specific goals of the workshop were to:
1. Define general requirements for the Study to identify technologies and technology-development areas in which "dual-use" capabilities are most likely to emerge.
2. Prioritize the most important of those areas.

A Dual-Use Project

⇕

PAYS OFF FOR BOTH

⇕ ⇕

Enhanced Geothermal Systems (Long Term) | **Hydrothermal Systems (Short Term)**

3. Develop criteria whereby importance relative to HDR/advanced reservoirs can be identified. R&D related to geothermal Drilling and Completion, and Conversion (power plant) technologies were not addressed in the Workshop because the EGS R&D Management Team considers these to be addressed adequately by OGT's current research in these areas.

Origin of the EGS Management Project

The Geothermal Energy Association, an industry association, held a workshop on hot dry rock R&D in December of 1995. Among the recommendations made was, "Make the name 'Hot Dry Rock' disappear." The other really strong recommendation was that they didn't say, "Make the work disappear." Rather, they said that hot dry rock could play an important role in thee future of the geothermal industry, and that future work to develop hot dry rock systems should be better integrated with R&D to improve hydrothermal-based energy systems.

DOE responded to this by releasing, in mid-1997, a Request for Proposals to contract with an industry-based team to manage DOE's future HDR-related R&D. Princeton Economics Research (PERI) and GeothermEx teamed to win the proposal. PERI brings experience on the policy side, the programmatic management side, and the long-term analysis side. GeothermEx brings the practical side and the deep economic evaluation side. We'll draw in expertise on other things as needed.

Lynn McLarty of PERI leads the EGS R&D Management Project. Subir Sanyal leads the GeothermEx component of the Project, and Ann Robertson-Tait assists him. We use "PERI/GX" as the acronym for the team.

The PERI/GX team includes Dr. Ted Mock and Cliff Carwile, both of whom are retired from many years of active participation in the DOE Geothermal R&D program and HDR R&D among many other related R&D fronts. The R&D program manager for EGS at DOE's Office of Geothermal Technologies in Washington, D.C., is Paul Grabowski. Willetia Amos is the DOE Idaho Operations technical manager for the Project. Bob Creed (DOE) and Joel Renner (INEEL) advise her.

One of primary needs laid out in the DOE solicitation for this work is to markedly intensify the involvement of U.S. industry in this area of R&D. This will be done in part by forming an industry-based Coordinating Committee that can guide us in planning the work. Lynn McLarty has been working very hard and successfully to get the nucleus of an EGS National Coordinating Committee (EGS-NCC) going. The Coordinating Committee reports to PERI and GeothermEx.

The National Coordinating Committee has come up with the new name to replace and subsume "Hot Dry Rock." This R&D area is now going to be called "Enhanced Geothermal Systems." This has been generally agreed to by the relevant people at the Department of Energy. We will not stop talking about hot dry rock, but HDR will be subsumed under the more general name. What is happening now is the transition from an HDR project that was run by a single lab for 20 years into a broader technical arena and a broader base of technnical experts and R&D performers.

SOME SUGGESTED DUAL-USE AREAS

- Stimulation (e.g., Hydrofracing)
- Fracture Detection & Analysis
- Simulation - Reservoir Modeling
- Risk Analysis / Economic Feasibility / Cost Models
- National Resource Assessment for R&D Investment Planning
- Low-cost Drilling in Hard Rock
- Assessment of Margins of Hydrothermal Reservoirs

PERI/GX's general method is to identify critical needs and define reasonable approaches to meeting the needs. Our initial perceptions of some of the main needs and approaches are listed here.

1. Need: Intensify involvement of U.S. industry in EGS R&D.
   Do: Form National EGS Coordinating Committee (EGS-NCC)
2. Need: Broaden technical expertise and contribution.
   Do: Form technical panels as needed
3. Need: Create and/or broaden constituency for EGS.
   Do: Enroll latent stakeholders, e.g., Environmental groups, Oil & Gas Firms
4. Need: Keep Practical R&D Moving
   Do: Promote Dual-Use cost-shared R&D projects.
5. Need: Benefit from other countries' ongoing work
   Do: International Interchange Projects.
6. Need: Broaden the R&D Performer Base for EGS.
   Do: Include industry performers as much as possible. Spread other R&D across a number of National Labs and universities.
7. Need: Return to Demonstration work as soon as possible
   Do: Develop Strategic Plan. Include Technology Development Path. Decide on type of systems to pursue, e.g., "Dry" versus "Moist" Rock. Promote support in Congress, DOE, via industry & environmental groups

PROCESSES FOR THE WORKSHOP

- Six short speeches, to prime the discussion pump.
- Three break out groups, tailored to the interests of the 29 participants.
- Whole-group reports and discussions at end.

Technical Presentations

The first part of the workshop consisted of six short talks about EGS and HDR. These provided background information and primed the discussion pump. Very brief extracts of those talks are provided here.

1. Donna Smith, Los Alamos National Laboratory: "Lessons from the Fenton Hill Experiments."

Smith reviewed some of the experience at the Fenton Hill program, and listed some for dual use and for continued research.

The "enhanced systems" concept is to be able to look at dead zones within a geothermal system or at the margin and are there ways that we could make those systems productive as a first step before moving out to the hot dry rock that's not near anything. There are main issues in: well completion, fracturing, high pressure versus low pressure systems and workover, impedance - particularly in a hot dry rock system, diagnostics and engineering of the reservoir, and the bottom line of economics. (Smiths's more detailed analysis of issues will be included in the full report of this workshop.)

Some of the main areas for Dual-Use technology development are:

<u>Hydro fracturing and stimulation</u>
- Currently not a reliable tool in hydrothermal systems.
- Research and technology development is needed to make this a reliable useful tool for hydrothermal applications.

<u>Improved geophysical sensors and analysis</u>
- Currently a labor-intensive, expert dependent process.
- Hardware for long-term seismic monitoring and software for analysis may make this a

useful tool for hydrothermal applications and system management.

Improved Reservoir Models

- Need to integrate data from geology, geochemistry, geophysics into a tool to manage the reservoir.

The answer for many of the issues and needs is in proving it out in field work. Proving it in one demonstration, unfortunately, probably isn't the answer. Because if it works everybody will say that it was a special case, that field was particularly amenable to that. So the real issue is can the workability and value of Enhanced Geothermal Systems and Hot Dry Rock be proven systematically.

2. Prame Chopra, Australian National University: Hot Dry Rock Beginnings in Australia

The Australian HDR project is very new. The project web site at http:\\hotrock.anu.edu.au has much detailed information. An extensive geophysics-based geothermal exploration program surveyed the entire continent. The program found a very nice correlation between gravity lows and the existence of granites that are very high in radiogenic elements that generate a very large amount of heat. The heat is being kept in by three plus kilometers of low conductivity sediments.

The HDR prospect chosen for the first, $30 million, development is just north of Sydney in Hunter Valley. It's close to population centers and has the right things for commercial development. The area is believed to contain enough energy for 20 percent of Australia's electricity for 50 years. A company, Hot Rock Energy Propriety, Ltd., has been formed to do this as a commercial arrangement. Its shareholders include some of Australia's largest companies. Seven of those companies are billion dollar asset companies. The plan is to go forward with $30 million demonstration project in Hunter Valley.

There are a few technical issues that are relevant to Australian problems when we get going. One key issue is that there is a sedimentary basin cover about 3 to 4 kilometers thick. Can we do accurate monitoring of microseismicity, with the likely degree of attenuation that will occur?

The reservoirs are expected to be horizontal pancakes, a series of cells stacked one on top of the other. A serious issue is how to control flow through the different cells of the reservoir? What do you do if one of the cells is very high in flow rate and the others low? You have to be able to valve this somehow. The economics of the approach hangs on the idea that we're going to get lots of cells from a single hole. That's going to be the same problem world-wide. If this technology is to be successful, you've got to reduce the major cost in the project which is the cost of the drilling. So you need to be able to somehow fabricate multi-cell reservoirs and manage them responsibly whether the reservoirs are vertical or horizonal.

3. Jörg Baumgärtner, Soultz Project: Status of Soultz Hot Dry Rock Project

The Soultz project is a multi-national project of the European Community located in western Europe at the border between France and Germany. The permeability in the wells before we stimulate the outmost sections is in the order of a couple of hundred microdarcies which means, from a technological point of view, that they are impermeable. A main difference compared to Fenton Hill, is that whatever we do in scientific drilling, we never encounter a real tight formation.

We are dealing with something here which is surprising. We know that granites and crystalline rocks have very little porosity. We talk about less than one percent normally. Here, in these altered zones, we find porosities which are peaking up to 20 percent and are not in the heart of the alterations; they are usually at the boundary. So when you stimulate, you have a two mechanism process. You are going into the main vein and you're also stimulating the high porosity rocks.

Last year saw a four month circulation experiment in which we circulated 244,000 tons of water through our reservoir at zero fluid loss. We also have to say that the system is so large we have never seen a temperature drop so far.

We see so far, temperature increases. The flow rate was on the order of about 75 to 90 tons per hour as we accelerate the system and the energy we produced was in the order of 10 to 11 megawatts-thermal, of which we dissipated about 6 or 7 megawatts-thermal on the surface through cooling, simulating a user on the surface. We have no user so far. Energy used by the system for circulation was on the order of 250 kilowatts electrical; that is rather low. I think this gives us hope for the future.

What have we learned for the pilot from an operational point of view? We have tested enough to have some basis for our outlook for the future. What needs to be done, first of all, is a careful cost-risk analysis.

Concerning Wells:

- Careful cost and risk analysis between:
  - a 3-platform vertical well system, and
  - a 1-platform deviated well system.
- We need an even larger well separation, at least 600-700 meters at depth.
- Better adapted well completions (diameter, length of pumping chamber).
- Applied Research:
  Targets: Reduce cost, Reduce technical risk
  - high temperature cementing
    (cheap, efficient ... power plant ashes??)
  - temperature hardening of existing tools
    - multi-lateral wells
    - new drilling technologies

Our present separation between the wells is 450 meters. That's about a good 1500, 1600 feet and we want to drag it further apart based on recent experience. We feel comfortable enough to go to 600 or 700 meters in the future.

Concerning Stimulations:

- If we want to approach commercially interesting circulation rates, we need to use higher flow rates & larger volumes during stimulations.
- Applied Research:
  We need to test new stimulation techniques:
  - need to learn how to perform multi-stage stimulations safely
  - chemical treatments (acidizing (?) - under lab-testing)
  - use of fluids with varying densities proppants in crystalline rocks (?)

We feel in principle rather comfortable with the stimulation technology we have developed so far. We perform large scale stimulations. Our stimulation jobs usually involve something like 50,000 cubic meters of fluid volume each time. But we need to improve them nevertheless because we have to increase our circulation flow a lot, so we need to use higher flow rates and larger volumes during stimulation.

Concerning Circulation and Surface Installations:

- What about cycling operations (peak load) using the formation's storage capacity?
- Surface installations at SOULTZ did perform (surprisingly) well; the degree of automation still has to be improved
- Applied Research:
  Targets: Improve environmental friendliness (closed loop, binary cycle). Improve energy conversion efficiency!

The circulation experiment is very important. On the research operation side for circulation, I think we have to improve the environmental friendliness of all operations. I think geothermal, although it has been called environmental friendly, is not really environmental friendly in most operations. So we have to learn to really operate totally closed loops, because if we want to gain support for our technology it comes from the environmental side and their money comes in quicker than from the technological side. And also we have to improve the energy conversion efficiency on the surface for low temperature cycles, whatever you tend to gain on the surface, you don't have to gain underground.

4. Bill Wood, B.J. Services: Stimulation of Geothermal Wells

This talk was a brief introduction to hydraulic fracturing, and its application to hot dry rock (HDR) reservoirs.

Fracturing is a fairly simple technique in permeable rock. By injecting fluid rapidly into a porous rock, it is possible to initiate a fracture. This occurs when the strength of the rock is

exceeded by the pressure required to force the fluid through the pores of the rock. The fracture will propagate away from the well bore as long as pumping continues. Once fractures have been effectively placed, there must be communication of fluids from one wellbore to another to allow for heat exchange. In impermeable rock, fracturing is more difficult to accomplish, but can be done.

The fracture will "heal" or close up after pumping ceases. In order to prevent healing, proppants are injected with the fluid to hold the fracture open. Proppants are sand, or manufactured resin coated sand or ceramic materials. Proppants are highly permeable when placed in a fracture.

Fractures are normally oriented vertically at depths below 3000 feet. Above 3000 feet fractures usually have a horizontal component. Fractures can range in size from a few feet to hundreds of feet from the wellbore. Fracture heights and widths are determined by rock properties, but are generally as follows: (a) Heights are roughly equal to length from wellbore, (b) Widths range from 0" to 1+", depending on rock type and fluid properties. (c) Fractures generally tend to decline in length as formation permeability increases. For HDR, low permeability may require longer fractures.

Complex fracturing fluids incorporating cross-linked polymers are used to conduct fracturing operations. The fluids have a consistency like Jell-O® which allows them to open the fracture wider, while carrying sand deep into the fracture. Once the job is over these fluids "break" (return to a low viscosity state like water) and flow out of the well, leaving the proppant behind.

Temperatures above 350°F require special fluids and techniques to successfully place a propped fracture. Pre-job cool down injections must be performed to assure fracture fluid stability for job duration. Special proppants may be required due to temperature and mineralogy of rock. Ceramic proppants or sintered bauxite would have higher temperature stability than a natural Ottawa sand, but may be just as susceptible to dissolution due to the corrosivity of superheated steam.

5. Subir Sanyal, GeothermEx: Assessing Enhanced Reservoirs

One of the problems I believe everybody working in HDR acknowledges is figuring out how much energy you can get, and how to engineer the recovery of energy. We need to improve the definition of the fractured network. Before we even start drilling and planning to make a fracture, we have to understand what the natural rock conditions are in terms of rock mechanics, distribution of rock types, hydraulic properties, and the existing fracture network. A lot of advances have been made within the last 10 to 20 years in trying to use seismic technology and other geophysical methods to understand better where one should drill for an HDR project and how one should plan a project.

Once drilling is done, the question then is to test the well and to understand what kind of fracture we can create. Or after the fracture is created, what kind of fracture have we got? From working with Golder Associates, I believe that there are technologies available in the nuclear waste disposal area that we can borrow to understand and define the fracture network.

In the area of prediction, I believe that with the technology developed with DOE funding of numerical modeling of heat transfer and hydraulics, prediction is not that big a challenge. The area where I think we still need to improve in the rock mechanics area is to combine rock mechanics with the conventional heat transfer and fluid flow equations that these models already handle.

Well testing, which will actually consider only the free production or free injection fractured conditions and post-injection situation, needs to be improved because now well testing technology really looks at only very simple fracture systems. In the area of tracer technology, significant improvements have been made over the last few years, but I think tracers have not yet become a quantitative tool even in hydrothermal reservoir testing.

Once the fracture is developed, once you can define the fracture network from the well test geophysics and so on, then we can model it and we can design a project to optimize the energy recovery. In that, I think the main problem will

be to control the breakthrough of cooler water coming from injection wells to the production wells, and the possible encroachment of cooler water in various cells in the reservoir. That is very important. In the petroleum industry, almost 30 years have been spent in trying to control mobility of injected water in oil fields. The problem people have found repeatedly is that if you have multiple zones, multiple fractures, multiple layers of sand; there is a tendency for the injected fluid to break through to the easiest path. Therefore recovery is sharply curtailed.

However, there is hope in this area. I worked for three years on a DOE R&D program in enhanced oil recovery, where you inject a surfactant with the water that forms a solid and that blocks the hyperlabile zones and selectively keeps the low permeability zone more open. This has also been done with polymers in the oil industry. So I think that's an area of research we ought to look into. I think we'll succeed in controlling the mobility of the advancing injection front.

There remain some chemical issues, for example, corrosion, gases that will come out, and noxious elements, arsenic and so on, including hydrogen sulphide. These have not yet been addressed.

The final question is a question of pumping versus self-flow, high pressure versus low pressure. The need is to have adequate flow. We have to have a large steam fracture and chances are in these deep wells, we have to depend only on self-flowing wells. The energy loss at the well is small. Pressure loss will be significant. On the other hand, pump technology today does not allow you to go much deeper than 1500 feet in pump setting depth and the pumps are designed to run at temperatures less than 180 degrees C. There are significant limitations there. So we don't want to have it be like some hydrothermal projects, where we find it is too hot to pump but too cool to self flow.

John Sass, U.S. Geological Survey: Margins of Hydrothermal Systems

Let's begin with a quote from an article that appeared about three or four years ago, by Dave Tenenbaum.

> *"There are abundant reserves of heat beneath the earth's surface, and new technologies could improve our ability to use them as an energy source. But in the United States, at least, few people seem to care."*

The sentiments expressed there are still very true and in particular they apply to my employer who in their wisdom sacrificed their geothermal program to the god of reinventing government. Those of us who are still hanging in are very dependent and very grateful to Marshall Reed and Al Jelacic for keeping us in the business.

Another quotation may make the appellation "dual use" moot.

> *"An HDR system is any geothermal system where (re)injection is necessary to extract heat at a commercial rate for a prolonged period."*

It's something that John Garnish said several years ago and I subscribe to this philosophy. I put brackets around the "re" because I think any geothermal system where injection is necessary to extract heat is, in fact, an enhanced geothermal system or in our old terminology, hot dry rock.

What we're seeing now is that most of geothermal production is at the end of the scale where you have naturally very high permeabilities. You're sucking that fluid out and injecting condensate and spent brine, but not doing much of anything else. At the other end is the Fenton Hill type model, hot dry rock.

If geothermal is going to reach single-digit percentage of U.S. electricity production, where we're going to get it is in the middle of the range of permeabilities. We're not going to get that much more from the high permeability systems. We're not going to get political support or industry support for doing the archetypal hot dry rock stuff. So we're going to have to look at existing low-permeability hydrothermal systems like Soultz, like Hijiori, in other words, like every other project that's going on now and try to enhance both the longevity and the productivity of those

reservoirs.

I've been working on geothermal resources in the Western U.S. for about 30 years, in terms of heat flow and trying to interpret it. [He shows a map.]

What we show here is the heat flow distribution in the Southwest. The stars are geothermal plants. The reds are higher than 100 milliwatts heat flow per square meter. The yellows are typical Basin and Range 80 milliwatts per square meter. Most of the existing hydrothermal power plants are within or adjacent to these red areas. The prospects for potential enhanced reservoir systems are all the ones that are labeled here: The Geysers, Imperial Valley, Coso, Roosevelt, Cove Fort, Long Valley, and Dixie Valley. Dixie Valley, I think, is at the moment the most carefully and completely studied of the potential enhanced geothermal systems.

The Imperial Valley is intriguing because all of the power production now is either from flash steam or from closed systems in the hydrothermally convecting, very high salinity brines of the region. There are, however, conductive areas and conductive caps over the hydrothermal systems that might be good enhanced systems above the top of the hydrothermal systems.

This illustrates the situation in the Basin and Range when we're talking about how widespread is the resource. This is in the yellow area of the map, 80 milliwatts per square meter and you can see if we look just at the crystalline rock outcrops and assume that 4 kilometers is where we're going to be drilling with enhanced type and more efficient drilling that 4 kilometers is going to be the target. So we're not looking at terribly exciting temperatures. In crystalline rocks, we put a kilometer of sediments on and they get a bit more interesting. If we put a couple of kilometers of sediments on, we're in business at 13,000 feet (4 kilometers).

In the red areas it looks even better. So overall, there are places like the Basin and Range, the Rio Grande rift, and other places where we have red dots on that map that, if we can get the engineering problem settled, are very viable and credible regions for developing enhanced geothermal reservoirs exist.

We're basing our generalizations on heat flow. These are the heat flows in the vicinity of Dixie Valley and most of these are crystalline rocks and most of them are high temperature. If we go back into areas that have some sedimentary cover, and even some that don't where we have this regional heat flow of 100 milliwatts per square meter, we're likely, if we drill to depths like 13,000 feet to be in an area where, if we can develop the kind of permeability that we need, we'll have a very widespread, very productive resource.

General Discussion

This discussion occurred after the breakout groups met, but before the groups reported.

Lynn McLarty (PERI): My comment basically comes from Jörg Baumgärtner. He said we would have to be careful to not allow the Dual Use concept to become a mechanism for hydrothermal interests to siphon money from EGS projects and interests over the long term. That's a very important point. We need to keep the long-term focus really on Enhanced Geothermal Systems.

Mike Wright (EGI, University of Utah): In the Geothermal Energy Association HDR workshop (December, 1995) the notion of Dual Use came up, and the thought was that, in the process of getting to solutions for Hot Dry Rock or Enhanced Geothermal Systems, we're going to spin out some stuff that is of use to the hydrothermal industry. So that's one thought.

The other thought was that there's already a lot going on in hydrothermal research that doesn't have to be repeated in a HDR program. The thing that industry was really very critical of, and I think actually led in large measure to the recommendation to shut down Fenton Hill, was that the project had throughout the years appeared to have been operating entirely in isolation from the hydrothermal industry. And, the fact is that these technologies are very closely related. So, I think we have to be careful about "Dual Use." I'm not sure that basing a program around "Dual Use" is even a good idea.

John Sass: I generally agree with what Mike said. Once again getting back to John Garnish's

definition, which I like, any system where you have a significant amount of injection, not just reinjection of condensate, etc., but using injection to either increase the longevity or increase the productivity of the field, should be considered as an enhanced system. There are good reasons to do this at the moment, in this competitive environment. But if there's some DOE interest and some money coming in, then it's going to be pushed in that direction and might reach the point where this becomes a self-sustaining and economic thing. But it needs a little nurturing at this point in the game.

McLarty: Another good reason to pursue that is that, in the next eight to ten years, we'll probably see declines in production in other fields. What's happened to The Geysers starting about 15 years ago is a precedent to what is likely to happen at other fields.

Unknown: And most of the heat is still going to be there.

Moderator: I want add something to those thoughts, about the history of U.S. Department of Energy Geothermal R&D program. It was roughly in 1974 or 1975 as ERDA and then DOE were being created, that Ron Toms of the DOE Geothermal R&D Program was locked in a room and told, "In six weeks, come up with a grand strategy for geothermal R&D." The result was: We will use hydrothermal electric systems as a technology-improvement test bed for almost every thing else. And then we are going to spin out into three other areas: geopressured, hot dry rock, and direct heat. (Magma energy came later, from scientific work started at Sandia.) The idea was that there would be some technology work, some resource assessment work done for geopressured and hot dry rock, but that almost all of the technology development R&D would be funded under the hydrothermal program, because it would almost all eventually spin off into the other more challenging areas.

Reports of Breakout Groups

Breakout Group 1. Finding the Next Sites for Enhanced Geothermal Systems

Facilitator: John Sass, U.S. Geological Survey

The group concentrated on Enhanced Geothermal Systems in the United States that are not Hot Dry Rock; that is, there is expectation of some permeability and perhaps some fluid in the natural state reservoir. We had a very diverse group, but one that rapidly reached consensus.

We adopted a fairly stringent set of Criteria for such sites:

A. Criteria for Site Selection

1. Public acceptance.
2. Near an established hydrothermal resource.
3. A field with low permeability wells interspersed with productive ones
4. Transmission - main lines not too far away.
5. Commercially relevant - i.e. conditions are such that there is interest from major players in the industry.
6. Easily accessible - roads, general commercial services, housing.
7. Sources of water are available for injection.
8. A known reservoir, preferably of a single lithology whose boundaries and hydrologic source are well defined
9. Mechanically well characterized: Stress orientations and magnitudes, and their vertical and lateral variation are known. Locations and orientations of major producing fractures are identified.
10. Existing wells available. For example, from previous hydrothermal exploration and/or reservoir confirmation efforts. Or, at relative dry patches in the center or edges of producing hydrothermal systems.
11. Knowledge gained at this site could be transferred to other sites. That is, this site is not so unusual that what is learned or developed here would have low likelihood of being useful at other potentially attractive sites.
12. Extensional stress regime: All existing

hydrothermal plants are in extensional settings. Provides lower breakdown pressures than compressional or strike-slip regimes. Tradeoffs are between easy establishment of hydrologic communication and difficulty in containing injected fluid and avoiding short circuits.

13. Temperature. Meaning, as high as we can get, all other things being equal.
14. Relatively large reservoir volume and surface-reflected area.
15. Pre-existing knowledge of general geology and hydrology of the area.
    (a) Lithology, stratigraphy, and structure.
        i. Sedimentary blankets provide shallower targets for a given heat flow, but make monitoring from the surface more difficult.
        ii. Will affect well costs, and predictability of reservoir enhancement strategies.
    (b) Young volcanic activity or evidence for subsurface magmatism: some of the most productive hydrothermal reservoirs and most promising engineered reservoir sites are in regions of high heat flow with no evidence for upper crustal magmatism.
    (c) Sources of recharge, injectate, etc. should be known and water rights established.
    (d) Mineralogy of thermal reservoir rocks will determine the extraction technology.
16. Political considerations
    (a) Serves folks and Congressional districts not already served by geothermal energy production.
    (b) Reservoir development has not already received a great deal of funds from DOE. E.g., on this one, we maybe should avoid The Geysers and Heber. Roosevelt H.S., Steamboat, Coso, East Mesa, Glass Mountain, and Newberry would be OK. [Sass disagrees. Subject to marketability of power, increasing the productivity or longevity of a field like the Geysers would have a greater political appeal than getting a little plant going at Newberry, irrespective of what's already been spent.]
    (c) There are not already fairly large-scale hydrothermal operations in operation. For this we would tend to exclude The Geysers, Coso, Salton Sea, and East Mesa.
    (d) Sass believes the California Energy Commission would like to contribute to any good effort being made in California, and perhaps in Nevada sites that might serve California load.
17. There is some chance of a power sales agreement or sales to a green power marketer (Enron, PG&E Energy, Edison Energy, others).

B. <u>Known Sites that fit the Criteria</u>

1. Primary Sites: All of the primary sites meet all of the criteria, insofar as the participants in the breakout group knows.
    a. Upper Steamboat Hot Springs, Reno, NV
    b. Geysers-Clear Lake KGRA, CA
    c. Dixie Valley, NV
    d. Roosevelt Hot Springs, UT
    e. Soda Lake, NV
    f. Salton Sea, CA [Here, there is large untapped potential for competitive power from brine conversion, but mining heat from high-temperature cap rocks might be an attractive, environmentally friendly alternative].
2. Secondary Sites: Each of these sites is believed to miss on one or more of the criteria.
    a. Coso
        i. Source of injectate is not clear.
        ii. Legal contention re ownership of reservoir fluids.
    b. Long Valley
        i. Shallow reservoir shows drawdown.
        ii. Deep reservoir is not understood.
    c. Puna, HI
        i. Hydrothermal reservoir probably adequate for near-term local demand.
        ii. Strong environmental, cultural and religious opposition.
    d. Cove Fort
        i. Small, poorly characterized system.

e. Salton Trough
   i. Any of the KGRAs outside of the current production areas should be considered secondary.

As mentioned, this was a diverse group, but it rapidly reached consensus. Note that we're down to five sites in the United States that are the top candidates for research on Enhanced Geothermal Systems. The projects would be to stimulate production from unproductive parts of fields. We're not talking about new power plants here yet.

Breakout Group 2. Stimulation of Enhanced Geothermal Reservoirs

Facilitator: Dan Entingh, PERI

Stimulation means stressing a reservoir or specific geological formation to increase its permeability. In general, the desire is to create relatively long fractures, perhaps with length of 1000 meters or more, that will serve as flow paths between injection and production wells.

Reservoir stimulation is one area where fundamental science hits the rubber of the real road. There seems to be a lot of Rock Mechanics work that might be applicable to stimulation practice and theory. It's done in labs, on very small samples, but should be able to elucidate when and how stimulation might be useful in practical geothermal reservoirs. But a bridge between small sample work and large expanse work isn't there yet.

- We talked first about explosive stimulation, which may not apply to EGS work.
- Then solution mining, which we don't think will apply directly to most geothermal reservoirs, but is part of the techniques for creating space in some mineralogies.
- Then gas stimulation. Nitrogen is usually used.

The group considered, "How would we use stimulation if we were trying to stimulate a body of rock at The Geysers." That is, a body of rock that now is hot but not very productive. What came out is that hydrothermal rock is very different from sedimentary rock. There is a lot of rock mechanics work that needs to be done in the lab to understand better how to go after these harder and hydrothermally-altered rocks.

There are a lot of questions you would get into at The Geysers, or any other real-world location:

- Fractures you make might be parallel to existing fractures, and not connect to them.
- A big issue in most parts of the country, is that we have to understand the principal stress fields at depth, which we don't understand very much at all at The Geysers, because the measurements are hard to do.
- Self-propping is expected to occur in fracturing in some reservoirs and not others, and at least in the geothermal and hot dry rock literature, there is little about this.
- The composition of the fracturing fluids is very important, and needs to be worked on.
- Always for geothermal, high temperatures downhole will have large effects on stimulation schemes. The nature of the rock is very important. The needed information for crystalline rock is not nearly as certain as that for the sedimentary rocks found in oil and gas strata.
- The first big task is to integrate what we know about basic rock mechanics, geochemistry, and some geophysics at the lab and small-scale levels. Then the next big task is to integrate that knowledge into assisting with the experimental design of field tests of stimulation of interest to industry. A lot of this kind of work is going on at Yucca Mountain right now (the probable site of the civilian high level nuclear waste repository.)

When asked, "What are some of the criteria by which we would identify projects that are important Dual-Use projects?" the group said, "Get to the field. Get to work!"

Mike Wright said that many of the things you'd want to do for EGS, Enhanced Geothermal Systems, are being well covered in the R&D program right now. But stimulation R&D is a great big gap. The group recounted that in the late 70's and early 80's, DOE stimulate eight or ten hydrothermal wells, without much success in increasing productivity. We believe we could have spent another two hours or so discussing this topic fruitfully.

Breakout Group 3. Reservoir Analysis and Management

Facilitator: Subir Sanyal, GeothermEx

We too didn't really finish our discussion, but have identified some priority things to look at.

- The first priority is fracture characterization. Everybody felt this an area of crying need for technology development. We did not discuss specifics of what needs to be developed, but this is the first priority.
- The next important product, although not part of this group's mandate, is to prepare an inventory of all the HDR/EGS resources in the West so that industry has some sense of where to work.
- For well testing and tracer testing, what is important is to have some tools to run into the well to measure various factors.
- Numerical modeling technology has to be brought up to date for HDR/EGS. Rock mechanics has to be integrated into the modeling.
- We referred to, but did not discuss enough, the topic of mobility control.
- Finally, is the question of whether to operate systems at low pressure or high pressure, as first mentioned in Donna Smith's talk. For example, we are seeing now at the same field in the Imperial Valley, both self-flowing wells and pumped wells, and in both cases, the decision has to be very site-specific. So decisions about "high-pressure" or "low-pressure" are not easy, and will have to be studied.

Dick Benoit raised the issue about how to approach developers and operators about use of a well to do experiments. The understanding I got from that is if one can show the developer that a technology has a real chance of success, and the risks are reasonably low, they will be willing to come forward and offer their wells and even share the costs.

Summary and Wrap Up

Moderator: Joel Renner has agreed to try to summarize what's gone on here.

Joel Renner: It's difficult to make a summary of a workshop that's this short. Some of the most interesting things came from the initial presentations and discussions, more so than from the breakout groups. I think Mike Wright's caution about much of the technology being produced for hydrothermal systems will be useful for hot dry rock is important. The discussions in the breakout groups have already been summarized.

Bill D'Olier: I think much of what happened here is of very high quality. You need to provide all of us with at least the lists of issues from the break out groups.

Anna Carter: You defined part of this workshop to be setting up criteria for what R&D to pursue. I'm uncomfortable about predetermining criteria before we know where the ideas for R&D are going to come from. This may screen out very good projects simply because they don't meet the criteria.

Moderator: That's a good point. Procurements can be structured in a number of ways. I've seen many that included technical criteria and many that didn't.

So now we're done. Thank you all very much for coming to the workshop and working in the groups. I am very pleased at the breadth of what we've covered today. This is a good start on defining specific research ideas to pursue in the EGS program.

Notes

This report is an account of work under U.S. Department of Energy Contract DE-AM07-97ID13517 to Princeton Economic Research, Inc. (PERI), Rockville, Maryland. Opinions expressed herein are those of the speakers and not necessarily those of the Department of Energy, PERI, or GeothermEx.

file: pr2pro3 7/30/98

Appendix A:

Presentation Notes

Planning:
Creating the Path to Success

Dr. Allan Jelacic, Director
Office of Geothermal Technologies
U.S. Department of Energy

Geothermal Program Review XVI
Berkeley, CA

April 1, 1998

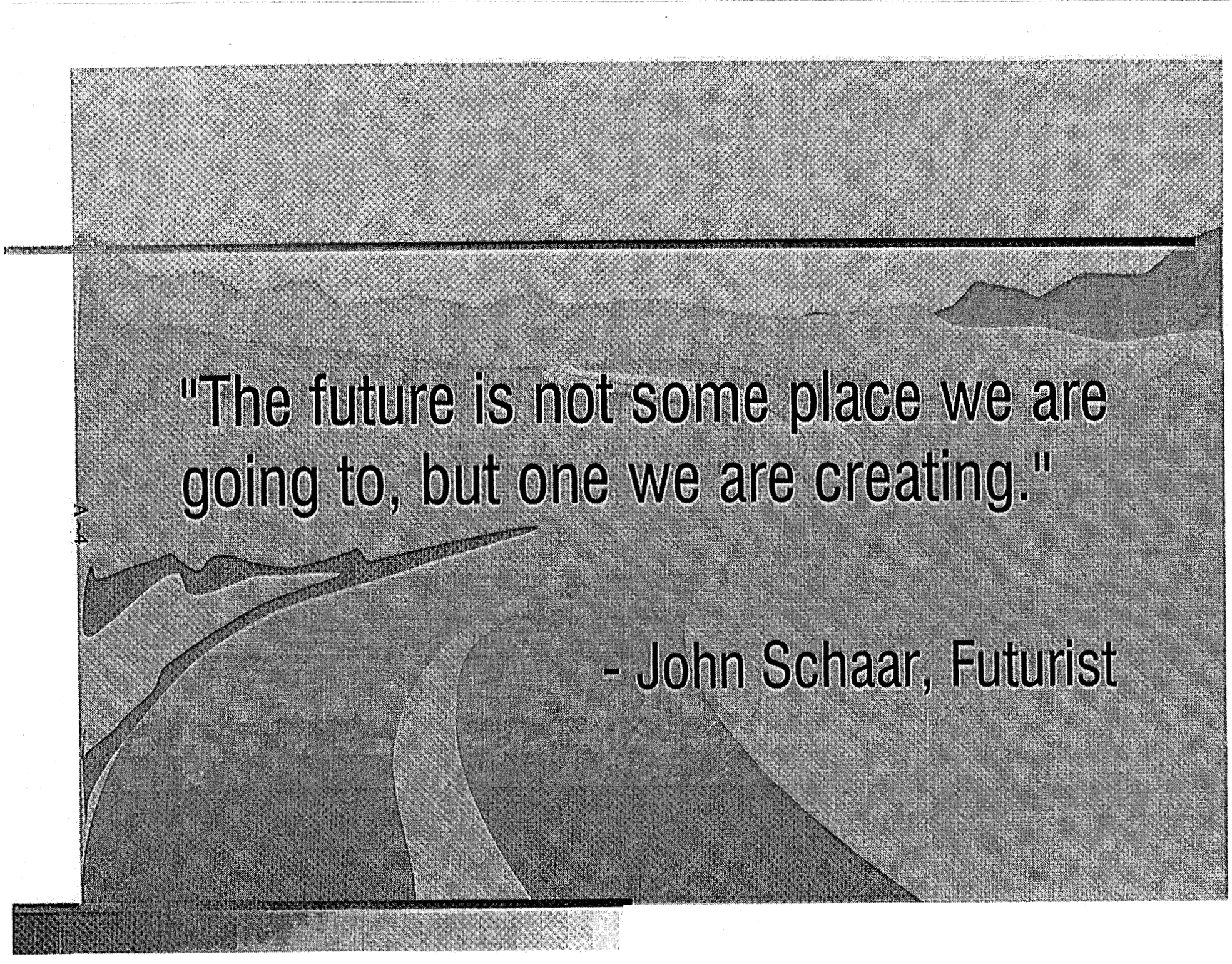
"The future is not some place we are going to, but one we are creating."
- John Schaar, Futurist

Failing to plan = Planning to fail

- Anonymous

Linear Path, Circular Process

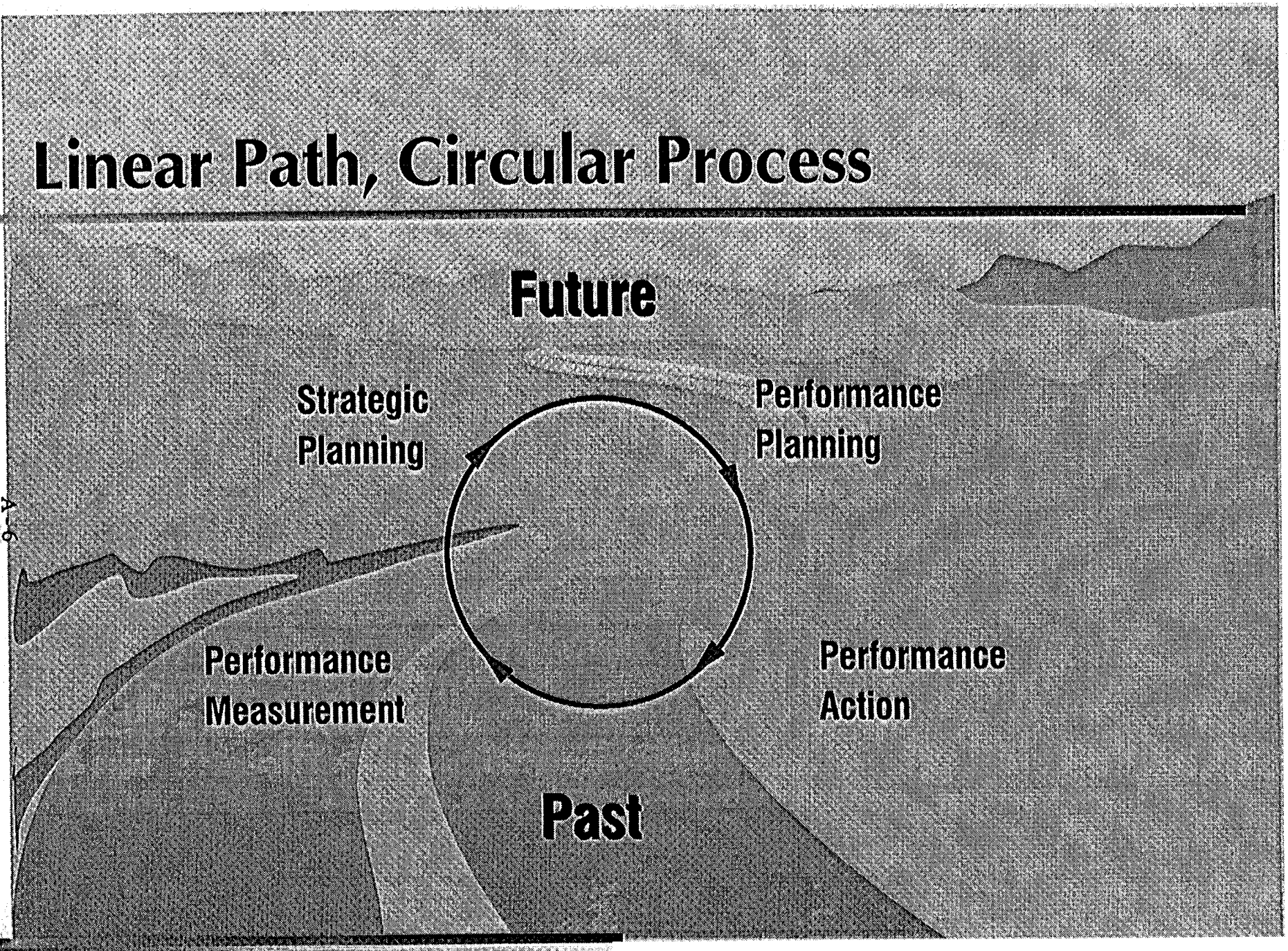

Government Performance & Results Act of 1993

- Purpose
  - To shift focus from what we are doing to what we are accomplishing
- Requirements
  - Strategic plans
  - Annual performance plans
  - Annual performance reports

DOE Comprehensive National Energy Strategy

Pursuit of market-based energy policy that supports higher living standards, economic security, and a clean environment through 5 specific goals:

- Improve Energy Efficiency
- Ensure against energy disruptions
- Promote energy production and use in ways that reflect human health and environmental values
- Expand future energy choices
- Cooperate internationally on energy issues

Government-Industry Interactions on Setting Geothermal R&D Priorities

1995	May	Meeting with Secretary O'Leary
	July	R&D Priorities Workshop
	December	Hot Dry Rock Workshop
1996	April	Drilling Workshop
	June	Reservoir Technology Workshop
1997	April	Energy Conversion Workshop
	August	Strategic Planning Workshop
	October	Planning Review Meeting
1998	January	Draft Strategic Plan
	February	Strategic Plan Survey

Geothermal Strategic Vision

By 2010, geothermal energy will be the preferred alternative to polluting energy sources throughout the world.

Geothermal Strategic Mission

Mission: OGT will work in partnership with U.S. industry to establish geothermal energy as a sustainable, environmentally sound, economically competitive contributor to the U.S. and world energy supply.

Strategic Plan Goals

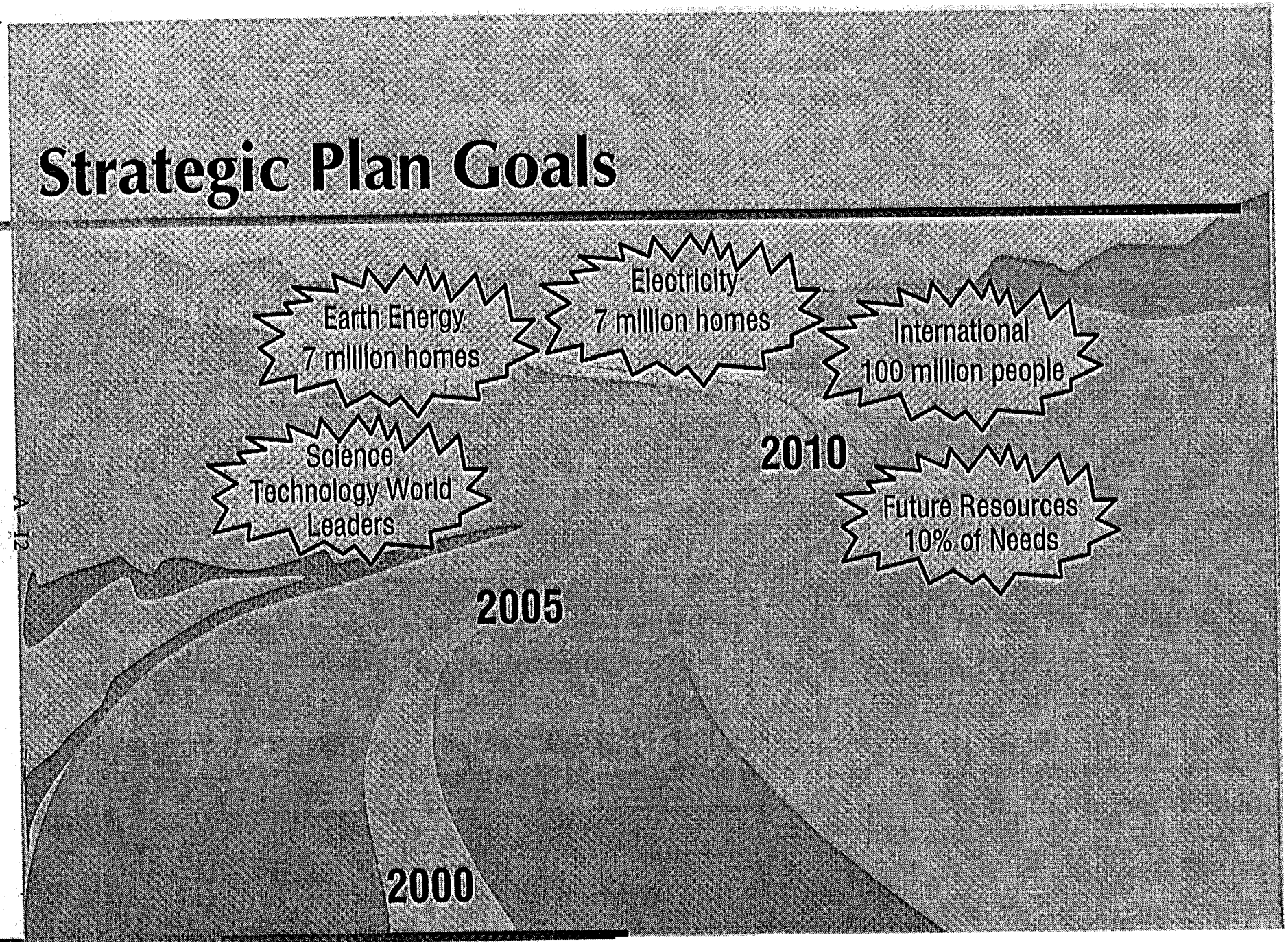

Survey Results

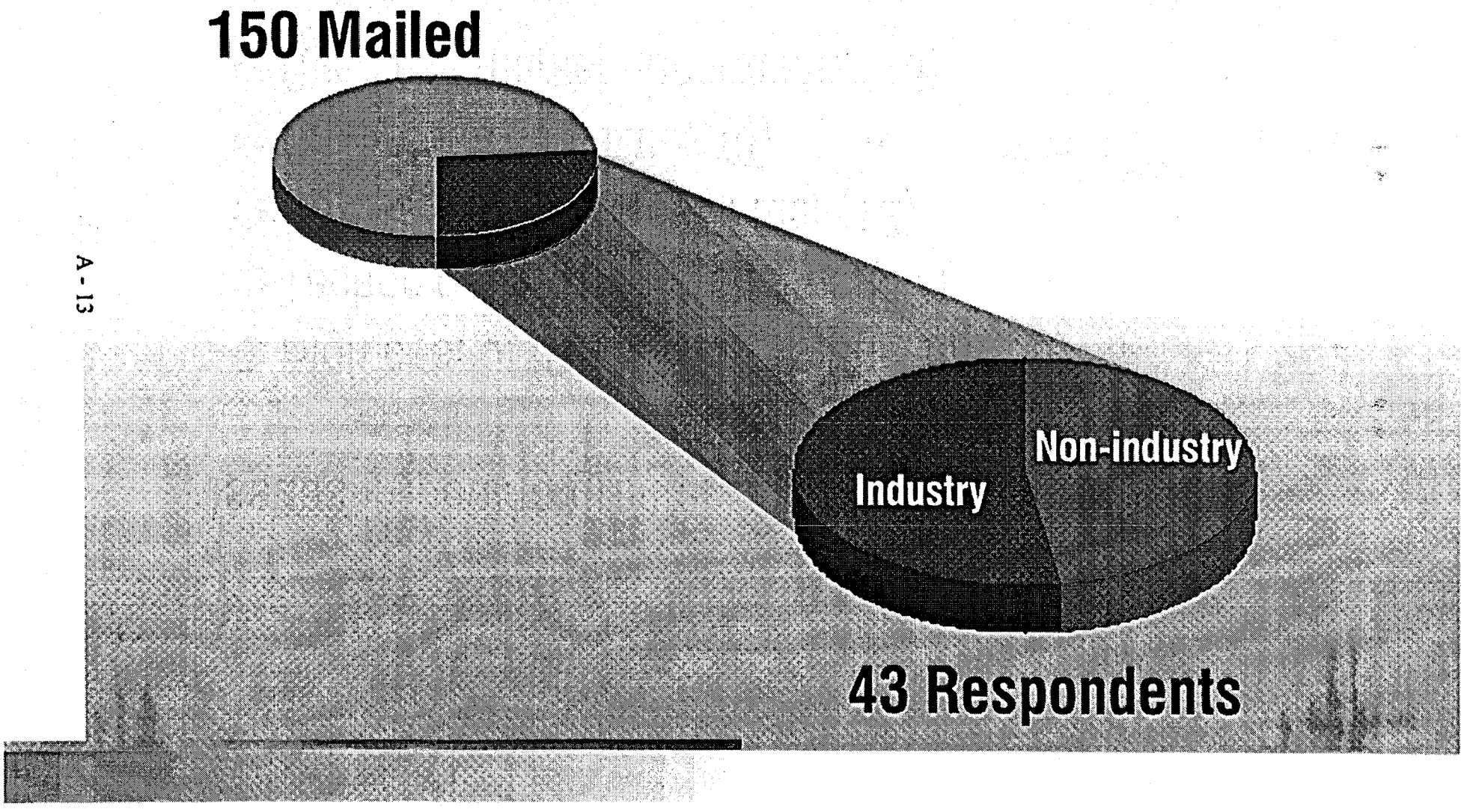

Survey Results

- Issues impeding greater use of geothermal energy
  - High cost of geothermal production (30)
  - Technology-related problems (17)
  - Competition from fossil fuel (12)
  - Credit for externalities (8)
  - Overseas market uncertainties (6)

Survey Results

- Do goals achieve vision?

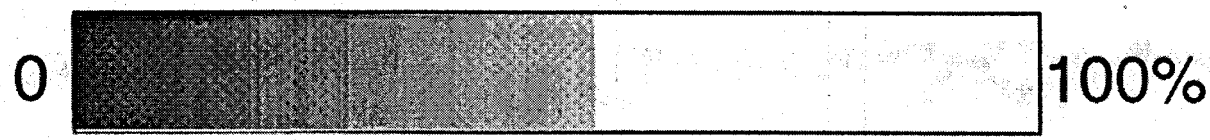

- Comments
  - Vision unrealistic
  - 7 million homes not enough
  - Better funded and conducted program needed
  - Show me how
  - Too little, too late

Survey Results

Ranking the Objectives Against the Goals

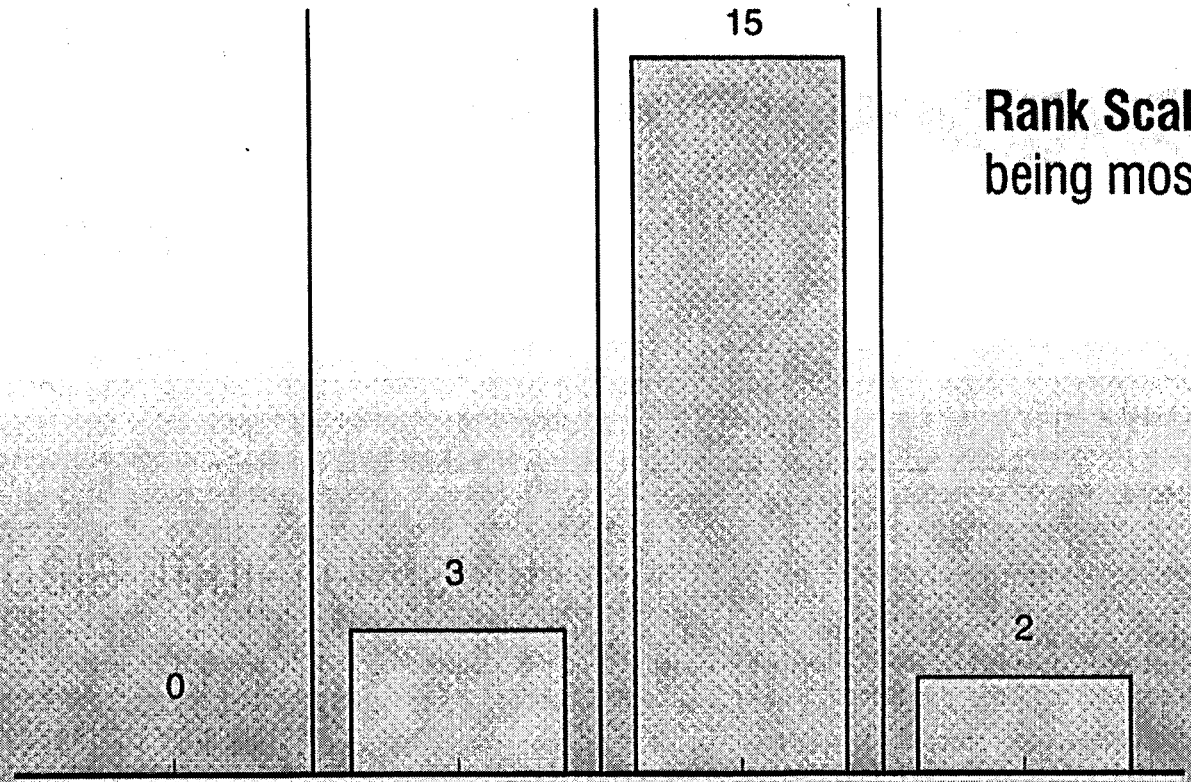

Rank Scale: 1-5, with 5 being most important

Survey Results

Ranking the Plan's Objectives

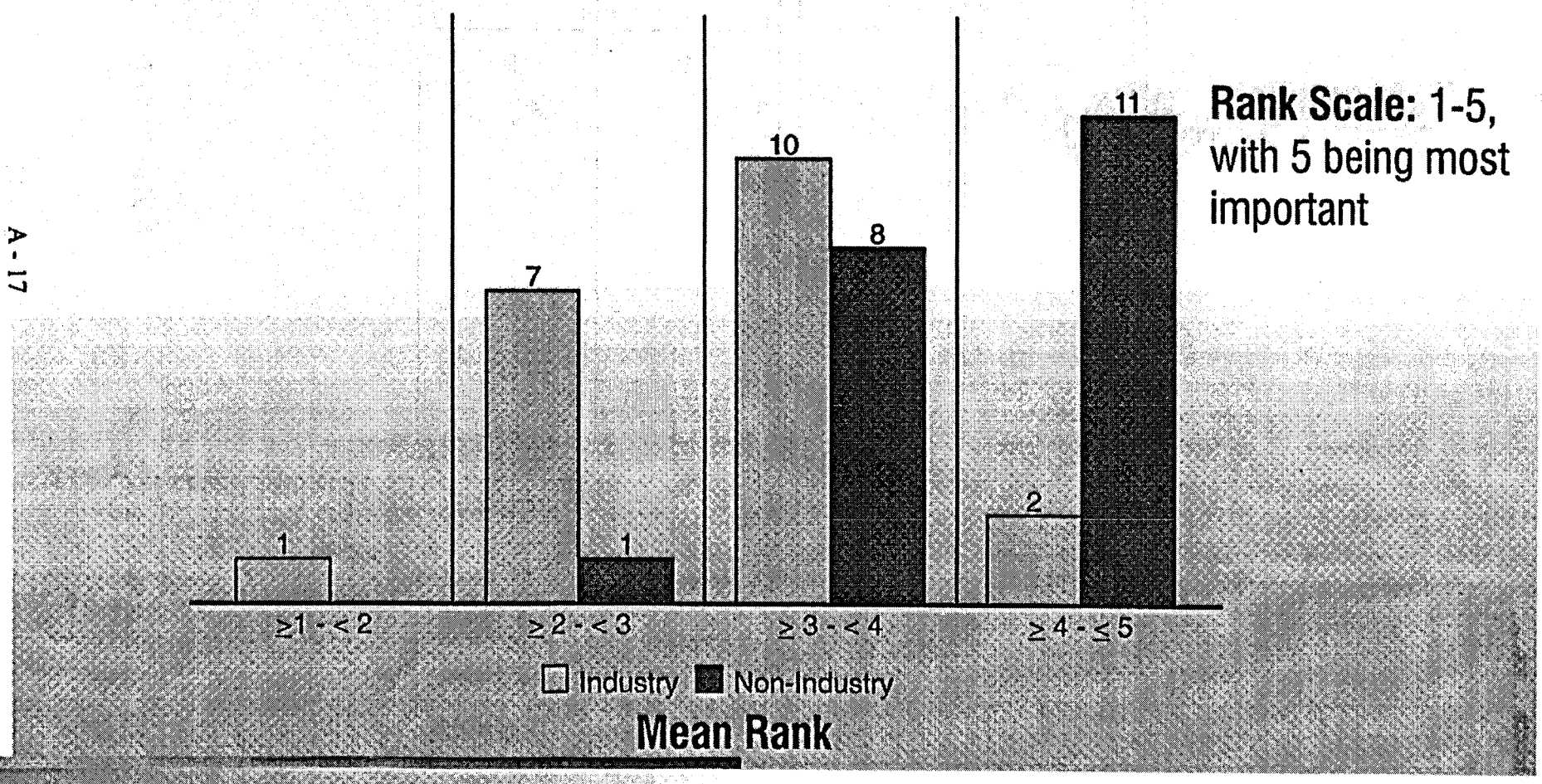

Survey Results

Strategic Budget Plan

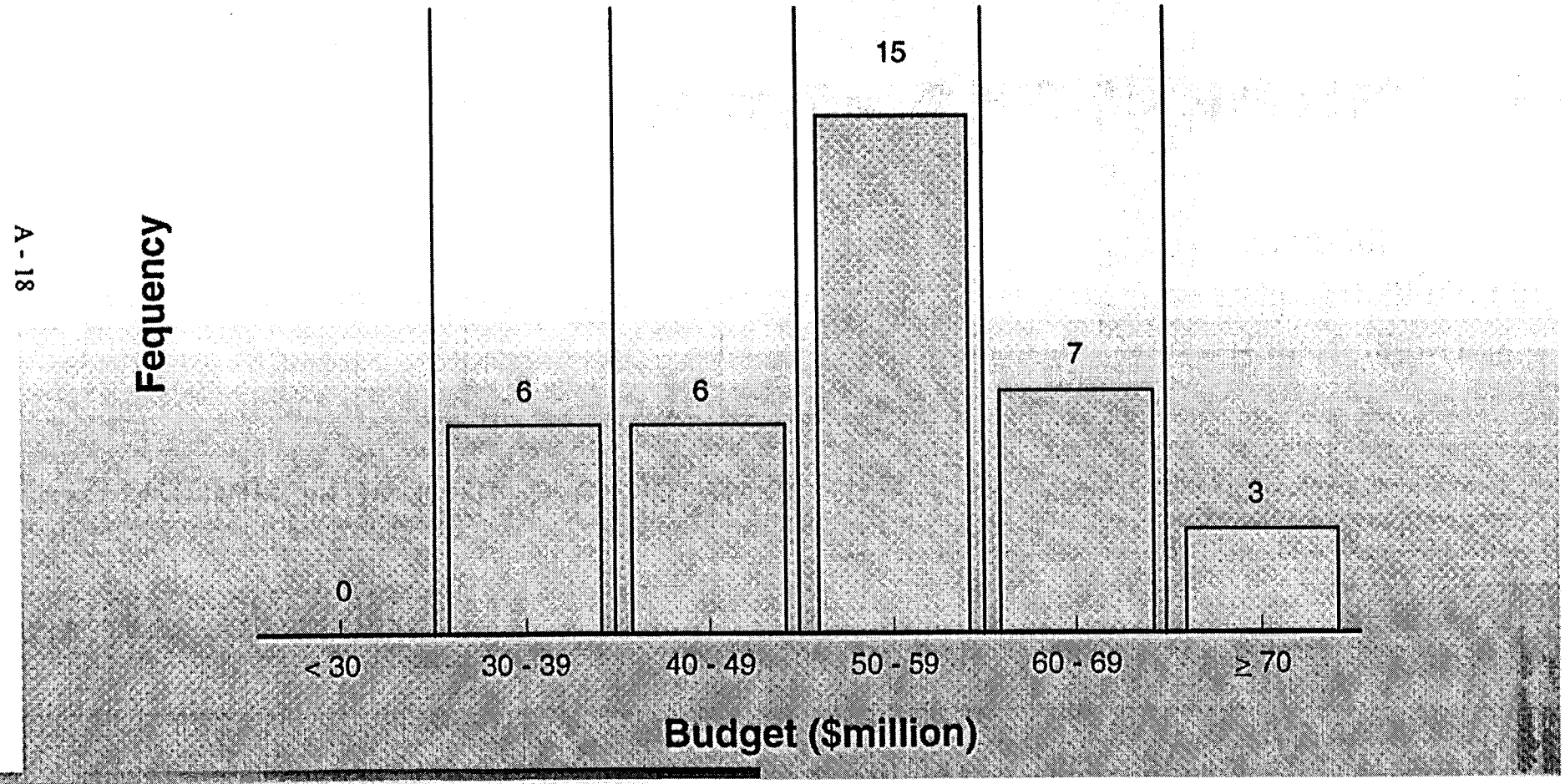

Planning Hierarchy

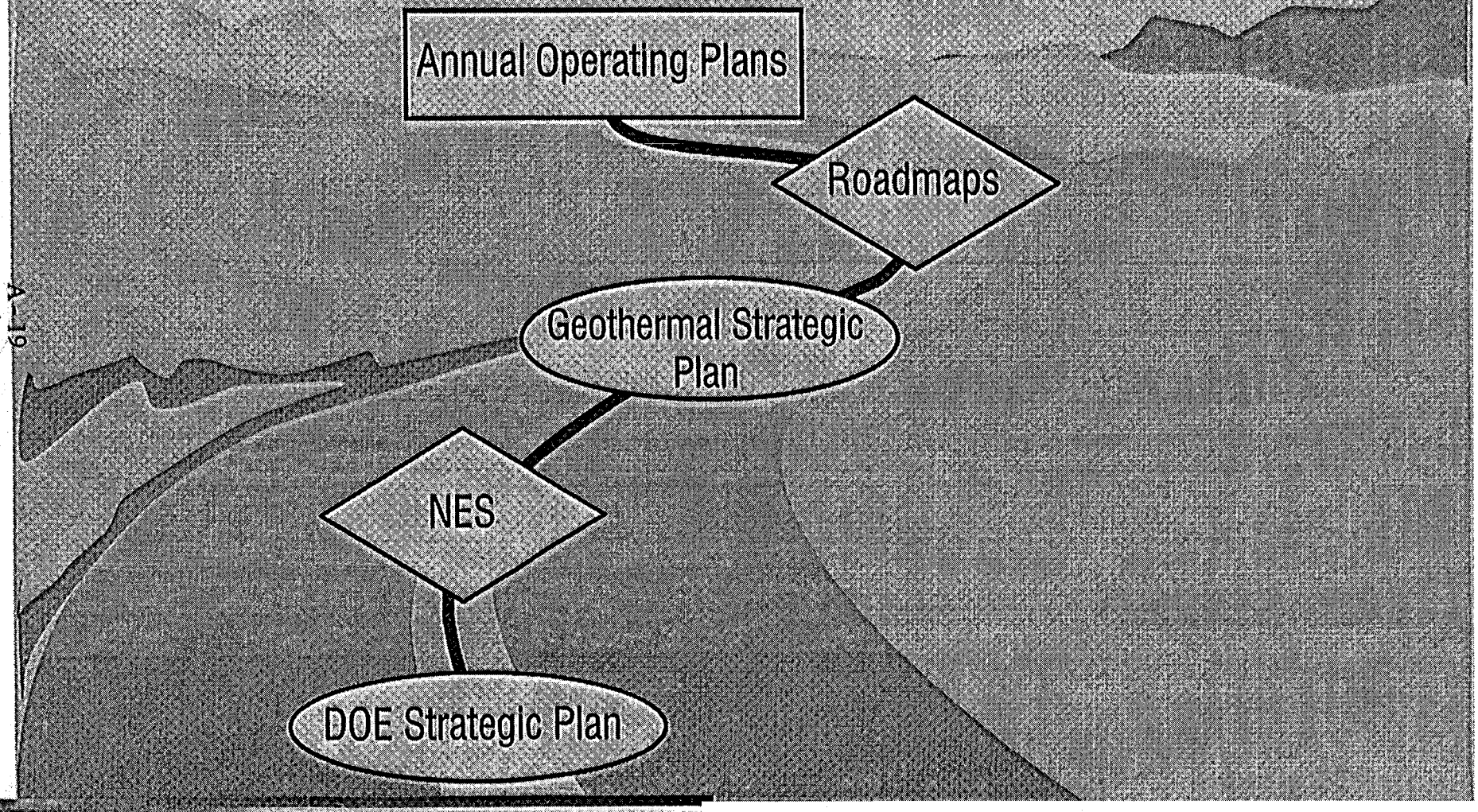

Survey Results Program Priorities

Program Element	Industry	Non-Industry
Exploration	3.83	4.10
Conventional Drilling	4.33	3.81
Advanced Drilling	4.17	3.71
Reservoir Technology	4.22	4.10
Conversion Technology	3.72	3.38
O&M	3.69	2.90
Hot Dry Rock	2.11	3.19
Direct Use	2.94	3.00
Geothermal Heat Pump	3.11	3.38
Education & Outreach	3.28	3.05

Rank Scale: 1 - 5, with 5 being the highest priority.

Survey Results
Program Priorities

Next Steps....

- Finalize Strategic Plan
- Develop Multi-Year Performance Plan (Roadmap)
- Develop Detailed FY 99 Annual Operating Plan

Don't Doubt the Future

"Where a calculator on the ENIAC is equipped with 18,000 vacuum tubes and weighs 30 tons, computers in the future may have only 1,000 vacuum tubes and weigh 1.5 tons"

Popular Mechanics, March 1949

Linear Path, Circular Process

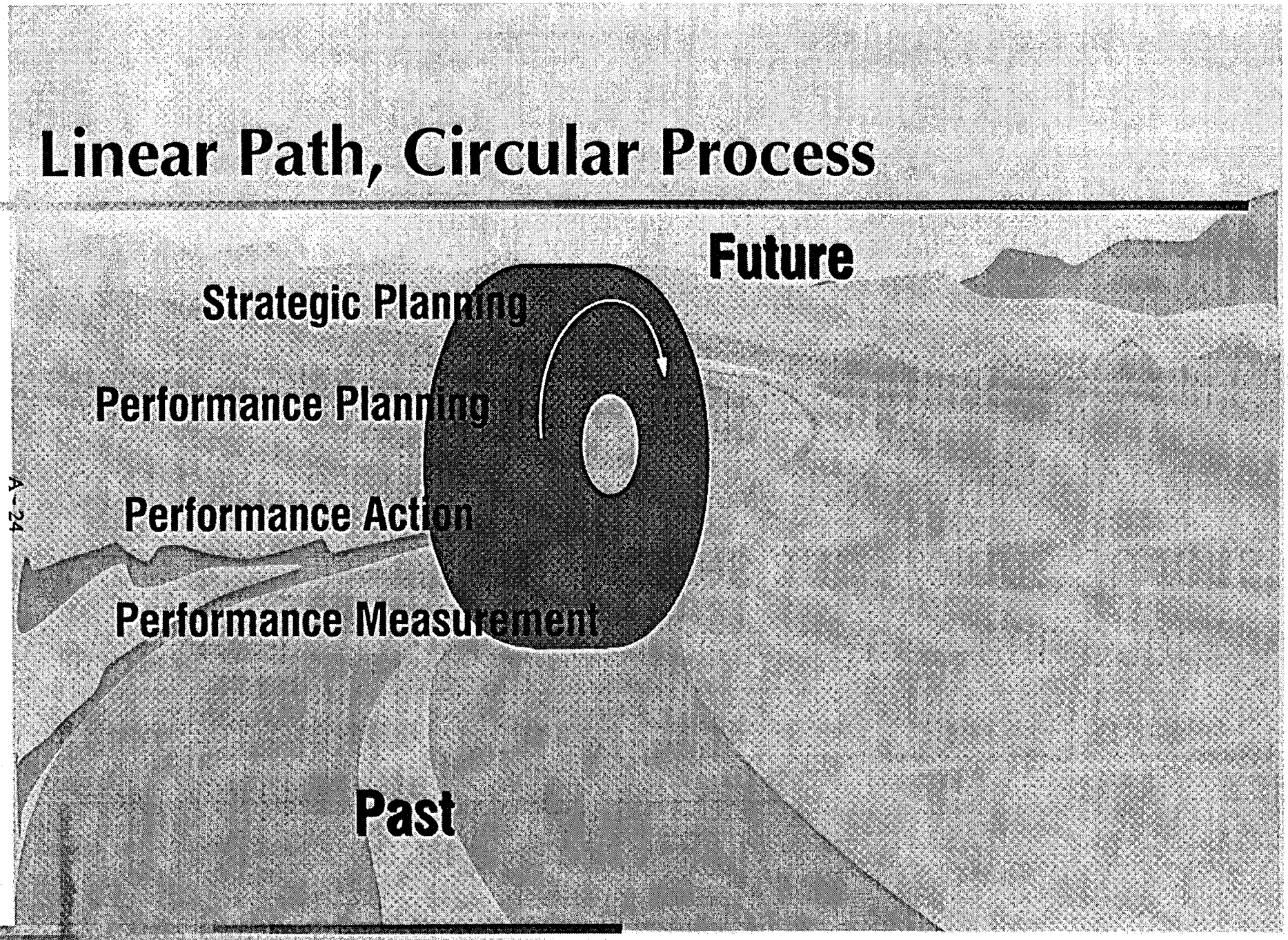

Appendix B:

Summary of Conference Evaluation
Final Agenda
List of Participants

Geothermal Program Review 16

Conference Evaluation Comments

Suggestions for future conference topics/sessions keynote speakers and presenters):

- Mack Kennedy from LBL - noble gas geochemistry.
- More emphasis on direct use, especially district energy systems.

Suggestions to improve future conferences:

- I'd prefer that future conferences be held in a more central location, i.e. downtown San Francisco or downtown Berkeley. In my opinion, the Berkeley Marina is too isolated a location. That's the only reason I put "disagree" in number 4.
- Too many speakers wasted our time presenting talks on research that has been covered in past years where little new information or progress has been made.
- Extend room block prices 3 days before and after the conference.
- No concurrent sessions.
- Focus on specific topics.

Other Comments:

- Mount a concerted effort to define, point out, and promote geothermal energy in the Renewables Technologies.
- This program had a nice mix of industry and regulatory input in the opening program.
- Crowded in rooms and between sessions.
- Concurrent sessions greatly reduce time available for discussions and don't allow sufficient time for "side meetings."
- Nice facility, smoothly run conference, but very isolated.

GEOTHERMAL PROGRAM REVIEW XVI
EVALUATION

		Strongly Agree	Agree	Disagree	Strongly Disagree
1.	The information presented has increased my knowledge and/or understanding of the DOE Geothermal Energy R&D Program.	50%	50%		
2.	Holding concurrent sessions was an effective way for me to spend my time at the conference.	22%	57%	14%	7%
3.	The panel discussion format facilitated information exchange among government, industry, and utility participants.	70%	30%		
4.	The conference logistics (facility, registration, meals, materials, etc.) were appropriate and effective.	25%	67%	8%	
		Excellent	**Good**	**Fair**	**Poor**
5.	Overall, I felt the conference was...	50%	50%		

6. Suggestions for future conference topics/sessions (including keynote speakers and presenters):

7. Suggestions to improve future conferences:

8. Other comments:

9. I work for:

36% Industry: _____ *(please specify)* 14% University/Research Organization 14% National Laboratory

DOE HQ | Other DOE Office | 7% Other Federal Agency | 29% Other _____ *(please specify)*

GEOTHERMAL PROGRAM REVIEW XVI

"STRATEGIC PLANNING FOR GEOTHERMAL RESEARCH"

TUESDAY EVENING, MARCH 31, 1998

7:00 - 9:00 PM	**OPENING RECEPTION AND CONFERENCE REGISTRATION**

WEDNESDAY, APRIL 1, 1998

8:00 AM	**REGISTRATION AND CONTINENTAL BREAKFAST**
9:00 - 11:45 AM	**OVERVIEW SESSION**
9:00 - 9:15 am	**Welcome and Announcements** Allan Jelacic, Director, Office of Geothermal Technologies, U.S. Department of Energy
9:15 - 9:35 am	**Keynote Presentation** Michal C. Moore, Commissioner, California Energy Commission
9:35 - 10:00 am	**Industry Keynote Presentation** Thomas Mason, President and Chief Operating Officer, CalEnergy Company, Inc.
10:00 - 10:30 AM	**BREAK**
10:30 - 10:55 am	**Industry Keynote Presentation** Randolph L. Howard, Vice President, Geothermal Operations, Unocal Corporation Geothermal
10:55 - 11:20 am	**Industry Keynote Presentation** Daniel Schochet, Vice President, Ormat International, Inc.
11:20 - 11:45 am	**Office of Geothermal Technologies Keynote Presentation** Allan Jelacic, Director, Office of Geothermal Technologies, U.S. Department of Energy
11:45 AM - 1:30 PM	**GEA LUNCHEON - "CHALLENGES AND OPPORTUNITIES GLOBAL WARMING PRESENTES FOR THE GEOTHERMAL INDUSTRY IN THE EMERGING COMPETITIVE MARKETS"** Ralph Cavanaugh, Co-Director, Energy Program, Natural Resources Defense Council

WEDNESDAY AFTERNOON, APRIL 1, 1998

TIME	EXPLORATION	ENERGY CONVERSION
1:30-1:50 pm	**Overview**, Marshall Reed, Office of Geothermal Technologies, U.S. Department of Energy	**Investigation of Innovative Cycles**, Desikan Bharathan, National Renewable Energy Laboratory
1:50-2:10 pm	**Geophysical Methods: Three-Dimensional SP Modeling**, Alan C. Tripp, Energy & Geoscience Institute, University of Utah	**Ammonia/Water Condensation Experiments**, Vahab Hassani, National Renewable Energy Laboratory
2:10-2:30 pm	**Geochemical Methods: Geothermal Chemistry in Exploration**, Deborah Bergfeld, Los Alamos National Laboratory	**Condensate Detection in Hydrocarbon Turbines**, Bob Evans or Greg Mines, Idaho National Engineering and Environmental Laboratory
2:30-2:50 pm	**Geological Methods: Mapping and Geologic Interpretation in the Coso Geothermal Area**, J. Douglas Walker, University of Kansas *(invited)*	**Kalina Demonstration Project at Steamboat Springs**, Hank Leibowitz, Exergy
2:50-3:10 pm	**The Awibengkok, Indonesia, Geothermal Research Project**, Jeff Hulen, Energy & Geoscience Institute, University of Utah	**Field Tests of Heat Exchanger Coatings**, Joint presentation by Keith Gawlick (National Renewable Energy Laboratory) and Toshifumi Sumaga (Brookhaven National Laboratory)

3:10-3:40 PM **BREAK**

TIME	RESERVOIR TECHNOLOGY	ENERGY CONVERSION (continued)
3:40-4:00 pm	**Development and Application of Inverse Modeling Techniques to Geothermal Problems**, Stefan Finsterle, E.O. Lawrence Berkeley National Laboratory	**Geothermal Heat Pump Grouting Materials**, Marita L. Allan, Brookhaven National Laboratory
4:00-4:20 pm	**Reservoir Physics: Water Adsorption**, Miroslaw Gruszkiewicz, Oak Ridge National Laboratory	**H2S Monitoring Using Laser Spectroscopy**, Judy Partin, Idaho National Engineering and Environmental Laboratory
4:20-4:50 pm	**Reservoir Chemistry: Chemical Models for Optimizing Geothermal Energy Production**, John Weare, University of California at San Diego	**H2S Monitoring Using Laser Spectroscopy**, Charles G. Stevens, Lawrence Livermore National Laboratory
4:50-5:10 pm	**Dixie Valley Field Studies: Fracture Permeability and In Situ Stress in the Dixie Valley, Nevada, Geothermal Reservoir**, Stephen Hickman, U.S. Geological Survey	**Geothermal Biocorrosion**, P.A. Pryfogle, Idaho National Engineering and Environmental Laboratory
5:10- 5:30 pm	**The Geysers Field Studies: Experimental Studies of Geysers Rock and Impacts on Exploration**, Brian Bonner, Lawrence Livermore National Laboratory	**Biochemical Processes for Geothermal Brine Treatment**, Eugene Premuzic, Brookhaven National Laboratory

5:30 PM **ADJOURN FOR THE DAY**

THURSDAY, APRIL 2, 1998

7:30 AM **REGISTRATION AND CONTINENTAL BREAKFAST**

TIME	DRILLING	HOT DRY ROCK WORKSHOP
8:30-8:50 am	**Overview of Sandia's Drilling Research,** David Glowka, Sandia National Laboratories	**Generate Concepts and Selection Criteria for "Dual-Use Technology" Research to Benefit Future Engineered Geothermal Systems and Near-Term Hydrothermal Systems** Moderators - Ted Mock and Dan Entingh, Princeton Economic Research, Inc.
8:50-9:10 am	**High-Temperature Electronics for Downhole Use,** Randy Normann, Sandia National Laboratories	
9:10-9:30 am	**Wireless Telemetry,** Doug Drumheller, Sandia National Laboratories	
9:30-9:50 am	**Mud Jet Augmented Bit,** TBA, Sandia National Laboratories	

9:50 AM **BREAK**

TIME	DRILLING (continued)	HOT DRY ROCK WORKSHOP (continued)
10:20-10:40 am	**Mini-Disc Cutter Bit,** James Fryant, Excavation Engineering	**Generate Concepts and Selection Criteria for "Dual-Use Technology" Research to Benefit Future Engineered Geothermal Systems and Near-Term Hydrothermal Systems (continued)** Working Breakout Groups and Reports
10:40-11:00 am	**High-Speed Bearing for Roller Cone Bits,** M.S. Kalsi, Kalsi Engineering	
11:00-11:20 am	**Advanced Bonding Technique for TSP Cutters,** Dan Goodman, Science and Research Lab	
	DIRECT USE	
11:20-11:40 am	**Direct Use Utilization at the Geo-Heat Center,** John Lund, Geo-Heat Center, Oregon Institute of Technology	
11:40am-Noon	**Geothermal Heat Pumps,** John Geyer, John Geyer & Associates, Inc. *(invited)*	

NOON **HOSTED LUNCH**

TIME	A STRATEGIC PLAN FOR GEOTHERMAL RESEARCH
1:30-3:00 pm	**Electric Power Generation,** Tim Anderson, Unocal Corporation **Direct Use Applications,** John Lund, Geo-Heat Center, Oregon Institute of Technology **International Geothermal Development,** Gerald Huttrer, Geothermal Management Company, Inc. **Science and Technology,** Roland Horne, Stanford University **Advanced Engineered Geothermal Systems,** Daniel Schochet, Ormat International, Inc.

3:00PM **CLOSING REMARKS**
Allan Jelacic, Director,
Office of Geothermal Technologies, U.S. Department of Energy

Address Listing of Registrants: Complete List

Jeff W. Adams
Energy Commission Specialist
California State Lands Commission
200 Oceangate, 12th Floor
Long Beach, CA 90802
Phone: (562) 590-5201
Fax: (562) 590-5295
Internet: adamsj@slc.ca.gov

James N. Albright
Group Leader
Los Alamos National Laboratory
Earth and Environmental Sciences Division
MS D-443
Los Alamos, NM 87545
Phone: (505) 667-4318
Fax: (505) 667-8487
Internet: albright@seismo5.lanl.gov

Marita Allan
Associate Scientist
Brookhaven National Laboratory
Building 526, 12 North Sixth Street
Upton, NY 11973
Phone: (516) 344-3060
Fax: (516) 344-2359
Internet: allan@bnl.gov

Tim D. Anderson
Research Coordinator
Unocal Corporation
1300 North Dutton Avenue
Santa Rosa, CA 95401
Phone: (707) 521-7611
Fax: (707) 521-7604
Internet: tanderson@unocal.com

Leon D. Ballew
Owner
Ballew Tool Company
P.O. Box 361
Cobb, CA 95426
Phone: (707) 987-0837
Fax: (707) 987-0696

Bill Barham
Technical Director
Johnston Pump Company
3215 Producer Way
Pomona, CA 91768
Phone: (909) 594-9959
Fax: (909) 594-2609
Internet: bill_barham@compuserve.com

Ronald C. Barr
President
Earth Power Resources, Inc.
2534 East 53rd Street
Tulsa, OK 74105
Phone: (918) 743-5593
Fax: (918) 743-5594
Internet: erthpower1@aol.com

Liz Battocletti
Senior Associate
Bob Lawrence & Associates, Inc.
424 North Washington Street
Alexandria, VA 22314
Phone: (703) 836-0304
Fax: (703) 836-6068
Internet: ecbatto@aol.com

Jorg Baumgartner
Project Coordinator
Socomine
Route de Kutzenhausen - B.P.39
F-67250 Soultz-Sous-Forets, France
Phone: 33-03-88-80-53-63
Fax: 33-03-88-80-53-51
Internet: baria@zeus.pandemonium.fr

Douglas Bell
Ansaldo North America, Inc.
430 Mountain Avenue
New Providence, NJ 07974
Phone: (908) 771-7410
Fax: (908) 771-5972

Dick Benoit
Resource Manager
Oxbow Power Services, Inc.
9790 Gateway Drive, Suite 220
Reno, NV 89511
Phone: (702) 850-2229
Fax: (702) 850-2211
Internet: dick_benoit@opsi.oxbow.com

John J. Berger
Environmental Consultant & Author
LSA Associates, Inc.
157 Park Place
Point Richmond, CA 94801
Phone: (510) 231-7714
Fax: (510) 236-3480
Internet: hfws90a@prodigy.com

Deb Bergfeld
Graduate Research Assistant
Los Alamos National Laboratory
EES-1, MS D462
Los Alamos, NM 87545
Phone: (505) 667-1812
Fax: (505) 665-3285
Internet: debberg@lanl.gov

Desikan Bharathan
Senior Engineer
National Renewable Energy Laboratory
1617 Cole Boulevard
Golden, CO 80401
Phone: (303) 384-7418
Fax: (303) 384-7495
Internet: desikan_bharathan@nrel.gov

D. Jo Blais
Conference Coordinator
Princeton Economic Research, Inc.
1700 Rockville Pike, Suite 550
Rockville, MD 20852
Phone: (301) 468-8412
Fax: (301) 230-1232
Internet: jblais@perihq.com

R. Gordon Bloomquist
Senior Scientist
Washington State University Energy Program
Box 43165
Olympia, WA 98504
Phone: (360) 956-2016
Fax: (360) 956-2030
Internet: bloomquistr@energy.wsu.edu

Brian Bonner
Group Leader, Experimental Geophysics Group
Lawrence Livermore National Laboratory
7000 East Avenue
P.O. Box 808, L-201
Livermore, CA 94551
Phone: (510) 422-7080
Fax: (510) 423-1057
Internet: bonner1@llnl.gov

Tonya "Toni" Boyd
Research Assistant
Geo-Heat Center
Oregon Institute of Technology
3201 Campus Drive
Klamath Falls, OR 97601
Phone: (541) 885-1750
Fax: (541) 885-1754
Internet: boydt@oit.edu

Marc A. Brennen
District Sales Engineer
BJ Services Company
80 Bee Jay Way
Woodland, CA 95776
Phone: (530) 662-3932
Fax: (530) 662-1972

Carol J. Bruton
Lawrence Livermore National Laboratory
L-219
P.O. Box 808
Livermore, CA 94550
Phone: (925) 423-1936
Fax: (925) 422-0208
Internet: brutonl.@llnl.gov

Kerry L. Burns
165 Chamisa Street
Los Alamos, NM 87544
Phone: (505) 662-4254
Fax: (505) 662-1561

Ken Byers
Director
Central California Power Agency
9500 Coldwater Creek Road
Kelseyville, CA 95451
Phone: (707) 928-5208
Fax: (707) 928-5144

Louis E. Capuano, Jr.
Drilling Engineer
ThermaSource, Inc.
P.O. Box 1236
Santa Rosa, CA 95402
Phone: (707) 523-2960
Fax: (707) 523-1029
Internet: lcapuano@cds1.net

Donald Carder
President
Cobb Mountain Estates, Inc.
9820 Kelsey Creek Drive
Kelseyville, CA 95451
Phone: (707) 279-8648
Fax: (707) 279-8927

Anna Carter
Geothermal Support Services
3125 Carvel Drive
Santa Rosa, CA 95405
Phone: (707) 578-3979
Fax: (707) 578-3979

Ralph Cavanaugh
Co-director, Energy Program, NRDC
Natural Resources Defense Council
71 Stevenson Street
San Francisco, CA 94105
Phone: (415) 777-0220
Fax: (415) 495-5996

Ravi Chhatre
Corrosion Engineer
Pacific Gas & Electric
3400 Crow Canyon Road
San Ramon, CA 94583
Phone: (510) 866-5311
Fax: (510) 866-5511
Internet: rmc3@pge.com

Prame N. Chopra
Australian National University
ACT Australia
fax: 61-2-62495544
0200
Internet: prame.chopra@anu.edu.au

Ted Clutter
Executive Director
Geothermal Resources Council
P.O. Box 1350
Davis, CA 95617
Phone: (530) 758-2360
Fax: (530) 758-2839
Internet: tclutter@concentric.net

Jim Combs
Principal
Geo Hills Associates
27790 Edgerton Road
Los Altos Hills, CA 94022
Phone: (650) 941-5480
Fax: (650) 941-5480
Internet: jimjeany@ix.netcom.com

Dean Cooley
Generation Coordinator
Pacific Gas & Electric Company - Geysers
P.O. Box 456
Healdsburg, CA 95448
Phone: (707) 431-6077
Fax: (707) 431-6207
Internet: ldc3@pge.com

Bob Creed
Geotechnical Scientist
U.S. Department of Energy
Idaho Operations Office
850 Energy Drive, MS 1220
Idaho Falls, ID 83401
Phone: (208) 526-9063
Fax: (208) 526-5964
Internet: creedrj@inel.gov

William L. D'Olier
Geothermal Energy Consultant
310 Hume Lane
Bakersfield, CA 93309
Phone: (805) 832-5786
Fax: (805) 837-1478

Alicia D. Decina
Publications & Administration Coordinator
Geothermal Energy Association
122 C Street, NW, Suite 400
Washington, DC 20001
Phone: (202) 383-2666
Fax: (202) 383-2678
Internet: adecina@geotherm.org

Donald J. DePaolo
Department Head, Center Isotope Geochemistry
E.O. Lawrence Berkeley National Laboratory
Department of Geology & Geophysics
395 Earth Sciences Building, MS 90-1116
Berkeley, CA 94720
Phone: (510) 495-2228
Fax: (510) 486-7070
Internet: depaolo@socrates.berkeley.edu

Perle M. Dorr
Director of Outreach Programs
Geothermal Energy Association
122 C Street, NW, Suite 400
Washington, DC 20001
Phone: (202) 383-2673
Fax: (202) 383-2678
Internet: pdorr@geotherm.org

Douglas S. Drumheller
Distinguished Member of the Technical Staff
Sandia National Laboratories
P.O. Box 5800, MS 1033
Albuquerque, NM 87185
Phone: (505) 844-8920
Fax: (505) 844-3952
Internet: dsdrumh@sandia.gov

Dan Entingh
Senior Economist
Princeton Economic Research, Inc.
1700 Rockville Pike, Suite 550
Rockville, MD 20852
Phone: (301) 881-0650
Fax: (301) 230-1232
Internet: dentingh@perihq.com

Mel Erskine
Consulting Geologist
5413 Silva Avenue
El Cerrito, CA 94530
Phone: (510) 234-6214
Fax: (510) 234-5371
Internet: merskine@ix.netcom.com

Gracio Fabris
President
Fas Engineering, Inc.
2039 Dublin Drive
Glendale, CA 91206
Phone: (818) 952-0217
Fax: (818) 952-0217

D. D. Faulder
Advisory Scientist
Idaho National Engineering & Environmental Laboratory
P.O. Box 1625
Idaho Falls, ID 83415
Phone: (208) 526-0674
Fax: (208) 526-0969
Internet: ddf@inel.gov

Stefan Finsterle
E.O. Lawrence Berkeley National Laboratory
One Cyclotron Road, MS 90-1116
Berkeley, CA 94720
Phone: (510) 486-5205
Fax: (510) 486-5686
Internet: safinsterle@lbl.gov

Raymond Fortuna
Senior Program Manager
U.S. Department of Energy
Office of Geothermal Technologies
1000 Independence Avenue, SW
Washington, DC 20585
Phone: (202) 586-1711
Fax: (202) 586-8185
Internet: raymond.fortuna@hq.doe.gov

George Frye
1412 Lorraine Way
Santa Rosa, CA 95404
Phone: (510) 486-4889
Fax: (510) 486-7070
Internet: gafrye@lbl.gov

Sabodh K. Garg
Senior Scientist
Maxwell Technologies
8888 Balboa Avenue
San Diego, CA 92123
Phone: (619) 576-7752
Fax: (619) 637-7411
Internet: garg@maxwell.com

Karl Gawell
Executive Director
Geothermal Energy Association
122 C Street, NW, Suite 400
Washington, DC 20001
Phone: (202) 383-2674
Fax: (202) 383-2678
Internet: kgawell@geotherm.org

Keith Gawlik
Staff Research Engineer
National Renewable Energy Laboratory
1617 Cole Boulevard
Golden, CO 80401
Phone: (303) 384-7515
Fax: (303) 384-7540
Internet: keith_gawlik@nrel.gov

John Geyer
President
Sound Geothermal
P.O. Box 84490
Vancouver, WA 98684
Phone: (306) 694-9123
Fax: (306) 694-9201
Internet: jgeyer@soundgt.com

David A. Glowka
Manager, Geothermal Research Department
Sandia National Laboratories
P.O. Box 5800, MS 1033
Albuquerque, NM 87185
Phone: (505) 844-3601
Fax: (505) 844-3952
Internet: daglowk@sandia.gov

Paul E. Grabowski
Program Manager
U.S. Department of Energy
Office of Geothermal Technologies
1000 Independence Avenue, SW
Washington, DC 20585
Phone: (202) 586-0478
Fax: (202) 586-8185

Murray G. Grande
Plant Engineer
Northern California Power Agency
P.O. Box 663
Middletown, CA 95461
Phone: (707) 987-4033
Fax: (707) 987-4039
Internet: mggncpa@inreach.com

Ken Green
Senior Technical Staff
BCS, Inc.
5550 Sterrett Place, Suite 216
Columbia, MD 21044
Phone: (410) 997-7778
Fax: (410) 997-7669
Internet: bcs@clark.net

Jerry P. Greenberg
Staff Scientist
San Diego Supercomputer Center
P.O. Box 85608
San Diego, CA 92186
Phone: (619) 534-5138
Internet: jpg@sdsc.edu

M. S. Gruszkiewicz
Research Staff Member
Oak Ridge National Laboratory
Lockheed Martin Energy Research
P.O. Box 2008, Building 4500S, MS 61
Oak Ridge, TN 37831
Phone: (423) 574-4965
Fax: (423) 574-4961
Internet: xuk@ornl.gov

Raymond Guenther
Professor
University of Nebraska at Omaha
Department of Physics
Omaha, NE 68182
Phone: (402) 554-3726
Fax: (402) 554-3100

Mohinder S. Gulati
Chief Engineer
Unocal Corporation
P.O. Box 2390
Brea, CA 92822
Phone: (714) 985-6402
Fax: (714) 985-6301
Internet: mgulati@unocal.com

Douglas S. Hackley
Project Manager, Geothermal & Power Operations
Unocal Corporation
1300 North Dutton Avenue
Santa Rosa, CA 95401
Phone: (707) 521-7644
Fax: (707) 521-7603
Internet: dhackley@unocal.com

Jeff Hahn
Project Manager
U.S. Department of Energy
Golden Field Office
1617 Cole Boulevard
Golden, CO 80401
Phone: (303) 275-4775
Fax: (303) 275-4753
Internet: jeff_hahn@nrel.gov

Bob Hare
Technology Transfer Specialist
California Energy Commission
1516 Ninth Street, MS 43
Sacramento, CA 95814
Phone: (916) 653-8685
Fax: (916) 653-6010
Internet: bhare@energy.state.ca.us

Christopher K. Harris
Shell International Exploration & Production B.V.,
Research and Technical Services
2280 AB Rijswijk, P.O. Box 60
The Netherlands
Phone: 31-70-311-2845
Fax: 31-70-311-3366
Internet: c.k.harris@siep.shell.com

Vahab Hassani
Senior Engineer
National Renewable Energy Laboratory
1617 Cole Boulevard
Golden, CO 80401
Phone: (303) 384-7464
Fax: (303) 384-7495
Internet: vahab_hassani@nrel.gov

Lance Hays
President
Douglas Energy Company
181 West Orangethorpe Avenue, Suite D
Placentia, CA 92670
Phone: (714) 524-3338
Fax: (714) 524-3341
Internet: deco@interserv.com

Joe Henfling
Principal Technologist
Sandia National Laboratories
P.O. Box 5800, MS 1033
Albuquerque, NM 87185
Phone: (505) 844-6720
Fax: (505) 844-3952
Internet: jahenfl@sandia.gov

Stephen Hickman
Geophysicist
U.S. Geological Survey
345 Middlefield Road, MS 977
Menlo Park, CA 94025
Phone: (650) 329-4807
Fax: (650) 329-5163
Internet: hickman@thepub.wr.usgs.gov

Gale Higgins
Plant Superintendent
Sacramento Municipal Utility District
P.O. Box 1269
Cobb, CA 95426
Phone: (707) 987-3136
Fax: (707) 987-2024

Donald G. Hill
Senior Associate Geophysicist
Weiss Associates
5500 Shellmound Street
Emeryville, CA 94608
Phone: (510) 450-6000
Fax: (510) 547-5043
Internet: dgh@weiss.com

Susan Hodgson
Editor
California Division of Oil, Gas, & Geothermal
Resources
801 K Street, MS 20-20
Sacremento, CA 95814
Phone: (916) 445-9686
Fax: (916) 323-0424
Internet: shodgson@consrv.ca.gov

Tim Hollingshead
TSS Supervisor
Pacific Gas & Electric Company - Geysers
PO Box 456
Healdsburg, CA 95448
Phone: (707) 431-6042
Fax: (707) 431-6207
Internet: twh4@pge.com

Ben Holt
Chairman Emeritus
Ben Holt Company
201 South Lake Avenue, Suite 300
Pasadena, CA 91101
Phone: (626) 795-6866
Fax: (626) 584-9210

Roland N. Horne
Professor & Chairman
Stanford University
Department of Petroleum Engineering
Green Earth Science Building, Room 064
Stanford, CA 94305
Phone: (650) 723-9595
Fax: (650) 725-2099
Internet: horne@pangea.stanford.edu

Randolph L. Howard
Group Vice President, International Operations/Geothermal
Unocal Corporation
2929 East Imperial Highway, Room 200
Brea, CA 92821
Phone: (714) 985-6994
Fax: (714) 985-6301
Internet: gtlarlh@unocal.com

Jeffrey B. Hulen
Senior Geologist
Energy & Geoscience Institute
University of Utah
423 Wakara Way, Suite 300
Salt Lake City, UT 84108
Phone: (801) 581-8497
Fax: (801) 585-3540
Internet: jhulen@egi.utah.edu

Shirley M. Hunt
Area Underwriter
Chicago Title Company
2425 West Shaw, Suite A
Fresno, CA 93711
Phone: (209) 228-5562
Fax: (209) 226-2879

Gerry Huttrer
President
Geothermal Management Company, Inc.
P.O. Box 2425
Frisco, CO 80443
Phone: (970) 668-3465
Fax: (970) 668-3074
Internet: ghuttrer@colorado.net

Cathy J. Janik
Geochemist/Geologist
U.S. Geological Survey
345 Middlefield Road, MS 910
Menlo Park, CA 94025
Phone: (650) 329-5213
Fax: (650) 329-5203

Allan Jelacic
Director
U.S. Department of Energy
Office of Geothermal Technologies
1000 Independence Avenue, SW
Washington, DC 20585
Phone: (202) 586-6054
Fax: (202) 586-8185
Internet: allan.jelacic@hq.doe.gov

Mary Johannis
Targeted Technologies Manager
California Energy Commission
1516 Ninth Street, MS 43
Sacramento, CA 95814
Phone: (916) 654-4611
Fax: (916) 653-6010
Internet: mjohanni@energy.state.ca.us

Edward A. Johnson
Senior Engineer
MSE-TA
Box 4078
Butte, MT 59701
Phone: (406) 494-7337
Fax: (406) 494-7230
Internet: cajohn@in-tch.com

Stuart D. Johnson
Geologist
Oxbow Power Systems, Inc.
9790 Gateway Drive, Suite 220
Reno, NV 89511
Phone: (702) 850-2248
Fax: (702) 850-2211
Internet: stu_johnson@opsi.oxbow.com

Ron Judkoff
Director, Center for Thermal Systems
National Renewable Energy Laboratory
1617 Cole Boulevard
Golden, CO 80401
Phone: (303) 384-7520
Fax: (303) 384-7540
Internet: ron_judkoff@nrel.gov

Douglas Jung
Principal Engineer
Two-Phase Engineering
3209 Franz Valley Road
Santa Rosa, CA 95404
Phone: (707) 523-4585
Fax: (707) 528-2071
Internet: two-phase@juno.com

Erick Kaarlela
Senior Petroleum Engineer
Bureau of Land Management
3620 Elderberry Place
Fairfax, VA 22033
Phone: (202) 452-0341
Fax: (202) 452-0386
Internet: ekaarlel@wo.blm.gov

M. S. Kalsi
President
Kalsi Engineering, Inc.
745 Park Two Drive
Sugar Land, TX 77478
Phone: (281) 240-6500
Fax: (281) 240-0255

Paul Kasameyer
Geothermal Program Leader
Lawrence Livermore National Laboratory
7000 East Avenue
P.O. Box 808, L-203
Livermore, CA 94551
Phone: (510) 422-6487
Fax: (510) 423-2163
Internet: kasameyerl@llnl.gov

Dennis Kaspereit
Manager, Resource Technology
CalEnergy Company, Inc.
900 North Heritage Drive, Building D
Ridgecrest, CA 93555
Phone: (760) 499-2326
Fax: (760) 499-2348
Internet: dennis.kaspereit@calenergy.com

Mack Kennedy
Staff Scientist
E. O. Lawrence Berkeley National Laboratory
MS 70A-3363
Berkeley, CA 94720
Phone: (514) 866-6451
Fax: (510) 486-5496
Internet: dmkennedy@lbc.gov

Brian A. Koenig
Senior Geochemist/Geologist
Unocal Geothermal and Power Operations Group
1300 North Dutton Avenue
Santa Rosa, CA 95401
Phone: (707) 521-7645
Fax: (707) 521-7603
Internet: bkoenig@unocal.com

Michael Kramer
Energy Specialist/Project Manager
California Energy Commission
1516 Ninth Street, MS 43
Sacramento, CA 95691
Phone: (916) 654-4599
Fax: (916) 653-6010

Zvi Krieger
Director, System Engineering
Ormat Technologies, Inc.
980 Greg Street
Sparks, NV 89431
Phone: (702) 356-9029
Fax: (702) 356-9039

Chuck Kutscher
Senior Engineer
National Renewable Energy Laboratory
1617 Cole Boulevard
Golden, CO 80401
Phone: (303) 384-7521
Fax: (303) 384-7540
Internet: chuck_kutscher@nrel.gov

Raymond J. LaSala
Senior Program Manager
U.S. Department of Energy
Office of Geothermal Technologies
1000 Independence Avenue, SW
Washington, DC 20585
Phone: (202) 586-4198
Fax: (202) 586-8185
Internet: raymond.lasala@hq.doe.gov

L.R. Lawrence, Jr.
President
Bob Lawrence & Associates, Inc.
424 North Washington Street
Alexandria, VA 22314
Phone: (703) 836-3654
Fax: (703) 683-4379
Internet: boblaw424@aol.com

Hank Leibowitz
Vice President Engineering
Exergy, Inc.
22320 Foothill Boulevard, Suite 540
Hayward, CA 94541
Phone: (510) 537-5881
Fax: (510) 537-8621

Bill Livesay
Livesay Consultants
126 Countrywood Lane
Encinitas, CA 92024
Phone: (760) 436-1307
Fax: (760) 942-8375
Internet: livesay@worldnet.att.net

David B. Lombard
Technical Director
6640 Hazel Lane
McLean, VA 22101
Phone: (703) 356-1848
Fax: (703) 821-1729
Internet: dlombard@erols.com

John W. Lund
Director
Geo-Heat Center
Oregon Institute of Technology
3201 Campus Drive
Klamath Falls, OR 97601
Phone: (541) 885-1750
Fax: (541) 885-1754
Internet: lundj@oit.edu

Ernie Major
E.O. Lawrence Berkeley National Laboratory
One Cyclotron Road, MS 90-1116
Berkeley, CA 94720
Phone: (510) 486-6709
Fax: (510) 486-5686
Internet: elmajor@lbl.gov

Thomas R. Mason
President and Chief Operating Officer
CalEnergy Company, Inc.
307 South 36th Street, Suite 400
Omaha, NE 68131
Phone: (402) 341-4500
Fax: (402) 231-1403

Grace Mata
Geothermal Resources Council
P.O. Box 1350
2001 Second Street, Suite 5
Davis, CA 95617
Phone: (916) 758-2360
Fax: (916) 758-2839

Ann McKinney
Director, Export Programs
Geothermal Energy Association
122 C Street, NW, Suite 400
Washington, DC 20001
Phone: (202) 383-2553
Fax: (202) 383-2678
Internet: annmck@geotherm.org

Lynn McLarty
Senior Engineer
Princeton Economic Research, Inc.
1700 Rockville Pike, Suite 550
Rockville, MD 20852
Phone: (301) 881-0650
Fax: (301) 230-1232
Internet: lmcclarty@perihq.com

Tsvi Meidav
President
Trans-Pacific Geothermal Corporation
1901 Harrison Street, Suite 1590
Oakland, CA 94612
Phone: (510) 763-7812
Fax: (510) 763-2504
Internet: tgcorp@california.com

Philip H. Messer
Manager, Specilaist Projects
Unocal Corporation
2929 East Imperial Highway
Brea, CA 92822
Phone: (714) 985-6432
Fax: (714) 985-6305
Internet: philm@unocal.com

Greg L. Mines
Advisory Engineer/Scientist
Idaho National Engineering & Environmental Laboratory
P.O. Box 1625
Idaho Falls, ID 83415
Phone: (208) 526-0260
Fax: (208) 526-0969
Internet: minesgl@inel.gov

Michal C. Moore
Commissioner
California Energy Commission
1516 Ninth Street, MS 34
Sacramento, CA 95814
Phone: (916) 654-3787
Fax: (916) 654-4420

Paul B. Mount II
Chief, Mineral Resources Management Division
California State Lands Commission
200 Oceangate, 12th Floor
Long Beach, CA 90802
Phone: (562) 590-5201
Fax: (562) 590-5210
Internet: mountp@slc.ca.gov

Address Listing of Registrants: Complete List

Marty Mutsch
President
Ben Holt Company
201 South Lake Avenue, Suite 300
Pasadena, CA 91101
Phone: (626) 795-6866
Fax: (626) 584-9210

Larry Myer
Head, Energy Resource Department
E.O. Lawrence Berkeley National Laboratory
One Cyclotron Road, MS 90-1116
Berkeley, CA 94720
Phone: (510) 486-6456
Fax: (510) 486-5686
Internet: lrmyer@lbl.gov

Manuel Nathenson
U.S. Geological Survey
345 Middlefield Road, MS 910
Menlo Park, CA 94025
Phone: (650) 329-5292
Fax: (650) 329-5203
Internet: mnathnsn@mojave.wr.usgs.gov

Marilyn Nemzer
Executive Director
Geothermal Education Office
664 Hilary Drive
Tiburon, CA 94920
Phone: (415) 435-4574
Fax: (415) 435-7737
Internet: geo@marin.org

Randy A. Normann
Senior Member of the Technical Staff
Sandia National Laboratories
P.O. Box 5800, MS 1033
Albuquerque, NM 87185
Phone: (505) 845-9675
Fax: (505) 844-3952
Internet: ranorma@sandia.gov

Judy K. Partin
Advisory Scientist
Lockheed Martin Idaho Technologies Company
P.O. Box 1625
Idaho Falls, ID 83415
Phone: (208) 526-2822
Fax: (208) 526-2814
Internet: jk6@inel.gov

Purna Patnaik
Senior Scientist
Maxwell Technologies
8888 Balboa Avenue
San Diego, CA 92123
Phone: (619) 576-7760
Fax: (619) 637-7411
Internet: purna@maxwell.com

Susan Patterson
Manager, Technology Transfer Program
California Energy Commission
Energy Technology Development Division
Technology Evaluation Office
1516 9th Street, MS 45
Sacramento, CA 95814
Phone: (916) 654-4992
Fax: (916) 653-8251
Internet: spatters@energy.state.ca.us

Roger Peake
Energy Specialist/Project Manager
California Energy Commission
1516 Ninth Street, MS-43
Sacramento, CA 95691
Phone: (916) 654-4609
Fax: (916) 653-6010

Carl Peterson
Director, NADET Institute, Professor of Mechanical Engineering
NADET Institute/Massachusetts Institute of Tehnology
77 Massachusetts Avenue, MIT E40-473
Cambridge, MA 02139
Phone: (617) 253-5782
Fax: (617) 253-8013
Internet: marygal@mit.edu

David S. Pixton
Vice President Engineering
Novatek
2185 South Larsen Parkway
Provo, UT 84606
Phone: (801) 374-2755
Fax: (801) 373-9839
Internet: dpixton@novatekonline.com

Eugene T. Premuzic
Scientist/Energy Science & Tech. Div. Head
Brookhaven National Laboratory
P.O. Box 5000, Building 318
Upton, NY 11973
Phone: (516) 344-2893
Fax: (516) 344-2060
Internet: premuzic@bnl.gov

Karsten Pruess
Senior Scientist
E.O. Lawrence Berkeley National Laboratory
University of California
One Cyclotron Road, MS 90-1116
Building 90, Room 2024K
Berkeley, CA 94720
Phone: (510) 485-6732
Fax: (510) 486-5686
Internet: k-pruess@lbl.gov

Pete Pryfogle
Staff Scientist
Biotechnologies Group
P.O. Box 1625 - IRC/MS2203
Idaho Falls, ID 83415
Phone: (208) 526-0373
Fax: (208) 526-0828
Internet: wck2@inel.gov

Marshall J. Reed
Senior Program Manager
U.S. Department of Energy
Office of Geothermal Technologies
1000 Independence Avenue, SW
Washington, DC 20585
Phone: (202) 586-8076
Fax: (202) 586-8185
Internet: marshall.reed@hq.doe.gov

Dan W. Reicher
Assistant Secretary of Energy Efficiency and Renewable Energy
U. S. Department of Energy
Energy Efficiency and Renewable Energy
1000 Independence Avenue, SW
Washington, DC 20585
Phone: (202) 586-9220
Fax: (202) 586-9260
Internet: dan.reicher@hq.doe.gov

Joel L. Renner
Geothermal Program
Idaho National Engineering & Environmental Laboratory
P.O. Box 1625
Idaho Falls, ID 83415
Phone: (208) 526-9824
Fax: (208) 526-0969
Internet: rennerjl@inel.gov

Ann Robertson-Tait
Senior Geologist
GeothermEx, Inc.
5221 Central Avenue, Suite 201
Richmond, CA 94804
Phone: (510) 527-9876
Fax: (510) 527-8164
Internet: geothermex@compuserve.com

John C. Rowley
Senior Scientist
Pajarito Enterprises
3 Jemez Lane
Los Alamos, NM 87544
Phone: (505) 672-9770
Fax: (505) 672-0358
Internet: 75033.2375@compuserve.com

Dan A. Sanchez
Program Manager
U.S. Department of Energy
Albuquerque Operations Office
P.O. Box 5400
Albuquerque, NM 87185
Phone: (505) 845-4417
Fax: (505) 845-4430
Internet: dsanchez@doeal.gov

Paul M. Santi
Assistant Professor
University of Missouri-Rolla
129 McNutt Hall
Rolla, MO 65409
Phone: (573) 341-4927
Fax: (573) 341-6935
Internet: psanti@umr.edu

Subir K. Sanyal
President
GeothermEx, Inc.
5221 Central Avenue, Suite 201
Richmond, CA 94804
Phone: (510) 527-9876
Fax: (510) 527-8164
Internet: 76612.1411@compuserve.com

John H. Sass
Geophysicist
U.S. Geological Survey
Volcano & Earthquake Hazards
Geothermal Studies Project
2255 North Gemini Drive
Flagstaff, AZ 86001
Phone: (520) 556-7226
Fax: (520) 556-7169
Internet: jsass@flagmail.wr.usgs.gov

Hiroshi "Brett" Sato
Manager, Engineering & Sales
Fuji Electric Corporation of America
1 Park Plaza, Suite 580
Irvine, CA 92614
Phone: (714) 251-9600
Fax: (714) 251-9611
Internet: brettsato@msn.com

Allan R. Sattler
Distinguished Member of the Technical Staff
Sandia National Laboratories
P.O. Box 5800, MS 0706
Albuquerque, NM 87185
Phone: (505) 844-1019
Fax: (505) 844-0240
Internet: arsattl@sandia.gov

Daniel Schochet
Vice President
ORMAT International, Inc.
980 Greg Street
Sparks, NV 89431
Phone: (702) 356-9029
Fax: (702) 356-9039
Internet: ormatintl@ormat.com

Greg G. Scott
Chief, Engineering
California State Lands Commission
200 Oceangate, 12th Floor
Long Beach, CA 90802
Phone: (562) 590-5201
Fax: (562) 590-5210
Internet: scottg@slc.ca.gov

Dan Shawhan
Research Associate
Geothermal Energy Association
122 C Street, NW, Suite 400
Washington, DC 20001
Phone: (202) 383-2626
Fax: (202) 383-2678
Internet: dshawhan@geotherm.org

Manuchehr Shirmohamadi
Principal
Material Integrity Solutions, Inc.
3254 Adeline Street, Suite 200
Berkeley, CA 94703
Phone: (510) 594-0300
Fax: (510) 594-0333
Internet: mshir@misolution.com

Gary Shulman
Geothermal Power Company, Inc.
1460 West Water Street
Elmira, NY 14905
Phone: (607) 733-1027
Fax: (607) 734-2709

Gunter Siddiqi
Shell International Exploration & Production B.V.,
Research and Technical Services
2280 AB Rijswijk, P.O. Box 60
The Netherlands
Phone: 31-70-311-6122
Fax: 31-70-311-3366
Internet: g.siddiqi@siep.shell.com

J. M. Simonson
Staff Scientist
Oak Ridge National Laboratory
P.O. Box 2008, Building 4500S, MS-6110
Oak Ridge, TN 37831
Phone: (423) 574-4962
Fax: (423) 574-4961
Internet: simonsonjm.@ornl.gov

Donna Smith
Program Manager, Extractive Industries Technologies
Civilian and Industrial Technology Programs Office
P.O. Box 1663, MS C331
Los Alamos, NM 87545
Phone: (505) 667-9473
Fax: (595) 665-8874
Internet: smith_d@lanl.gov

Curtis Sommer
Graduate Student
Arizona State University
2416 East Laird Street
Temple, AZ 85281
Phone: (602) 967-2087
Internet: curtis@imapl.asu.edu

Thomas R. Sparks
Manager, Government Relations & Utility Affairs
Unocal Corporation
P.O. Box 2390
Brea, CA 92822
Phone: (714) 985-6404
Fax: (714) 985-6301
Internet: tom.sparks@unocal.com

Ken Speer
Plant Manager
Pacific Gas & Electric Company - Geysers
P.O. Box 456
Healdsburg, CA 95448
Phone: (707) 431-6047
Fax: (707) 431-6207
Internet: kdsi@pge.com

Charles G. Stevens
Project Leader
Lawrence Livermore National Laboratory
7000 East Avenue
P.O. Box 808, L-183
Livermore, CA 94551
Phone: (510) 422-6208
Fax: (510) 422-2499
Internet: stevens2@llnl.gov

Toshi Sugama
Chemist
Brookhaven National Laboratory
Building 526, 12 North Sixth Street
Upton, NY 11973
Phone: (516) 344-4029
Fax: (516) 344-2359
Internet: sugama@bnl.gov

Robert J. Sunderland
Vice President
Trans Pacific Geothermal Corporation
1901 Harrison Street, Suite 1590
Oakland, CA 91462
Phone: (570) 763-7812
Fax: (510) 763-2504
Internet: tgcorp@california.com

Daniel Swenson
Professor
Kansas State University
Mechanical and Nuclear Engineering
Rathbone Hall
Manhattan, KS 66506
Phone: (785) 532-2320
Fax: (785) 532-7057
Internet: swenson@ksu.edu

Kristi Theis
Technical Communications
National Renewable Energy Laboratory
1617 Cole Boulevard, MS 1713
Golden, CO 80401
Phone: (303) 275-3652
Fax: (303) 275-3619
Internet: theisk@tcplink.nrel.gov

Richard Thomas
Geothermal Officer
California Division of Oil, Gas, & Geothermal Resources
801 K Street, MS 20-21
Sacremento, CA 95814
Phone: (916) 323-1787
Fax: (916) 323-0424
Internet: dthomas@consrv.ca.gov

Alan C. Tripp
Research Associate Professor
Energy & Geoscience Institute
University of Utah
423 Wakara Way, Suite 300
Salt Lake City, UT 84108
Phone: (801) 581-5126
Fax: (801) 585-9249
Internet: actripp@mines.utah.edu

Alfred Truesdell
Chief Scientist
Entropy, Inc.
700 Hermosa Way
Menlo Park, CA 94025
Phone: (650) 322-6135
Fax: (650) 324-4009
Internet: ahtruesdell@lbl.gov

Laura Vimmerstedt
Environmental Analyst
National Renewable Energy Laboratory
1617 Cole Boulevard
Golden, CO 80401
Phone: (303) 384-7346
Fax: (303) 384-7411
Internet: laura_vimmerstedt@nrel.gov

Marina M. Voskanian
Chief of Planning and Development
State Lands Commission
Mineral Resources Management Division
200 Oceangate, 12th Floor
Long Beach, CA 90802
Phone: (562) 590-5291
Fax: (562) 590-5295
Internet: voskanm@slc.ca.gov

J. Douglas Walker
University of Kansas
Department of Geology
120 Lindley Hall
Lawrence, KS 66045
Phone: (785) 864-2735
Fax: (785) 864-5276
Internet: jdwalker@kuhub.cc.ukans.edu

Mark Walters
Geoscience Manager
CalEnergy Company, Inc.
900 North Heritage Drive, Building D
Ridgecrest, CA 93555
Phone: (760) 499-2336
Fax: (760) 499-2348
Internet: mark.walters@calenergy.com

Charlene L. Wardlow
Environmental Manager
Calpine Corporation
P.O. Box 11279
Santa Rosa, CA 95406
Phone: (707) 527-6700
Fax: (707) 544-2422
Internet: charlene@calpine.com

John Weare
Professor of Chemistry
University of California, San Diego
Department of Chemistry
Mail Code 0340
La Jolla, CA 92093
Phone: (619) 534-3286
Fax: (619) 534-7244
Internet: jweare@ucsd.edu

Ken Williamson
Manager, Geoscience
Unocal Corporation
P.O. Box 6854
Santa Rosa, CA 95406
Phone: (707) 521-7627
Fax: (707) 521-7604
Internet: kwilliamson@unocal.com

Michael Wilt
Vice President
Electromagnetic Instruments, Inc.
1304 South 46th Street
Richmond, CA 94804
Phone: (510) 232-7997
Fax: (510) 232-7998
Internet: wilt@emiinc.com

William D. Wood
Region Technical Manager
BJ Services Company, USA
1401 South Union Avenue
Bakersfield, CA 93307
Phone: (805) 831-5084
Fax: (805) 836-8903
Internet: bwood@bjservices.com

Phillip Michael Wright
Deputy Director
Energy & Geoscience Institute
423 Wakara Way
Salt Lake City, UT 84108
Phone: (801) 585-7783
Fax: (801) 585-3540
Internet: pwright@egi.utah.edu

David Zippin
Senior Associate
MHA Environmental Consulting, Inc.
520 South El Camino Real, Suite 800
San Mateo, CA 94402
Phone: (650) 373-1200
Fax: (650) 373-1211
Internet: zippin@mha-inc.com

Vince Zodiaco
Executive Vice President
Oxbow Power Corporation
9790 Gateway Drive, Suite 220
Reno, NV 89511
Phone: (702) 851-1199
Fax: (702) 850-2211
Internet: vince_zodiaco@oopsi.oxbow.com